AD-A163 218 AIRCRAFT NUCLEAR SURVIVABILITY METHODS(U) AIR FORCE INST OF TECH WRIGHT-PATTERSON AFB OH SCHOOL OF ENGINEERING H A UNDEM SEP 85 AFIT/DS/PH/84-3 1/3

UNCLASSIFIED F/G 18/3 NL

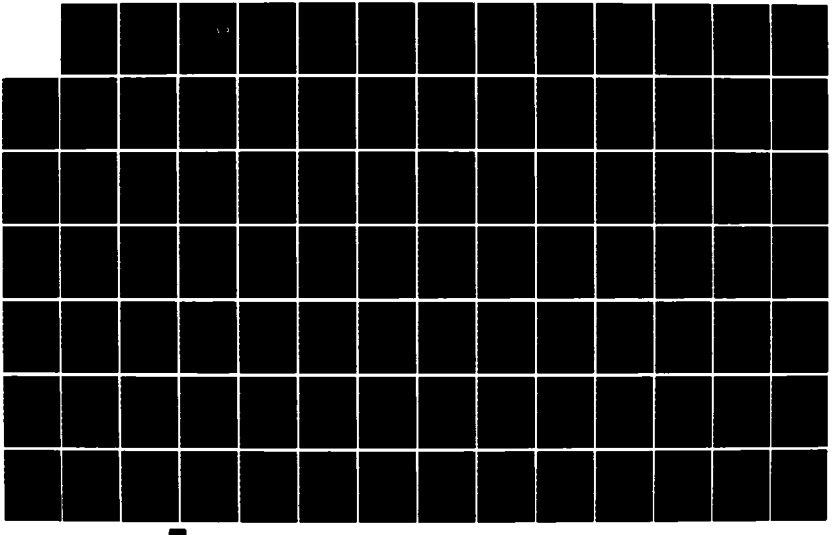

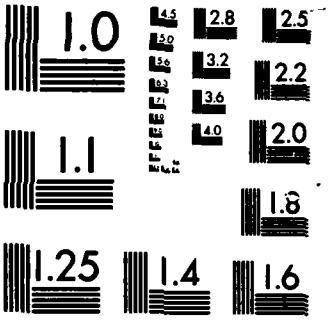

MICROCOPY RESOLUTION TEST CHART
NATIONAL BUREAU OF STANDARDS-1963-A

[illegible] AIR FORCE

AIRCRAFT NUCLEAR SURVIVABILITY METHODS

DISSERTATION

Halvor A. Ulden
Captain, USAF
AFIT/DS/PH/84-3

AFIT/DS/PH/84-3

AIRCRAFT NUCLEAR SURVIVABILITY METHODS

DISSERTATION

Halvor A. Undem
Captain, USAF
AFIT/DS/PH/84-3

AFIT/DS/PH/84-3

AIRCRAFT NUCLEAR SURVIVABILITY METHODS

DISSERTATION

Presented to the Faculty of the School of Engineering

of the Air Force Institute of Technology

Air University

In Partial Fulfillment of the

Requirements for the Degree of

Doctor of Philosophy

Halvor Andrew Undem, B.S., M.S.

Captain, USAF

September 1985

AFIT/DS/PH/84-3

AIRCRAFT NUCLEAR SURVIVABILITY METHODS

Halvor A. Undem, B.S., M.S.

Captain, USAF

Approved:

Charles J. Bridgman, Chairman — 30 July 85

Albert H. Moore — 31 July 85

D. Wallace Breuer — 31 July 1985

Michael F. Baran — 12 Aug 1985

Robert N. Davie, Jr. — 6 AUGUST 1985

Louis T. Montulli — July 31, 1985

Accepted:

J. S. Przemieniecki
Dean, School of Engineering — 9 Sep. 85

Dedicated to an immigrant of 1906, Sverre L. Undem, who gave up his native Norway to bequeath to me these great United States.

Preface

In the Winter of 1981, Dr. Charles J. Bridgman provided a unique and enlightening experience for me and several other graduate students. He led a special study in Nuclear Survivability, drawing on current research in the field, and provoking each of us to wrestle with that problem in a fundamental way. Just how does one measure the probability of failure for a structure exposed to the effects of nuclear weapons? The questions raised in this class were so intriguing that I chose the field for my research area under the direction of Dr Bridgman. My thanks to him for his inspiration, his encouragement, and his discipline.

My thanks also to the Defense Nuclear Agency who sponsored the work. Their willingness to sponsor travel to DNA and other locations for consultation was very beneficial.

A few words about some special items in the text are in order. Words can mean different things in different disciplines. A design engineer, for example, will see 'sigma' in pounds per square inch, while a statistician will see the normal distribution. To prevent these misunderstandings, a glossary can be found in Appendix F.

This problem covered a broad range of disciplines--from nuclear effects, to nonparametric statistics, to aircraft structures. The bibliography is topically indexed as an aid in sorting out the literature.

A good deal of statistics had to be learned in all this. A special thanks goes to Dr. Albert H. Moore. His courses in Reliability Theory provided insight into the nature of my research problem. I cannot omit the statisticians that Dr. Moore has "raised" either--Major James Sweeder and Major Ron Fuchs both contributed substantially to this research effort.

My thanks to Dr. Wallace Breuer for his help and consultation in the area of aircraft structures, and especially for assistance with the stress model in Chapter VI and Appendix E.

Thanks also to Lt Col Robert N. Davie and Dr. Louis T. Montulli, committee members at large and to Dr. Michael F. Baran, who reviewed and commented on an early version of Chapter V. I am also indebted to Major Max Stafford, who examined the proof in Appendix C. Thanks are due two members of the Air Force Weapons Laboratory. Chris Ashley and Al Sharp both took the time to patiently listen during an early stage of the research. I am especially grateful to Al Sharp for his fine work in documenting his thermal pulse routine.

Finally, a heartfelt thanks to my wife Becky, who again surrendered our home to books, and computer printouts, and plots piled high--and to Julia Susann--who made me a father just as this task was being finished.

Table of Contents

List of Figures

List of Tables

Abstract

A new approach for assessing the survivability of aircraft components in nuclear blast and thermal environments is presented in this dissertation. A nonparametric technique is developed for use in calculating the reliability interference integral. This approach eliminates the need for density function identification and parameter estimation. Furthermore, the method can be used without resorting to large-sample random Monte Carlo simulation or propagation of moments. In addition to this, the derived cumulative distribution function using such a technique exactly interpolates the true distribution function at selected points. The method is applied to the problem of aircraft survivability in nuclear blast environments using failure (strength) distributions found in the literature. It is also applied to the case of aircraft survivability in nuclear thermal environments where direct failure data is not available. Inputs to the engineering models involved are treated statistically, and the method is used to rigorously determine the statistical nature of the output variables.

I. Introduction

The objective of this dissertation is to find a logical way of inferring the probability of failure of an aircraft component when exposed to the effects of nuclear weapons. A reliability theory approach is taken that is distribution free. This approach, which exploits some recent developments in nonparametric statistics, eliminates the need for density function identification and parameter estimation. Furthermore, it provides a new way of finding the distribution of a function of random variables without using large-sample Monte Carlo simulation. The method is applied to the problem of aircraft survivability in nuclear blast environments using test data found in the literature. It is also applied to the case of aircraft survivability in nuclear thermal environments where direct failure data is not available. Inputs to the engineering models involved are treated statistically, and the method is used to rigorously determine the statistical nature of the output variables.

A review of nuclear survivability/vulnerability (S/V) methods is provided in Chapter II. The deterministic approach for aircraft is reviewed. Little work on probabilistic methods for aircraft has been done up to this time. Attempts to logically develop a probabilistic model from stated aircraft hardness specifications are noted as are other approaches. Ground system survivability methods are

examined. Probabilistic methods have been used for some time in this area. The earliest approaches involve direct modeling of system failure probability as a function of range from the weapon. Modern methods include Monte Carlo simulation. This has been used in Minuteman survivability studies and more recently to investigate electromagnetic pulse (EMP) survivability. Other studies include survivability assessment of horizontal and vertical missile shelters and interruption of low frequency communications by nuclear effects.

A review of classical stress/strength interference theory is provided in Chapter III. Strength and stress distributions are discussed, and the reliability interference integral presented. Engineering determinism, or "cookie-cutter" damage distributions, are shown to be a special case of the general interference theory approach. Stress/strength interference theory is thus a natural choice as a theoretical approach. Serious problems have existed in applying interference theory to failure assessment of large engineering systems. These include development of the system reliability model from component structures, the numerical difficulty of finding the distribution of a function of one or several random variables, and the serious limitation presented by the lack of data. This last limitation in particular makes density function identification and parameter estimation difficult. Attempts to solve the above diffi-

culties include fault tree analysis, propagation of moment methods, direct and indirect Monte Carlo simulation, variable transformation techniques, Bayesian analysis, and survey of expert opinion.

A new solution to the above difficulties using an extension of recently developed nonparametric estimation techniques is presented in Chapter IV. While the system reliability modeling problem remains, the new numerical technique provides a tool for finding the distribution of a function of multiple random variables. An example from the engineering literature is presented as a benchmark problem. The advantages of the nonparametric method are noted. These advantages include (a) elimination of the requirement for density function identification and consequent parameter estimation, (b) freedom from a priori distributional assumptions, (c) elimination of the requirement for large Monte Carlo samples, and (d) protection against drawing unwarranted inferences from a small data set.

The analysis of aircraft survivability to nuclear induced blast environments is presented in Chapter V. In this case, actual failure distributions for piece-parts are taken from an analysis of some 20 years of static test data conducted at Wright-Patterson AFB, OH. A general discussion of the survivability problem is presented, and a series reliability model for the mission developed. Blast vulnerability is determined for the fuselage, wing, and vertical

tail assemblies. This is done by using the statistical variation of overpressure versus range to determine the applied stress distributions. The actual failure distributions determined from the test data then allow the component failure probabilities to be determined as a function of range. These provide the required information for finding the system failure probability as a function of range from the weapon.

The analysis of aircraft survivability to nuclear thermal environments is presented in Chapter VI. The difficulty of sparse data is noted. In particular, no probabilistic description of the thermal environment could be found from the literature. Also, no failure data for the failure mode of interest could be found in the literature. As an alternative, the statistical distribution of radiated power is developed by regressing the output of a complex radiation hydrodynamics code on that of a more approximate model. The study is restricted to the radiated power from a 1 Kiloton (KT) burst in a sea level atmosphere. The statistical environmental input is then used to determine the distribution of peak skin temperature in a thin skin assembly. Two thermal failure models are compared, and failure probabilities versus range are displayed.

The results are summarized in Chapter VII, and recommendations for future work are given. The recommendations include needed developments in both methodology and applica-

tions. The greatest need for applications is for standardized statistical descriptions of nuclear effects environments.

The development of the primary numerical method used in the applications problems is detailed in Appendix A. The documentation of several modifications to a nonparametric estimation method is included.

A source code listing of the computer program NOSWET is presented in Appendix B.

In Appendix C, a new method is presented for finding the distribution of monotonic functions of random variables. Functions of a single random variable are considered first, and examples presented. The theory is then extended to functions of two random variables, and two examples of this are given. The theory, with some restrictions, is extended to functions monotonic in N random variables.

In Appendix D, the numerical technique used to calculate the integral of conditional density functions is explained and documented. The reliability interference theory integral is a special case of this type of problem.

Further consideration of the vulnerability of a box-beam wing structure in nuclear thermal environments is presented in Appendix E. In particular, the relative vulnerabilities of the parts of the beam are discussed.

Finally, a glossary of acronymns and nomenclature is presented in Appendix F, keyed by Chapter.

II. A Review of Survivability Methods

Overview

The problem to be considered is this: An aircraft flys in the vicinity of a nuclear weapon at the time that it detonates. If the aircraft position with respect to the burst is known, can one predict the probability of aircraft failure due to the effects of the nuclear weapon? What is the justification for such a prediction? The literature is reviewed below. This literature search leads to a preferred approach to solving this problem.

Deterministic Methods

The Defense Nuclear Agency (DNA) document DNA2048-H, Handbook For Analysis of Nuclear Weapon Effects on Aircraft [68] is representative of deterministic methods for assessing aircraft survivability. The basic objective of the handbook is the determination of sure-safe (SS) and sure-kill (SK) ranges. SS and SK ranges correspond to range locations where SS and SK responses of an aircraft subsystem are expected. A SS response corresponds to incipient damage, or limit loads. A SK response corresponds to a catastrophic damage condition. This way of thinking has its origins in aircraft design. SS loads are limit loads, while SK loads are ultimate loads, or loads beyond ultimate. Ultimate loads are often taken to be

limit loads times a factor of safety, typically 1.5. This approach to survivability allows one to find those regions of space where the aircraft is sure-safe or sure-killed. Typical outputs of the method of Reference [68] are shown in Figures 2.1 and 2.2. These pictures require some explanation.

In Figure 2.1, the target occupies the origin of coordinates. A nuclear detonation may be placed anywhere in the plane of the figure. Any burst that falls on the solid contour, or outside of it, leaves the target at the origin completely undamaged. Hence, the region of space outside of the contour is called the 'sure-safe' region. The probability of damage is nonzero (but unspecified) in the region of space inside the contour.

In Figure 2.2, the target also occupies the origin. In this case, however, any nuclear burst that falls on the contour or inside of it results in the destruction of the target. Hence, the region inside the contour is now the 'sure-kill' region. Outside of the contour, the probability of damage is unspecified (but it is not unity).

The chief disadvantage of the technique is that it is ambiguous. There are regions of space left over where the state of the aircraft subsystem cannot be determined.

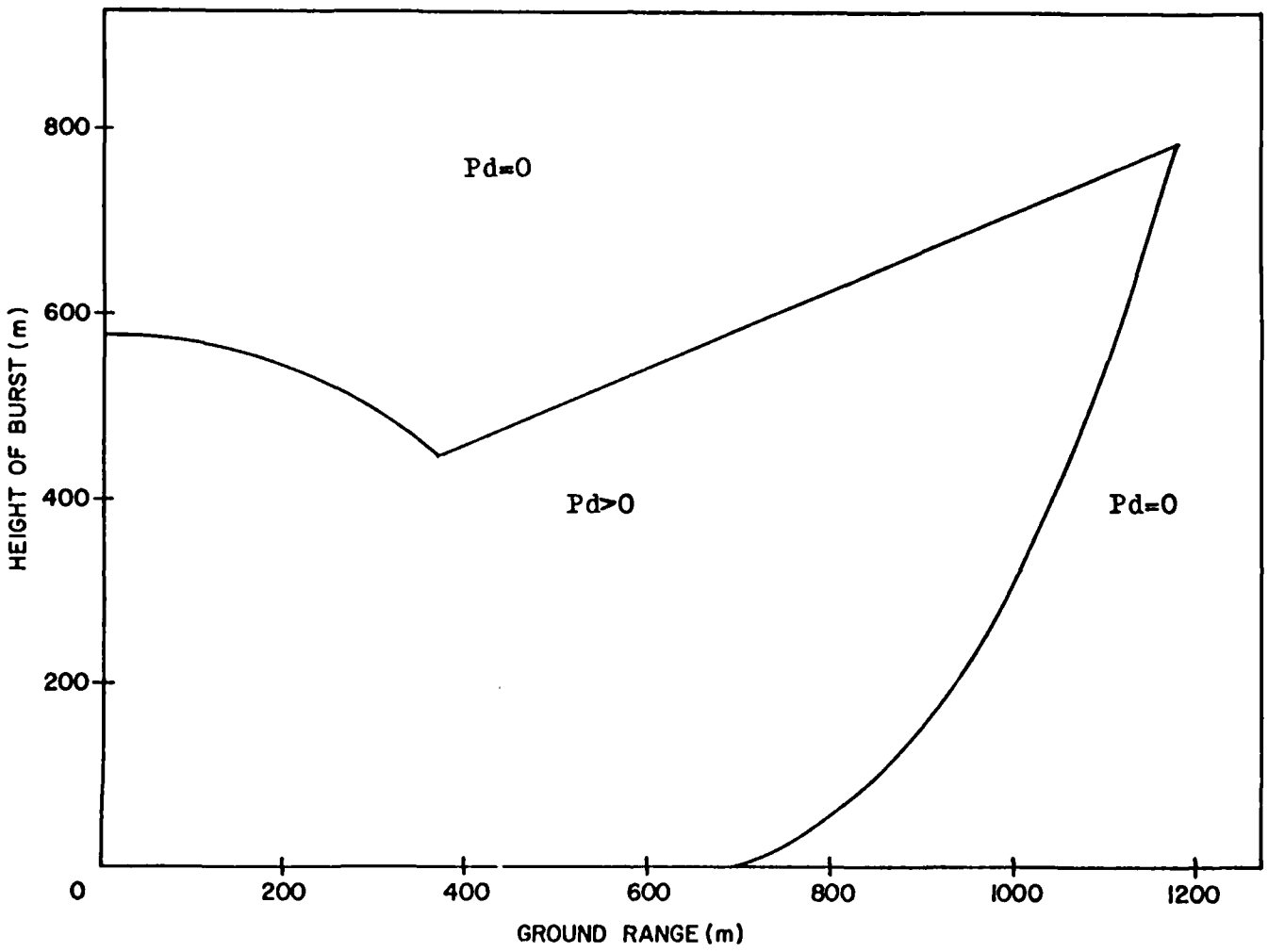

Figure 2.1. Sure Safe Range Envelopes for Aircraft
(Adapted From Reference [60])

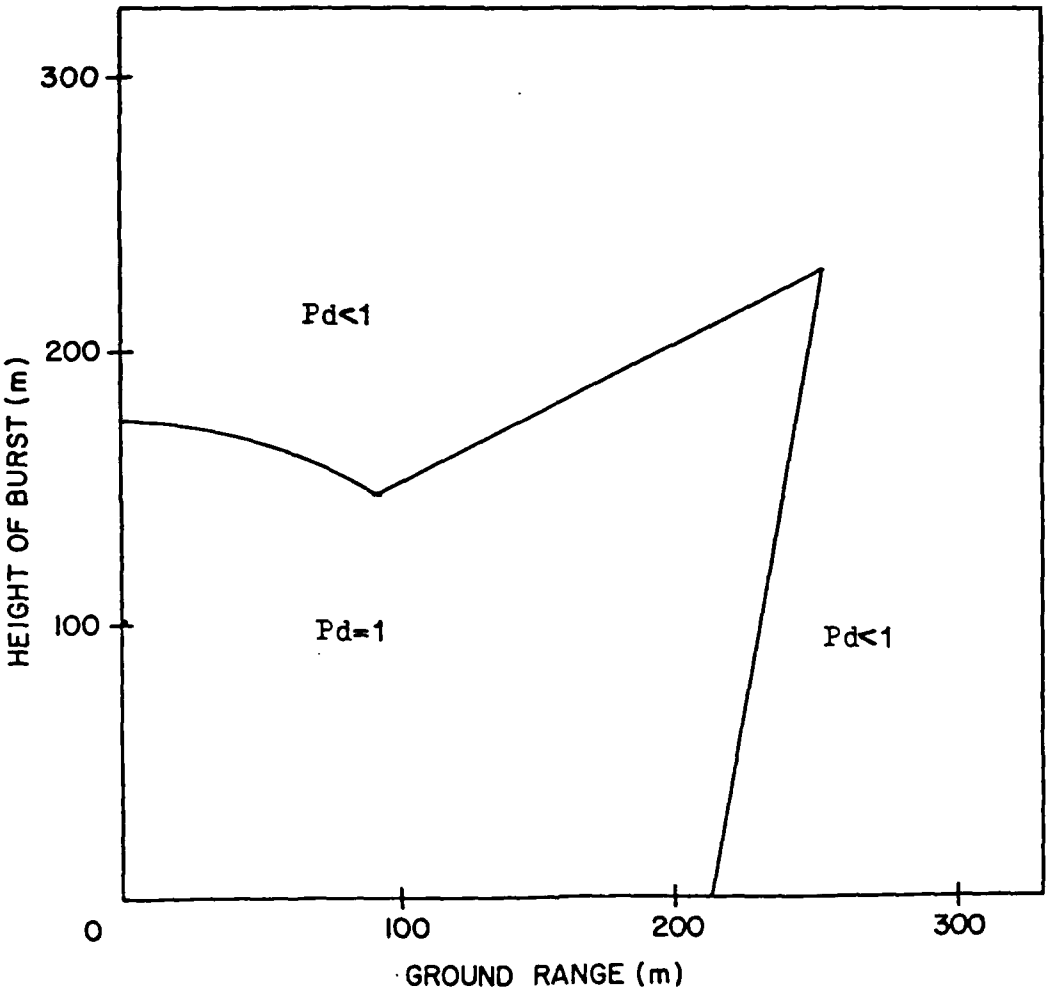

Figure 2.2. Sure Kill Range Envelopes for Aircraft (Adapted From Reference [60])

Probabilistic Methods

The obvious problem with the deterministic technique can be eliminated if one recognizes that the failure probability should vary smoothly from some low value in the SS region to some high value in the SK region. A number of approaches have been used to attempt this, and they are reviewed below.

Aircraft Structures. Bridgman [44], in an early Technical Note, attempted to find a continuous probability of damage curve by postulating a damage function as a cumulative lognormal distribution in the range space. This approach closely parallels that of AP-550 [53], discussed later. Since the lognormal is a two parameter distribution, an infinite number of possibilities exists for the continuous damage curve. Bridgman took the novel approach of coupling the information in DNA-2048H so as to find the optimum continuous damage model. He did this by postulating the damage probability to be some arbitrarily low number (.02) at a known SS range, and an arbitrarily high number (.98) at a known SK range. The SS and SK ranges were determined by the methods of DNA-2048H. Such a specification leads to a unique solution for the two parameters of the lognormal distribution, and thus specifies the damage function.

In some later papers [45,46], Bridgman recognized that the range specifications depended not just on the target,

but on the entire source, transmission, and interaction problem as well. He then postulated a continuous failure distribution in the stress space, again finding the distribution by coupling the information in DNA-2048H to the lognormal model so as to specify the survivability function.

There have been other attempts to treat survivability as a statistical problem at the component level. The Studies and Analysis group at Hq USAF [42] used an approach similar to Bridgman's. Sure-safe and sure-kill specifications in the stress space were assigned as percentiles of the component failure distribution. The possibilites using parametric statistics were surveyed as shown in Figure 2.3. Other contributors to this field include Gragg [63]. The probabilistic survivability literature for aircraft systems is quite limited compared to that of ground systems, which will be considered next.

Ground Structures. Ground system survivability has been studied for a considerably longer time than has aircraft survivability. One of the earliest probabilistic treatments is the method of AP-550 [53]. The failure probability of a structure is given as a complementary cumulative lognormal function, with the parameters of the lognormal depending on the target hardness. This method is still in use by the targeting community, as represented by the Defense Intelligence Agency (DIA). In this method one models damage directly as a function of range, based on

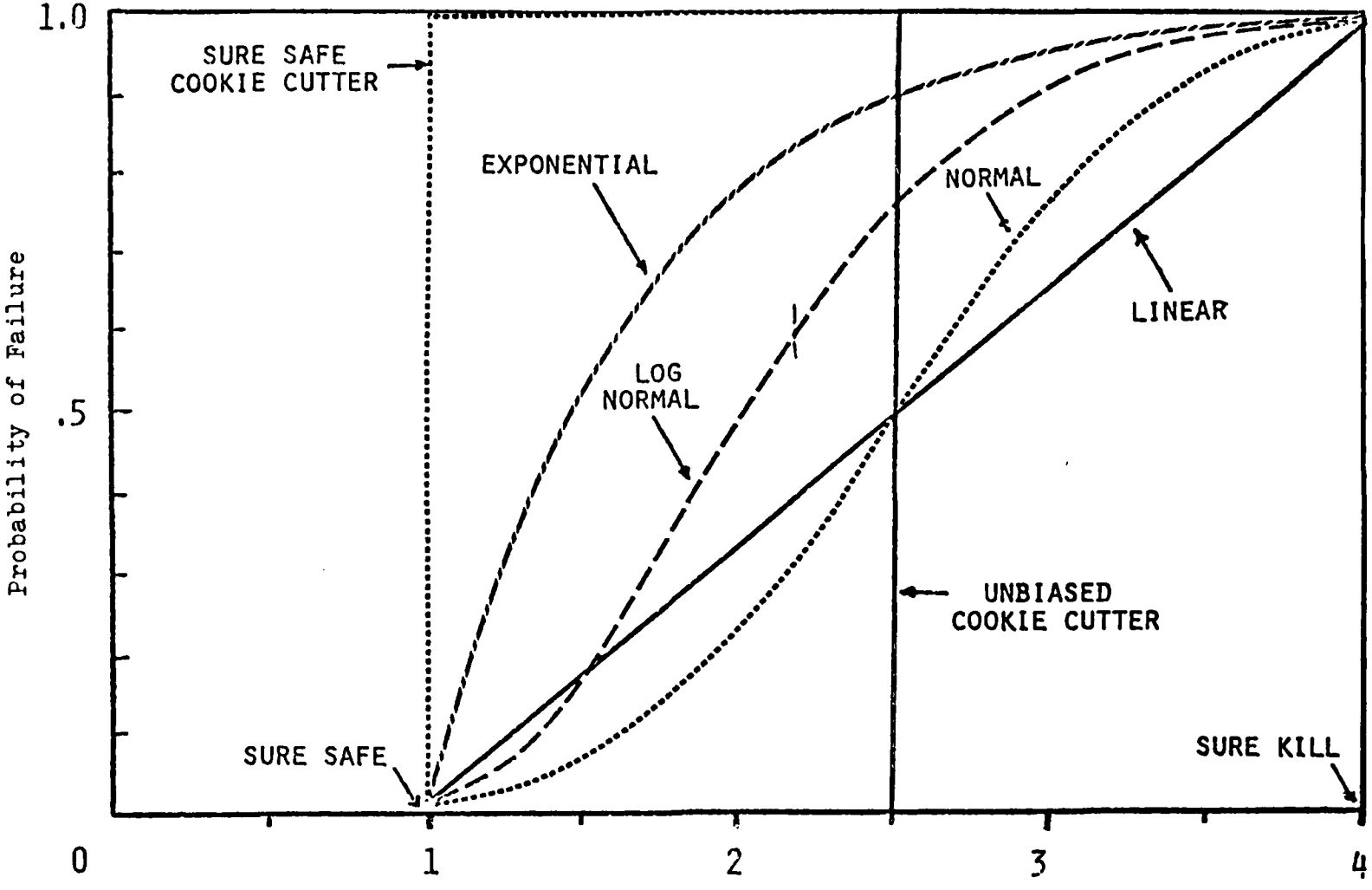

Figure 2.3. Hypothetical Failure Distributions
(From Reference [42])

early observations of the Hiroshima blast damage. Targets are coded by a special number as being either overpressure sensitive or dynamic pressure sensitive. The special coding of a target type yields parameters for the determination of the continuous damage function.

A quite different probabilistic method was developed by the Defense Nuclear Agency (DNA) in the late 1960's and applied to problems of Minuteman Missile survivability. This technique was developed independently of the method used by DIA. DNA published the FAST (Failure Analysis By Statistical Techniques) code in 1974 [57]. FAST is an ambitious Monte Carlo code, including correlated nuclear weapon environments, variable system reliability models, and arbitrarily input component fragilities, or subsystem failure distributions. The publication of FAST was a significant milestone. It was one of the first, if not the first, Department of Defense (DOD) products that treated survivability along the lines of classical reliability theory. After being used in the Nuclear Hardness and Evaluation Program (NHEP) [58], it was not used much until 1980. At that time a group at Lawrence Livermore National Laboratory (LLNL) began using it to investigate probabilistic modeling of survivability to EMP [40,41].

Recent probabilistic survivability studies include examination of MX survivability in both its horizontal and vertical shelters [55]. These studies, also conducted by

DNA, did not use FAST, but a combination of approximate probabilistic techniques [37] and Monte Carlo simulation [55]. Other studies of hardening of ground facilities may be found in the literature [49,50,75].

Another notable study conducted recently by DNA is that of Jordano [67]. He investigated the uncertainty of nuclear effects on low frequency (LF) communication links. He calculated the probability of LF signal loss, based on statistical inputs to nuclear debris cloud stabilization altitude and location. This work differed both from the FAST and the approximate probabilistic techniques. Rather than make distributional assumptions, Jordano directly calculated the distribution of a function of a random variable based on a variable transform method.

To summarize, ground system survivability is done in two ways. The targeting community, as represented by DIA, treats all damage as an empirical function of range [53]. The nuclear effects community, as represented by DNA, has developed some probabilistic damage models based on classical reliability theory [37,55,57] and direct variable transformation techniques [67]. The DNA publications just mentioned form the nucleus of modern probabilistic survivability literature for the DOD. However, there has been a good deal of work done outside of DOD, and some of this will be reviewed at this time.

Other Structures. Two groups in the engineering community outside of DOD have extensively studied methods for determining the probability of failure of structures. Civil engineers have been conducting research in the area since the late 1960's. Most of the literature here involves the method of propagation of moments of random variables, about which more will be said in Chapter III. This technique has been applied to a broad range of structural reliability problems [7,27,28,30,31]. Some of these even deal with nuclear blast damage [71]. Textbooks on the subject of structural reliability are beginning to be published [15,23]. Since about the early to mid 1970's, the nuclear engineering community has also taken an active interest in the subject. Proceedings of the conferences on Structural Mechanics in Reactor Technology (SMIRT) include many papers on the application of probabilistic methods to problems of nuclear safety. Here too, books are being written [25,29]. In most cases, these methods and applications are based on mathematical reliability theory, coupled with standard propagation of moments techniques.

Summary

The literature just reviewed includes deterministic and probabilistic methods. Deterministic methods do not provide for continuous failure (or survivability) functions. This violates intuition. On the other hand, probabilistic models that are based on direct modeling with range are justified

only by early observations of nuclear blast damage. Some recent publications suggest that the fundamentals of reliability theory are applicable to the problem. In Chapter III, classical reliability theory is more carefully reviewed. The strengths and weaknesses of this method as an applications tool for survivability analysis will be noted.

III. Stress-Strength Interference Theory

Overview

The mathematics of reliability theory, and the field of reliability analysis, came about as a result of problems the DOD had with electronics piece-parts in the early 1940's [8]. Only since about the mid 1960's has the field been extended to problems of large-scale engineering systems. In the paragraphs that follow, the basic theory of reliability mathematics is reviewed. Engineering determinism is shown to fit naturally into the theory as a special case. The problems in applying the theory to engineering systems are reviewed, as are previous approaches to solving those problems.

Mathematical Reliability Theory

Strength Distributions. The strength distribution is a statistical property of a population of devices operating in some stress environment. Examples include light bulbs operating for a given number of hours, or samples of wing materials under tensile testing. The strength distribution is sometimes called the failure distribution or the resistance distribution. It is a measure of how well the devices resist a stress load. The distribution is most easily determined for the case when a number of items can all be tested to failure. In that case, one can plot the

fractional number of failures occuring in a given stress interval versus the midpoint of the interval. The resulting histogram approximates the underlying probability density function (PDF) for failure. This statistical information is a measure of the strength of the item, since the central value of the distribution indicates the value of stress where most failures occur. In addition, the amount of scatter about the central value measures the variability in the quality of the item. The stress value at which an item will fail is a random variable. The probability that an item will fail at a particular stress value s is then expressed by:

$$p_f = Pr\{S \leq s\} = \int_{-\infty}^{s} f_S(s)ds = F_S(s) \qquad (3.1)$$

where p_f is the failure probability, S the strength random variable, s a particular value of S, $f_S(s)$ the strength PDF, and $F_S(s)$ the strength cumulative distribution function (CDF).

If the testing of n items resulted in every single item failing precisely at the value SK, then a true cookie-cutter distribution would result. The PDF would be a Dirac delta function [2] located at SK, and the CDF would be a step function as shown in Figure 3.1 (top). A more likely result is that every item fails at a slightly different value, resulting in a CDF similar to that of Figure 3.1 (bottom).

Cookie-Cutter Distribution

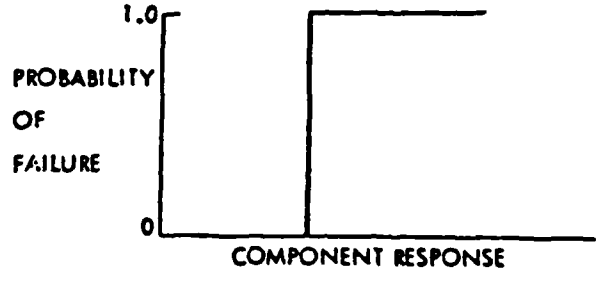

Uniform Distribution

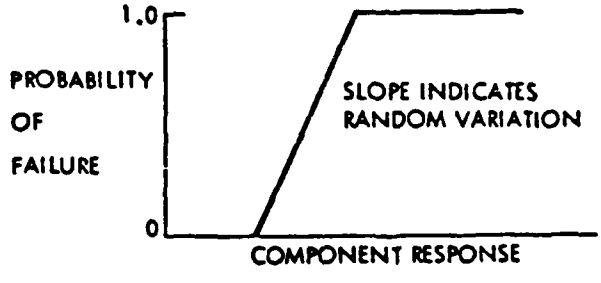

Figure 3.1. Cookie-Cutter (Top) and Random (Bottom) Failure Distributions
(Adapted From Reference [57])

Stress Distributions. Equation 3.1 gives the failure probability for the item provided the stress is exactly known. As in the case of the failure point of the device, the applied stress may not be known exactly. Repeated measurements of the free field stress may yield a central or expected value for the measurements, but also dispersion about the central value. The applied stress, s, would then also be a random variable, described by a statistical distribution.

The Interference Integral and Related Random Variables. If the distributions of S and s have been determined, then the general expression for the failure probability is given by:

$$p_f = Pr\{S \leq s\} \tag{3.2}$$

Provided the strength and stress variables are independent, Equation 3.2 can be written as:

$$Pr\{S \leq s\} = \int_{-\infty}^{\infty} f_s(s) F_S(s) ds \tag{3.3}$$

where p_f is the failure probability as before, S the strength random variable, s the stress random variable, $f_s(s)$ the PDF of the stress distribution, and $F_S(s)$ the CDF of the strength distribution. In words, the failure probability is just the chance that a random selection from the sample space of all strength values yields a number less than or equal to a random selection from the sample space of all stress values. Equation 3.3 is often referred to as the reliability interference integral, or just the interference

integral, since contributions to the integral occur only in the variable space where the density functions overlap or "interfere". The shaded portion of Figure 3.2 illustrates the interference region. Equation 3.3 is seen to reduce to Equation 3.1 if the stress PDF is a Dirac delta function.

If the stress and strength random variables are not independent, Equation 3.3 cannot be used as written. However, Equation 3.2 is still valid, and the failure probability can be calculated by finding the distribution of either the margin variable, ξ , or the safety factor variable, η . The margin variable is defined by:

$$\xi = S - s \tag{3.4}$$

Consequently, in terms of the margin variable, the failure probability could also be calculated by:

$$p_f = Pr\{\xi \leq 0\} \tag{3.5}$$

Also, the safety factor variable, provided the applied stress is not zero, is defined by:

$$\eta = S / s \tag{3.6}$$

In terms of the safety factor, the failure probability can be calculated by:

$$p_f = Pr\{\eta \leq 1\} \tag{3.7}$$

At this point, examination of Equations 3.4 and 3.6 shows that one of the requirements for solving the problem is the ability to find the distribution of a function of two random variables. This can be a difficult problem, and it will be discussed in more detail below. Before considering

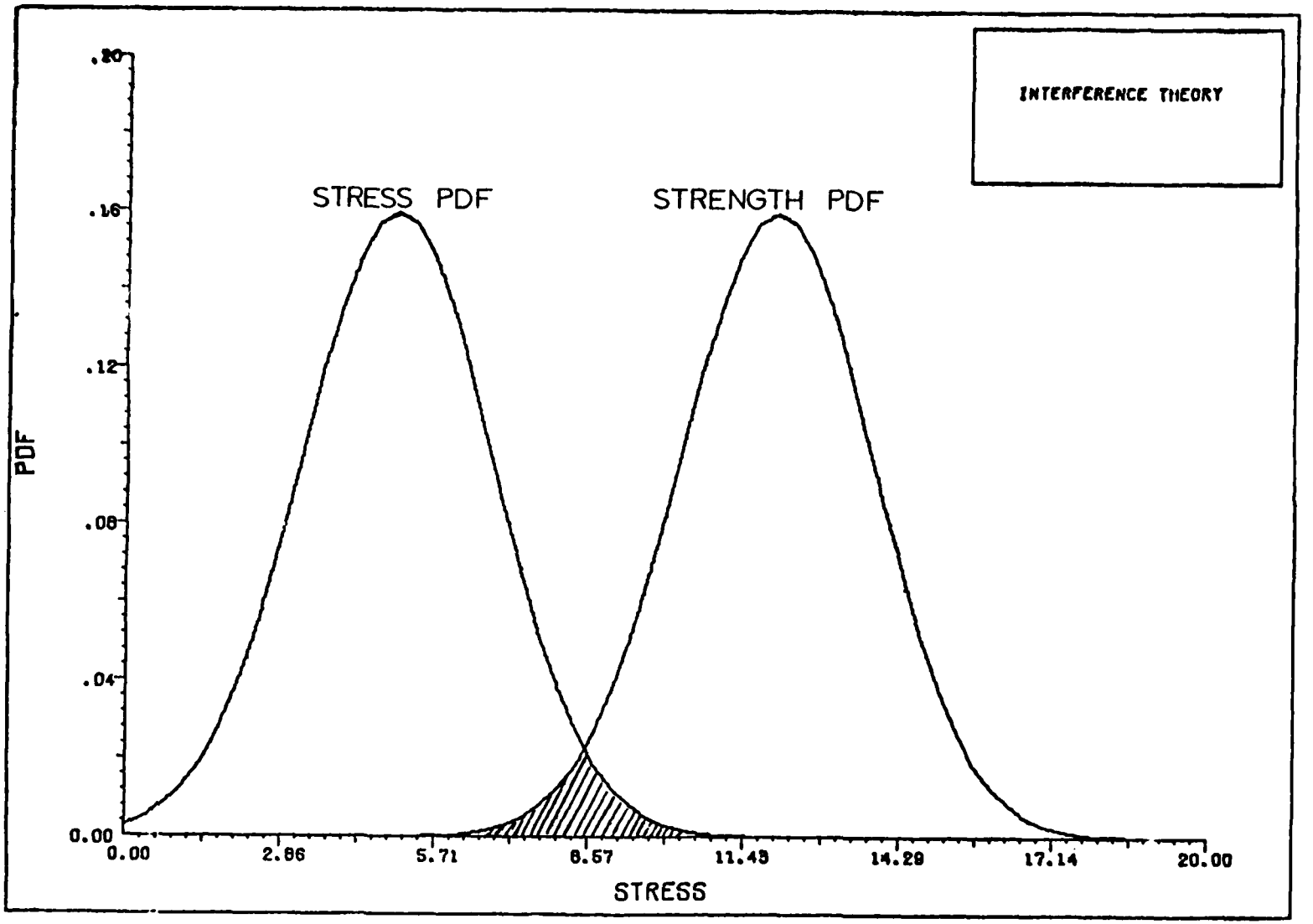

Figure 3.2. Interference Theory

that, a discussion of the reduction of the interference integral for the deterministic case is presented.

Reduction To Engineering Determinism. If the stress is deterministic, the PDF of s may be represented by a Dirac delta function centered at the known stress value, say $\bar{s}$. That is,

$$f_s(s)=\delta(s-\bar{s}) \tag{3.8}$$

Using Equation 3.8 in the interference integral of Equation 3.3 reduces the integral to:

$$p_f=F_S(\bar{s}) \tag{3.9}$$

If the strength is also deterministic, then the strength CDF is given by:

$$F_S(\bar{s})=0 \quad \forall \ \bar{s}<SK \tag{3.10}$$

$$F_S(\bar{s})=1 \quad \forall \ \bar{s}\geq SK \tag{3.11}$$

The results of Equations 3.10 and 3.11 are the familiar deterministic cookie-cutter damage functions.

Going the other way, Equations 3.10 and 3.11 can be used first inside the interference integral of Equation 3.3. Since the integrand is zero for every s<SK, the limits are changed so that:

$$p_f=\int_{SK}^{\infty} f_s(s)ds \tag{3.12}$$

But Equation 3.12 is just the statement that:

$$p_f=Pr\{s>SK\} \tag{3.13}$$

Again, by hypothesis, only one value of s is ever observed, namely $\bar{s}$. Consequently, Equation 3.12 takes only two values:

$$p_f=1 \quad \blacktriangledown \quad \bar{s} \geq SK \tag{3.14}$$

$$p_f=0 \quad \blacktriangledown \quad \bar{s} < SK \tag{3.15}$$

The set of Equations 3.14 and 3.15 is identical in meaning to the set of Equations 3.10 and 3.11. Cookie-cutter damage distributions are the result.

The reduction of the general reliability integral approach to the cookie-cutter case for Dirac delta PDF's makes it a natural choice for adding probabilistic information to the survivability problem. One sees that engineering determinism is nothing more than a subset of a more general probabilistic approach. The subset is found by replacing all continuous probability density functions by a very special probability density function--the Dirac delta, which has a single parameter. Seen in this light, engineering determinism would *seem to have no* inherent theoretical superiority over probabilistic methods based on reliability theory. Even so, probabilistic approaches to survivability problems are not common. The reasons for this are examined next.

Applications Difficulties For Engineering Systems

The direct application of stress-strength interference theory has been thwarted by problems in system reliability modeling, analytic and numerical intractability in finding the distribution of functions of random variables, and a serious lack of hard data. These are all discussed in turn below.

System Reliability Modeling. Even if data were abundant and mathematical methods available, it is still difficult to determine how individual component failures can combine to create a system failure. An example from the aircraft survivability problem is the melting or rupturing of non-structural skin panels. It simply is not true that the loss of a single skin panel will mean the loss of the aircraft. It is true that as panels are lost, the drag coefficient increases, and that at some point, as more and more panels are lost, the drag coefficient is such that the mission cannot be completed--i.e, the system has failed. The difficulty in constructing a model of system reliability or survivability as a function of component survivability is apparent. System reliability modeling is discussed in most reliability engineering textbooks [8].

An approach used in reactor safety studies is that of fault tree analysis [29]. Basically, a list is created of every event that is to be the subject of analysis. These events are termed top events. A functional diagram of the system is then studied so as to identify contributing events that may directly cause the top event to occur. These contributing events typically cause the top event to occur through AND/OR Boolean operations. For example [29], a circuit breaker may fail to trip because it fails randomly by itself, OR a trip signal is not received. The contributing events can also be further analyzed. To continue

the example, perhaps the trip signal is not received because relay 1 AND relay 2 remained closed. Fault tree construction can become a substantial task for a large engineering system.

At this point, it should be noted that whatever number is obtained by a probabilistic assessment of survivability, it will not represent an absolute measure of the frequency of system failure. Since no system reliability diagram can be perfect, a probabilistic estimate of survivability is a conditional probability measure. At the very minimum, it is conditional due to the system reliability model. Since it is not possible to know all the failure mechanisms of a system, the resulting survivability number is an upper bound to the system survivability. Thus, for military applications, targeters have more to gain by this type of analysis than do defenders.

Mathematical Methods. Another difficulty in the direct application of reliability theory is the analytic and numerical intractability of the mathematics of statistics. The most common problem, and one already hinted at, is that of finding the distribution of a function of one or more random variables. Very few problems have exact analytic or closed-form solutions. Methods that have been used by survivability analysts include propagation of moments with a priori distributional assumptions, Monte Carlo simulation, and variable transformation techniques.

Propagation of moments methods have been used by DNA in some of the studies of missile basing [55]. Basically, given an equation of the form:

$$Z=g(X_1,X_2, \ . \ . \ .X_n) \tag{3.16}$$

moment information about the X_i is collected (usually the mean and variance). The mean and variance of Z are then calculated by means of Taylor Series expansions about some point [8,12]. This requires the determination and evaluation of partial derivatives. Once the mean and variance of Z have been estimated, a lognormal distribution function for Z is usually assumed [71]. Correlations among the X_i must be accounted for. Along these same lines, a new technique based on a linear algebra has been developed by Ditlevsen [23]. This approach assumes that only moment information is available for all inputs, and thus only moment information can be used for all outputs. Ditlevsen's linear algebra approach seeks to accomplish the same goals as a probability theory, yet can be presented without a reference to probability theory.

There are several disadvantages to using propagation of moments. One is that not all combinations of random variables yield distributions that have moments. The Cauchy, for example, cannot be estimated efficiently by such methods [23,13]. Another disadvantage is the common use of a priori distributional assumptions. However, perhaps the worst disadvantage is the tediousness of calculating many

partial derivatives. For example, in Appendix B of Reference [12], one can find an expression for the expected value of a fourth moment. This single expression occupies 48 lines of typewritten text! Needless to say, tasks of this magnitude are prone to errors. Most of these objections can be overcome by using Monte Carlo simulation.

Direct Monte Carlo simulation is described by Stancampiano [32]. This is basically a brute force counting operation. One samples randomly the distribution of margin or safety factor. This is done by randomly drawing from the strength and stress distributions, which may be functions of multiple random variables, and counting the relative number of times the margin variable is less than 0, or the safety factor less than 1. If the part has a very high reliability, this counting operation can become expensive.

Monte Carlo with fitting seeks to overcome the expense of brute force Monte Carlo counting. In this case, one fits the simulated data to a distribution function, perhaps a normal, or some other type. Stancampiano shows [32] that some problems can be sensitive to the choice of distribution function chosen. An elegant technique is to calculate high order moments of the data and use the Shannon maximum entropy method to find the minimally prejudiced probability distribution [13]. This is not always straight-forward, since the solution for the minimally prejudiced PDF involves

solving a non-linear programming problem. Also, there is no a priori guarantee that the distribution of the output variable has moments.

Other Monte Carlo techniques exist, though they will not be useful for the nuclear survivability problem. Importance sampling [32] can be used if one knows that the location parameter for the stress distribution is relatively fixed. In that case, one can improve the Monte Carlo efficiency by concentrating the sampling in the area of interference between the strength and stress density functions. This will not be useful for the problem at hand since the applied stress from a nuclear weapon cannot, in general, be confined to a limited range of values.

Other methods include the use of specialized mathematics, such as Cook's work with H Functions [4]. These methods are still cumbersome and unattractive at present for engineering applications.

Sparse Data Sets. Finally, the lack of data for the required inputs to a probabilistic assessment limits the usefulness of the reliability theory approach. The most serious limitation of the lack of data is in the ability to identify parametrically the input distributions. With a small sample, it is possible that a number of density functions would slip through even the best of goodness of fit tests. Ashley [3] has shown how the use of a weak test, such as the Chi-square which is popular among engineers, can

lead to erroneous conclusions about the underlying distribution, and unwarranted confidence statements about survivability. Without a good idea of the underlying density function for the inputs, it is hard to know just how to estimate the parameters--indeed, one may not even know how many there are.

The dearth of hard data has led many to consider Bayesian estimation techniques. The use of Bayesian statistics in reliability theory is discussed by Kapur and Lamberson [8]. Bayesian statistics combines subjective judgment or experience with hard data to provide statistical information similar to the classical statistical inference approach. The method is controversial since "no experimental or analytical methods exist for the quantification of . . .belief" [8]. Nevertheless, Bayesian methods have been widely used in doing probabilistic risk assessments. The reasons for this are best represented by direct quotes from the literature:

Ang writes in 1975, "When the observed data are limited, as is often the case in engineering, the statistical estimates have to be supplemented (or even superseded) by judgmental information. With the classical statistical approach, there is no provision for combining judgmental information with observational data in the estimation of parameters." [1]

McCormick, in a 1981 book on risk analysis [29], writes "The interpretation of" (the law of large numbers) "is clear enough for experiments that can be repeated. There are many occasions in which the knowledge available is less precise, especially when the engineer deals with rarely occurring events that form the basis of many risk evaluations. Then it is necessary to resort to the axiomatic or subjective approach to the concept of probability, which we shall use from now on."

Subjective probabilistic assessment is also mentioned by Bevensee [41]. The lack of hard data for EMP survivability assessment is apparently so serious, that in a 1981 follow-up study to that of Reference [41], fully 29 pages of a draft Lawrence Livermore National Laboratory (LLNL) report are devoted to methods of polling expert opinion [39]. Personal conversations with experts in the study of ground systems survivability confirm that opinion surveys are a common source of information [48].

This lack of hard data, combined with the controversy surrounding the use of Bayesian statistics, leads to a perplexing dilemma. Faced with the difficulties in rigorously pursuing an approach along classical statistical lines, one may wish to retain the traditional approach of engineering determinism. On the other hand, engineering determinism cannot deal with uncertainty other than by worst case analysis or by parametric surveys. From a probability

theory point of view, one has not avoided subjectivity by retaining engineering determinism. One has simply chosen the Dirac delta function as the underlying PDF for all variables of interest. The present probabilistic alternatives to that are to choose continuous distributions, and somehow to estimate the parameters for those distributions.

Summary

To summarize the Chapter then, three of the more serious difficulties in applying stress-strength interference theory to engineering systems have been noted. These include: (a) the problem of system survivability modeling based on component survivability, (b) the difficulty inherent in the mathematical methods for propagating statistical information, and (c) the sparseness of the databases for engineering inputs.

In Chapter IV (with related appendices), a new approach for dealing with problems (b) and (c) above will be presented. It will be shown that newly developed methods in nonparametric estimation provide a tool for finding the distribution of a function of multiple random variables. It will also be argued that nonparametric estimation provides a logical method for propagating uncertainty in an engineering model.

IV. Nonparametric Estimation-A New Interference Theory Tool

Overview

In this Chapter, an effort will be made to deal with some of the problems mentioned in Chapter III. However, the problem of system survivability modeling from knowledge of component survivability will not be dealt with. In the chapters that follow, an aircraft system will be treated as a simple series reliable assembly. However, much more can be done in overcoming the problems involved with mathematical methods, and with sparse data bases. These are presented at this time.

Distribution of a Function of Multiple Random Variables

Some recent developments [14] in nonparametric estimation techniques provide a new and powerful statistical tool for use in survivability calculations. This tool can be used as an empirical one, for use on observed sets of data. It can also be used as a numerical method in its own right. Although most of the details are discussed in Appendixes A and C, a basic outline of the approach is discussed below, and an example from the reactor risk analysis literature is presented.

As noted earlier, one of the tasks that must be done in order to make stress-strength interference theory work is that of finding the distribution of a function of one or

more random variables. With the nonparametric estimation technique, the following can be demonstrated:

(a) Given the random variable equation $Z=g(X)$, with $g(x)$ monotonic, and the distribution function of X (whether parametric or non-parametric), the distribution function of Z can be exactly determined at selected points.

(b) Given the random variable equation $Z=g(X,Y)$, the distribution functions of X and Y, and the restriction that $\partial g/\partial x \neq 0 \ \forall x$, $\partial g/\partial y \neq 0 \ \forall y$, then the distribution function of Z can be determined at a selected number of points by using the equation of conditional probability as a sampling rule. The accuracy in the distribution function of Z is limited only by standard problems of numerical integration.

(c) Given the random variable equation

$$Z=g(X_1,X_2, \ldots X_n) \tag{4.1}$$

the distribution functions of the X_i, and the restriction that $\partial g/\partial x_i \neq 0 \ \forall \ x_i$, then the distribution function of Z can be determined at a selected number of points, provided the X_i are independent or have known correlations. The accuracy in the resulting distribution function of Z is limited only by standard problems of numerical integration.

This technique is best illustrated by working an example from the actual survivability literature. The density function for the safety factor of a reactor pressure vessel will be calculated by the above method, and compared to a standard Monte Carlo calculation [32].

A Benchmark Problem-Safety Factor of a Reactor Pressure Vessel

A very long ductile steel cylinder is subjected to an applied internal pressure P. The applied pressure P is found to be a random variable with a three-parameter Weibull distribution. That is:

$$F_P(p)=1-\exp[-((p-c)/a)^b] \quad \forall \; p>c \tag{4.2}$$

$$F_P(p)=0 \quad \forall \; p\leq c \tag{4.3}$$

where p is a particular pressure value in KPa (kilopascals), a is the Weibull scale parameter in KPa, b the dimensionless Weibull shape parameter, and c the Weibull location parameter in KPa. Stancampiano gives the values as:

$$a=.10665P_0 \tag{4.4}$$

$$b=4.212 \tag{4.5}$$

$$c=.9P_0 \tag{4.6}$$

$$P_0=4316 \text{ KPa } (626 \text{ psi}) \tag{4.7}$$

The random variable P is the stress variable, and it has the parametric representation just noted. However, one may represent P nonparametrically rather than parametrically. This is done by solving Equation 4.2 for the m values of p_i that satisfy the equation:

$$p_i=F_P^{-1}(G_i) \tag{4.8}$$

where the G_i are given by:

$$G_i=(i+\alpha)/(m+\beta); \; i=1,m \tag{4.9}$$

and α and β are constants satisfying:

$$-1\leq\alpha\leq\beta\leq 1 \tag{4.10}$$

The m values of p found by solving Equation 4.8 are ordered from smallest to largest and denoted by the set of values:

$\{p_i\}; i=1,m$

As discussed in Appendix C, if, for every i from 1 to m, the G_i of Equation 4.9 are plotted versus the ordered p_i in the set just described, then the result in general is an approximation to the distribution function $F_p(p)$. However, for this case, the result is exact at the data points p_i. This is because the data (the p_i) were drawn by the rule of Equation 4.8. Such a set of points will be defined as a **stylized set** (Reference Appendix C).

The distribution of P derived from a set of 50 stylized points is shown in Figure 4.1. The plotting rule used was Hazen's Rule where α and β are given by -.5 and 0 respectively. The distribution function of Figure 4.1 is exact at the percentiles .01(.02).99 and in-between values are simply linearly interpolated from these. As discussed in Appendix A, the end-point values are found by requiring the integral of the PDF to be unity.

At this point, it might appear that this representation of the distribution of P is needlessly complicated, since (a) the distribution of P is already known parametrically, and (b) the parametric form was used anyway to provide the data to the nonparametric technique.

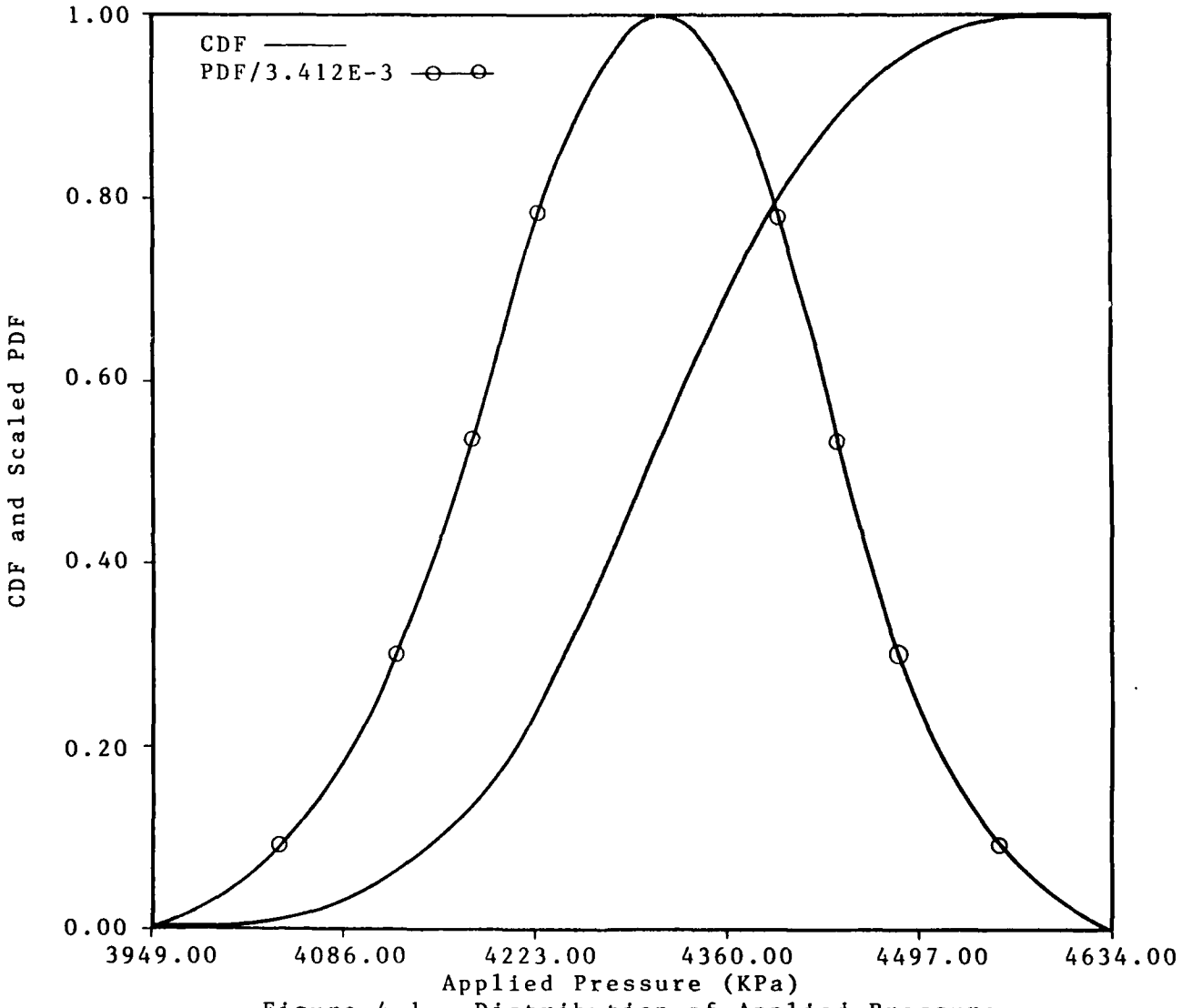

Figure 4.1. Distribution of Applied Pressure

IV.5

The answer to the first objection is that, although it seems complicated now, the application of this method will make more difficult problems much simpler later on. To find a distribution function parametrically, one must first know the density function or distribution function, and then all the parameters that go into it. If these were always known for every conceivable combination of random variables, then density function identification would be greatly simplified. As it is, some of the simplist combinations of random variables (Reference Appendix C) have complicated density and distribution functions.

As to the second objection, the fact that the nonparametric technique is using data drawn from a parametric model is just a property of the example. Stancampiano [32] does not say how the distribution of P was found to be three-parameter Weibull. If one simply believes him, then the parametric input is accepted. If one does not believe him, then one obtains the data for himself, and estimates the distribution of P independently, using another parametric model, or perhaps a nonparametric one. In any case, every input variable will have its distribution function specified somehow. No matter how it is done, the nonparametric representation can be used.

To continue the calculation of the survivability of the pressure vessel, one now needs to find the distribution of the strength, having determined the distribution of the

applied stress. At this point, a subtle departure from the norm of classical reliability theory occurs--a departure shared by most problems in nuclear survivability. Classically, the strength distribution would be found by taking a large number of cylinders, and testing them all to failure. The strength distribution would then be determined by the standard methods of statistical inference. However, in this case, as in most cases involving nuclear survivability, the items in question are far too few in number, and too expensive per copy, to test to destruction. Instead, one models the response of the part. For the cylinder example, the point at which the vessel is believed to burst is given by the equation:

$$P_b = A\sigma'_u F_{cyl} \ln W \tag{4.11}$$

where A is a dimensionless modeling coefficient, σ'_u is the engineering ultimate tensile strength in KPa, F_{cyl} is a dimensionless function of strain and elongation given by:

$$F_{cyl} = .25/(\epsilon_u + .227)(e/\epsilon_u)^{\epsilon_u} \tag{4.12}$$

ϵ_u is the true strain at maximum tensile test, and is given as a function of the uniform elongation , ϵ'_u by:

$$\epsilon_u = \ln(1+\epsilon'_u) \tag{4.13}$$

$$W = D/d \tag{4.14}$$

$$d = D - 2t \tag{4.15}$$

t being the wall thickness of the cylinder, D the outer diameter, and d the inner diameter.

The distribution of the strength variable, that is, the distribution of P_b, is determined by finding the distribution of the individual input variables, and then finding the distribution of the function of the inputs. The input distributions are given by:

A is normally distributed with mean 1.0478 and standard deviation .0948. σ_u' is normal with a mean of 433,000 KPa and standard deviation of 21,200 KPa, ϵ_u' is normal with a mean of .4485 and standard deviation of .0377. The correlation between the tensile strength and elongation is an additional complication. The correlation coefficient was found to be -.498. The outer diameter D was taken as uniformly distributed between 60.639 cm and 61.281 cm. The wall thickness t was taken as uniformly distributed between 1.237 cm and 1.532 cm [32]. The nonparametric representations of the input variables are shown in Figures 4.2 through 4.6.

The strength distribution can now be found by a sequence of binary operations. Some variable changes simplify the equation for the burst pressure, P_b. The geometrical factors can be represented by:

$$X_1 = \ln W = \ln(D/(D-2t)) \tag{4.16}$$

The distribution of X_1, found by the method described earlier, is shown in Figure 4.7. With the distribution of X_1 determined, the dimension of the random variable equation is reduced, and the burst pressure can be written as:

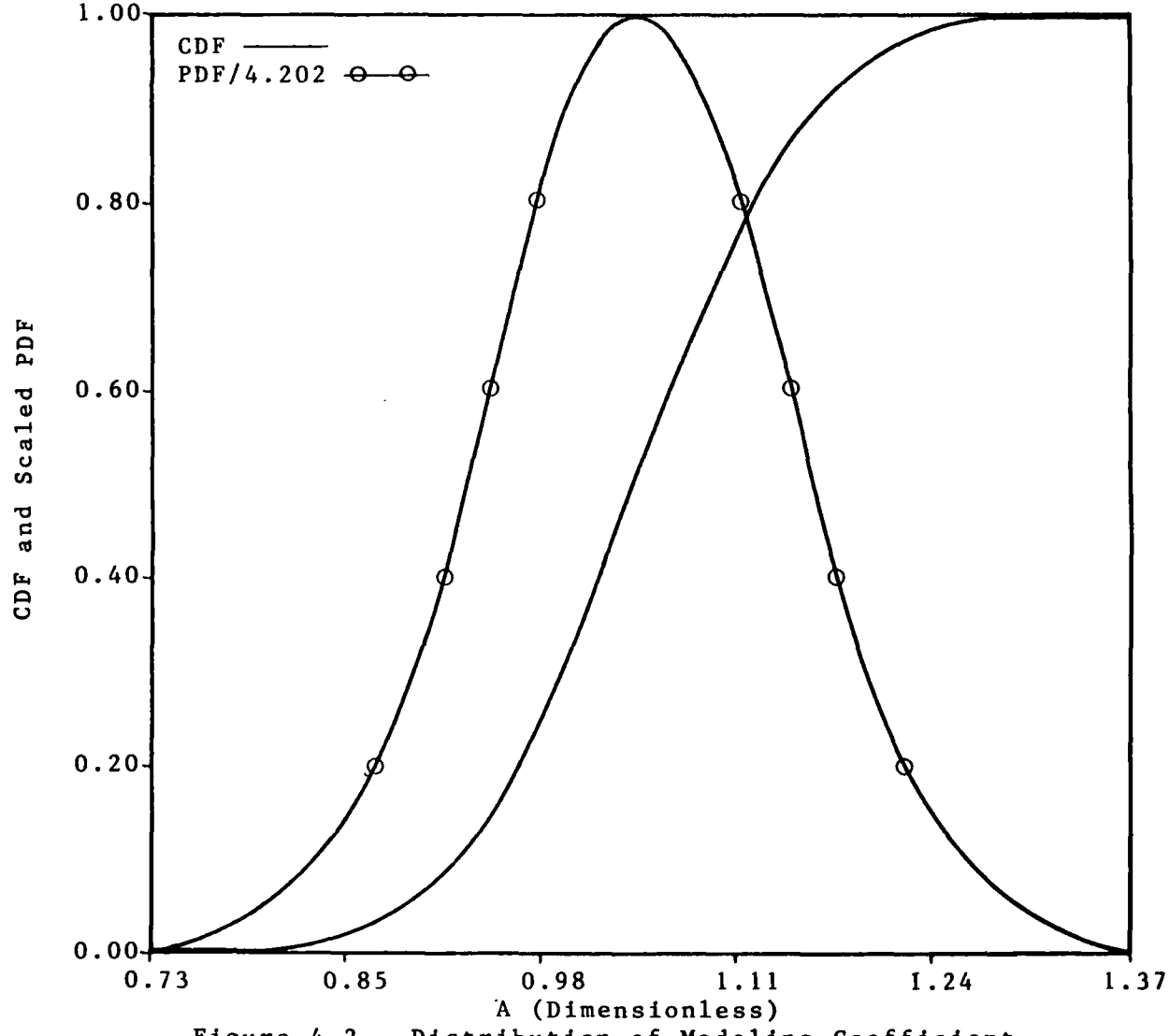

Figure 4.2. Distribution of Modeling Coefficient

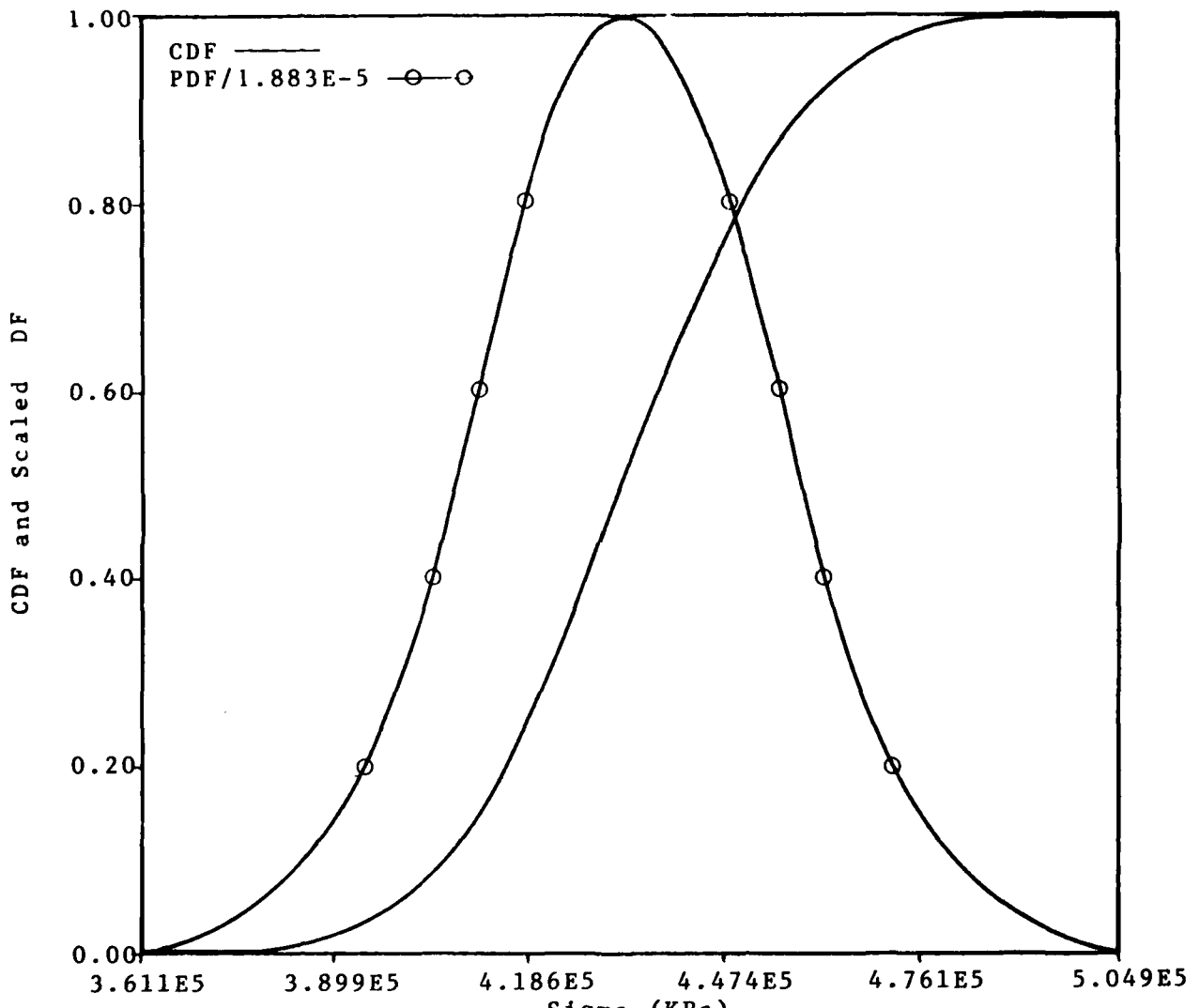

Figure 4.3. Distribution of Tensile Strength

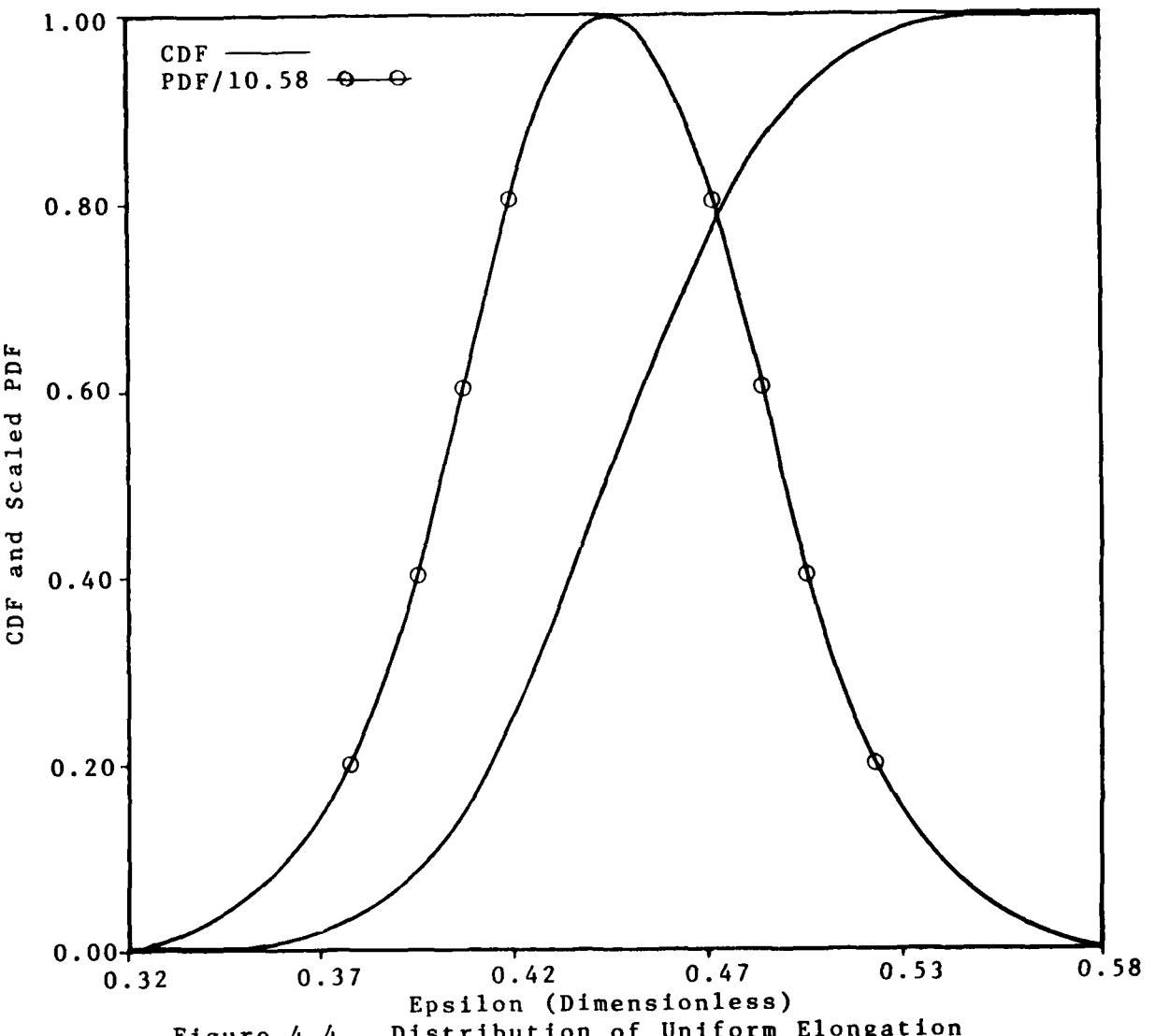

Figure 4.4. Distribution of Uniform Elongation

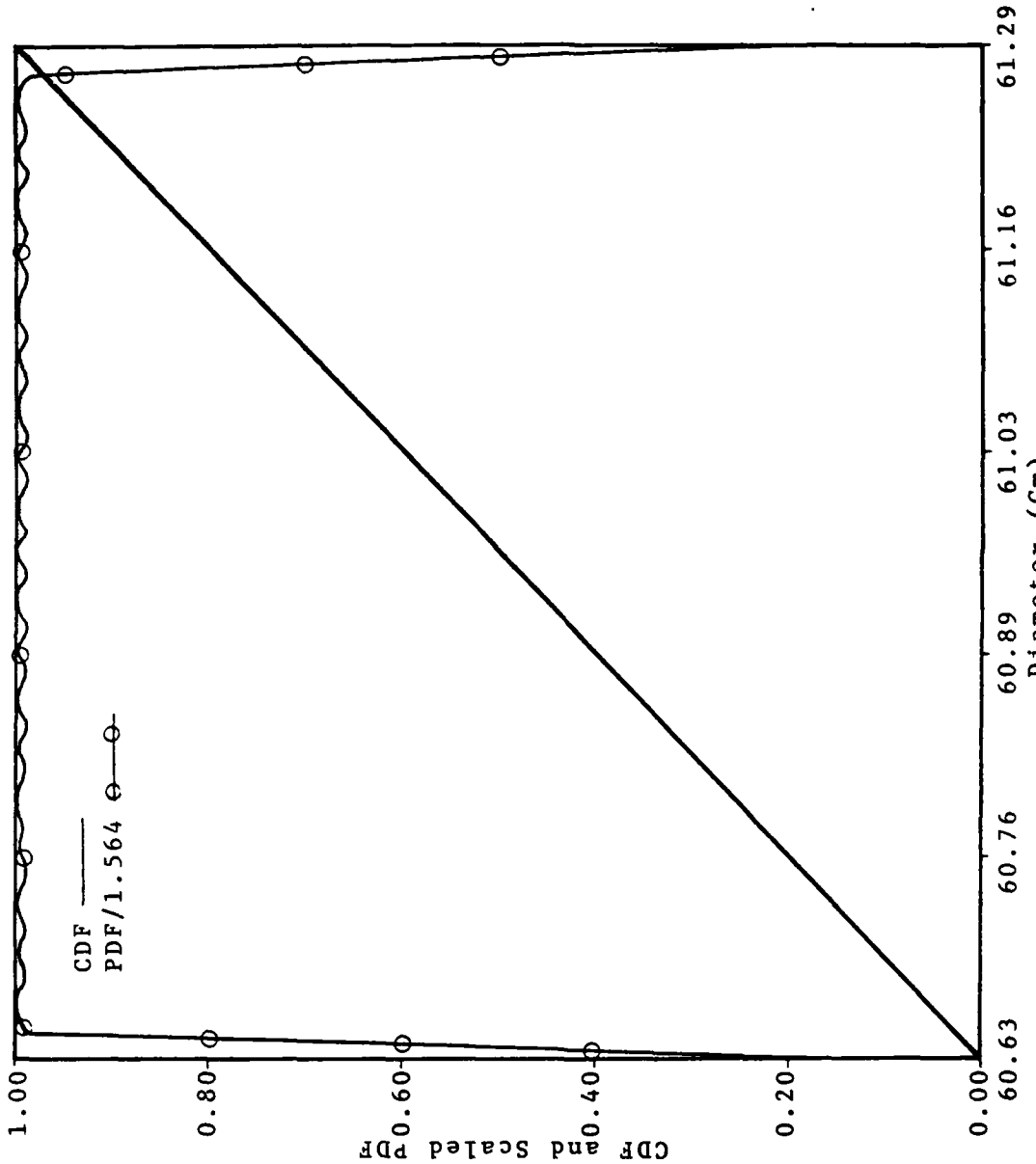

Figure 4.5. Distribution of Outer Diameter

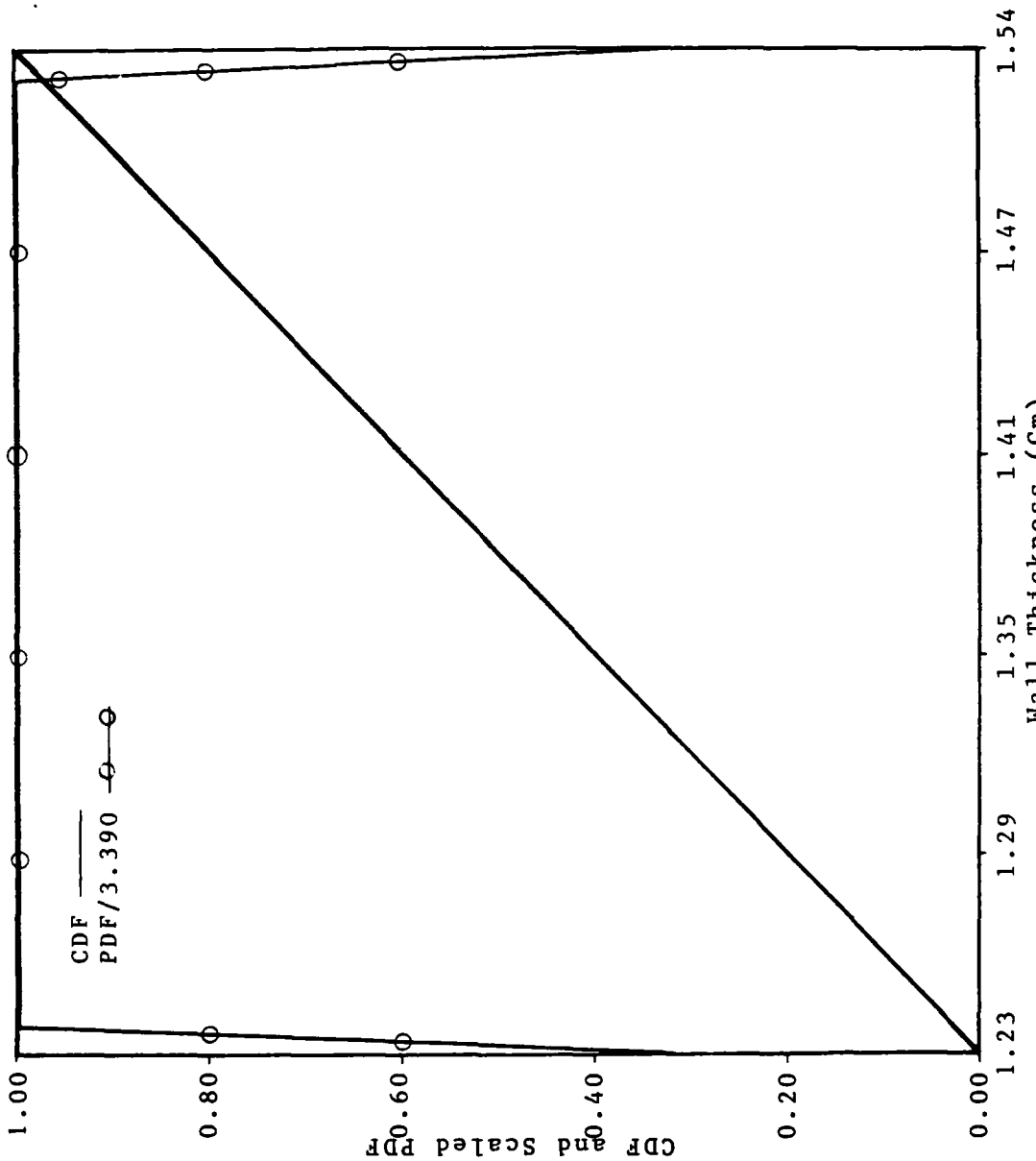

Figure 4.6. Distribution of Wall Thickness

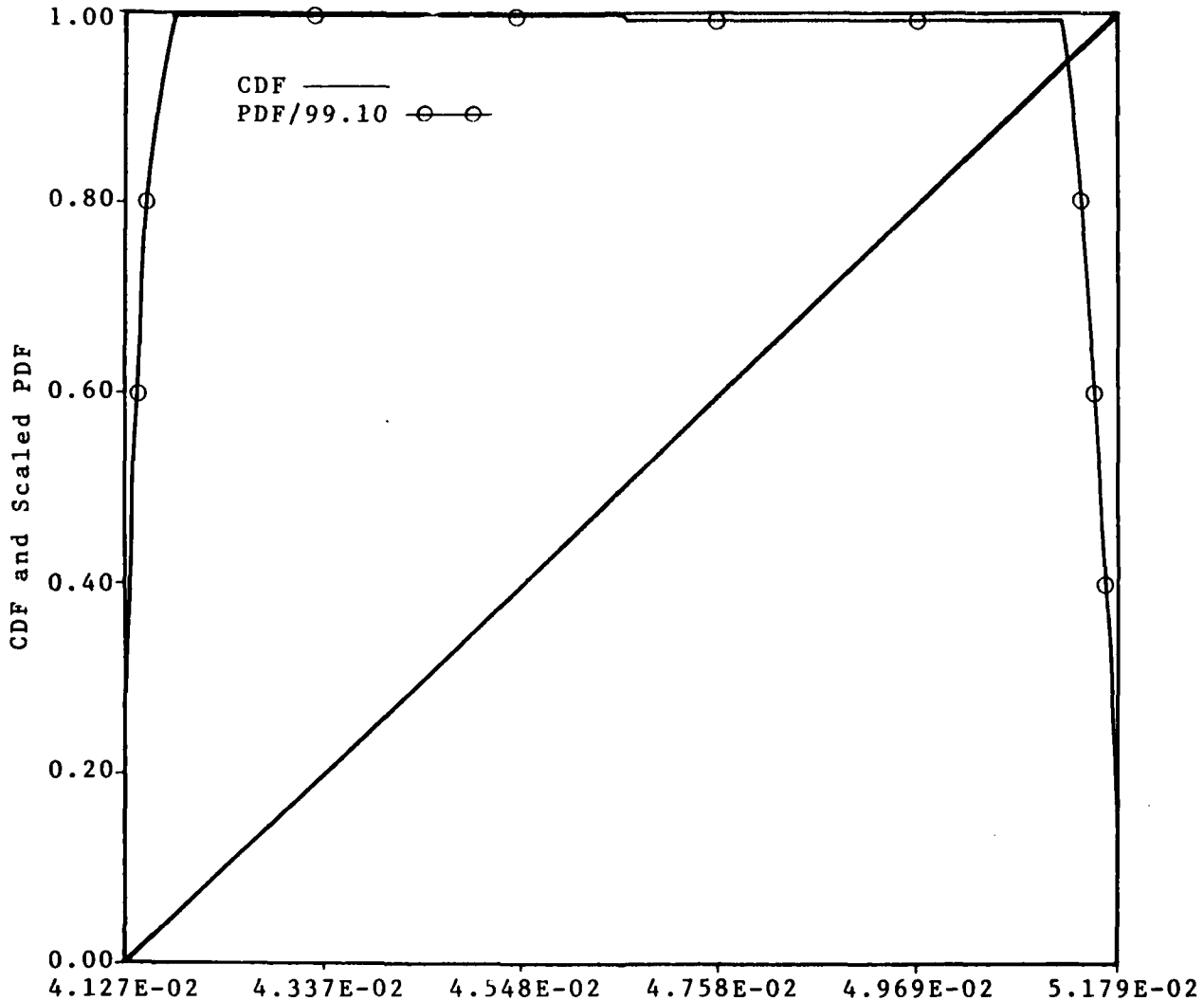

Figure 4.7. Distribution of Ln(D/(D-2T))

$$P_b = A\sigma'_u F_{cyl} X_1 \tag{4.17}$$

To handle the correlated variables, the variable X_2 is defined by:

$$X_2 = \sigma'_u F_{cyl} \tag{4.18}$$

The distribution of X_2 is shown in Figure 4.8. At this point, the random variable equation for the burst pressure has been reduced to an independent set of variables:

$$P_b = AX_2 X_1 \tag{4.19}$$

One can now proceed with a sequence of binary operations to find the distribution of the burst pressure. Defining the variable X_3 by:

$$X_3 = AX_1 \tag{4.20}$$

the equation for the burst pressure is reduced to:

$$P_b = X_2 X_3 \tag{4.21}$$

The distribution of X_3 is illustrated in Figure 4.9.

At this point, there are at least three ways to proceed. One could find the distribution of P_b from Equation 4.21 above, and then directly integrate to find the failure probability. The integration technique is discussed in Appendix D. It is analagous to the graphical estimation technique [8], or the Mellin transform technique [9]. Alternately, we could evaluate the distribution of the margin variable, ξ, or the safety factor variable η. The latter will be done. In this case, η is given by:

$$\eta = P_b / P = X_2 X_3 / P \tag{4.22}$$

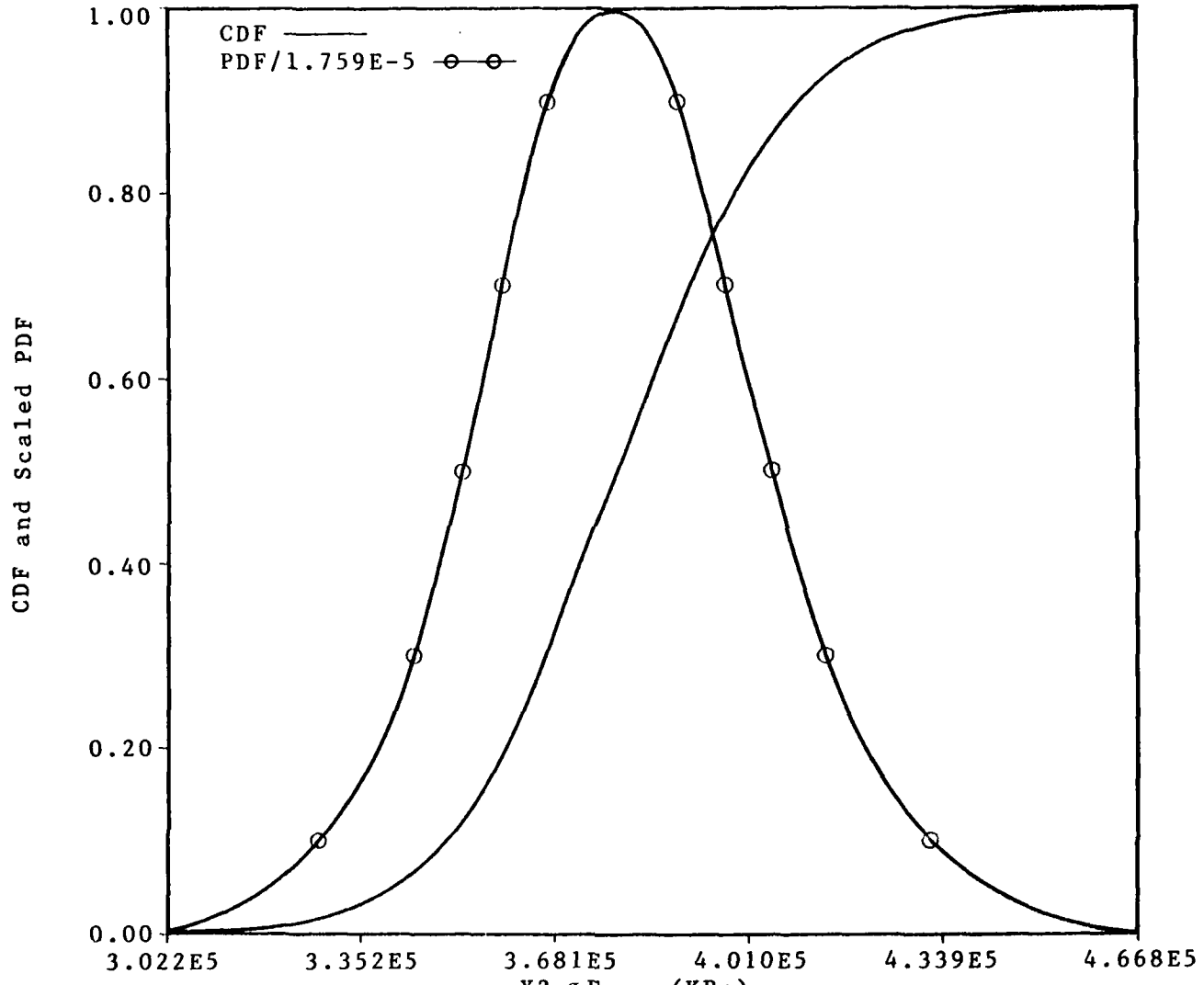

Figure 4.8. Distribution of σF_{cyl}

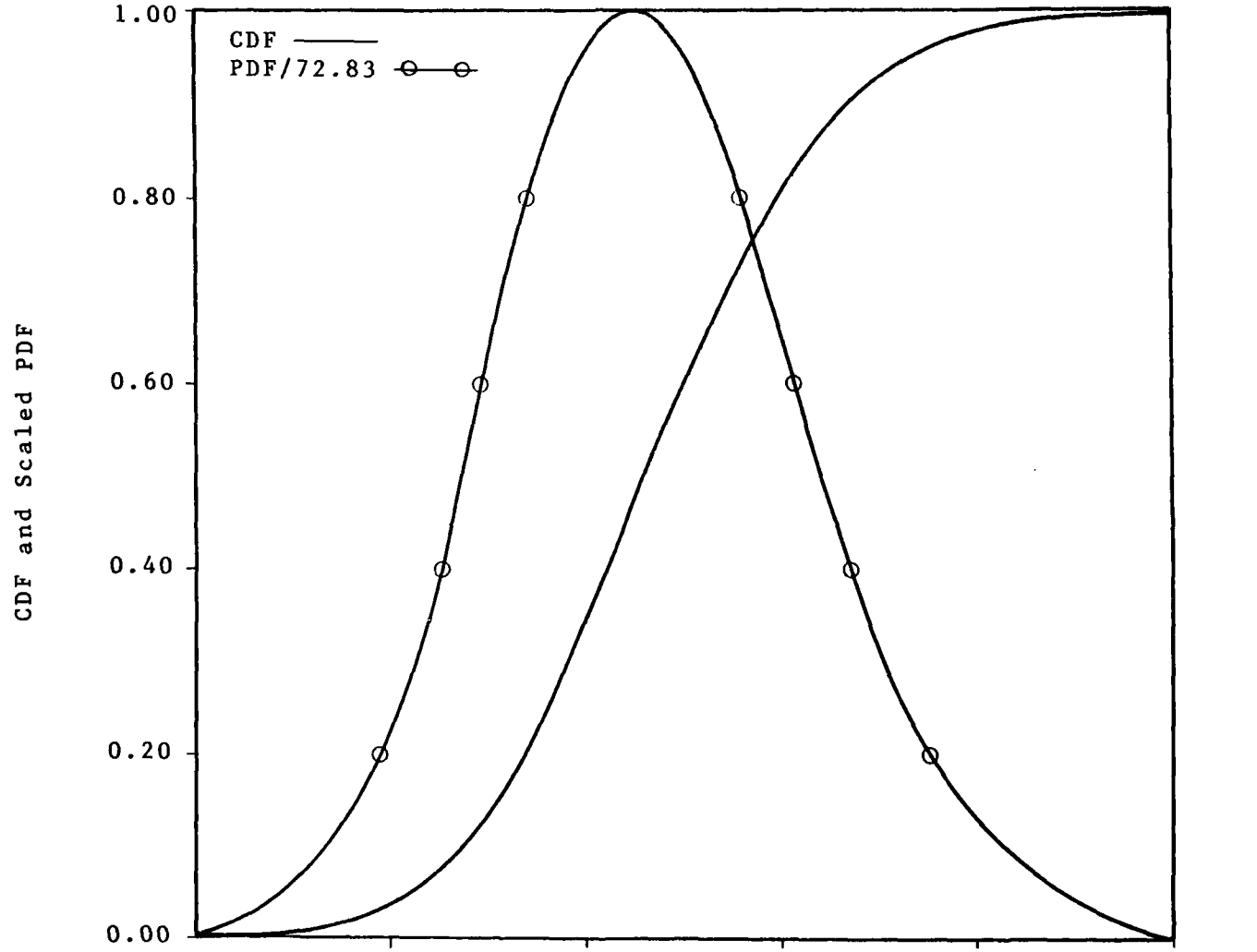

Figure 4.9. Distribution of ALn(D/(D-2T))

Defining X_4 by:

$$X_4 = X_3/P \tag{4.23}$$

the distribution of X_4 is determined and illustrated in Figure 4.10. The final distribution of the safety factor, given by:

$$\eta = X_2 X_4 \tag{4.24}$$

is illustrated in Figure 4.11.

One of Stancampiano's single random samples of the safety factor is displayed in Figure 4.12. It is of size 3500. In Figure 4.13 the results of the nonparametric technique are overlayed with that of the random sample method. As mentioned earlier, the nonparametric results are exact (within integration errors) at the percentiles .01(.02).99. Also, the nonparametric technique is efficient enough to run on a Z-80 microcomputer. The results of Figures 4.1 to 4.11 were done on such a computer. A check was made on the results by doing the problem on a CYBER 750 also. For this check, 100 stylized points were used to represent each distribution. Except for increased tail information, the results were identical to that for 50 stylized points.

Of course, one need not use the nonparametric algorithm in such a rigorous fashion as just described. Instead, one may use random Monte Carlo sampling just as Stancampiano did, and then use the nonparametric method on the simulated data. This was done also, and the results displayed in

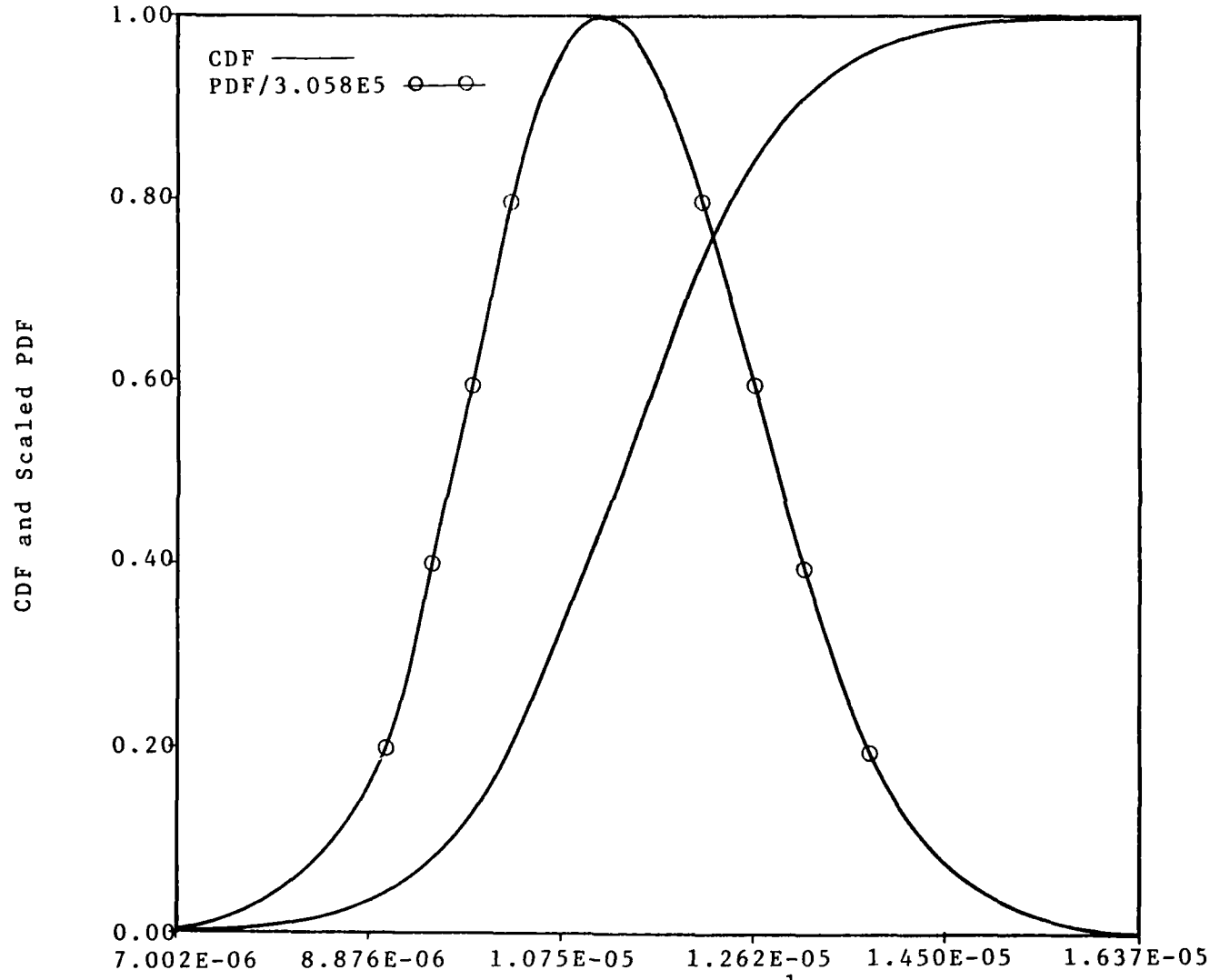

Figure 4.10. Distribution of ALn(D/(D-2T))/P

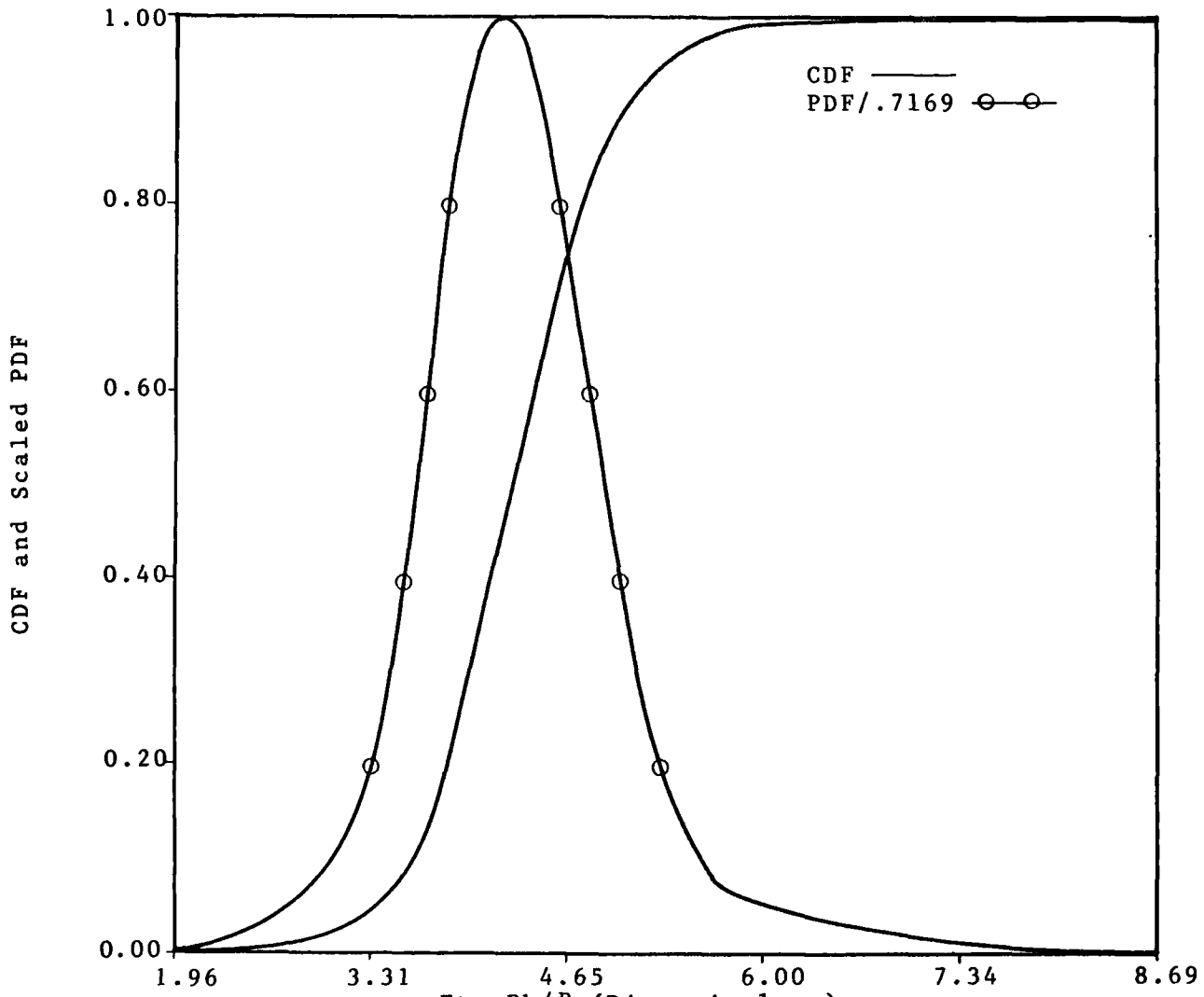

Figure 4.11. Distribution of Safety Factor

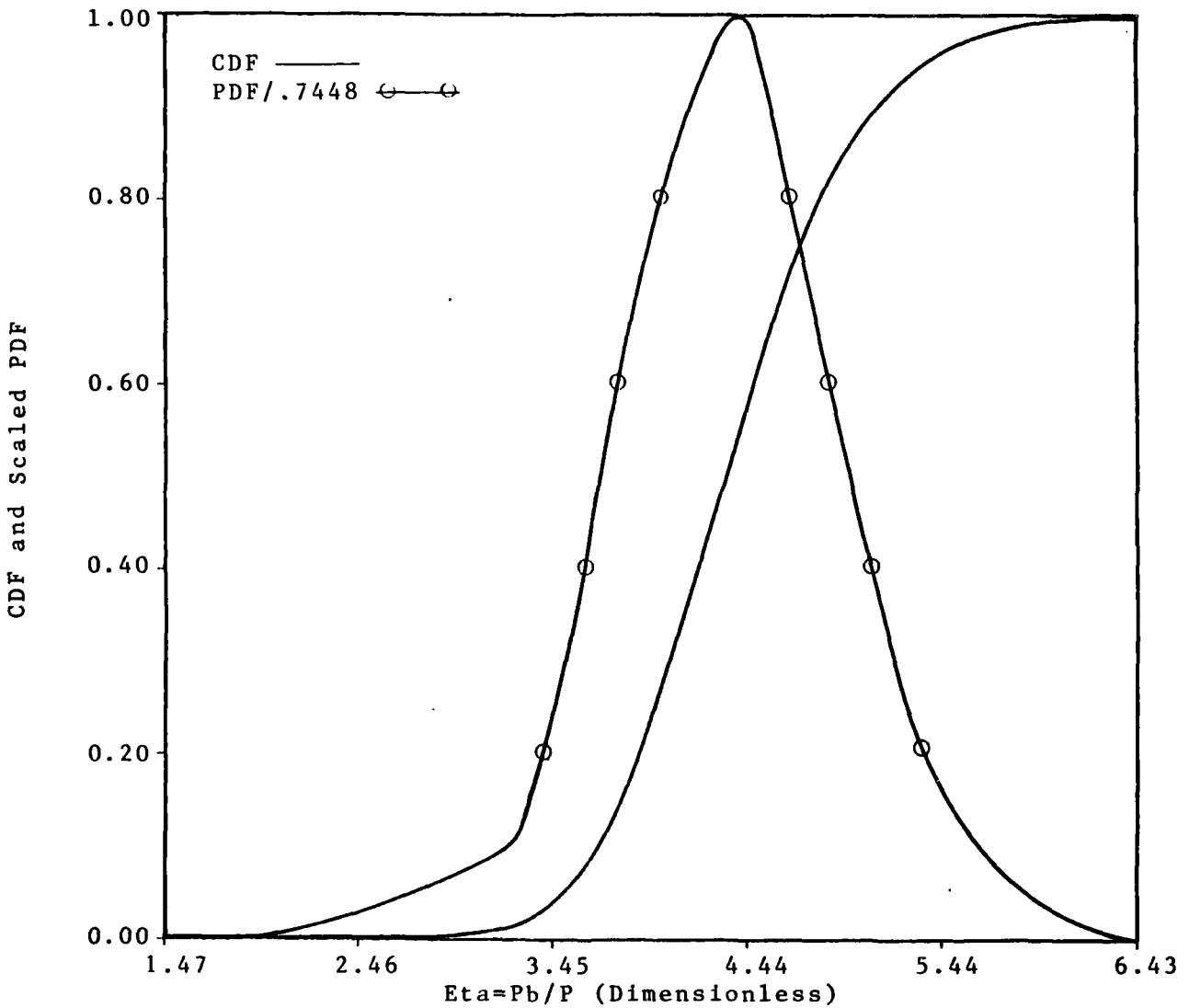

Figure 4.12. A Monte Carlo Sample of the Safety Factor

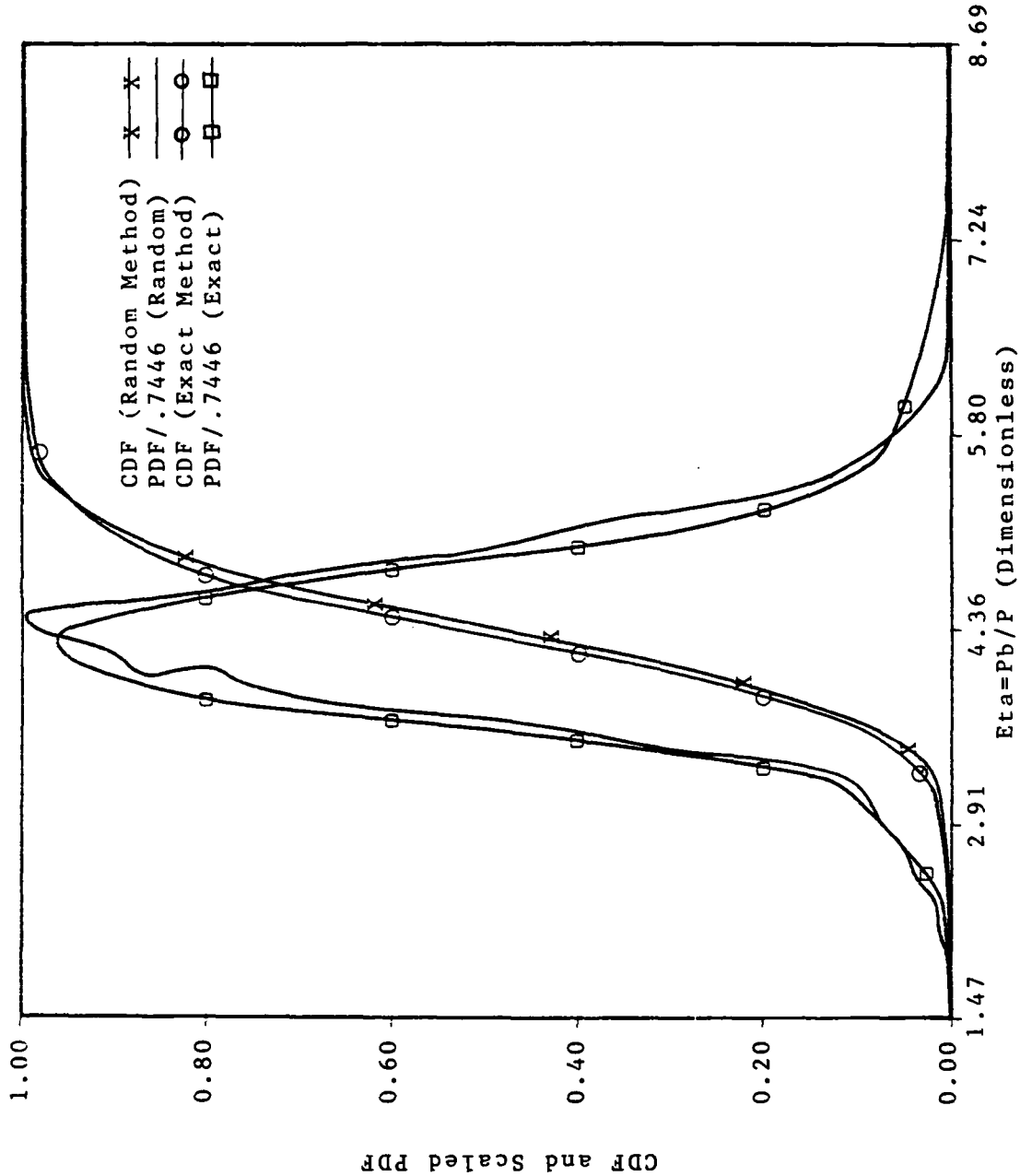

Figure 4.13. Comparison of Exact and Random Methods

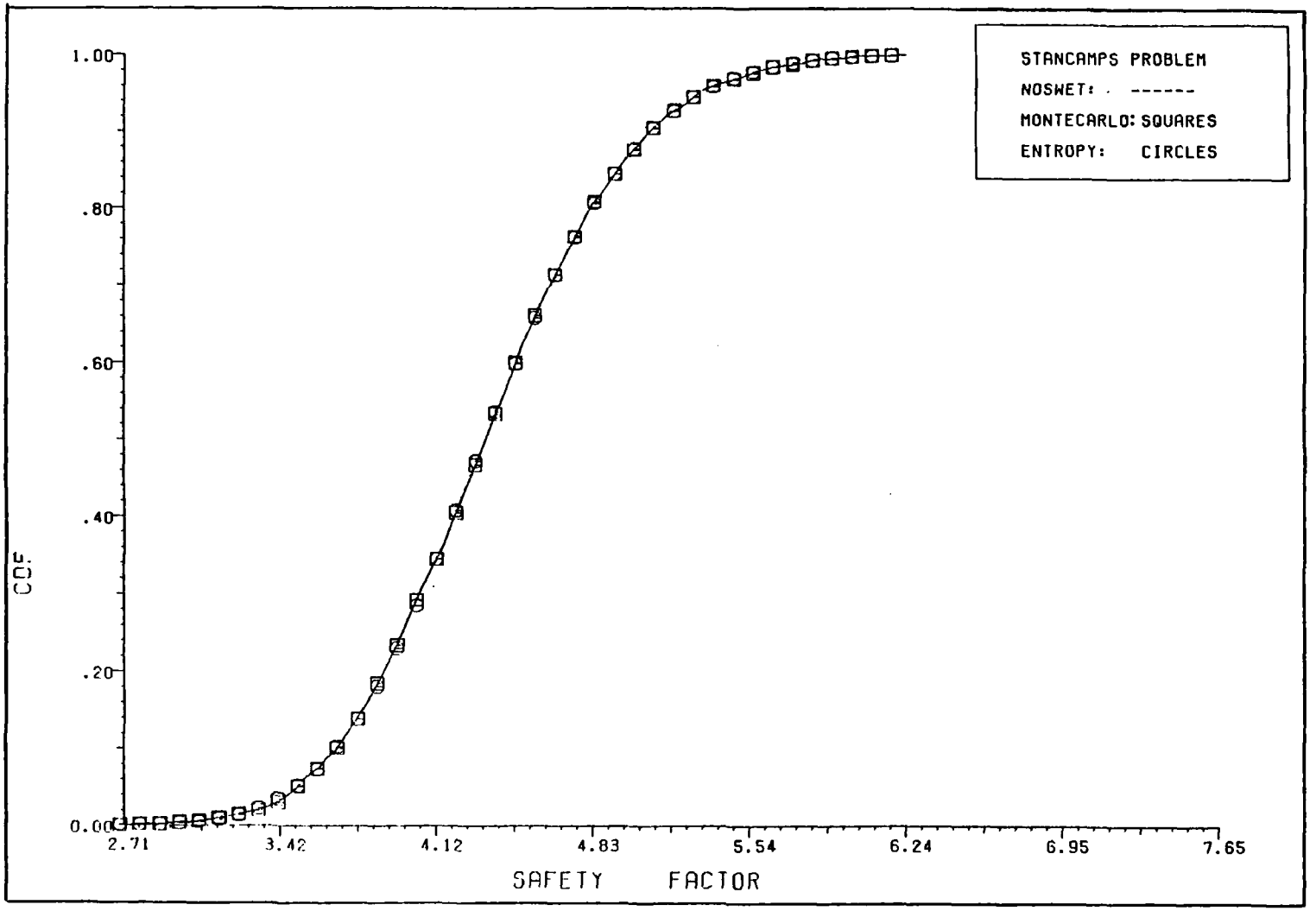

Figure 4.14. Comparison of Nonparametric Method with Maximum Entropy Method

Figure 4.14. The root mean square error by the nonparametric method is a factor of 20 smaller (1.021E-4 versus 2.040E-3) than by using Shannon maximum entropy. Thus, the nonparametric tool can be used as either a rigorous numerical method for finding the distribution of a function of multiple random variables, or as a direct estimator of distribution functions given a data set.

A Comment on Sparse Data Sets

The problem of sparse data sets for the inputs still remains. It is still true, that if one is attempting to measure the failure probability for a highly reliable part, and the data for the inputs is limited, then one is forced to estimate the area in the tail of some distribution. If one is using parametric models, then the relative error can be large for different parametric models. For example, Stancampiano [32] found a failure probability of 7E-10 $\pm$ 5E-10 using normal fitting; 2E-31 $\pm$ 2E-31 using importance sampling, and 2E-16 $\pm$ 4E-16 using Shannon maximum entropy. There is a large relative variation within each method and between the methods, even though the absolute value is close to zero. The nonparametric estimate for the same problem is zero.

Tail estimation is always difficult. Shapiro and Gross [12] point out that great care needs to be exercised when one seeks probability values that are outside the range of

the set of data obtained. The use of an erroneous parametric model can be costly in this case. The advantage of the nonparametric approach taken here is that one cannot infer probabilities far beyond the range of the data. Protection against unreasonable inference is built in.

Further research in applying the nonparametric tool to highly reliable assemblies is in order. However, that is not a problem in aircraft nuclear survivability. As mentioned earlier, this tail issue is not important for this application. One only has a tail problem if one can guarantee that the location parameter for the stress variable is fixed in the stress space. For the aircraft nuclear survivability problem no such guarantee can be given. Besides this, extremely small failure probabilites (sure-safe regions) and extremely large failure probabilites (sure-kill regions) are not the regions where one worries about what happens. It is clear what happens. It is the space between that one wonders about, and any techique that can accurately find the shape of the distributions in this region is a valuable tool. Such is the case for the nonparametric model.

Summary

To summarize, the nonparametric method that will be used to find the survivability of aircraft in nuclear weapon environments has been described. A benchmark problem from the reactor risk analysis literature has been worked, and

the results compared to more standard methods. The nonparametric method has been shown to be numerically efficient, and useful as a stand-alone numerical algorithm or a tool for direct application on existing data sets. Its use on sparse data sets has been mentioned. Its chief advantage here is that it provides protection against unreasonable extrapolation beyond the information contained in the sparse data set.

In the next two Chapters the tool just described and demonstrated will be applied to the problem of aircraft survivability in nuclear weapon environments.

V. Aircraft Vulnerability In Nuclear Blast Environments

Overview

The prescription for a survivability calculation can now be specified succinctly. One needs to first construct a reliability model of the system as a whole. For each component that goes into the model, one then requires a stress and a strength function for the component. For nuclear survivability, the nuclear weapon effect (in this case overpressure) appears in the stress model. If the weapon effect is a random variable, then the applied stress is also. The strength model may be a single number, that is, a sure-kill (SK) specification, or it may be a functional equation as in Chapter IV. For the present Chapter, a single number will suffice provided one can test enough items so that the distribution of such numbers can be determined. This distribution, of course, is the strength distribution. Having obtained both distributions, which may vary in space and time, the failure probability is determined.

Mission Survivability

A systems approach to the problem of nuclear survivability analysis must begin with a description of the intended mission and the threats to that mission. Every mission may be thought of as a series chain of mission

phases. Each phase must be executed in order for the mission to be completed. These ideas have been recognized [45]. An illustration of the base escape problem (from a paper by Bridgman [45]) is shown in Figure 5.1.

During each mission phase, the weapon system may encounter one or more nuclear bursts at particular points in space and time. Thus each phase may be modeled as a chain of burst encounters. Each encounter will cause various nuclear-induced stresses to be placed on the weapon system, and these stresses must be survived. For each nuclear weapon induced stress some subsystems will be vulnerable and some will not. Those subsystems that can fail must be identified. The calculation of the survivability may then proceed as suggested by Bridgman [45]. His flow diagram from Reference [45] is shown in Figure 5.2.

Two of the most difficult parts of the calculation are shown in Figure 5.2 within the dashed lines. Regarding the first box, 'Find Intensity on Target', Bridgman writes "The calculation of free field intensities . . . . is a challenging business involving all manner of calculation on the hydrodynamics of blast waves on the transport of neutrons, gamma rays and x-rays on the propagation of the electromagnetic pulse, etc. All of this has occupied our attention for too long a period. Our focus here is to go beyond the free field calculations and focus on the next block of the diagram--finding the probability of failure . . ." [46].

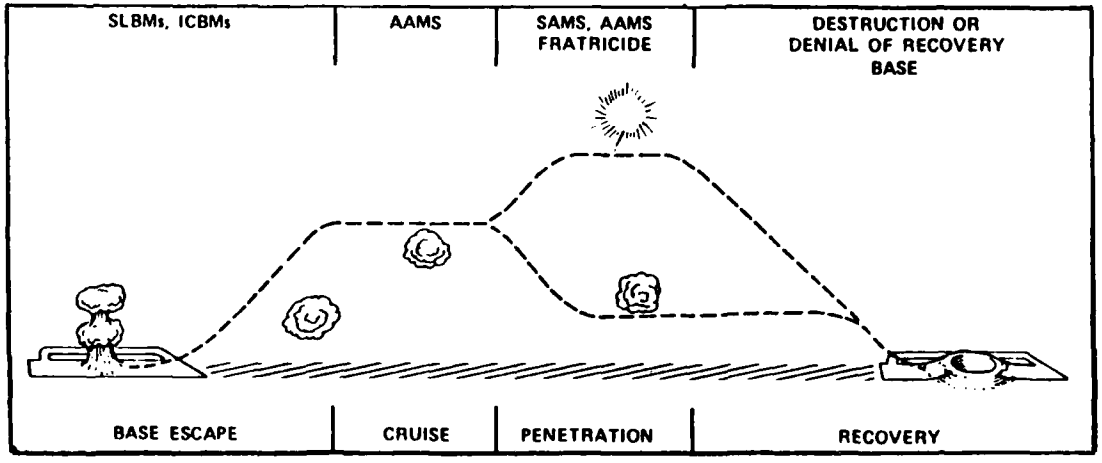

Figure 5.1. Pictorial of Base Escape
(From Reference [45])

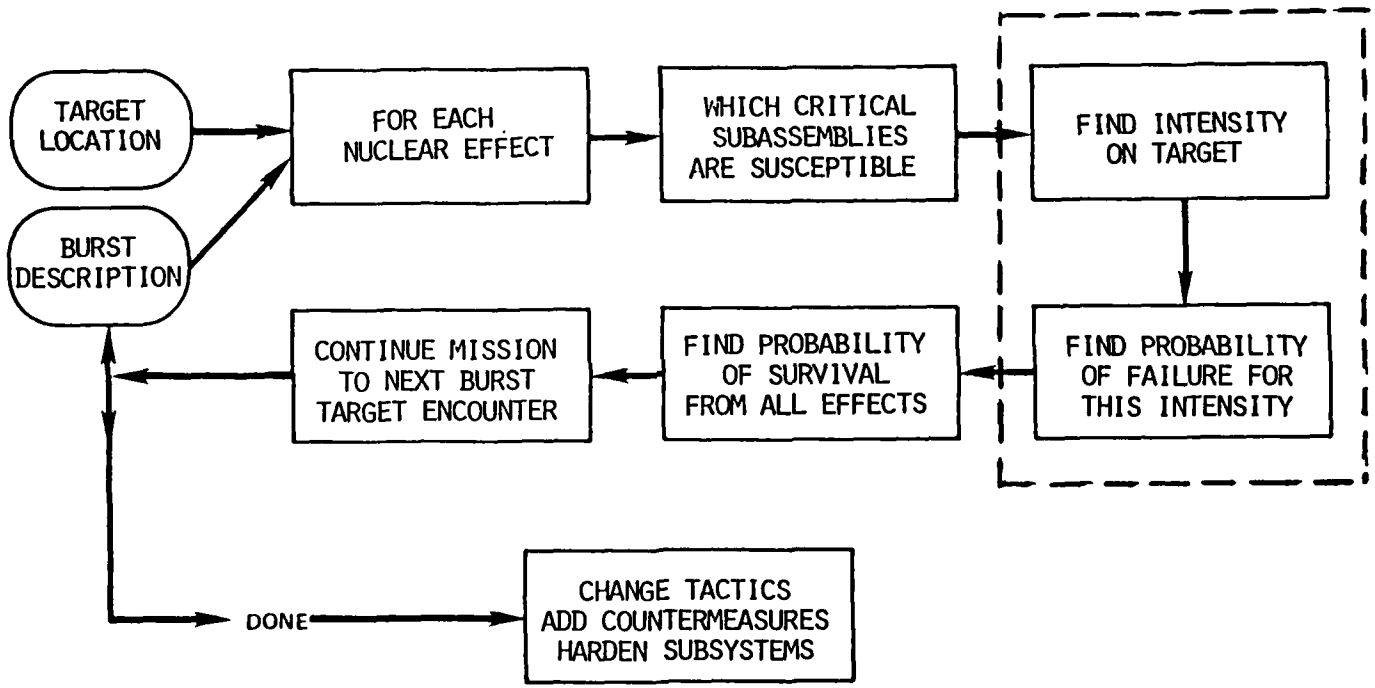

Figure 5.2. A Flow Chart for Calculating Survivability
(From Reference [45])

In all that follows, the focus of this dissertation will be limited to the two elements of the block diagram just mentioned. Actually, one can generalize those two blocks just a bit more by considering the intensity on the target as a random variable also. The scope of work in this Chapter and the next is illustrated in Figure 5.3, which expands on the two blocks of Figure 5.2. Some additional explanation of Figure 5.3 is in order.

In a deterministic model, one would find the intensity of the stress on target and then compare that stress value to the strength of the part. If the intensity exceeds the strength of the part, then the part fails. Otherwise, it does not.

If one uses a probabilistic model, then one finds, not the intensity on the target, but the **statistical distribution of intensities** on the target at the particular range and time of interest. Also, the strength of the item is not now represented by a single number, but by a statistical distribution of numbers. The failure probability, which is clearly a function of range and time and other variables, is now given by the interference integral of Equation 3.3.

The central problem is to determine the distributions of stress and strength at each range and time point of interest. There are three ways to do this, and each is discussed below.

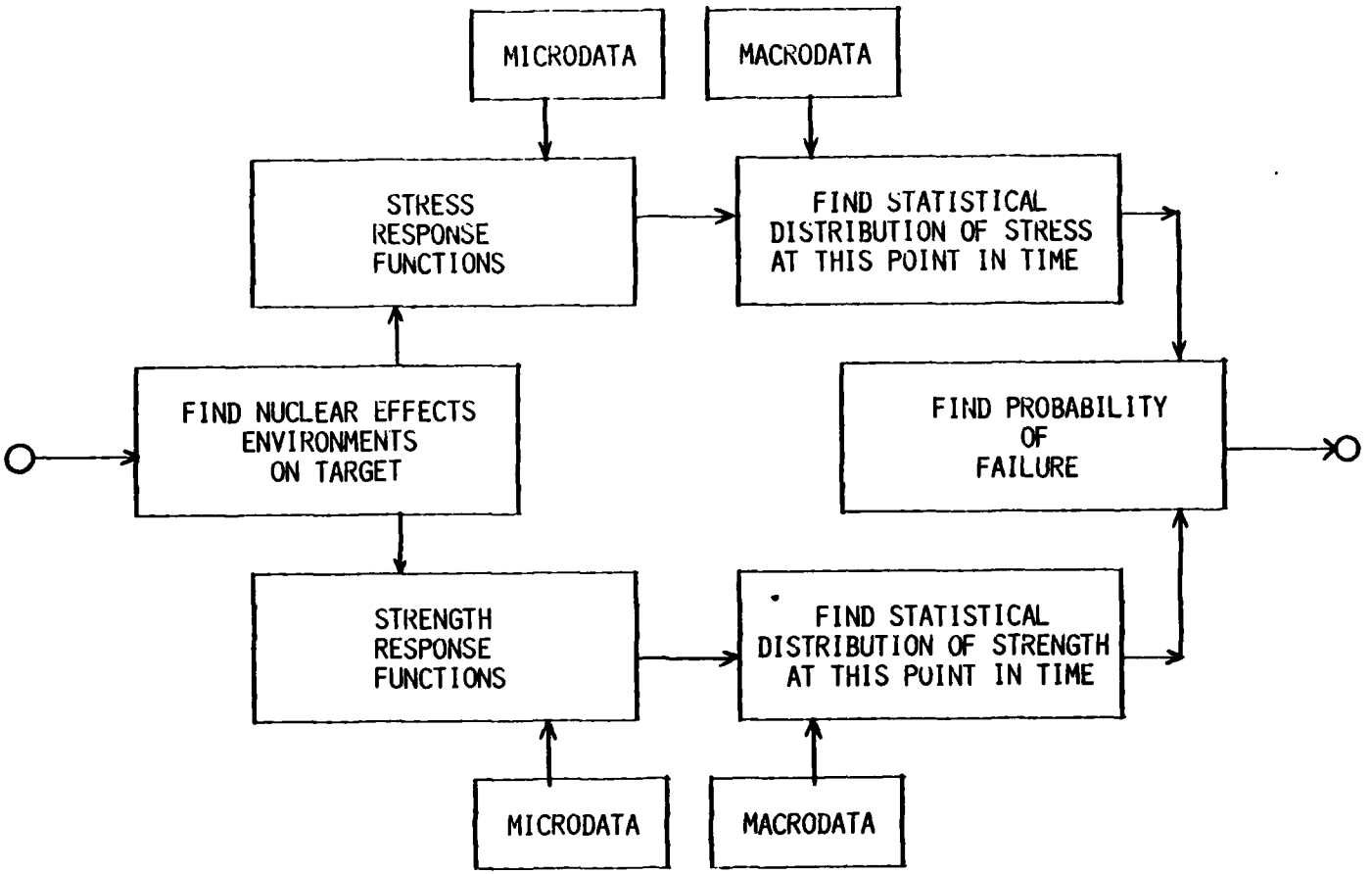

Figure 5.3. Survivability In Terms of Stress/Strength Interference Theory

First, one can simply claim to know the distributions, or rather, one can select them a priori. As has been previously discussed, selection of the Dirac delta function for the stress and strength PDF's leads directly back to the cookie-cutter way of doing business. One might select the Dirac delta function for the stress PDF and a lognormal for the strength PDF. This is precisely what is illustrated in Figure 5.2. The intensity on target is believed known. The part fails randomly. Of course, the disadvantage of this approach is that it may be difficult to defend the choice of distributions used.

A second approach is the straightforward one of measuring the quantities desired. The stress distribution is found by measuring the stress over a number of identical experiments so that the random character of the stress is determined. The strength distribution is determined by testing a number of items to complete failure. This method may be termed a **macrodata** approach, since the information obtained is directly applied to the failure calculation of the system as a whole. The disadvantage is that the testing requirements may be impossible.

Finally, one may infer the quantities desired. A deterministic model of the stress is formulated as in, for example, the bending moment on a wing of an aircraft. This model may depend on other variables whose distributions are known. The statistical distribution of the stress (bending

moment) is then found by propagating the statistical variation of all the input variables into the output variable. The strength distribution is found similarly. A good example of an inferred strength distribution is given by Equation 4.11 which predicts the burst pressure for a reactor pressure vessel [32]. One might call this a microdata approach, since the information collected is not applied directly to the system of interest but must be propagated into a larger model before one can calculate the failure probability. Although this approach is more rigorous and useful than the others considered, it has one potentially serious disadvantage. It depends critically on an accurate model of the processes being considered. Unlike direct testing, one is calculating the probability of failure given the modeling is accurate. Catastrophic events may well occur if the modeling is incomplete or inaccurate.

The central thrust of this Chapter will be to determine the stress and strength distributions for selected aircraft components vulnerable to the effects of overpressure and blast from a nuclear weapon. All of the above approaches will be considered, including mixtures of the approaches.

Stress Distributions in a 1 Kiloton Blast Environment

The overpressure environment from a nuclear burst in a homogeneous atmosphere may be described in three separate regions. These are the free air region, the transition region, and the mach stem region. In the free air region,

no ground effects perturb the blast wave. In the mach stem region, the reflected blast wave has caught up and constructively interfered with the primary wave so that a region of intense overpressure exists near the ground. The transition region is the region between the free air and mach stem regimes, typically in the vicinity above the triple point [45].

The overpressure environment in the free air region is usually described by the Air Force Weapons Laboratory (AFWL) 1 Kiloton (KT) standard [74], or the more recent DNA standard [73]. Research has been conducted to further refine this standard [47,51]. Reference [47] includes the 95% confidence intervals about the nominal pressure versus range curve. This is shown in Figure 5.4, which is a reproduction from that Reference. This information can be analyzed to construct the statistical distribution of overpressure as a function of range from the nuclear burst.

Polynomial fits exist for the nominal pressure versus range curve and are available in the literature [66]. Unfortunately, Reference [47] does not give the polynomial fits to either of the bounding curves that represent the 95% confidence interval. Since this information is lacking, a direct analysis of the graph of Figure 5.4 was made. Although the dispersion was found to increase slightly with range, an average value was used in the following analysis.

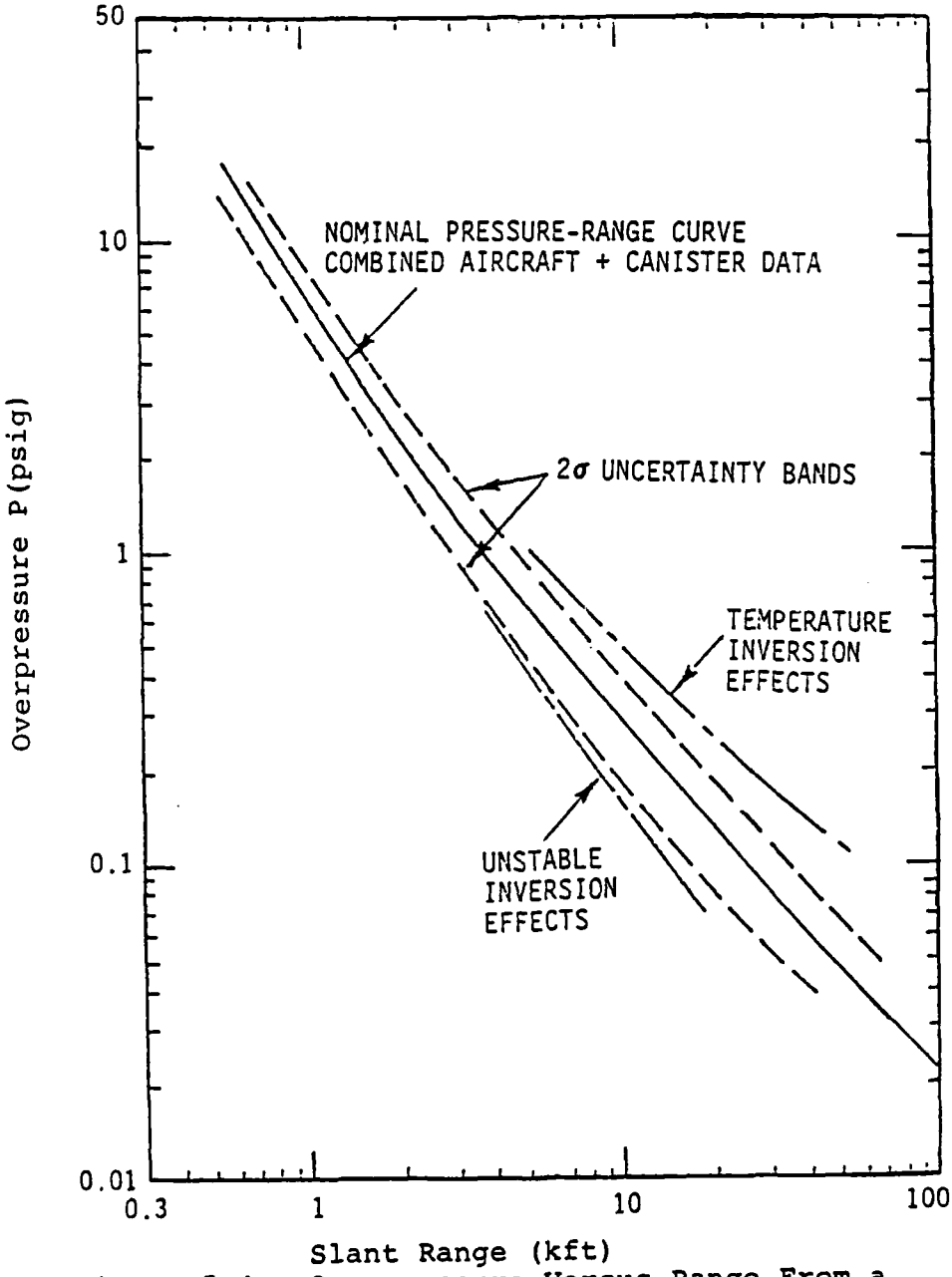

Figure 5.4. Overpressure Versus Range From a 1 Kiloton Sea Level Burst (From Reference [47])

Figure 5.4 is a log-log plot of p, the overpressure, versus r, the range from the burst. If it is assumed that a normal regression of ln p on ln r has been done, then, for a fixed value of r, the random variable P is log-normal with location parameter α_p and scale parameter β_p. Note that the lognormal distribution follows naturally from the standard assumption that the distribution of the residuals in the log space is normal. The location parameter is given by the regression equation, while the scale parameter is assumed constant. For any range r then, measured in meters, the distribution of P (in Pascals) is lognormal with parameters given by:

$$\alpha_p(r)=.19(\ln(r/1000))^2-1.51\ln(r/1000)+8.738 \qquad (5.1)$$

$$\beta_p(r)=.17 \qquad (5.2)$$

The stress distribution for particular components will take its random nature from the random character of the basic overpressure variable. In one case, this results in a simple analytic problem for the failure probability, but in most cases one must find the distribution of functions of the overpressure variable.

Strength Distributions for Aircraft Components

With the fundamental random variable input for the stress function identified, one can now consider strength functions and strength distributions. Three approaches will be examined, all of which have appeared in the literature at one time or another. These include cookie-cutter techniques

[54], probabilistic methods with an a priori lognormal assumption [45], and actual use of long-term test data [22,20].

Cookie-Cutter Distribution. For all of the work in this Chapter, the strength model is given by the simple equation:

$$S=SK \tag{5.3}$$

That is, the single sure-kill value SK characterizes the strength of the component. For the cookie-cutter case, as noted in Chapter III, the strength PDF is then given by:

$$f_S(s)=\delta(s-SK) \tag{5.4}$$

and the strength CDF by:

$$F_S(s)=0 \quad \forall \; s<SK \tag{5.5}$$

$$F_S(s)=1 \quad \forall \; s\geq SK \tag{5.6}$$

The parameter for the Dirac delta distribution is the sure-kill specification, given by sources such as Reference [54]. Some references [42] use an unbiased cookie-cutter specification which uses the average of the sure-safe (SS) and SK specifications as the parameter of the Dirac delta function.

These techniques, which remain in practice [56], result in cookie-cutter damage distributions with range, provided the stress distribution is also a Dirac delta function.

A Priori Lognormal Distribution. A second common approach is the assumption of a lognormal strength distribution, with a concurrent estimation of its parameters by some method [45,42,50,71].

Bridgman, for example [45], assigns the SS and SK specifications from Reference [54] as the 2nd and 98th percentiles, respectively, of the strength distribution of a specified component. Denoting SS and SK by $S_{.02}$ and $S_{.98}$ respectively, the parameters of the lognormal are found from the equations:

$$\alpha_S = \{\ln(S_{.02} S_{.98})\}/2 \tag{5.7}$$

$$\beta_S = \{\ln(S_{.98}/S_{.02})\}/(2z_{.98}) \tag{5.8}$$

where $z_{.98}$ is the 98th percentile of the standard normal variate and is approximately 2.054.

This approach satisfies qualitatively the concepts of SS and SK specifications, while at the same time providing a continuous probability of failure with range from the nuclear burst.

Strength Distributions From Test Data. The cookie-cutter approach does not take into account the probabilistic nature of failure phenomenon, while the alternate approaches of Bridgman [45] and others [42], though probabilistic, lack foundation in the actual database, and do not treat the uncertain nature of the applied stress environment. Consequently, the Department of Defense (DOD) database for nuclear gust and overpressure effects on aircraft was carefully surveyed to find aircraft component failure data. The results of that data search are presented at this time.

DOD Database For Blast Effects. The DOD database for blast effects on aircraft and aircraft structures falls into two broad classes--simulation testing and nuclear testing. The Defense Atomic Support Information and Analysis Center (DASIAC) has compiled complete bibliographies on both simulation and nuclear testing.

Simulation testing is largely carried out by the Defense Nuclear Agency (DNA), though others are involved in it also. A complete list of DNA and non-DNA reports on simulation testing may be found in Reference [35]. The purpose of simulation testing is to compare theoretical response predictions with actual response observations. There is little failure information in this database, since the objective of simulation testing is not to test to destruction. *Failures do occur sometimes* in simulation experiments, but these are almost always unintentional. An example of this can be found in Reference [60] where the tail section of an A-4C was destroyed in a simulation of a 1 KT yield device.

Nuclear testing has been carried out both above ground, prior to 1963, and by underground tests. Reference [35] also lists reports compiled from nuclear tests, most of them above ground. In addition, DASIAC has published two unclassified summaries of operations REDWING [70] and PLUMBBOB [69]. Besides these, DASIAC has also published a complete compendium of blast and thermal effects on aircraft gleaned

from a number of above ground nuclear tests [64]. Table V.1 shows the operations and shots that were examined. Some of these tests involved in-flight aircraft. Since these were manned, great care was taken to be sure that applied stress levels were well below limit loads of the components. Typical response data for these is given in Table V.2 taken from Reference [70]. The response data is displayed as a fraction of design limit load.

Although no failure information was found for in-flight aircraft response to nuclear overpressure effects, much is available for parked aircraft. Unfortunately, this data consists mostly of verbal descriptions of damage to a large number of different components. In many cases the exact failure mechanism is not known (e.g.--'The canopy was cracked and badly burned.') An attempt was made to quantify the information by constructing man-hours-to-repair versus overpressure plots, but these are difficult to extrapolate and remain classified. Consequently, the nuclear tests database does not contain the information needed to determine statistical failure distributions for aircraft components.

Even though the DOD database did not yield information that would allow reliability theory to be used, useful information was obtained. If drone aircraft in-flight tests had been conducted at higher levels, one might have observed failures or a number of failures. If the number of failures

TABLE V.1

NUCLEAR EVENTS INVOLVING VULNERABILITY TESTING

Vulnerability	Operation	Nuclear Shot
A/C In-Flight*	UPSHOT-KNOTHOLE	HARRY NANCY SIMON
* No Failures Observed--Max Load of 1.1 * Limit Load	REDWING	DAKOTA NAVAJO HURON APACHE
	HARDTACK	KOA WALNUT
	DOMINIC	AZTEC ENCINO YESO
A/C Structures+	UPSHOT-KNOTHOLE	ENCORE GRABLE
+ Yield Points Exceeded in 2 Cases		

TABLE V.2

REPRESENTATIVE RESPONSE DATA (From Reference [70])

SUMMARY DATA ON PROJECT 5.3

T_o is time of detonation. T_{sa} is time of shock arrival.

Shot	Absolute Altitude	Horizontal Range at T_o	Horizontal Range at T_{sa}	Radiant Exposure	Peak Overpressure	Percent of Design Limit
	feet	feet	feet	cal/cm^2	psi	
Cherokee	34,000	47,785	139,571			52 Wing
Zuni	14,000	27,000	97,760	34.0	0.400	47 Wing
Flathead	16,000	17,800	59,100			45 Wing
Dakota	16,000	13,100	35,050			88 Wing
Apache	8,000	23,500	60,500			48 Wing
Navajo	--	--	--			46.2 Wing
Huron	9,894	8,768	23,386			110 Wing
Tewa	19,000	27,250	65,750		0.900	65 Wing

SUMMARY DATA ON PROJECT 5.4

T_o is time of detonation. T_{sa} is time of shock arrival.

Shot	Absolute Altitude	Horizontal Range at T_o	Horizontal Range at T_{sa}	Radiant Exposure	Peak Overpressure	Percent of Design Limit
	feet	feet	feet	cal/cm^2	psi	
Lacrosse	13,700	6,750	28,200	1.17	0.283	35 Wing
Zuni	16,900	34,000	--	10.55		--
Erie	10,450	3,829	14,000			65 Wing
Flathead	25,700	13,466	44,659			50 Wing
Inca	9,815	2,624	11,572			--
Dakota	17,650	16,690	43,630			56 Wing
Apache	10,200	28,516	45,375			35 Wing
Huron	16,200	10,000	31,493			40 Wing

SUMMARY DATA ON PROJECT 5.5 CAPABILITIES AIRCRAFT (F-84F)

T_o is time of detonation. T_{sa} is time of shock arrival.

Shot	Absolute Altitude	Horizontal Range at T_o	Horizontal Range at T_{sa}	Radiant Exposure	Peak Overpressure	Percent of Design Limit
	feet	feet	feet	cal/cm^2	psi	
Lacrosse	15,200	8,640	600	1.65	0.80	51 Wing
Flathead	21,000	900	14,935			40 Wing
Dakota	20,374	300	11,065			115 Wing
Mohawk	19,920	3,729	19,700			65 Wing
Apache	31,614	18,614	64,300			--
Navajo	16,865	25,200	57,400			10 Wing

had been cataloged as a function of the ratio of stress to design allowable stress, a generic strength distribution might be constructed which should apply to any component that is produced by the same design process. Such data was indeed found in non-DOD publications, as discussed below.

Static Tests On Aircraft. A computer search of the DIALOG (a commercial literature search service) databases located two separate compilations of static test results on aircraft. The first is a compilation by Jablecki [26] done in 1955, and based on static test results conducted at Wright-Patterson AFB (WPAFB) from 1940-49. Jablecki did not actually do a statistical analysis. This was later done both by Chenoweth [22] and by Freudenthal and Wang [24]. A second set of static test data was obtained and analyzed by Chenoweth in 1972 [20]. This was a compilation of static tests conducted at WPAFB from 1950-1970. In both cases, the data involved static loadings of the wings, fuselage, horizontal stabilizer, vertical stabilizer, and landing gear. The data analysis was done in a normalized fashion by constructing the failure probability as a function of the ratio of applied stress to design ultimate stress. These analyses allow one to construct the failure distribution for an aircraft component as a function of the design parameters. Both of these data sets have been used in estimating the reliability of aircraft structures to thunderstorm gust loadings [24,21] and aircraft maneuver

loadings [21]. A more detailed discussion of these findings follows.

Large Aircraft Structures. Chenoweth fit the Jablecki data for the larger structures, the wings and fuselage, to a lognormal failure distribution with the random variable being

$$X = S / S_{UL} \tag{5.9}$$

where the random variable S is the stress on the component that causes it to fail and S_{UL} is the ultimate load design stress for the component. Consequently, the component failure distribution is given by

$$F_X(x) = \Phi((\ln x - \alpha_x)/\beta_x)) \quad \forall\ x > 0 \tag{5.10}$$

where $\Phi(z)$ is the standard normal cumulative distribution function (CDF) evaluated at z, and given by

$$\Phi(z) = \int_{-\infty}^{z} (2\pi)^{-1/2} \exp(-t^2/2)\,dt \tag{5.11}$$

The variable x is an arbitrary value of the random variable X, α_x is the location parameter for the lognormal density function, and β_x is the scale parameter for the lognormal density function. If one desires the distribution of the random variable S it can be shown that given X is lognormal with parameters α_x and β_x, then S is lognormal with parameters α_S and β_S given by

$$\alpha_S = \alpha_x + \ln S_{UL} \tag{5.12}$$

$$\beta_S = \beta_x \tag{5.13}$$

Small Aircraft Structures. Chenoweth fit the data from the smaller structures (vertical stabilizer,

horizontal stabilizer, and landing gear) to an asymptotic Weibull distribution function. This is just a power function, and the distribution of X in this case is given by

$$F_X(x)=0 \quad \forall \quad x \leq 0 \tag{5.14}$$

$$F_X(x)=(x/a_x)^{1/b_x} \quad \forall \quad 0 \leq x \leq a_x \tag{5.15}$$

$$F_X(x)=1 \quad \forall \quad x \geq a_x \tag{5.16}$$

In the above equations a_x and b_x are the parameters for the power function distribution. If the distribution of S is desired it can be shown that, given X has a power function distribution with parameters a_x and b_x then S has a power function distribution with parameters a_S and b_S given by

$$a_S=a_x S_{UL} \tag{5.17}$$

$$b_S=b_x \tag{5.18}$$

The 1972 data analysis is not broken out into large and small structures as was done for the Jablecki data. The data is instead lumped together and fitted to the power function model. Chenoweth shows [20] both sets of data fitted to this model, and notes that a slight improvement can be seen in the reliability of the design process from 1945 to 1960. The improvement is shown in Figure 5.5, taken from Reference [20]. For the more recent data set, the mean has improved by about 10% and the coefficient of variation (ratio of standard deviation to mean) has been reduced by about 33%.

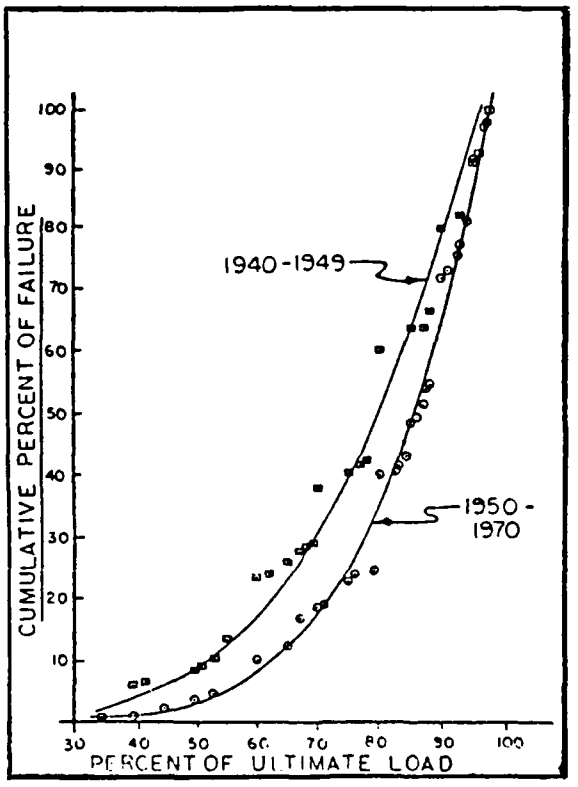

Figure 5.5. Aircraft Failures Versus Ultimate Design
(From Reference [20])

AD-A163 218 AIRCRAFT NUCLEAR SURVIVABILITY METHODS(U) AIR FORCE INST OF TECH WRIGHT-PATTERSON AFB OH SCHOOL OF ENGINEERING H A UNDEM SEP 85 AFIT/DS/PH/84-3 2/3

UNCLASSIFIED F/G 18/3 NL

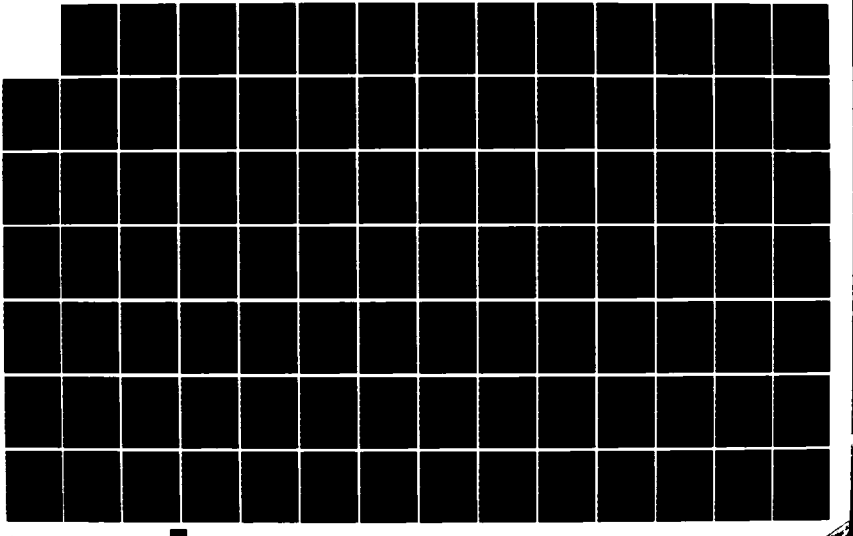

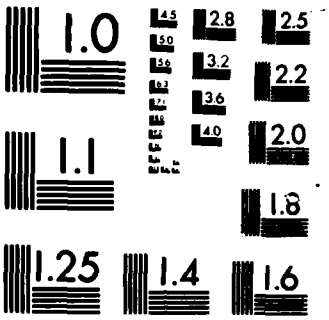

Chenoweth's data is somewhat surprising. It seems to imply that at nominal limit loads (2/3 of ultimate) the failure probability is significantly high--on the order of 10%. Chenoweth apparently insists on the validity of the data. Quoting from Reference [21], he says, "It is shown that a 'no static test' policy on major aircraft structural components yields extremely high probability of failure or unreliability." No formal rebuttal to this was found in the literature. Chenoweth goes on in Reference [21] to further show, based on the data, the vulnerability of aircraft to thunderstorm gust loads and maneuver loads. In both cases, the resulting failure probabilities range from 1E-4 to 1E-2. The following additional observations should also be noted.

First, the data as shown in Figure 5.5 is, at most, half the story. The distribution of stresses or loads can be as important, or perhaps more important, than the strength distribution in determining the actual probability of failure. For example, if the ultimate load design had been chosen in such a way that the limit load value (2/3 of ultimate, say) was extremely improbable, then the aircraft could be perfectly hard. It is the interference of the stress distribution with the strength distribution that governs the failure probability, and not either acting alone.

As a second consideration, Chenoweth says [21] the data is first time static test data. If these tests resulted in

redesign of the components, then the resulting product would of course be harder than the first time tests indicate.

Third, the data is admittedly old. The most recent data set is a mixture of aircraft from 1950 to 1970. The methods of aircraft design and hardness verification and validation have undoubtedly changed since the data was obtained, so that one should not infer that it applies to modern combat aircraft. Because of this, the resulting calculations in this Chapter should be considered worst case results.

Having said all this, the data is still a valuable collection of information. Here at least is some justification for choosing parametric failure distributions. The following calculations illustrate the use of such information.

Component Failure Probabilities

Fuselage Vulnerability. The general failure probability is, as stated earlier, given by the reliability interference integral. That is,

$$p_f = \int_{-\infty}^{\infty} f_s(s) F_g(s) ds \qquad (5.19)$$

Model 1. The result depends on the time dependent properties of both the strength and stress distributions. The stress function is presumed given by

$$s = P \qquad (5.20)$$

where P is just the random overpressure variable, lognormally distributed with parameters given by Equations

5.1 and 5.2. For this case, denoted as Model 1, the cookie-cutter strength distribution is assumed, reducing Equation 5.19 to the result:

$$p_f = 1 - F_s(SK) \tag{5.21}$$

where SK is 1.085E5 Pa (15.75 psi). Since the stress distribution is a lognormal, the results for this case have an analytical form as a function of range. Explicitly,

$$p_f(r) = 1 - \Phi\{(\ln SK - \alpha_p(r))/\beta_p\} \tag{5.22}$$

where $\Phi(z)$ is given by Equation 5.11.

The results of Model 1 are shown in both the stress space (Figure 5.6) and the range space (Figure 5.7). One notes that the use of a probabilistic model for the stress is sufficient to provide a continuous probability of failure in the range space. The tails in Figure 5.7 for Model 1 are due to the variation in the applied overpressure only, since the strength distribution is a step function. The median failure range for Model 1 corresponds to the SK stress specification.

Model 2. Keeping the stress distribution the same, if the lognormal assumption is made for the strength distribution, with parameters calculated from Equations 5.7 and 5.8, and SS=6891 Pa (1 psi), and SK=1.085E5 Pa (15.75 psi), then the failure probability may be written as:

$$p_f = Pr\{S \leq P\} = \int_{-\infty}^{\infty} f_p(p) F_s(p) dp \tag{5.23}$$

where S is the strength random variable, P the stress random variable (the applied overpressure), $f_p(p)$ the probability

density function of P, and $F_S(p)$ the CDF of S evaluated at p. Equation 5.23 could also be written as

$$p_f=Pr\{S/P\leq 1\} \tag{5.24}$$

or

$$p_f=Pr\{\ln(S/P)\leq 0\} \tag{5.25}$$

In the case of Equation 5.25, letting the random variable Y, sometimes called the log safety factor, be defined by

$$Y=\ln(S/P)=\ln S-\ln P \tag{5.26}$$

it is seen that Y is consequently normally distributed with mean μ_y and standard deviation σ_y given by

$$\mu_y=\alpha_S-\alpha_p \tag{5.27}$$

$$\sigma_y=(\beta_S{}^2+\beta_p{}^2)^{1/2} \tag{5.28}$$

Consequently, the failure probability for the fuselage can be shown to be

$$p_f=\Phi(-\mu_y/\sigma_y) \tag{5.29}$$

Since the parameter α_p is a function of distance from the burst, p_f as given by Equation 5.29 is also a function of distance from the burst. The results for Model 2 are also shown in Figures 5.6 and 5.7.

Model 3. Finally, the actual data for fuselage failures may be used to form the strength distribution while retaining the previous model for the stress distribution. Since the large structures were found to have lognormal strength distributions, the general form for the failure probability is given again by Equations 5.27 through 5.29.

However, in this case the parameters α_S and β_S are calculated from Equations 5.12 and 5.13 where the parameter S_{UL} is related to the sure-safe specification by:

$$S_{UL}=1.5(SS) \tag{5.30}$$

and the parameters SS, α_x, and β_x are given by:

$$SS=6891 \text{ Pa } (1 \text{ psi}) \tag{5.31}$$

$$\alpha_x=.1481 \tag{5.32}$$

$$\beta_x=.3159 \tag{5.33}$$

The vulnerability of the fuselage for this case is also illustrated in Figures 5.6 and 5.7. Model 3 (based on the Chenoweth data) seems to imply a much softer fuselage than either Model 1 or Model 2 would suggest. The failure probability rises steeply with increasing stress, with a median failure level at about 11.7E3 Pa (1.7 psi). Nevertheless, all three distributions agree qualitatively in the SS and SK regimes.

Not surprisingly, the softness of the fuselage as a function of range from the 1 KT standard is clearly demonstrated in Figure 5.7. If Model 3, based on the Chenoweth data, is accepted, the sure-safe range (denoted by RS--the distance where the failure probability is less than or equal to .02) is at 1160 meters, where the median overpressure is expected to be 5012 pascals (.73 psi). This stress value is about 27% smaller than that postulated by 2048, but is within the error bounds given by 2048 [54].

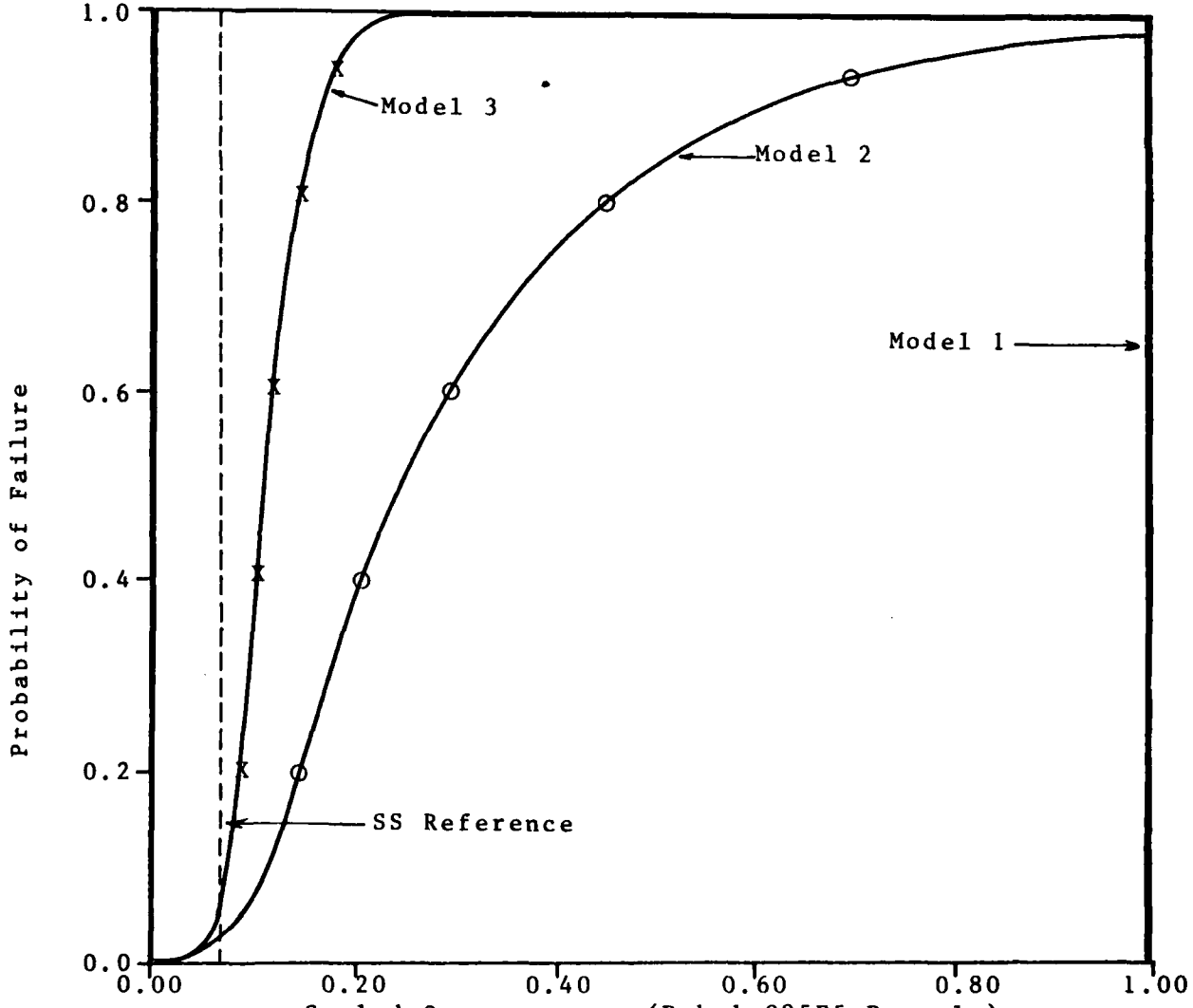

Figure 5.6. Fuselage Failure Probability Versus Overpressure

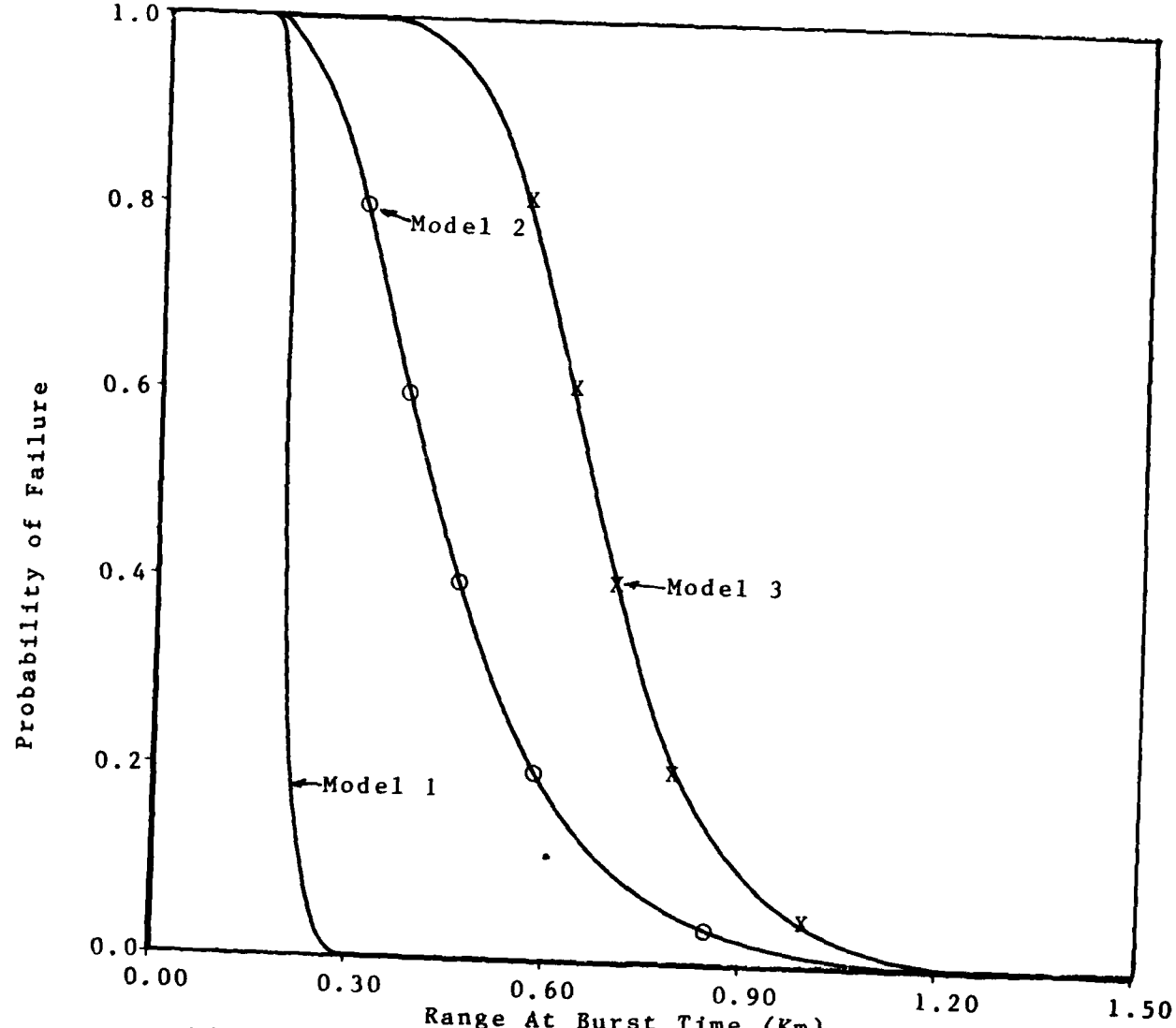

Figure 5.7. Fuselage Failure Probability Versus Range

This soft fuselage result qualitatively agrees with that of the work documented in Reference [60]. There it was noted that the 2048 Method 1 technique for overpressure was severely unconservative . In a test of the A-4C, the SK condition was reached at a farther range from a 1 KT simulation than was expected. In fact, the catastrophic failure occurred at 311 meters from ground zero. From Figure 5.7 (keeping in mind that our SS and SK specifications are somewhat different from that of Reference [60]) one sees that the cookie-cutter prediction is indeed one of no failures, while Bridgman's model (Model 2) would predict a failure probability of .76 at that point, and the actual test data would predict the fuselage to be sure-killed.

Again, the caveats previously mentioned should be remembered. In addition to those, there can still be an ambiguity regarding the uses of the terms SS and SK. Although Reference [68] clearly equates a SS condition to a limit load condition, it is not clear what the factor of safety is between SK and SS specifications. Indeed, for the fuselage specs it may be 15.75--the ratio of SK to SS. If that is the case, then the ultimate load should perhaps be given directly by 15.75 psi and not 1.5 times the SS specification. This would have a dramatic effect on the strength distribution, moving the median failure point to a higher level.

Wing Vulnerability-Fundamental Mode. For the case of the fuselage, the presumption that the fuselage responds directly to overpressure led to simple computational results. If instead a more complex response (i.e, stress) model had been chosen, no such simple results would have resulted. This is the case for even elementary models of wing-loading.

The general expression for the failure probability as shown in Equation 5.19 is still valid, but now has no closed-form solution. Although the distribution of P remains the same as in the fuselage analysis, the stress variable s is no longer the direct overpressure variable. The stress (using a simple fundamental mode analysis as in Reference [45]) is now the load factor (in g's--multiples of weight) given by:

$$n_L = .5\rho v^2 C_L A/W \tag{5.34}$$

where ρ is the air density behind the shock front (kg/m^3), v is the lifting wind velocity (m/sec), C_L is the coefficient of lift (dimensionless), A is the area of the wing (square meters) and W is the aircraft weight (Nt). At every range point r the distribution of the load factor is now the required stress distribution. The problem is analytically intractable, since ρ, v, and even C_L in Equation 5.34 depend nonlinearly on the overpressure.

As previously discussed, the general problem of propagating a random variable through a complicated response

function has been approached by distributional fitting [37,32] and by Monte Carlo analysis [32,57]. The former approach can lead to large differences in results [32,3] while the latter may require more computer resources than the simple strength or response function models justify. Fortunately, nonparametric estimation provides a powerful tool [14,Appendix A,Appendix C].

The distribution of load factor can be constructed at any range r by using the technique illustrated in Chapter IV. This is done by drawing a stylized sample from the assumed known distribution of P and propagating these sample values through the response equation to generate a load factor sample. This sample can then be used to construct the distribution [14,Appendix A,Appendix C].

With this tool in hand, the distribution of s (load factor) can be determined without a priori distributional assumptions, and without large-sample Monte Carlo analysis. Equation 5.19 can then be numerically integrated at each point r where the failure probability is desired.

For the case of wing-loading, the stress model is described by the following, where bold-faced variables indicate random variables. For every value of P drawn at range r,

(1) Determine the magnitude of the peak wind velocity, u_1, behind the shock front (from Rankine-Hugoniot).

$$u_1 = 5Ps_0/\{7p_a(1+6P/7/p_a)^{1/2}\} \qquad (5.35)$$

(A complete description of these variables may be found in the section on nomenclature.)

(2) Find the components of u_1 in the aircraft frame of reference.

$$u_{1ax}=(u_1/s_r)y_b \tag{5.36}$$

$$u_{1ay}=(u_1/s_r)(x_t-x_b) \tag{5.37}$$

$$u_{1az}=(u_1/s_r)d_z \tag{5.38}$$

(3) Determine the initial attack angle (straight and level flight assumed).

$$C_{L0}=2W/(\rho_0 v_0{}^2 A) \tag{5.39}$$

$$\alpha_0=(C_{L0}-.356)/1.243 \tag{5.40}$$

(4) Determine the resultant wind vector in the aircraft frame of reference.

$$u_{rx}=u_{1ax} \tag{5.41}$$

$$u_{ry}=u_{1ay}-v_0 \tag{5.42}$$

$$u_{rz}=u_{1az} \tag{5.43}$$

(5) Resolve the resultant wind vector into its lifting and non-lifting components.

$$u_p=u_{rx} \tag{5.44}$$

$$v=(u_{ry}{}^2+u_{rz}{}^2)^{1/2} \tag{5.45}$$

(6) Determine the angle between the lift wind and the aircraft chord vector.

$$\text{cosdel}=\{\cos(\alpha_0)u_{ry}+\sin(\alpha_0)u_{rz}\}/v \tag{5.46}$$

$$\text{del}=\text{Acos}(\text{cosdel}) \tag{5.47}$$

$$\alpha=\pm(\pi-\text{del}) \tag{5.48}$$

(7) Determine the coefficient of lift.

$$C_L = 1.243\alpha + .356 \tag{5.49}$$

(8) Determine the air density behind the shock front.

$$\rho = \rho_0 \{7+6P/p_a\}/\{7+P/p_a\} \tag{5.50}$$

(9) Determine the load factor (a sample value of s) from Equation 5.34, i.e,

$$n_L = .5\rho v^2 C_L A/W \tag{5.51}$$

Model 1. With the stress distribution determined nonparametrically, the strength distribution is now required. Again one may use the simple equation,

$$S = n_{sk} \tag{5.52}$$

For Model 1 a cookie-cutter strength distribution is assumed so that the strength variable has the PDF,

$$f_S(s) = \delta(s - n_{sk}) \tag{5.53}$$

where n_{sk} is taken from Reference [54] as 6.75 g's for *loading from below*.

As in the fuselage case, the results for the failure probability reduce to

$$p_f = 1 - F_s(n_{sk}) \tag{5.54}$$

where the CDF of the stress distribution is now found nonparametrically.

The results for loading from below are displayed in Figures 5.8 and 5.9. The failure probability as a function of applied stress is shown in Figure 5.8, while the corresponding failure probability with range is shown in Figure 5.9. The results for Model 1 are shown by the solid lines.

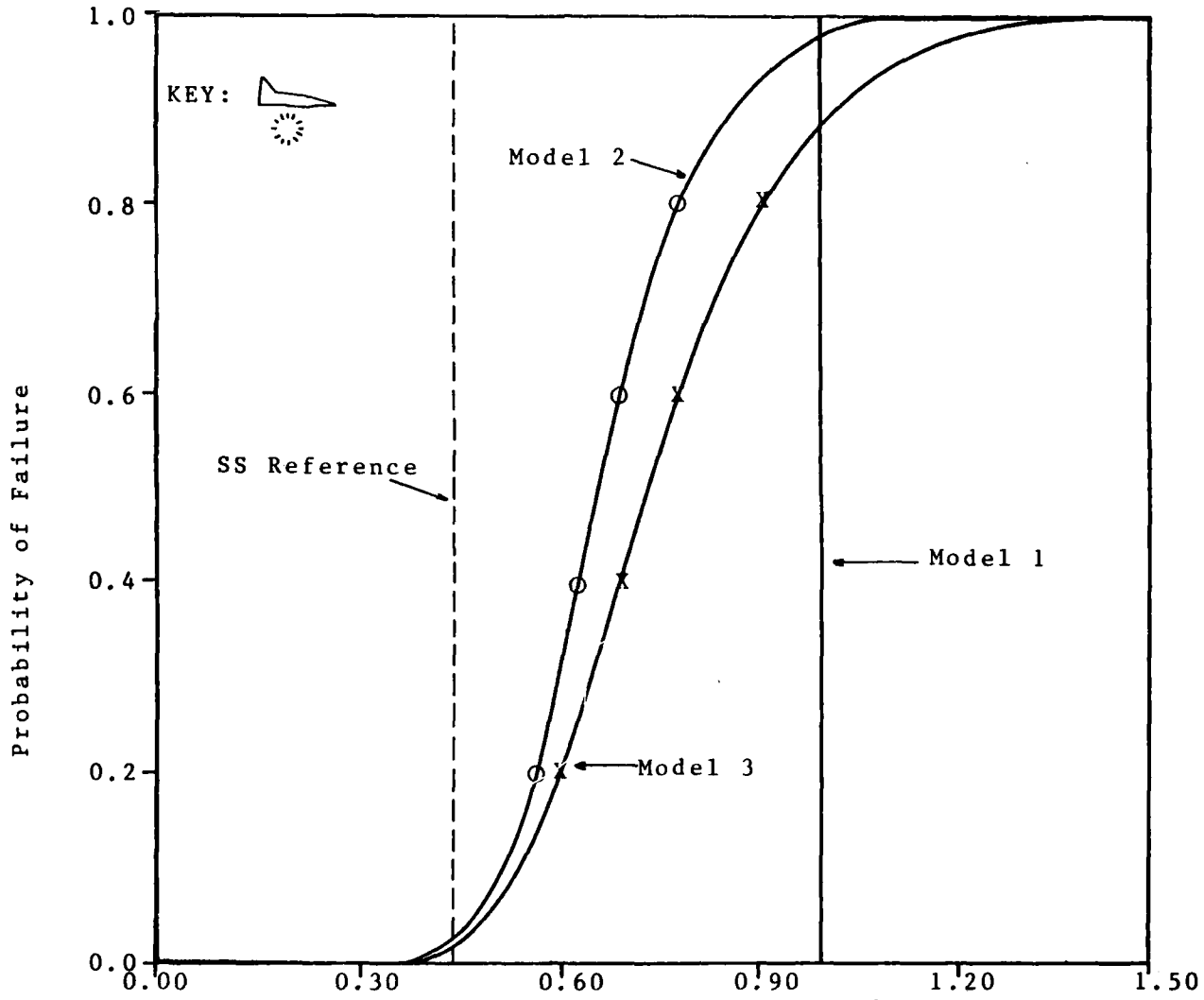

Figure 5.8. Wing Failure Probability Versus Gust Loads

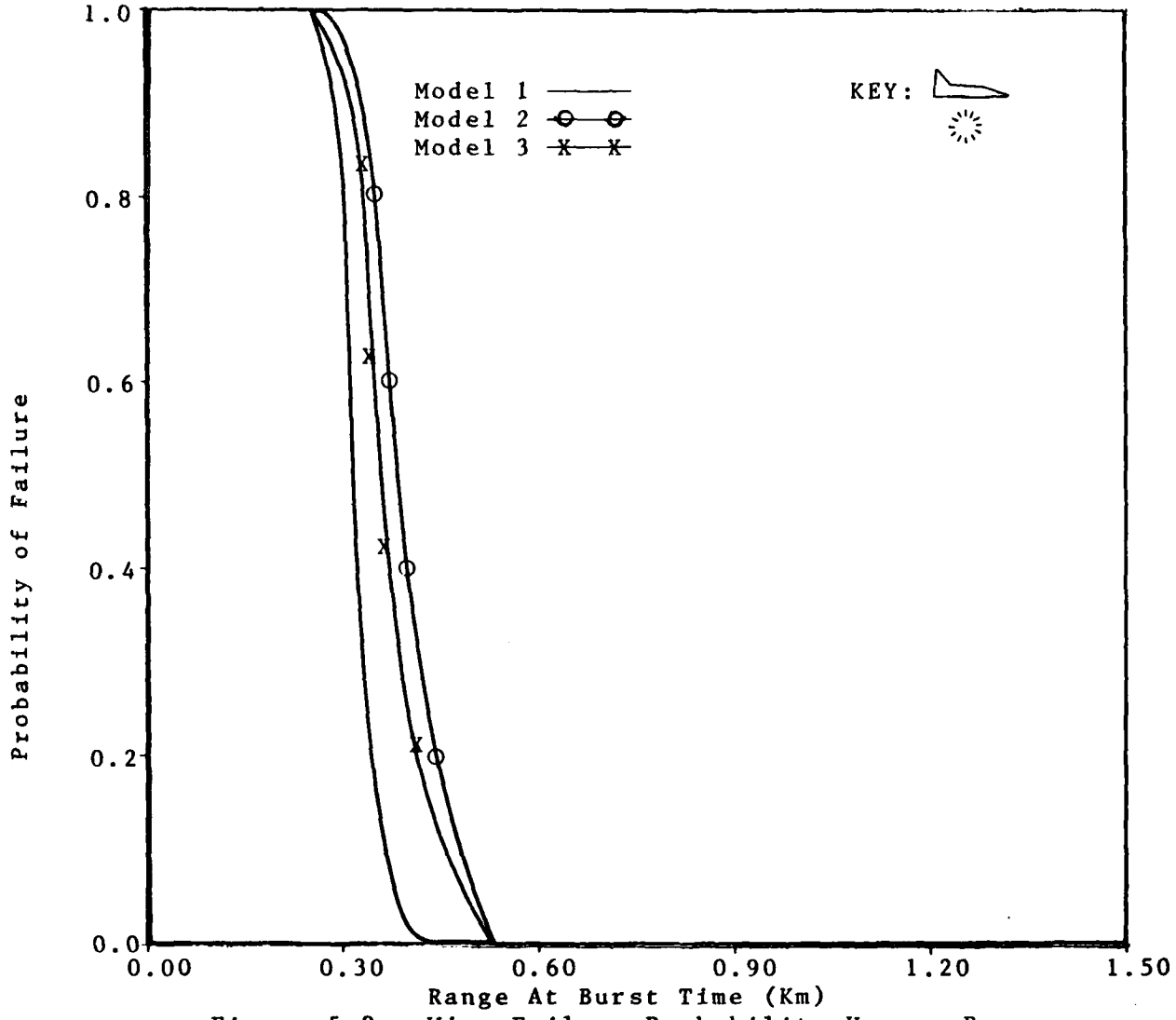

Figure 5.9. Wing Failure Probability Versus Range

Model 2. The stress distribution remains the same, but the lognormal assumption is now made for the strength distribution, with the parameters calculated from Equations 5.7 and 5.8, and with SS and SK given by 3 and 6.75 g's respectively (Method 1 of Reference [54]).

Since the stress distribution is known nonparametrically, the integral in Equation 5.19 must be solved numerically. The method for doing this is described in Appendix D. The results using the lognormal assumption are shown in Figures 5.8 and 5.9 also.

Model 3. Finally, the strength distribution derived from the test data is given as a lognormal, with parameters α_S and β_S calculated from Equations 5.12 and 5.13, and S_{UL} calculated from Equation 5.30. For the case of the wing, the necessary parameters are given by

$$SS=3 \text{ g's} \tag{5.55}$$

$$\alpha_x=.1076 \tag{5.56}$$

$$\beta_x=.2467 \tag{5.57}$$

The results for Model 3 are shown with those of the previous models in Figures 5.8 and 5.9. The results for the different models in both the stress and range spaces are much closer together than the comparisons for the fuselage were. In fact, the results of Figure 5.9 indicate that the cookie-cutter approximation for wing-loading is reasonably valid, especially for the higher values of the failure probability. There are at least three reasons for this.

First, the ratio of SK to SS is much smaller for the wing-loading case. The continuous probability models rise faster with increasing stress, and the differences between the cookie-cutter damage distribution and the continous ones are decreased. Second, the experimental results for the fuselage showed the largest variation of any of the aircraft components. This makes the fuselage a worst case as far as reliability goes. Finally, the aircraft response (load factor) is a very steep function of range, resulting in a step-function appearance. All three distributions are in near agreement on RK, the sure-kill range (point where failure probability equals or exceeds .98), while the difference in RS is only about 100 meters.

Vertical Stabilizer Vulnerability. The analysis of the vertical tail assembly can be done in the same way the wing-loading analysis was done. The stress variable s is now the combined bending moment of the vertical tail and fuselage. The overpressure variable P is sampled as before, the sample values are propagated through the response equations, and the distribution of s is determined at range points r. Equation 5.19 is then integrated numerically to determine the failure probability as a function of range from the 1 KT standard. The stress model is described as follows. For every value of P drawn at range r:

(1) Proceed with the response function for wing-loading through step (5) to find a_p, the component of the

resultant wind vector that acts on the vertical tail assembly.

(2) *Determine the combined bending moment due to this wind acting on the vertical tail and fuselage (a value of s).*

$$B_f = .5\rho u_p^2 C_{df} A_f L_f \tag{5.58}$$

$$B_t = .5\rho u_p^2 C_{dt} A_t L_t \tag{5.59}$$

$$B = B_f + B_t \tag{5.60}$$

Model 1. The SS specification is taken as 1.763E6 newton-meters, and SK specification as 3.7E6 newton-meters (again, after Method 1 of Reference [54]). For the cookie-cutter model of the strength distribution, one assumes the strength to be given by

$$S = b_{sk} \tag{5.61}$$

where b_{sk} *is the sure-kill value just mentioned.* This being the parameter of a Dirac delta function, the equation in the range space for the failure probability is given by

$$p_f = 1 - F_s(b_{sk}) \tag{5.62}$$

where again the distribution of the stress is found using nonparametric methods. The results are displayed in Figures 5.10 and 5.11.

Model 2. The strength distribution under the assumptions of Model 2 is a lognormal with parameters given by Bridgman's prescription [45] in Equations 5.7 and 5.8. The SS and SK specifications just mentioned provide the $S_{.02}$ and $S_{.98}$ percentiles that go into the calculation.

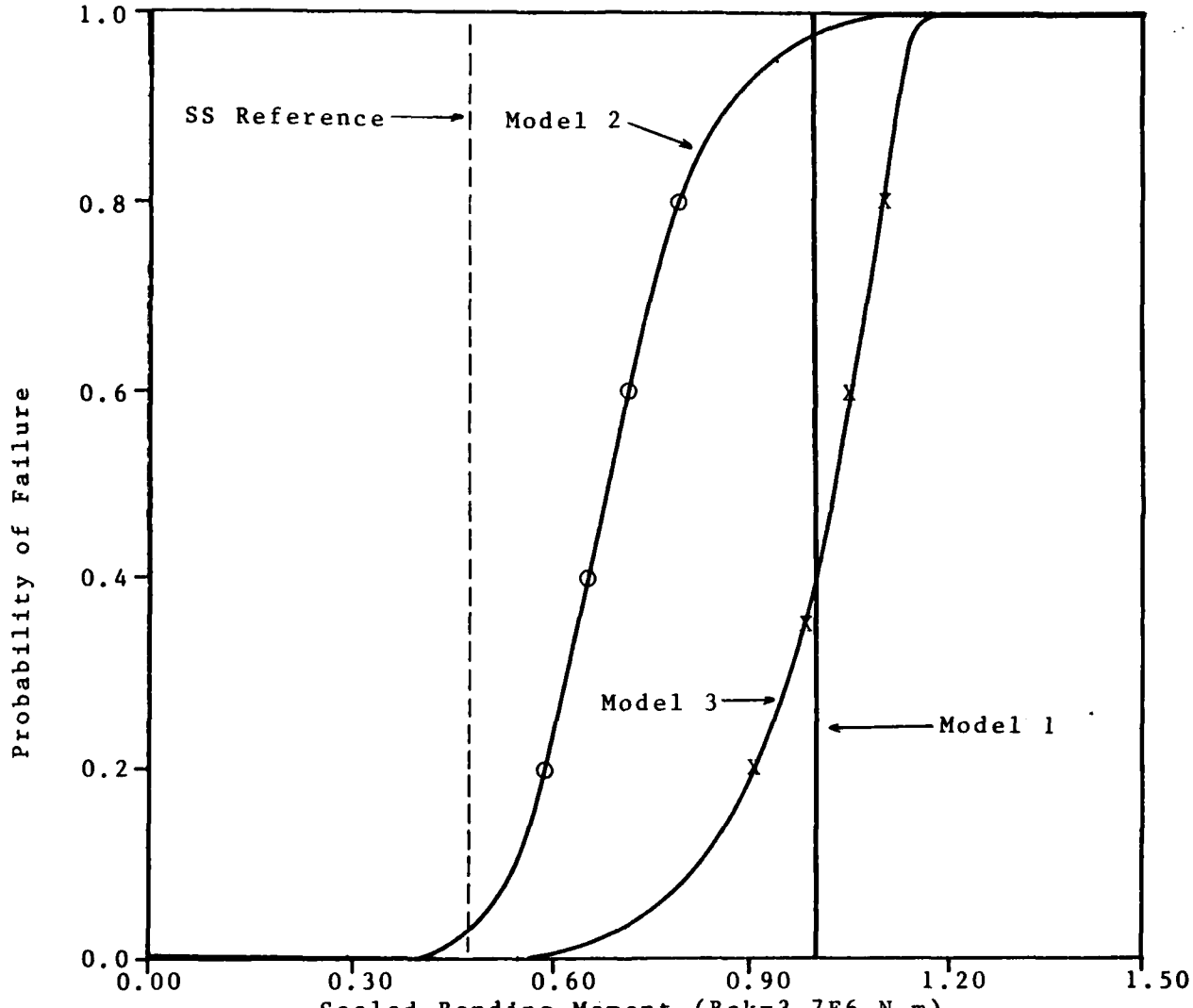

Figure 5.10. Vertical Stabilizer Failure Probability Versus Bending Moment

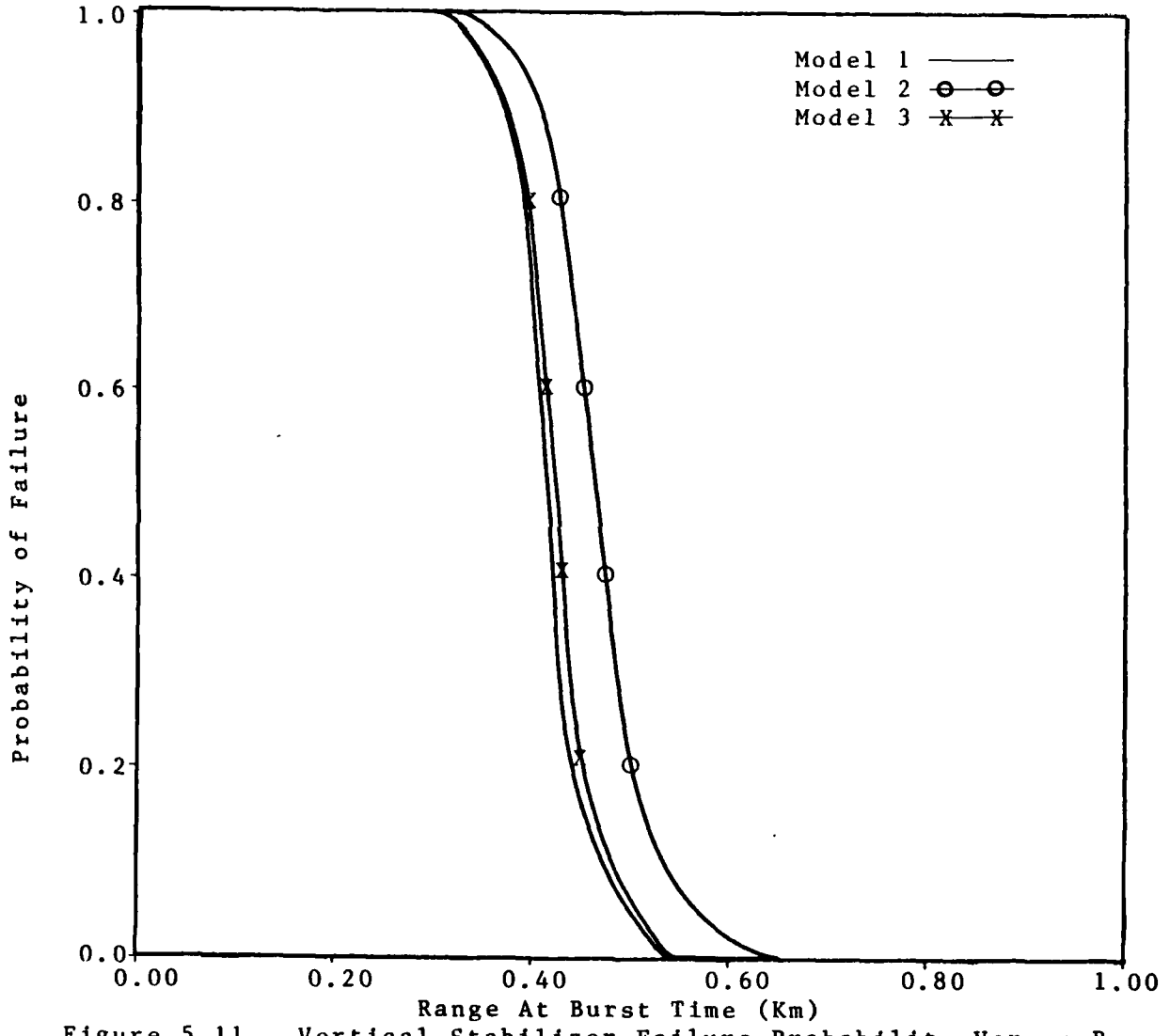

Figure 5.11. Vertical Stabilizer Failure Probability Versus Range

The failure probability must be found by numerically integrating Equation 5.19 at each range point r. The results are displayed along with those of Model 1 in Figures 5.10 and 5.11.

Model 3. Finally, under the assumptions of Model 3, the strength function is given by Equation 5.61, but the failures are distributed as determined by Chenoweth [20]. The strength distribution is asymptotic Weibull with parameters given by Equations 5.17 and 5.18. As usual, S_{UL} is taken as 1.5 times the SS specification. From the static test results, a_x and b_x are found to be:

$$a_x=1.606 \tag{5.63}$$

$$b_x=.1431 \tag{5.64}$$

and the SS specification is taken as 1.763E6 newton-meters.

The results of the analysis are displayed in Figures 5.10 and Figure 5.11 and are compared to the other models. Although there appears to be some differences in the distributions when viewed in stress intensity space, these differences are nil when viewed in range space. In particular, Model 3 and the cookie-cutter approximation are indistinguishable. This is a reasonable result since the ratio of SK to SS is low, and the experimental data yields a failure distribution that rises steeply. From Figure 5.11, RK is at about 330 meters, while RS is at about 520 meters.

Summary

The survivability of several aircraft components in a nuclear blast environment has been calculated. Stress distribution construction begins with stress functions. The nuclear weapon effect of interest here, the overpressure variable, is a random variable that enters into these stress functions. The distribution of these functions, found by nonparametric methods, defines the stress distributions for the components.

The strength distributions are surveyed. Two common approaches, cookie-cutter modeling and lognormal modeling, are compared to distributions found by analyzing twenty years of aircraft static test data.

The resulting failure probability with range from the weapon is calculated and compared. In general, one cannot say beforehand whether or not a parametric model is superior to a cookie-cutter model. For most cases, the results did not vary much. For the case of the fuselage, however, neither the cookie-cutter nor the lognormal was as conservative as the actual test data suggested.

In the next Chapter, the survivability to nuclear thermal effects will be considered, and the difficulties posed by the lack of failure data will be noted.

VI. Aircraft Vulnerability In Nuclear Thermal Environments

Overview

In this chapter, a stress-strength interference theory calculation of the probability of failure of skin panels in nuclear thermal environments is accomplished. A search of the database for nuclear effects on aircraft yields no direct information on either stress or strength distributions for the failure modes of interest. The temperature of a thin skin panel in a nuclear thermal environment is a fundamental stress. Although this is a deterministic response, statistical variation is introduced by treating the radiated power from the weapon as a random variable, and then finding the distribution of the functions of this random variable. Two failure modes are considered. The first is based on sure-safe and sure-kill specifications for aircraft, and is analogous to the work done on blast vulnerability. For this mode, two strength distributions are examined--a cookie-cutter and a lognormal. An alternate failure mode is investigated that considers skin panel yielding as a function of both gust and thermal loading. The calculation illustrates the use of the nonparametric interference theory technique in treating problems where multiple nuclear effects contribute to a failure mode.

A Data Search For Thermal Effects on Aircraft

As in the case of blast effects on aircraft, no direct failure data for aircraft components were found. Items of interest in the nuclear tests examined include thermal fluence and temperature time histories. Peak temperatures for the time histories of Operation REDWING are well below melt point. A typical result from Reference [70] is shown in Figure 6.1. Lacking actual service histories for the failure mode of interest, the only alternative is engineering modeling. An important variable, as displayed in Figure 6.1, is the temperature of a thin panel as a function of time. This is a fundamental thermal stress on the system, and is discussed in detail below.

A Deterministic Thermal Stress Model

A simple model of the temperature rise in a thin-skin assembly can be constructed by requiring an energy balance condition [45]. That is, the temperature in the thin skin obeys the differential equation:

$$\rho C_v \Delta x dT/dt = Y_{th}(t)/(4\pi r^2) - h(v)(T-T_0) \qquad (6.1)$$

where the term on the left of the equals sign is the time rate of change of the energy deposition in the material. The variables in this term include ρ, which is the material density in kg/m^3; C_v is the specific heat in Joules/(kg-°-Kelvin); Δx is the skin thickness in meters; T is the skin temperature in degrees Kelvin; t is the time in seconds.

The first term to the right of the equals sign is the source term, corrected for spherical divergence. The variables there are given by:

$$Y_{th}(t)=P_m(W)f(t)T_r\alpha_b\cos\theta(t) \qquad (6.2)$$

where $P_m(W)$ is the maximum radiated power (in watts) from the weapon and is a function of W, the weapon yield in kilotons (KT); f(t) is the fractional radiated power at time t; T_r is a transmittance factor to account for attenuation through the atmosphere; α_b is the absorptivity of the skin surface; θ is the look angle between the weapon and the aircraft skin and is a function of time due to the motion of the aircraft. The variable r in Equation 6.1 is the slant range (in meters) from the weapon at time t.

The last term in Equation 6.1 is the sink term, the rate of energy dissipated to the environment by convective cooling. The variables here include h(v), which is the (velocity dependent) heat transfer coefficient in Joules/(^{o}-Kelvin-meter^2-sec) and T_0, the temperature of the air adjacent to the skin in degrees Kelvin.

The equation can be made dimensionless by introducing some natural variables. Since the differential equation is one that couples temperature and time, the natural variables involve both times and temperatures. The natural time variables include t_m, the time (in sec) to peak thermal radiated power. The dimensionless time τ can then be defined as

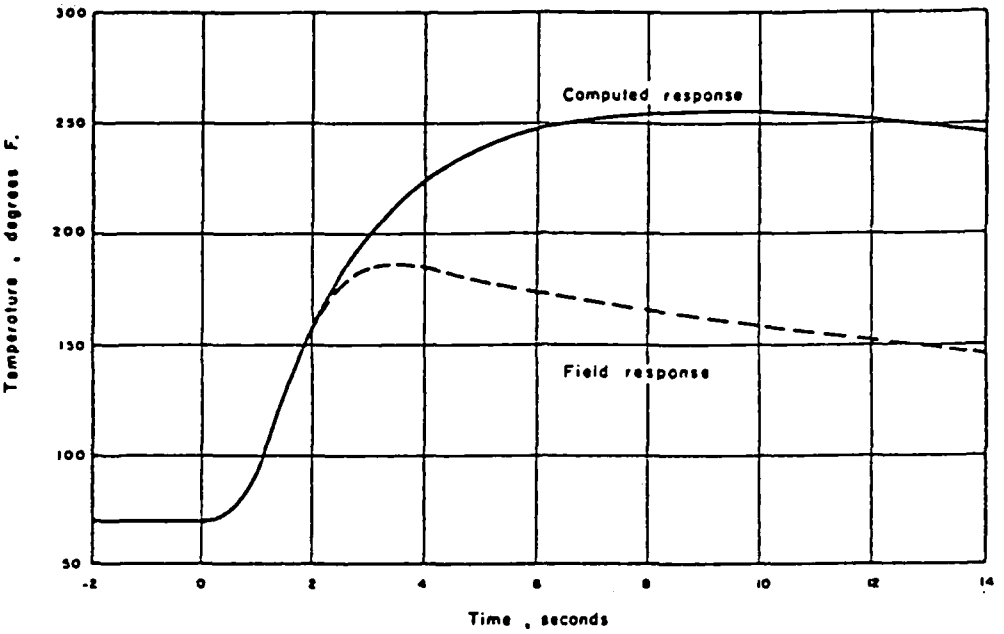

Exposed facing temperature-time histories of GLM specimen with 0.016-inch white-painted skin. (Computed peak temperature: 255°F.)

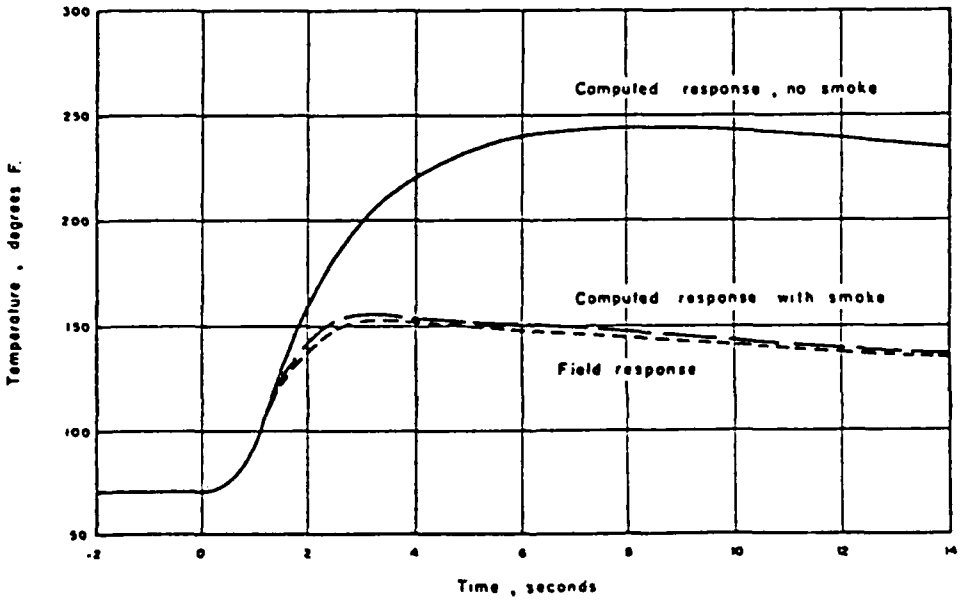

Exposed facing tempe. ture-time histories of NAA specimen with $\frac{1}{8}$-inch cell size and 0.016-inch white-painted skin. (Computed peak temperature: 243° F.)

Figure 6.1. Temperature Time History In A Thin Plate (From Reference [70])

$$\tau = t / t_m \tag{6.3}$$

Another important time variable is t_c, the cooling time, given by

$$t_c = \rho C_v \Delta x / h \tag{6.4}$$

where the right hand side variables have already been described. One can show that in the absence of any source term, the cooling time is the time for a preheated structure to cool to 1/e of its initial temperature, where e is the natural logarithmic base. Finally, the ratio of time constants will be denoted by

$$\gamma = t_m / t_c \tag{6.5}$$

The natural temperature variables include the ambient temperature, T_0, in degrees Kelvin. The dimensionless time dependent temperature T can be defined by

$$\hat{T}(\tau) = T(\tau) / T_0 \tag{6.6}$$

A time dependent characteristic temperature can also be defined. This temperature depends on geometrical and physical characteristics of the skin material, and on properties of the thermal pulse. The dimensionless characteristic temperature can be written as

$$\hat{T}_c(\tau) = \hat{T}_k(\tau) f(\tau) \tag{6.7}$$

where $\hat{T}_k(\tau)$ is given by

$$\hat{T}_k(\tau) = P_m(W) T_r \alpha_b \cos\{\theta(\tau)\} t_m / (4\pi r^2 \rho C_v \Delta x T_0) \tag{6.8}$$

The variables on the right hand side of Equation 6.8 have been described previously. The term $f(\tau)$ in Equation 6.7 is the relative radiated power at time τ. That is

$$f(\tau)=P(\tau)/P_m(W) \tag{6.9}$$

where $P(\tau)$ is the radiated power in watts at time τ. For stationary targets, $\hat{T}_k$ reduces to a time-independent constant. Dividing all times in Equation 6.1 by t_m, the time to thermal maximum, and all temperatures by T_0, the ambient temperature, leads to a dimensionless differential equation. Solving that equation by using an integrating factor and the natural variables just described leads to the solution

$$\hat{T}(\tau)=1+[T(0)-1+\int_0^{\tau} T_c(\tau')e^{\gamma\tau'}d\tau']\exp(-\gamma\tau) \tag{6.10}$$

Equation 6.10 is the deterministic equation for the stress function. It represents the anticipated response of the skin to a nuclear thermal pulse. The statistical distribution of this response can be determined by propagating statistical information about the input variables through the function. Of the many input variables one might consider, the radiated power from the weapon will be examined statistically and the others left as deterministic. Two reasons dictate this choice. First, it will provide a parallel development to the work of the previous chapter. In particular, a thermal analog to the work of Carpenter and Kuhl [47] will be developed. Second, it is difficult to find statistical data for the other variables of interest. In fact, the statistical information for the radiated power is not readily available, and one must analyze the data that one can find. In the next section, the deterministic stress

function is expanded into a random variable equation.

The Thermal Stress Distribution For A 1 KT Sea Level Burst

General Approach. The objective now is to find the statistical description of the temperature in a thin skin at any time desired. Equation 6.10 is the basic deterministic temperature response. The dependence on the basic weapon effect, the radiated power, can be explicitly demonstrated by writing the characteristic temperature in the form shown in Equation 6.7. The resulting integral equation is:

$$\hat{T}(\tau)=1+[T(0)-1+\int_0^{\tau}\hat{T}_k(\tau')f(\tau')e^{\gamma\tau'}d\tau']\exp(-\gamma\tau) \qquad (6.11)$$

If one now recognizes that the radiated power, $f(\tau)$, is statistically distributed, then the resultant output variable, $\hat{T}(\tau)$ is also statistically distributed, since it is a function of a random variable. In particular, if the distribution of the radiated power has been determined, then the particular sample value $f_i(\tau)$ results in a corresponding sample value $\hat{T}_i(\tau)$ where the two values are functionally related through Equation 6.11. Given the distribution of the radiated power, the distribution of the temperature in the structure can be determined by the methods already discussed. The determination of the distribution of the radiated power is the next task to be accomplished.

A Statistical Model Of The Radiated Power. As previously mentioned, a search of the database for thermal effects on aircraft did not yield any information about

statistical thermal source models--that is, no analog to the work of Carpenter and Kuhl [47] was found. In order to continue with an interference theory calculation one must have a source of data. There are several approaches that could be taken, but all depend in part on a deterministic model of the weapon effect. Two such deterministic models are discussed below.

A relatively simple model of the radiated power produced by a nuclear weapon is described by Glasstone [62]. Figure 6.2, reproduced from Reference [62], displays the normalized power as a function of normalized time. In this model, the time to (second) thermal maximum, and the peak radiated power at that time are scaled according to yield. Consequently, the plot of Figure 6.2 has been used for a variety of yields and burst altitudes. Glasstone quotes the results as being valid $\pm$ 25% for altitudes below about 4-5 kilometers (km) and $\pm$ 50% for altitudes above that. This statement acknowledges that the value of the radiated power is statistically uncertain.

Glasstone's pulse is synthesized from both experimental data gathered during the days of atmospheric testing and theoretical modeling. With the signing of the Limited Test Ban Treaty in 1963, theoretical calculations of thermal environments have largely replaced data collection techniques.

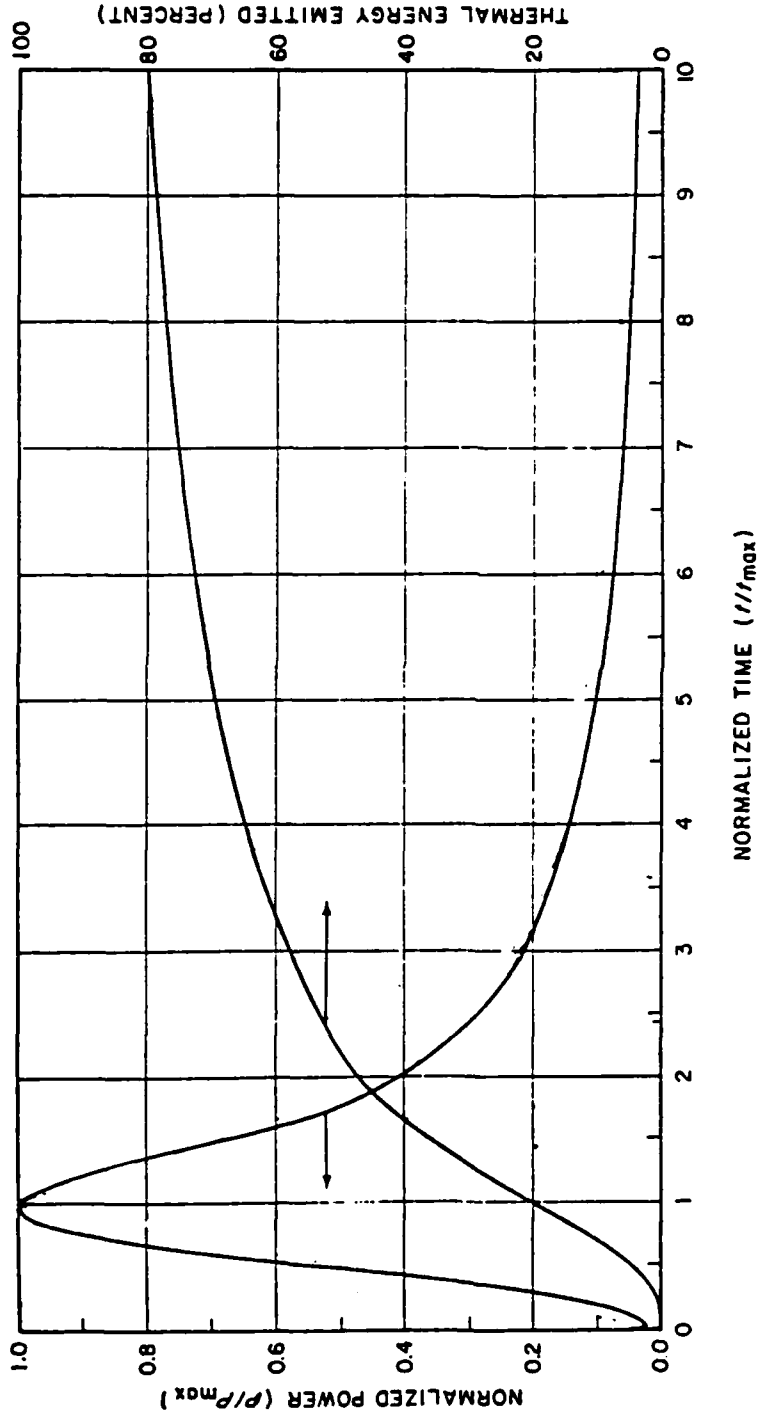

Figure 6.2. Glasstone's Thermal Pulse (From Reference [62])

Sharp of the Air Force Weapons Laboratory (AFWL) published an alternate model in 1973 [77]. The model was published as a FORTRAN subroutine, and includes variation of the thermal pulse shape with altitude. This feature was not available in the Glasstone model. This AFWL thermal power routine, called FLUX, is still in use. It is found, for example, in some computer codes that deal with nuclear survivability problems. These codes include TRAP [65], QUANTA [38], and FLEE.2 [36].

The problem of finding a statictical description of the radiated power from a nuclear weapon still remains. One approach which might be used is documented by Ostermann and Collins [75]. These authors specify a lognormal distribution for a nuclear weapon environment, using the output of a nuclear effects algorithm as the median of the distribution. The scale parameter of the lognormal (which is just the standard deviation of the log of the data) is said to be estimated by a combination of judgment and data. This technique is similar to Bridgman's approach to specifying the strength distribution [45].

As an alternate approach, one can examine the data that does exist, however sparse, and formulate the distribution of the radiated power from that alone. Choosing this as a rationale, the Glasstone model cannot be used. Although an uncertainty is stated, it is not clear how to translate $\pm 25\%$ into a statistical distribution. The AFWL FLUX routine

documentation, on the other hand, contains a good deal more information. This information allows one to construct a statistical radiated power model based on the data alone. Before proceeding with this, FLUX must be examined in a little more detail.

FLUX is a numerical model that seeks to duplicate the thermal power output of a more complex code called SPUTTER [80]. SPUTTER is a program used to dynamically model nuclear fireball phenomenology. Among the quantities available from a SPUTTER run are the thermal power and energy as a function of wavelength and time. Sharp used SPUTTER to obtain time-dependent power and energy in 35 wavelength bands covering the atmospheric transmission window. FLUX was then developed as a curve fitting technique to match the unattenuated source power and energy values as functions of time summed over the 35 wavelength bands.

FLUX therefore derives its sole credibility from the SPUTTER runs which it seeks to match. The statistical model to be developed is thus again conditional. SPUTTER is presumed to be true.

If the SPUTTER runs are taken to represent nature, then one needs to assess statistically the ability of FLUX to model SPUTTER output. The answer depends on the height of burst and yield regime. Figure 6.3 taken from Reference [77] illustrates a rather good result, while Figure 6.4

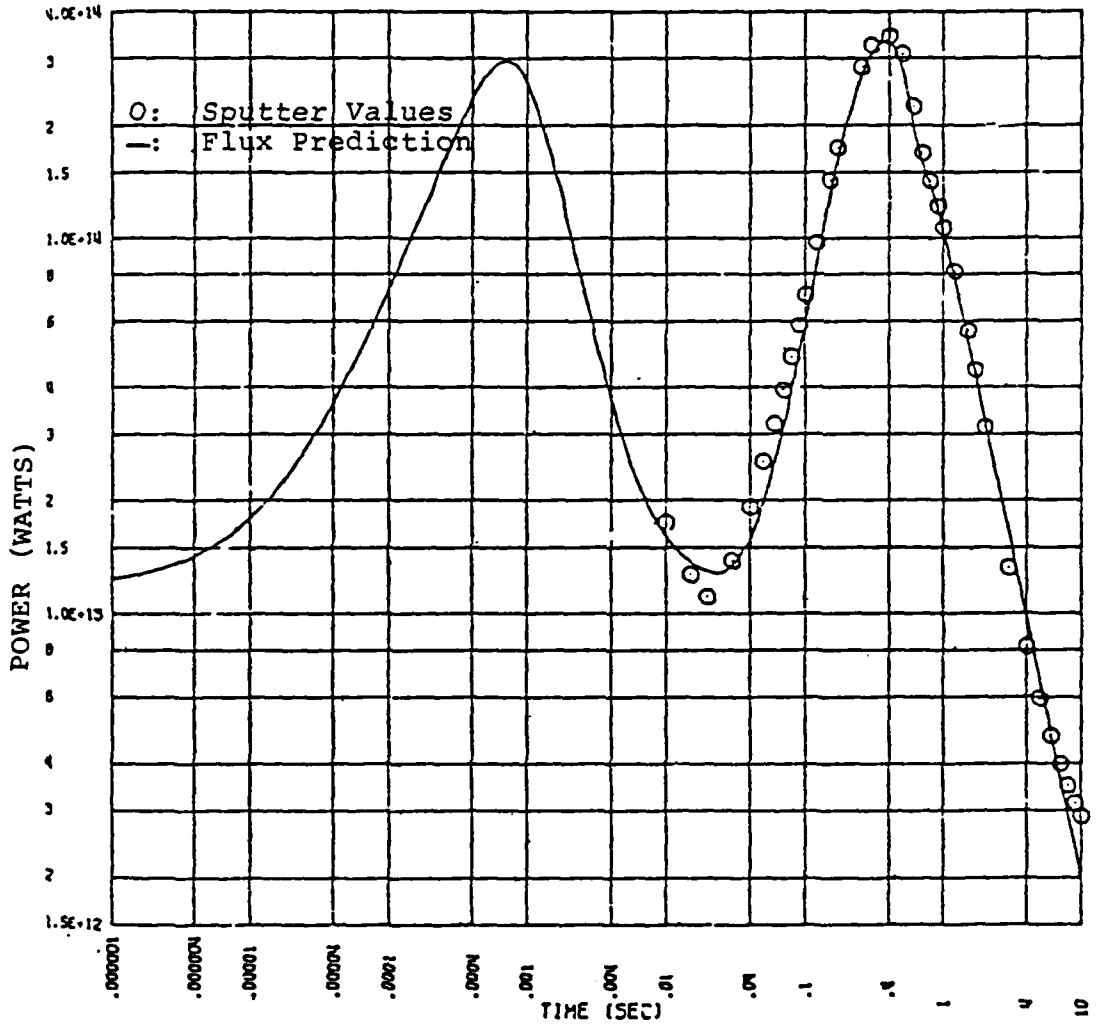

Figure 6.3. Thermal Power Versus Time -- 198 Kilotons At Sea Level (From Reference [77])

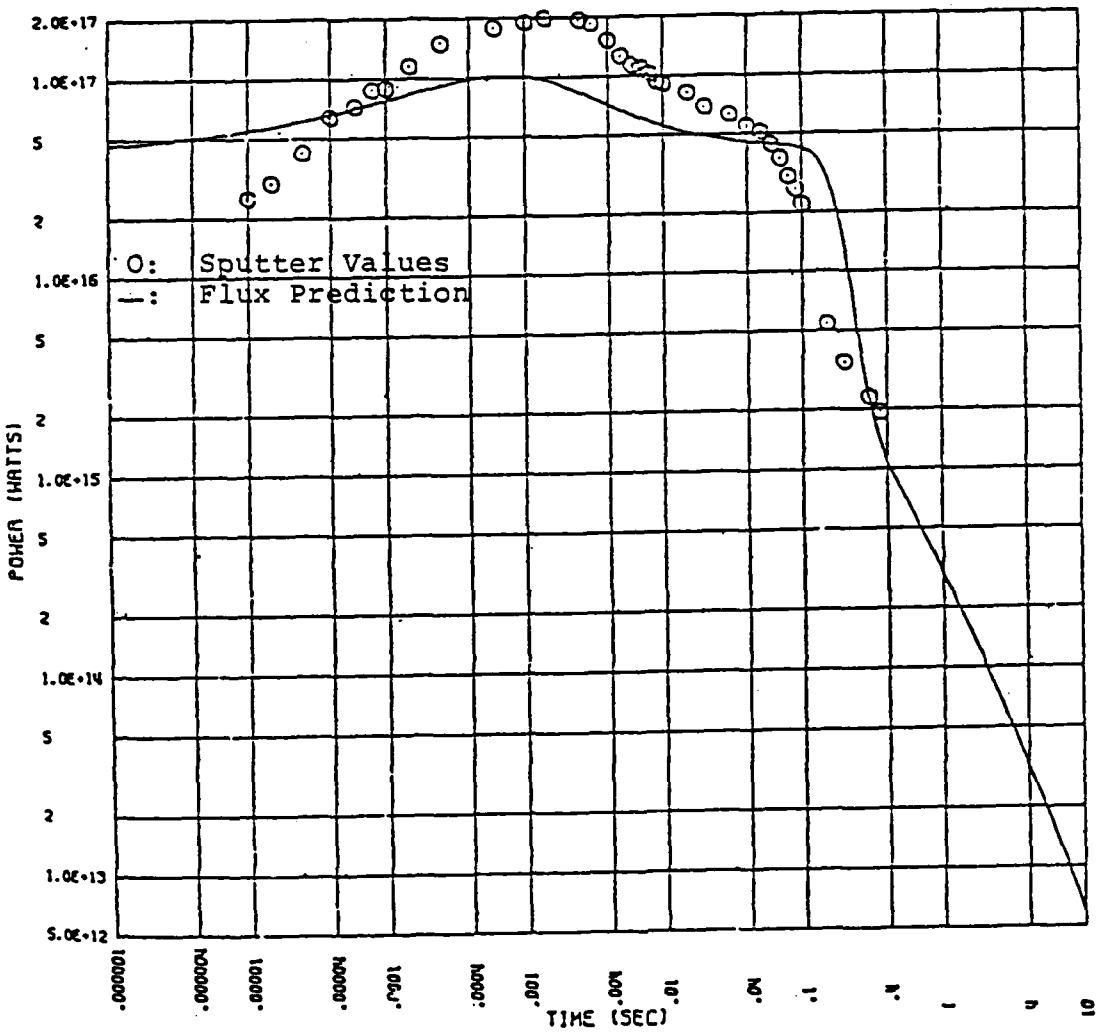

Figure 6.4. Thermal Power Versus Time - 3.8 Megatons At Sea Level (From Reference [77])

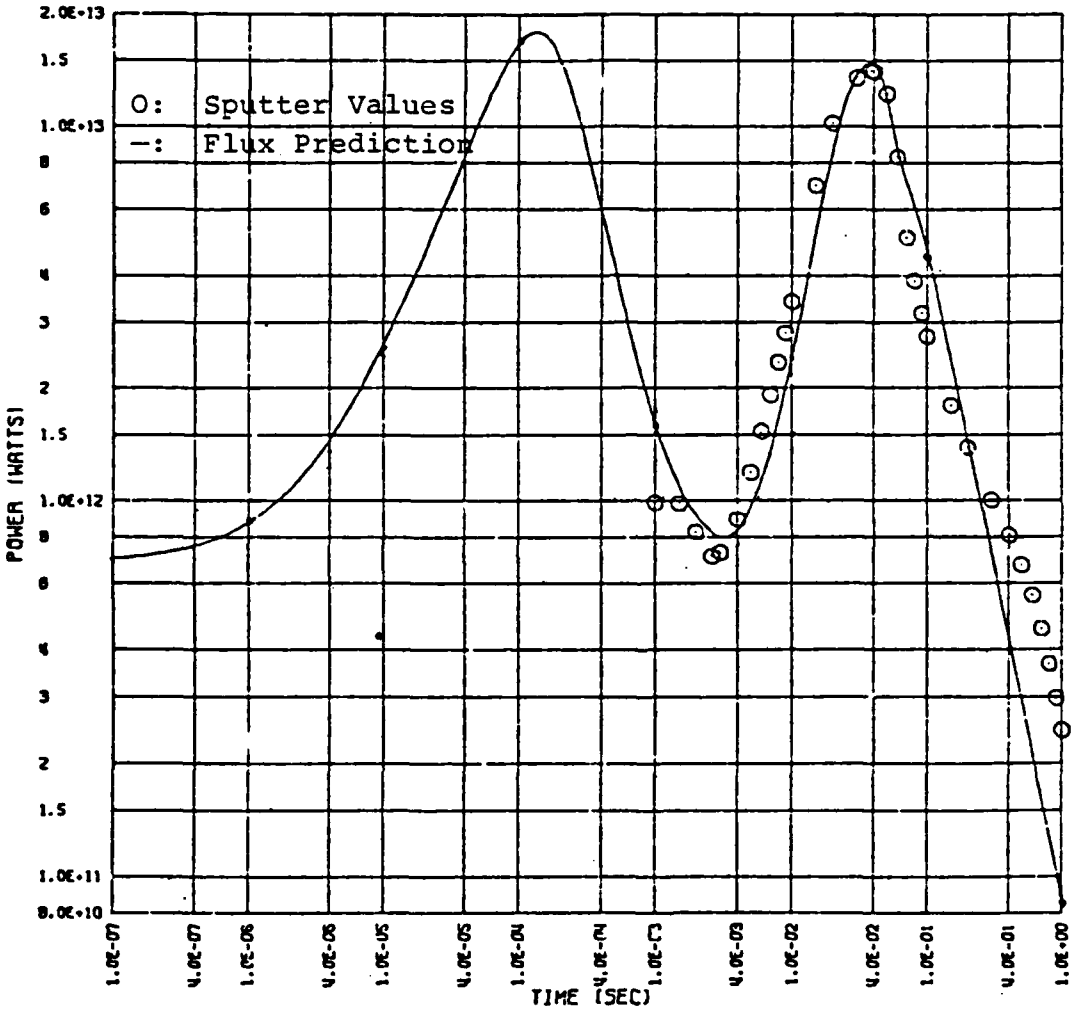

Figure 6.5. Thermal Power Versus Time - 1 Kiloton At Sea Level (From Reference [77])

illustrates a somewhat poorer one. Of special interest is Figure 6.5, which is the fit for a 1 KT burst in a sea level atmosphere. In these figures the solid line is the FLUX prediction line, while the circles are the SPUTTER output. The objective is to find a statistical measure of the quality of the FLUX fit.

One could make the lognormal assumption as done by Ostermann and Collins [75], and use FLUX output as the median radiated power value. The scale parameter for the lognormal could be estimated by the average root mean square error. That is, one might take β_p as:

$$\beta_p=\{\sum_{i=1}^{n}(\ln Y_f-\ln y_i)^2/n\}^{1/2} \qquad (6.12)$$

where y_i is a particular SPUTTER value and Y_f is the FLUX prediction at the same time. The only problem with this is that there is no guarantee that the FLUX line is the median line. This is borne out by a second examination of Figure 6.5. One sees that FLUX underpredicts SPUTTER in the late time regime in particular. A calculation of the mean residual, $\bar{R}$, defined by:

$$\bar{R}=\sum_{i=1}^{n}(\ln Y_f-\ln y_i)/n \qquad (6.13)$$

for the FLUX fit to SPUTTER run FB-21 (Figure 6.5) yields a value of -.18, showing the overall underprediction. The scale parameter as estimated in Equation 6.12 is about .50. This fit can be improved in the following way.

Since the objective of FLUX is to match SPUTTER point for point, FLUX may be thought of as a predictor variable for the SPUTTER output. Hence, if FLUX exactly matches SPUTTER, then a plot of SPUTTER versus FLUX for fixed yield and height of burst will yield a straight line with unit slope and zero intercept. The SPUTTER data for the 1 KT sea level case, with the corresponding FLUX prediction values is shown in Table VI.1. In this table, time enters in as an implicit variable. The regression of SPUTTER on FLUX is shown in Figure 6.6. As already noted, at late times FLUX underestimates the SPUTTER values. This is seen in Figure 6.6 in the low power regime. The one sigma boundaries are also shown on the plot. Linearity is pronounced, as expected, with a correlation coefficient of .96. The regression equations in the log space are given by:

$$\langle \ln Y_s \rangle = m \ln Y_f + b \tag{6.14}$$

$$\sigma_{S|F} = .3258 \tag{6.15}$$

where Y_s is the median SPUTTER output in watts, Y_f is the FLUX prediction in watts, m is .7626, b is 6.847, and $\sigma_{S|F}$ is the conditional variance of the SPUTTER output given FLUX as a predictor variable. As a comparison, the mean residual for this fit has been reduced to about 8E-6, while the root mean square error has been reduced to about .30. The least squares fit incorporates the standard assumption that the distribution of the residuals is normal.

TABLE VI.1

DATA FOR 1 KILOTON AT SEA LEVEL

Time (Sec)	Power (Watts)	FLUX Prediction (Watts)
1.0	2.444E11	8.668E10
0.9	2.977E11	1.043E11
0.8	3.660E11	1.284E11
0.7	4.539E11	1.624E11
0.6	5.581E11	2.130E11
0.5	6.709E11	2.935E11
0.4	8.049E11	4.345E11
0.3	1.000E12	7.201E11
0.2	1.383E12	1.462E12
0.15	1.792E12	2.396E12
0.1	2.744E12	4.604E12
0.09	3.166E12	5.343E12
0.08	3.864E12	6.193E12
0.07	5.056E12	7.134E12
0.06	8.269E12	8.594E12
0.05	1.223E13	1.200E13
0.04	1.402E13	1.466E13
0.03	1.348E13	1.374E13
0.02	1.019E13	8.504E12
0.015	6.941E12	5.105E12
0.01	3.392E12	2.387E12
0.009	2.804E12	1.992E12
0.008	2.342E12	1.651E12
0.007	1.909E12	1.364E12
0.006	1.525E12	1.132E12
0.005	1.185E12	9.539E11
0.004	8.886E11	8.347E11
0.003	7.248E11	7.960E11
0.0026	7.073E11	8.188E11
0.002	8.242E11	9.129E11
0.0015	9.794E11	1.092E12
0.001	9.851E11	1.602E12

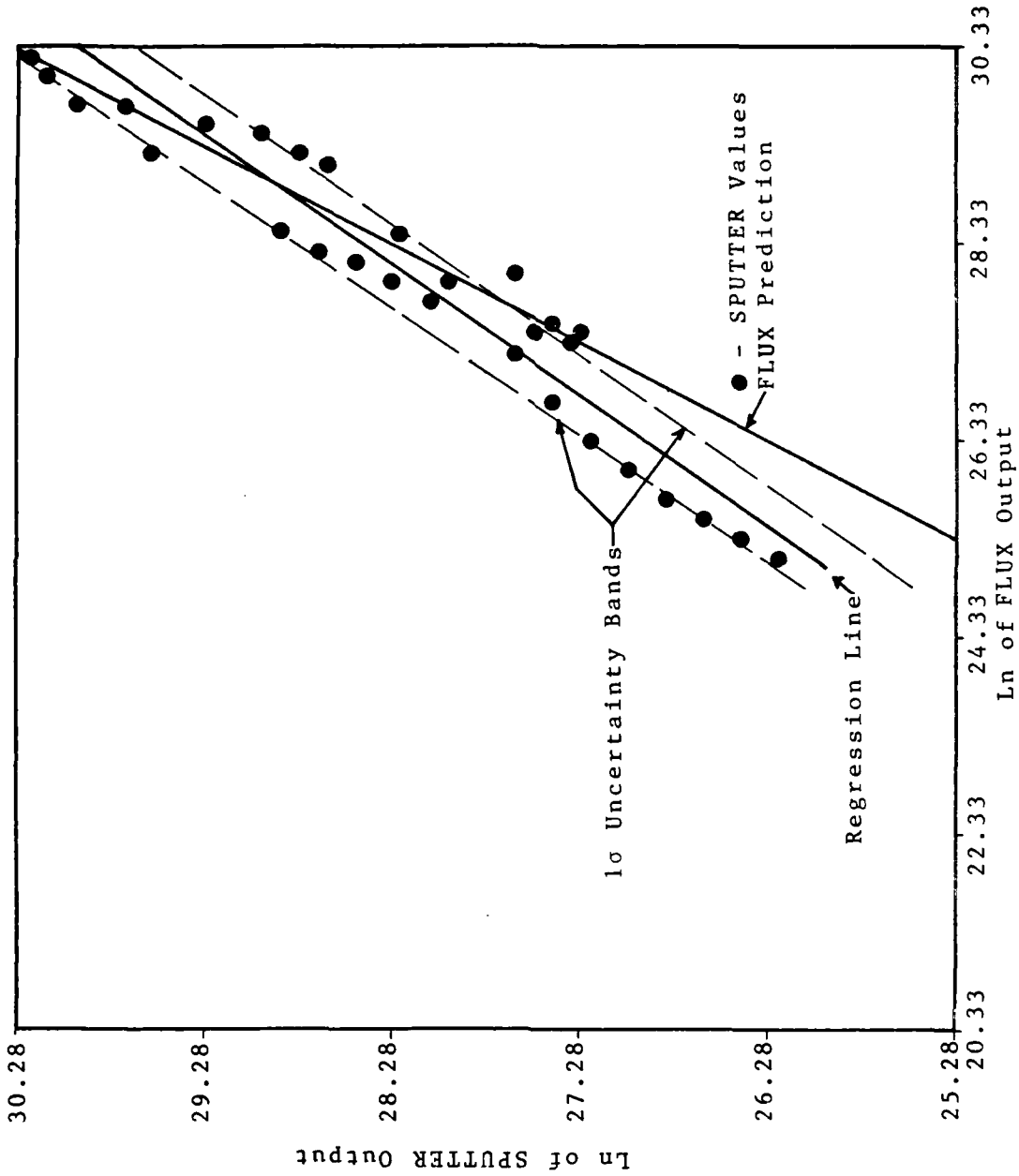

Figure 6.6. Regression of Ln SPUTTER on Ln FLUX

Since the plot is in the log space, the radiated power Y_s is a lognormal random variable with location parameter α_p and scale parameter β_p given by:

$$\alpha_p = \langle \ln Y_s \rangle \tag{6.16}$$

$$\beta_p = \sigma_{S|F} \tag{6.17}$$

The statistical model of the radiated power is thus determined. The explicit expression for a sample value of the relative radiated power can be written in terms of the above parameters. Given z_i, a value of the standard normal variate, $f_i(\tau)$ is given by:

$$f_i(\tau) = \exp(\alpha_p(\tau) + \beta_p z_i) \tag{6.18}$$

The i subscript denotes the statistical meaning of the particular value of f_i in terms of the standard normal variate z_i. In particular,

$$Pr\{F \leq f_i\} = Pr\{Z \leq z_i\} \tag{6.19}$$

Equation 6.18 may be directly inserted into Equation 6.11 to complete the expression for the distribution of the temperature in a thin skin assembly.

With a statistical model for the temperature in a thin skin completed, the stress distribution is known. The other half of the problem is the determination of the strength distribution. The choice of the strength variable depends on the failure mode of interest. Melt mode failures will be examined in the next section.

Thermal Vulnerability Modeling

The statistical description of the temperature in a thin skin has been completed. This may be the stress variable of interest, but it may also appear in the strength function, depending on the failure model chosen. The choice of the strength variable also depends on the failure mode of interest. Two failure models are considered below. In one, melt mode failures are considered. In the other, the temperature of the skin enters into both the stress and strength distributions.

Melt-Mode Vulnerability. In the previous chapter, methods from the nuclear survivability literature [54,45] were compared with data that allowed one to infer actual strength distributions for several aircraft components. Aircraft must be designed for a certain amount of gust hardness since atmospheric turbulence is a natural aircraft environment. It is not surprising, then, that enough data exists in regards to mechanical loading to formulate strength distributions directly from test data [22]. Some have even suggested that because of this, modern day aircraft have some inherent hardness to nuclear gusts [72].

In contrast, aircraft are not normally designed for thermal environments like that from a nuclear weapon. Consequently, no direct data exists from which to infer a strength distribution. There is then no choice but to model the strength function by choosing values of skin tempera-

tures that are considered critical. In Reference [54] two such values are chosen--a sure-safe (SS) temperature, T_{SS}, and a sure-kill (SK) temperature, T_{SK}. The sure-safe temperature is that temperature which results in a 20% reduction in the modulus of elasticity. The sure-kill temperature is the melt-point of the material. Two strength distributions will be considered. As in the case for blast, a cookie-cutter strength distribution will be called Model 1 while the a priori lognormal strength distribution will be referred to as Model 2.

Cookie-Cutter Failure Distribution. The structure fails upon encountering the SK temperature, and does not fail otherwise--i.e, the failure probability density function (PDF) is a Dirac delta function centered at T_{SK}.

A Priori Lognormal Failure Distribution. The probability of failure for the skin structure is .98 if the SK temperature is encountered; it is .02 if the SS stress value is encountered; the distribution of failures is lognormal [45].

These two distributions are illustrated in Figure 6.7. The stress space is now temperature. The circles represent Model 2, while the solid line represents Model 1. Model 1 yields the familiar cookie-cutter plot in the absence of any statistical model of the stress. However, since a statistical model of the stress does exist, the failure probability will be a continuous function of range. For Model 1, it is

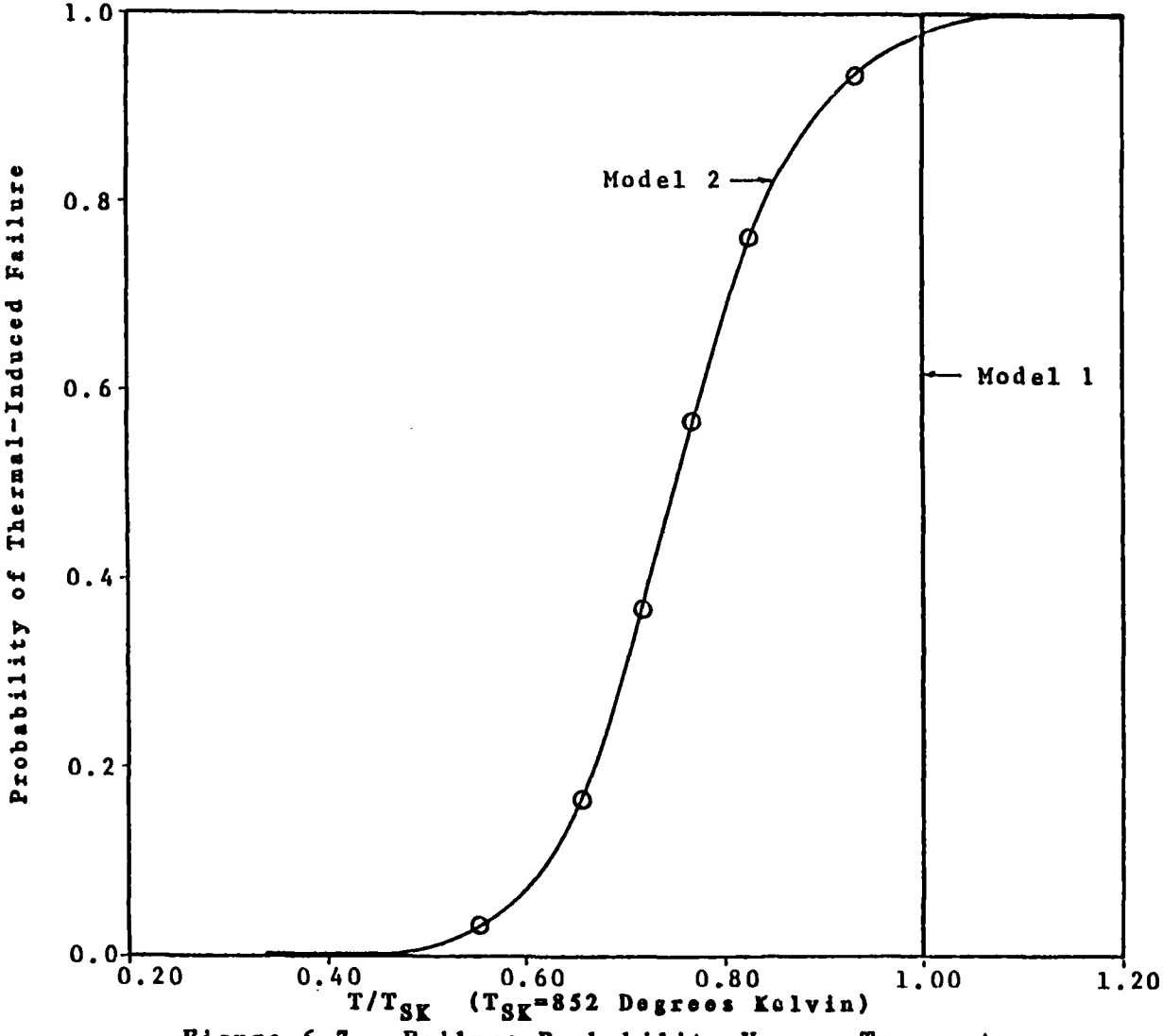

Figure 6.7. Failure Probability Versus Temperature

given by:

$$p_f(r)=1-F_s(T_{SK}) \tag{6.20}$$

where $F_s(T)$ is the cumulative distribution function (CDF) of the temperature (the stress variable) in the thin skin at the time of interest.

The resultant vulnerability of the skin is shown in Figure 6.8 for both Model 1 and Model 2 strength distributions. The cookie-cutter damage distribution is not very different from the lognormal one. The failure probability is a steep function of range, dropping from .98 to .02 in the span of 100 meters even for the lognormal assumption. The reason for this is the rapid decrease in peak temperature with range. This is true even if the structure is not cooled. If it is, the decrease is even faster. Thus, one sees that cookie-cutter techniques can work well depending on the rate of change of the critical response variable with other variables in the problem.

Before leaving the thermal vulnerability problem, one can consider an alternate failure mode. In particular, one can examine the effects of combined gust/thermal loading on the mechanical integrity of a structure. This is the last topic, and is considered in the next section.

Combined Blast/Thermal Vulnerability. The fundamental idea behind most thermal vulnerability calculations is to find the amount of heat required for some specific effect. The topic of yielding of skin panels due to thermal loads

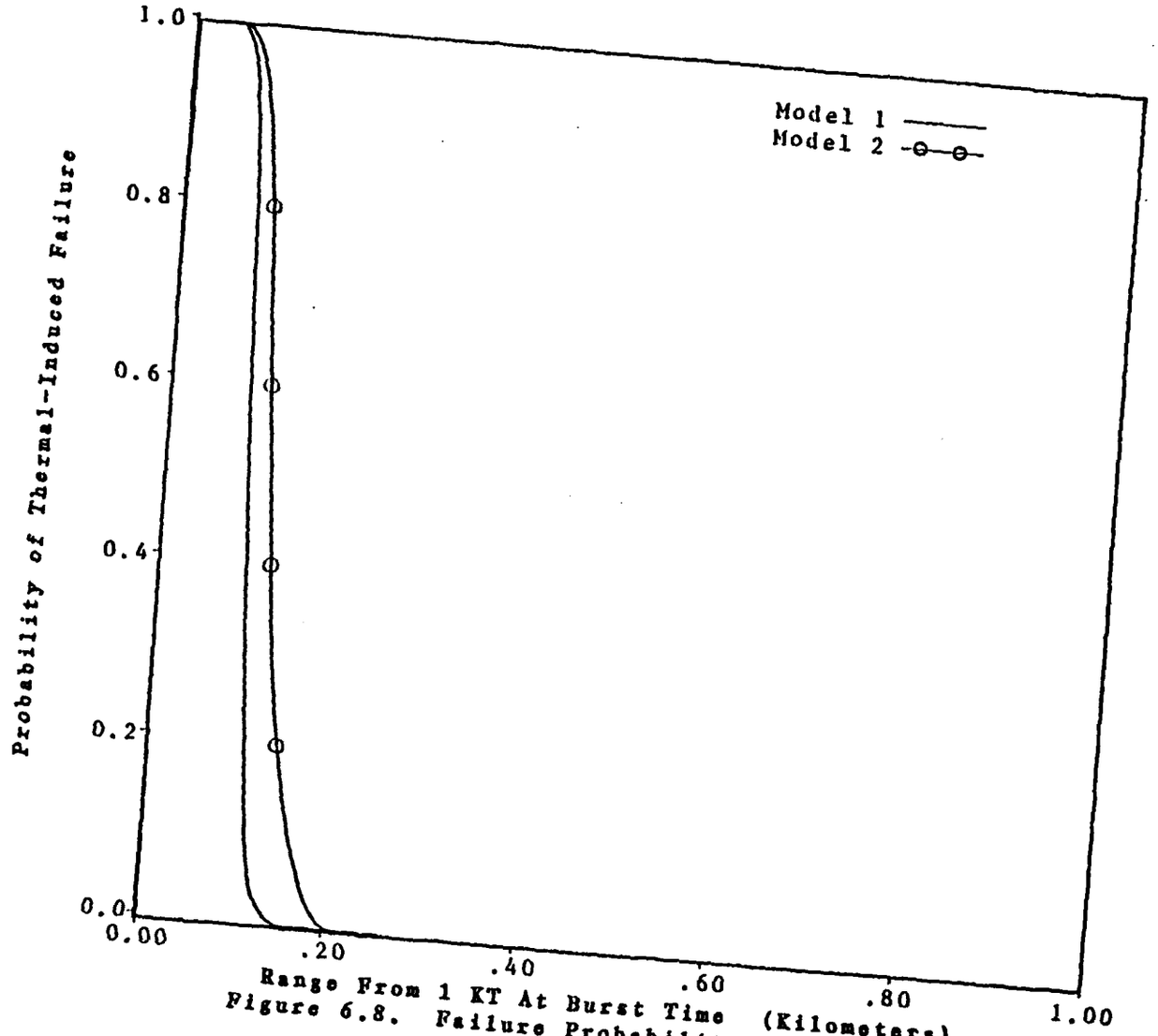

Figure 6.8. Failure Probability Versus Range

combined with internal pressurization loads is treated using Method 2 of Reference [54]. This problem demonstrates that a combination of conditions can precipitate failure rather than the primary weapon effects acting alone. On the other hand, a given failure mode might depend on more than one weapon effect. In the alternate failure model described below, the combined effects of blast and thermal in causing yielding of wing skin panels is investigated. This will illustrate the utility of the stress-strength interference theory technique in treating such problems.

Stress On A Skin Panel. A stress analyst would attempt to calculate the stresses in the skin rather than use the SS and SK specifications of the previous section [43]. A representative wing section is shown in Figure 6.9. Treated as a simple box beam with constant bending stress [76], and using a thermal model from a classical text like Gatewood [61], one can show that the stress in the lower section at position z and time t is given by:

$$\sigma_x(z,t)=\sigma_g(z,t)+\sigma_{th}(z,t) \tag{6.21}$$

where $\sigma_g(z,t)$ is the stress component due to the gust loading and $\sigma_{th}(z,t)$ is the stress component due to the thermal loading from the nuclear detonation. These two terms are given by:

$$\sigma_g(z,t)=-\sigma_{1g}N_L z/c \tag{6.22}$$

$$\sigma_{th}(z,t)=\sigma_{th1}(z,t)+\sigma_{th2}(z,t)+\sigma_{th3}(z,t) \tag{6.23}$$

The thermal stress terms [61] are given by:

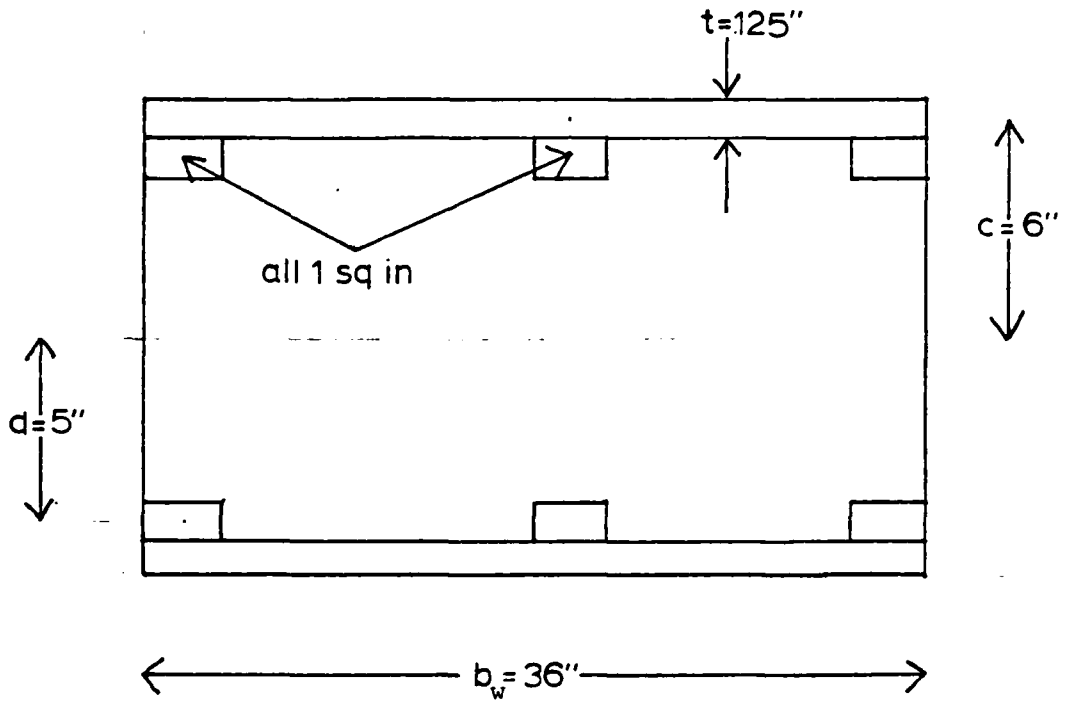

Figure 6.9. A Box-Beam Wing Model

$$\sigma_{th1}(z,t) = -\alpha_1 E(T)\Delta T(z,t) \tag{6.24}$$

$$\sigma_{th2}(z,t) = (\alpha_1 b_w E(T)/A_x)\int_{-c-\epsilon}^{-c+\epsilon} \Delta T(z,t)dz \tag{6.25}$$

$$\sigma_{th3}(z,t) = (\alpha_1 b_w z E(T)/I_x)\int_{-c-\epsilon}^{-c+\epsilon} z\Delta T(z,t)dz \tag{6.26}$$

The variables in the above equations are described as follows. σ_{1g} is the allowable design stress, taken as 6.891E7 pascals (10^4 psi). N_L is the load factor on the wings (dimensionless). The coordinate z is the location where the stress is desired (meters) measured relative to the center of the assembly. The variable c is the midpoint of the skin as measured from the center and is taken as .1524 meters (6 inches). ϵ is the half-thickness of the skin, taken as 1.588E-3 meters (.0625 inch). α_1 is the coefficient of linear expansion (2.286E-5 m/m-^{o}-Kelvin). E(T) is the modulus of elasticity (in pascals) at temperature T (in ^{o}-Kelvin). The room temperature modulus of aluminum is taken as 6.891E10 pascals (10^7 psi). As previously discussed, T is the temperature of the skin in degrees Kelvin. The term ΔT is given by:

$$\Delta T(z,t) = T(z,t) - T_0(z,t) \tag{6.27}$$

where T(z,t) is the temperature at location z and time t and T_0 is the ambient temperature in degrees Kelvin. The dimension b_w, as shown in the figure, is the chordwise length, taken as .9144 meter (36 inches). Finally, A_x is the cross-sectional area (15 square inches or 9.677E-3 meter^2), while I_x is the area moment of inertia (474 in^4 or 1.973E-4 meter^4).

Now, using the thin skin approximation as before, the temperature response of the skin is as shown in the previous section. The bottom skin panel is heated uniformly to a peak temperature T_p so that the temperature profile with z is given by:

$$T(z)=T_p \quad \text{w} \quad -c-\epsilon \leq z \leq -c+\epsilon \tag{6.28}$$

$$T(z)=T_0 \quad \text{elsewhere} \tag{6.29}$$

where ϵ is the skin half-thickness, as previously defined.

With the above temperature profile, the integrals in Equations 6.25 and 6.26 are calculable in closed form. The results for the lower wing station (z=-c) for the geometry of Figure 6.9 lead to the equation:

$$\sigma_x=\sigma_{1g}N_L-.3582\alpha_1 E(T_p)\Delta T_p \tag{6.30}$$

Equation 6.30 is a function of two random variables--N_L, the load factor on the wings, and T_p, the peak temperature in the thin skin. This equation is the stress response of the skin. The response is dependent on both the gust loading and the thermal loading caused by the nuclear weapon. Even though this is a function of two random variables, it is not clear that it needs to be treated that way. The gust loading and peak thermal loading can appear at very different times, and this would effectively decouple the two effects.

The relative vulnerabilities of the four parts of the box beam are discussed in more detail in Appendix E. In fact, the analysis there shows that the lower skin is not

the most vulnerable assembly. However, that part of the beam is interesting in that the gust dominates the stress distribution, while the thermal dominates the strength distribution. Since the thermal contribution to the load stress is slight, one can first consider the case of gust loading only.

The Case of Gust Loading Only. As a first approximation, Equation 6.30 is evaluated when the thermal environment is absent. This reduces the stress function to:

$$\sigma_x = \sigma_{1g} N_L \tag{6.31}$$

The strength function is taken as the yield point of 6061-T6 aluminum. That is, the critical, or sure-kill stress value is given by:

$$\sigma_{sk} = 2.756E8 \text{ pascals } (40{,}000 \text{ psi}) \tag{6.32}$$

Since this is a cookie-cutter strength distribution, the reliability interference integral reduces to the result:

$$p_f = 1 - F_s(\sigma_{sk}) \tag{6.33}$$

where s is the stress variable, and is just σ_x as given in Equation 6.31. The overlay of the wing stress model with the previously considered cookie-cutter and lognormal gust vulnerability models are shown in Figure 6.10. Model 1 is the cookie-cutter model for gust loads discussed in Chapter V, while Model 2 is the a priori lognormal model, and Model 3 is the results based on Chenoweth's data. The skin stress model just developed (represented by the □'s in the figure) is a bit more conservative than the other models considered.

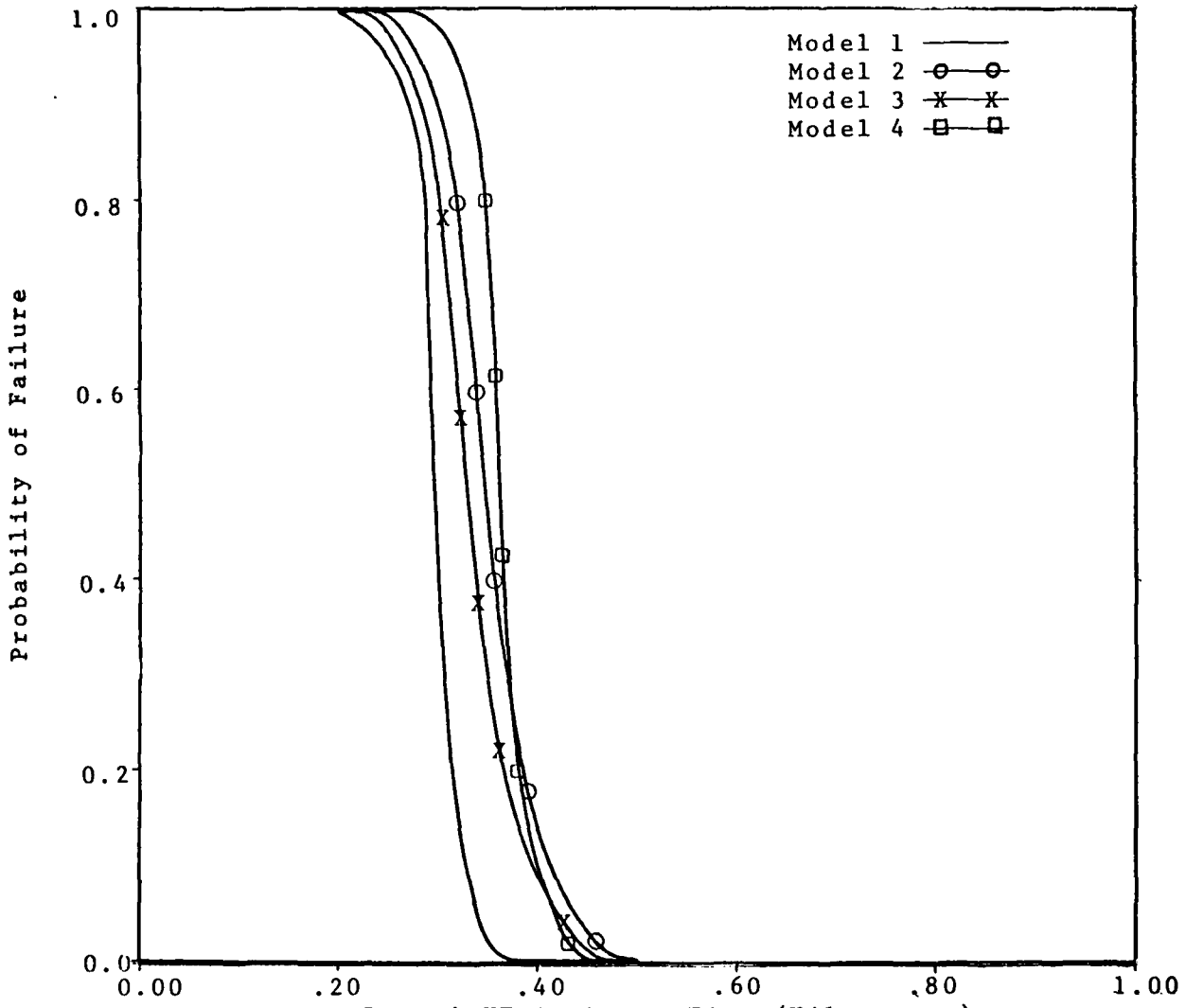

Figure 6.10. Gust Load Failure Probability Versus Range

This is in part because it is just another cookie-cutter damage model, but with a lower sure-kill specification. That is, the sure-kill load factor is taken as 4 instead of 6.75. This value of 4 is closer to what the authors of STRAT-SURVIVOR [42] would call the unbiased cookie-cutter damage specification. In any case one sees that a reasonable independently derived failure model gives about the same results as the others considered.

The Thermal Stress Contribution. Equation 6.30 can also be evaluated with the peak thermal environment present, and the aircraft in a straight and level flight condition. In that case, and for the geometry previously indicated, the response equation reduces to:

$$\sigma_x = \sigma_{1g} - .3582\alpha_1 E(T_p)\Delta T_p \qquad (6.34)$$

The thermal stress contribution adds a compressive stress term to an existing tensile load. The thermal stress contribution is quite small for the lower skin assembly. This is because not much heating has taken place by the time the blast wave arrives. For example, the statistical distribution of temperature at blast arrival time (.24 sec) is shown in Figure 6.11 for a target at 200 meters range. This variable is statistically distributed at each time step due to the statistical variation in the calculation of the thermal power (Figures 6.3-6.5). The position at 200 meters range is well inside the sure-kill region for gust acting alone. The illustration in Figure 6.11 shows a temperature

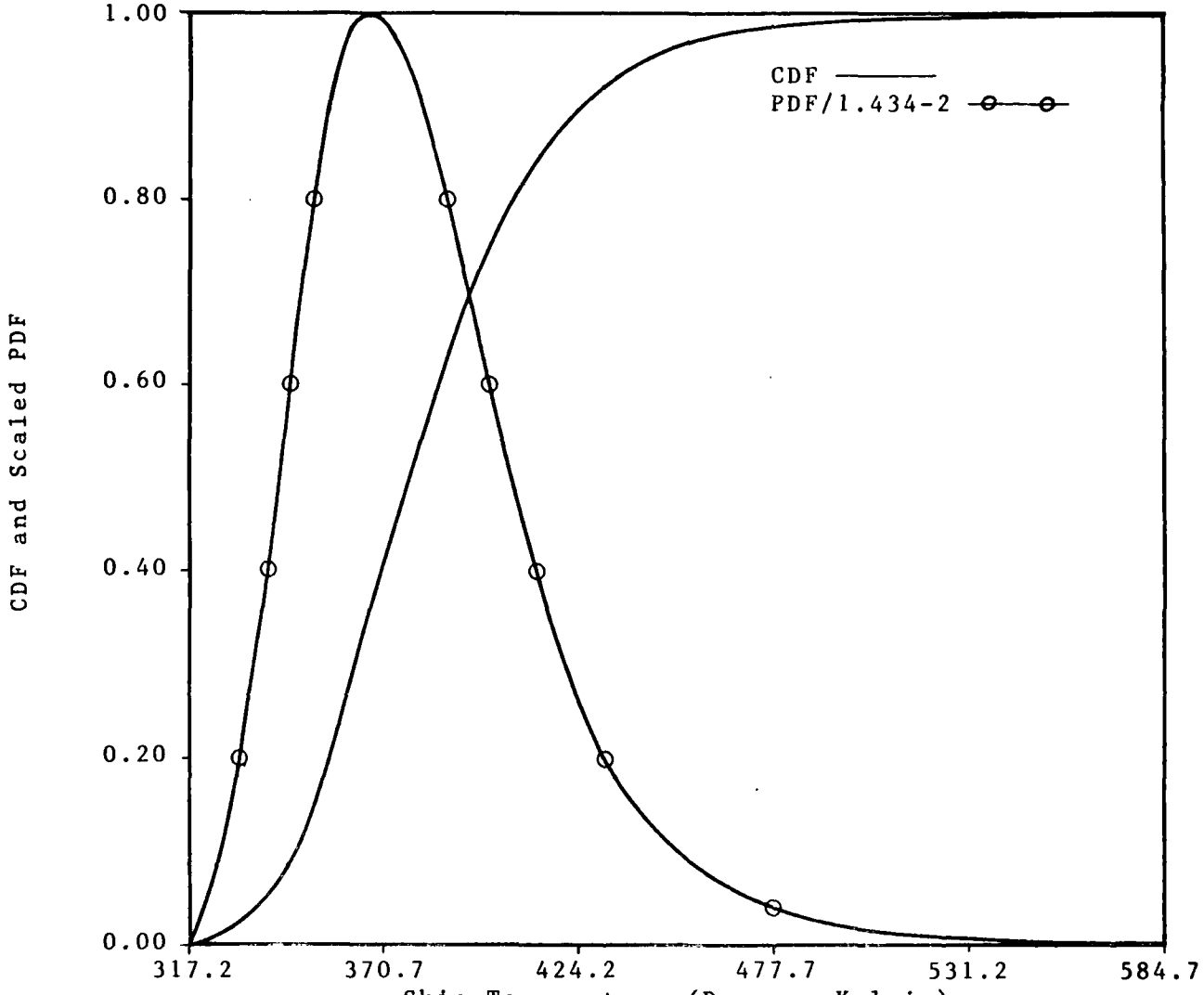

Figure 6.11. Statistical Distribution of Peak Temperature at 200 Meters Slant Range

maximum in the right hand tail of the distribution at less than 585^{o}.

This does not mean that a gust/thermal synergism does not exist. It only means that it does not exist in the stress function for the lower skin. The behavior of the strength function there is examined next.

Gust Dependent Stress--Thermal Dependent Strength. Even though the thermal loading does not contribute much to the stress function, a combined effects problem can still exist. The yield point of the material has been treated so far as a constant. Hence, the strength distribution has been considered as a cookie-cutter in the stress space. However, the yield point can vary with temperature. A possible variation of yield strength with temperature is illustrated in Figure 6.12. The authors of Reference [79] state that the degradation of yield strength parallels that of the elastic modulus out to about 480^{o} Kelvin. At that point, the length of time at a given temperature ("soak time") becomes an important variable as well. Since 480^{o} is a rarely observed temperature for the 1 KT scenario, the strength function and the elastic modulus can both be modeled by:

$$E(T)=E(T_0)g(T) \tag{6.35}$$

$$\sigma_{SK}(T)=\sigma_{SK}(T_0)g(T) \tag{6.36}$$

where g(T) is the approximately linear function shown by the dashed line in Figure 6.12, and $\sigma_{SK}(T_0)$ is given by Equation

6.32.

When the temperature dependence for the strength variable is taken into account, the previous cookie-cutter strength distribution is altered. The statistical uncertainty in the temperature of the skin propagates into the temperature dependence of the yield point of the material. A set of calculations was performed to determine the strength distributions from 200 to 500 meters at blast arrival time. The resulting continuous strength distributions are shown in Figures 6.13, 14, and 15 for range positions of 200, 400, and 500 meters respectively. The strength of the part is statistically distributed because the temperature of the part is (Figure 6.11) and the strength depends on the temperature as shown in Equation 6.36. Since the distribution of temperatures changes at each range step the strength distribution does also. For the close-in case (200 meters) the original step function damage distribution of Equation 6.32 centered at 2.756E8 pascals has been transformed into a continuous function with a long left-ward tail. The mid-range strength distribution (400 meters) shows a cookie-cutter shape beginning to form, with the most probable failure point being the room temperature failure point of 2.756E8 pascals. The cookie-cutter limit has essentially been reached in Figure 6.15 when the aircraft is 500 meters from ground zero at burst time. Hence, even an original cookie-cutter assumption (as in Equation 6.32) can lead to

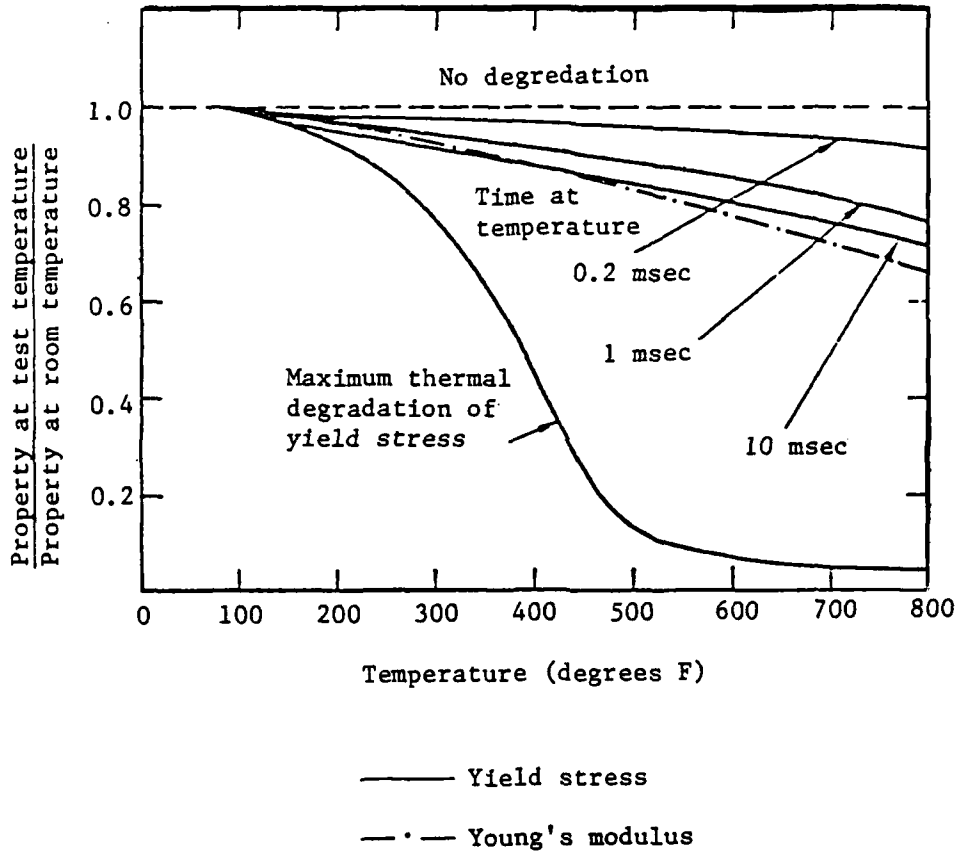

Figure 6.12. Degradation of Strength Properties With Instantaneous Heating (From Reference [79])

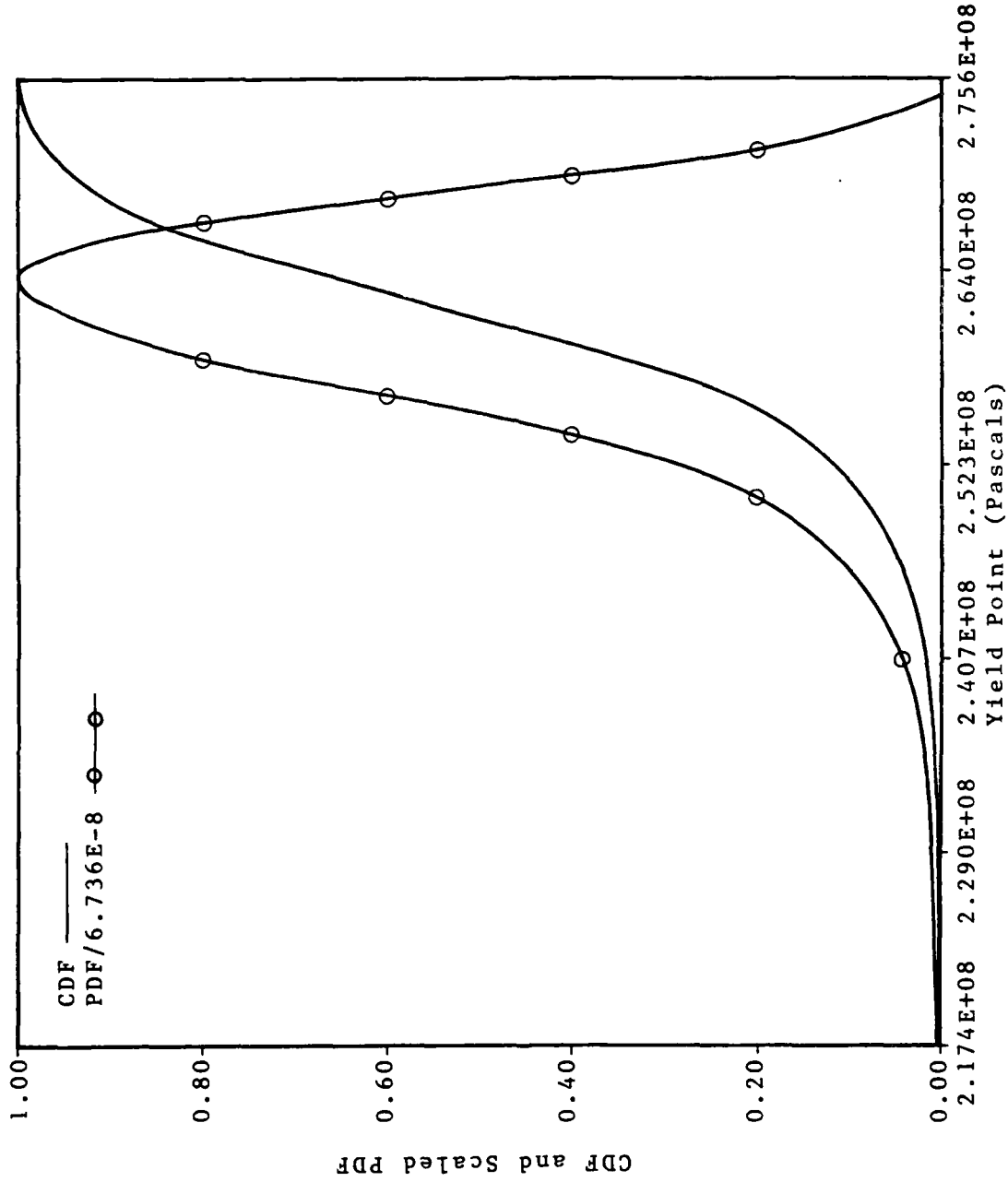

Figure 6.13. Statistical Distribution of Yield Strength at 200 Meters Slant Range

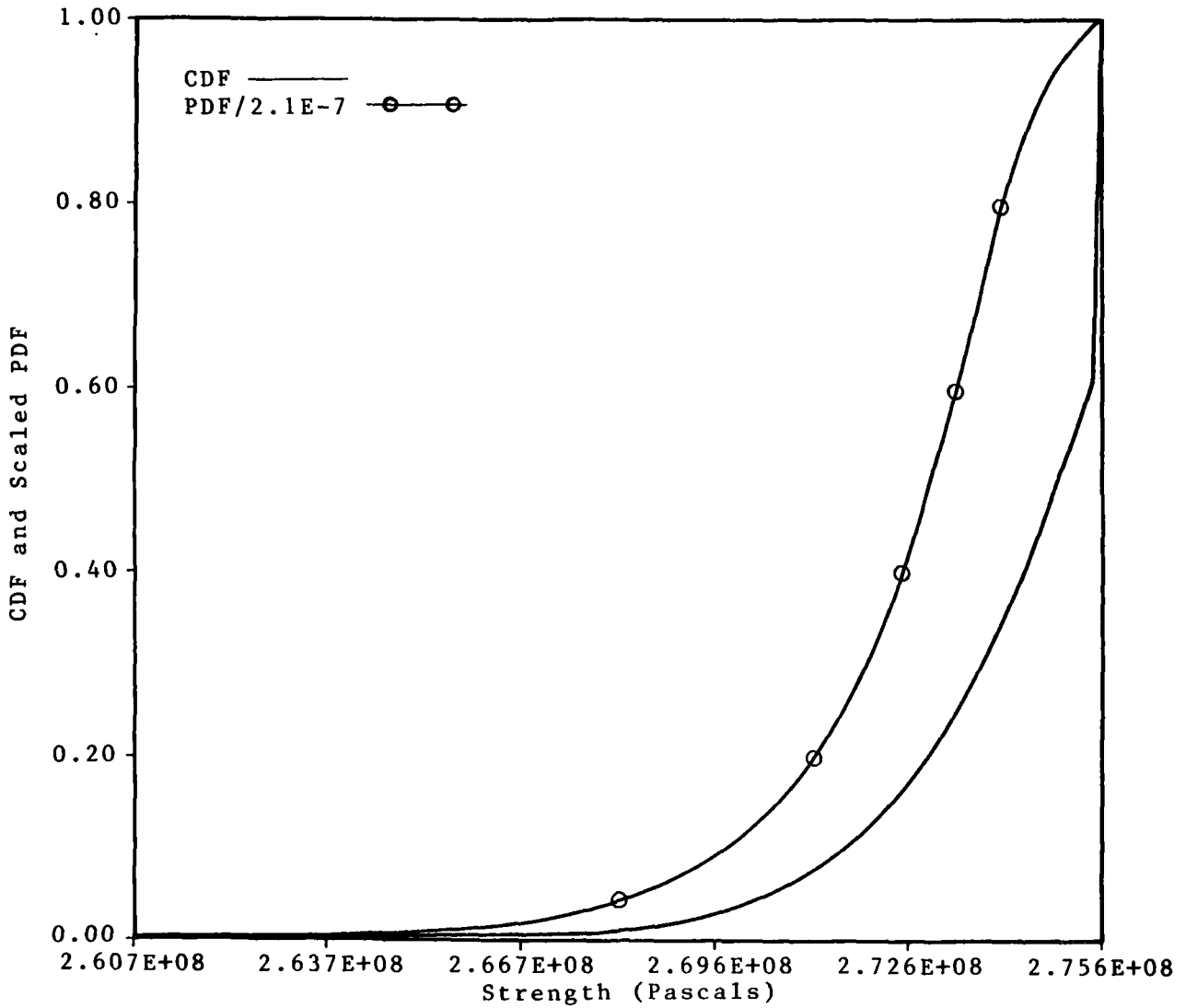

Figure 6.14. Statistical Distribution of Yield Strength at 400 Meters Slant Range

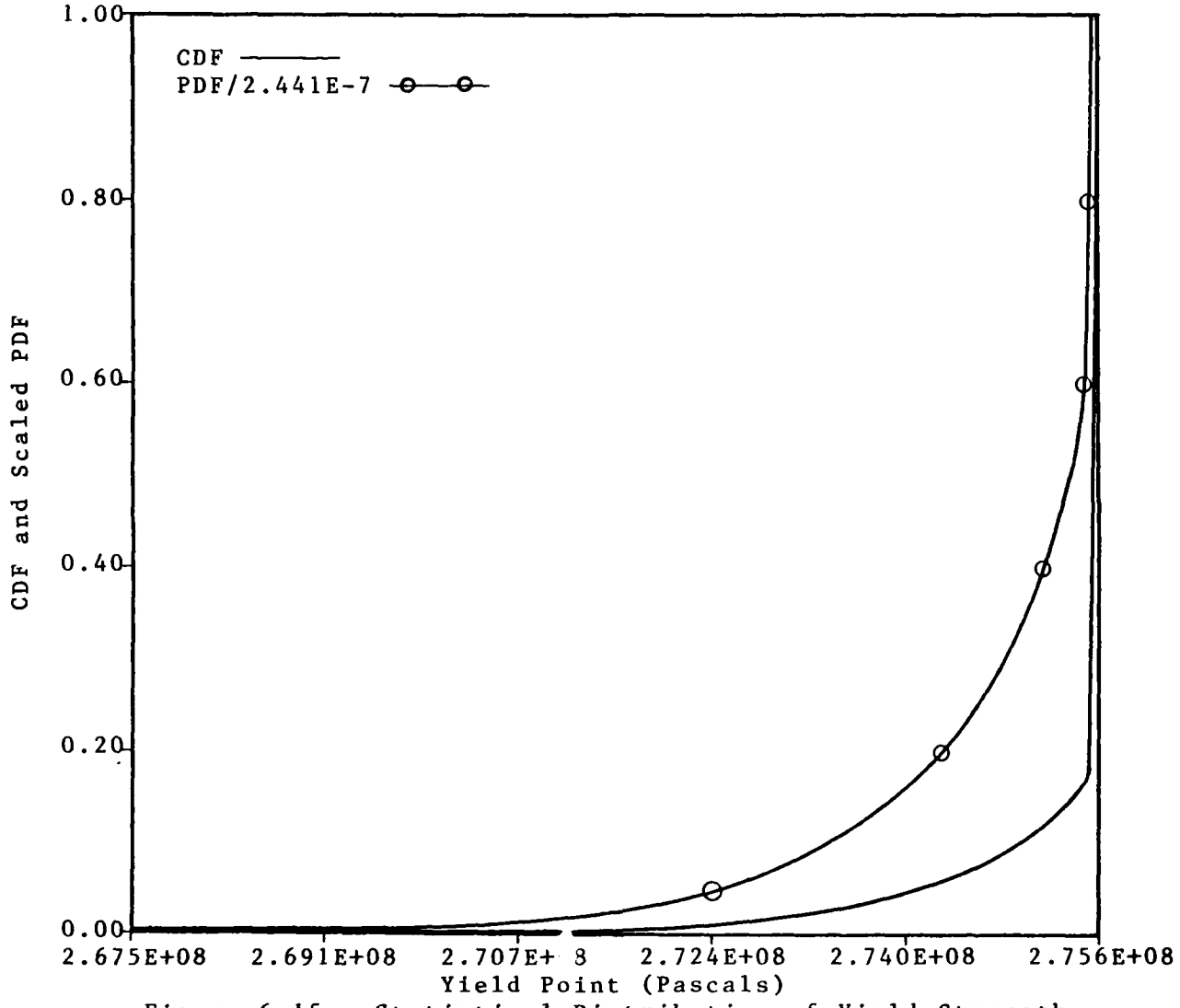

Figure 6.15. Statistical Distribution of Yield Strength at 500 Meters Slant Range

continuous probability distributions when the statistical nature of other variables is introduced.

The failure probability at each range point depends on more than the strength distribution alone. It is the combination of stress and strength at every instant of time that governs the failure probability. The stress function is given by Equation 6.31 for the lower skin since the gust loading dominates the stress, as just discussed. The load factor, N_L, is the random variable that gives the stress function its random character. The stress distributions for range positions of 200, 400, and 500 meters are shown respectively in Figures 6.16 through 6.18.

With both distributions determined, one from the nuclear blast effects, and the other from the thermal effects, the failure probability can be directly calculated by the methods previously described and illustrated. The failure probability as a function of range is displayed in Figure 6.19. The results are nearly indistinguishable from the approximation that considered gust effects only and the room temperature value of the yield stress. This is because very little heating has taken place at gust arrival time. One should not infer that gust/thermal combinations are never important, since results may be different for different parts of the beam and for other scenarios. However, the results do show the utility of the new nonparametric approach to stress-strength interference theory when direct

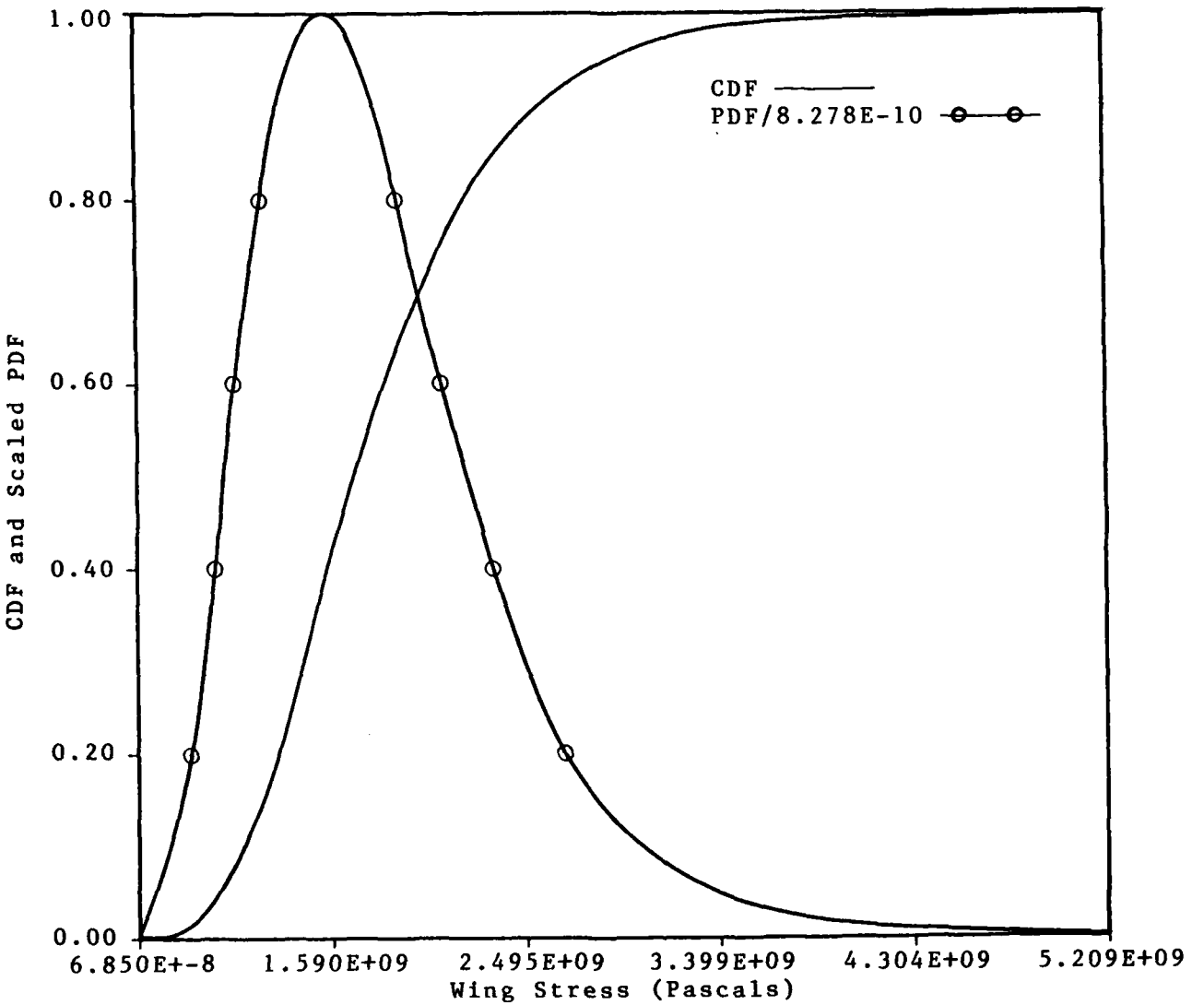

Figure 6.16. Statistical Distribution of Wing Stress at 200 Meters Slant Range

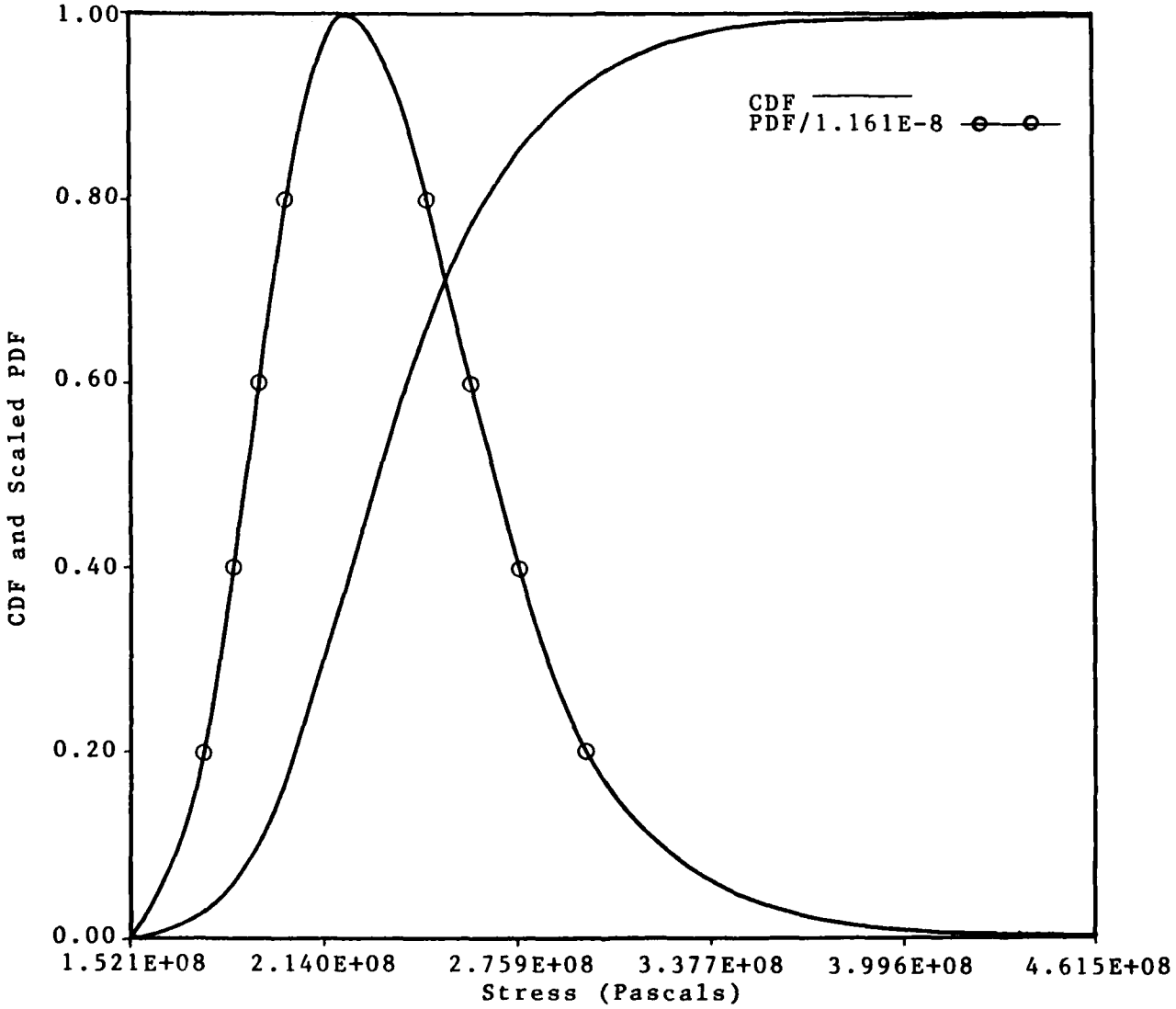

Figure 6.17. Statistical Distribution of Wing Stress at 400 Meters Slant Range

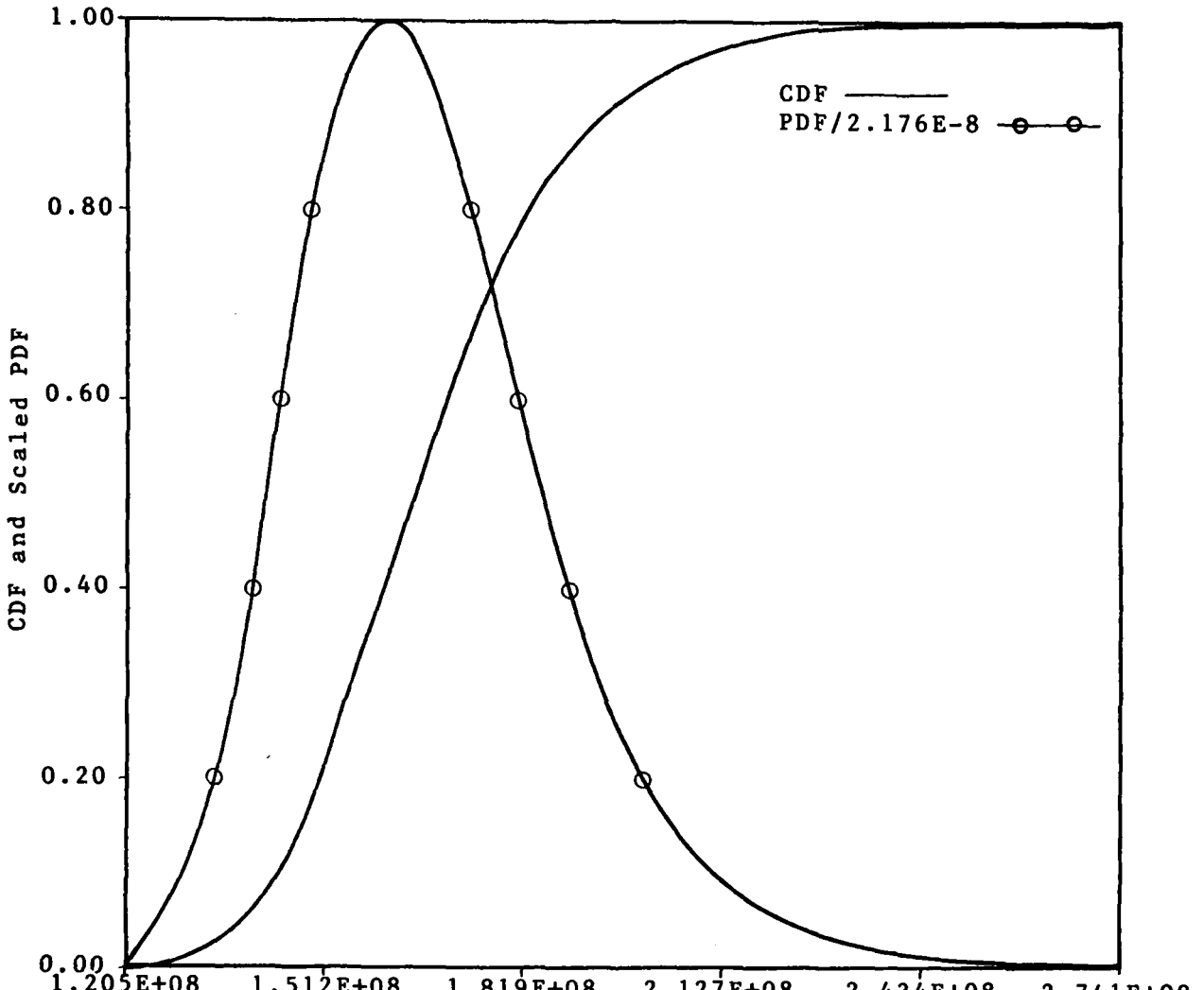

Figure 6.18. Statistical Distribution of Wing Stress at 500 Meters Slant Range

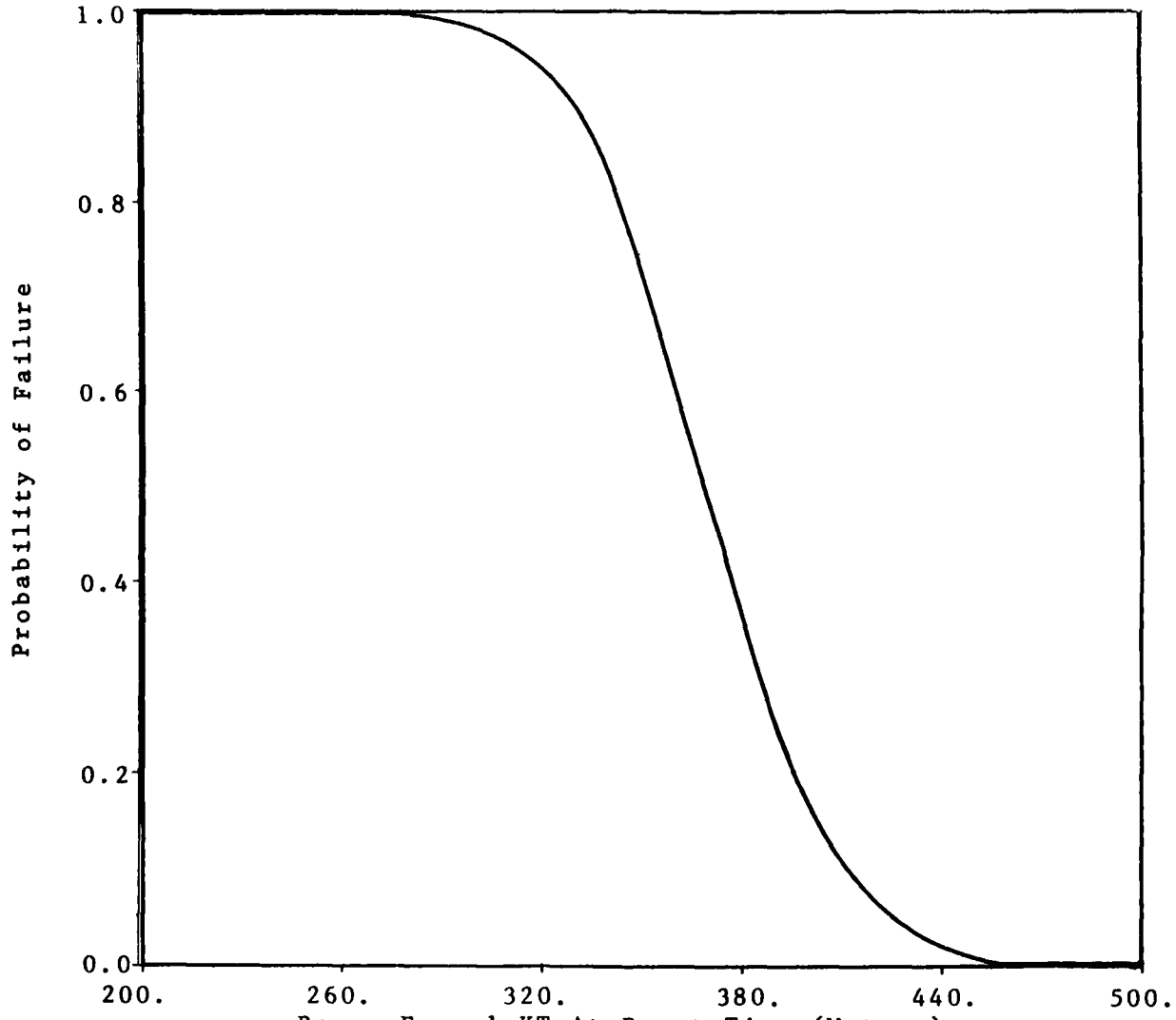

Figure 6.19. Gust/Thermal Failure Probability Versus Range From 1 Kiloton Burst

service data is not available.

Summary

Aircraft vulnerability to the nuclear thermal pulse from a low yield weapon has been considered. A search of the available data sources for thermal effects on aircraft yielded no direct information on either stress or strength distributions. A deterministic model of the stress was developed instead. The statistical variation in one of the input quantities to this model was determined from the nuclear effects literature. Stress distributions were then inferred by finding the distributions of functions of this random input variable. Melt mode failures were examined and the failure probability with range calculated. The results show little variation between a cookie-cutter and a log-normal strength distribution model. A combined effects problem was also analyzed. In this case the blast environment was found to dominate the stress distribution, while the thermal effect determined the strength distribution. The failure probability as a function of range was again calculated, with little synergistic effect noted. These problems further illustrate the utility of the nonparametric interference theory technique in assessing nuclear survivability.

VII. Summary And Recommendations

Summary

A new approach for assessing the survivability of aircraft components in nuclear blast and thermal environments has been presented. A nonparametric technique for finding the distribution of functions of random variables has been discovered and presented. This procedure allows one to rigorously determine the strength and stress distributions for aircraft components exposed to nuclear blast and thermal environments. If direct service histories are not available, strength distributions may still be inferred by considering the statistical variation in the inputs to a strength function. Similarly, stress distributions may be inferred even though direct stress measurements are not possible. The reliability interference integral can then be solved resulting in continuous failure probabilities as a function of range from a nuclear weapon. In the following paragraphs, each chapter is briefly reviewed, and recommendations for future work presented.

Chapter II provided a review of nuclear survivability/vulnerability methods, both deterministic and probabilistic. Deterministic methods do not provide for continuous damage probabilities with range. Probabilistic methods of two broad types have been used. Users of the first type model failure probabilities directly with range,

while users of the second model strength and stress functions as random variable processes. The latter is the basic approach of mathematical reliability theory.

Chapter III provided a brief review of mathematical reliability theory, including stress-strength interference theory and the interference integral. Engineering determinism was found to be a special case of this theory. That is, cookie-cutter failure distributions result if Dirac delta functions are used to represent the probability density functions for the stress and strength random variables. Even though these theoretical considerations are attractive, stress-strength interference theory is difficult to apply to large engineering systems. Three problems exist--(a) the difficulty of developing a system reliability model from component models, (b) the analytic difficulty of finding distributions of functions of random variables, and (c) the limited amount of data available. Some of the current methods of approaching these difficulties were reviewed. Fault tree analysis, expectation analysis, direct Monte Carlo simulation, indirect Monte Carlo simulation, variable transformation techniques, and Bayesian inference have all been used in attacking these problems.

In Chapter IV, a new application of nonparametric statistics was presented that allows one to find the distribution of functions of multiple random variables. The technique can be applied without using random number

generators. Although nothing can be done when little data is available, the nonparametric method does provide protection against drawing unwarranted conclusions from sparse data bases. In addition to this, the nonparametric approach eliminates the need for density function identification, parameter estimation, and the taking of partial derivatives. An example from the reactor safety literature was presented to illustrate the method, and provide a benchmark calculation.

In Chapter V, this new theory was applied to the problem of aircraft survivability in nuclear blast environments. In this case, the strength distributions for several aircraft piece-parts were taken from the literature. A statistical model of the overpressure from a nuclear weapon was also available from the literature. This information allowed the stress distribution to be determined using the new nonparametric tool. The stress-strength interference integral was then solved, resulting in a continuous probability of failure with range. Except for the fuselage, cookie-cutter approximations appeared to be adequate for the low-yield scenario chosen.

In Chapter VI, a more difficult problem was approached. The analysis of the thermal vulnerability of aircraft is difficult owing to the lack of available data. Strength distributions cannot be determined based on service histories. Stress distributions cannot be determined directly

either. However, stress and strength functions for failure modes of interest can still be postulated exactly as is done in the deterministic case. Any statistical information that affects the stress and strength functions can be incorporated using the nonparametric technique. Stress and strength distributions are thus rigorously inferred, based on any available data. The scatter in the prediction of the thermal radiated power was analyzed in this fashion, and the probability of failure for skin panels examined. In this case, cookie-cutter techniques were found to be completely adequate for the yield scenario chosen.

Recommendations for Future Work

Deterministic modeling will always be the mainstay of nuclear survivability assessment. The physics of nuclear weapon effects and the response of weapons systems to those effects will be a topic of study for years to come. Probabilistic modeling can and should augment this work. If data exists, however sparse, the nonparametric tool described in this dissertation can be used. Finding data and rigorously processing it is hard work. The survivability analyst must decide whether this task is worth it. Methods need to be developed to assist in answering the question, "Is this worth doing? Will a 'cookie-cutter' approximation be a good one?"

One of the more difficult problems in stress-strength interference theory is in the assessment of very low failure probabilites. The nonparametric tool applied in this dissertation could in principle be applied to these problems also. The assessment of a very low failure probability would require a large number of points and substantial computer resources. Research in this area should be conducted.

Work should definitely continue in the area of applied nonparametric statistics. This work should involve improvements in nonparametric tools themselves, and new applications of those tools.

As far as work on the tools themselves, several improvements need to be made. Survivability assessment based on direct probability density function (PDF) estimation might be useful. Since integration is well-posed, such a tool would not suffer from some of the defects that can arise when estimating a PDF by differentiation of a cumulative distribution function (CDF). Endpoint extrapolation is another area that could be improved. The currently used center-difference scheme for integrating the PDF might be enhanced by using higher-order polynomials or spline methods. Another area of study is stylized sampling from non-monotonic functions. A preliminary numerical investigation seemed to indicate that CDF estimation by stylized sampling worked well enough if one was willing to put up

with jumps in the CDF. The size of the jumps can be made as small as desired by simply taking more and more points. However, the PDF estimator derived by differentiating such a CDF can be a numerical problem. Beyond this, a good theoretical proof here would be welcome.

Nonparametric estimation techniques should also be applied to other problems in engineering and physics. One simple yet potentially useful application might be in Monte Carlo radiation transport. Even if used only as a tool to provide fast inversion of distribution functions, computer time might be substantially decreased in some of these large codes. Other applications will no doubt be found.

Finally, as applied to future work in nuclear survivability, the most useful efforts would be in determining the statistical uncertainty in nuclear effects predictions. This is a difficult task, involving a careful search of all known data; however, as noted earlier, if the environments of the nuclear effects can be statistically described, continuous failure probabilities with range will result, even if strength distributions must be taken as cookie-cutter. Furthermore, these environmental inputs would remain the same, barring further testing and discovery, and survivability assessment could proceed with these environments as a common input.

Appendix A: The Development Of Algorithm NOSWET

Overview

This appendix chronicles the development of NOSWET (NOnparametric 'after SWeeder' Estimation Technique), the primary algorithm used to find the distribution of functions of random variables. The actual use of NOSWET for this purpose is discussed in Appendix C. In this Appendix, the work of James Sweeder and A.J. Moore [14] is examined as a possible tool in reliability theory. One of Sweeder's early research models (Model 5332) is selected for further development. The Model is applied to random samples of size 50 from the uniform, normal, double exponential, and log-normal distributions. These results show unwanted variations due to the randomness of the samples. A second series of experiments are performed to show the performance of Model 5332 on stylized samples. The concept of a "stylized" sample [14] is explored and defined more precisely. The performance of the Model on stylized samples is investigated. The results indicate a need to change the part of the algorithm that affects the tails of the distributions. A third series of numerical experiments is presented that shows marked improvement in the estimate of the cumulative distribution function (CDF), but a very much degraded estimate of the probability density function (PDF). This mystery leads to a fourth series of experiments. In

this series, Sweeder's original trigonometric interpolation of the CDF is abandoned, as is his method of estimating the PDF. A linear interpolation scheme is implemented, along with a centered-difference scheme for finding the PDF. The results are a much improved estimate of both the CDF and the PDF for the distributions studied. Finally, a fifth series of experiments is performed in order to find an adaptive endpoint extrapolation technique. Turning again to numerical analysis, one finds that enforcing the conservation of probability in the tails of the distribution leads to optimum selection of the endpoints. Sweeder's extrapolation rule is shown to be a special case of the general endpoint selection algorithm. These results are incorporated in the computer code NOSWET, and used in nuclear survivability assessments.

Sweeder's Model 5332

In a recently published work [14], Sweeder has demonstrated a nonparametric technique for estimating distribution and density functions. Sweeder showed that, given a set of observations denoted by

$\{z_i\}$, i=1,m, where $z_i < z_{i+1}$

then the sample distribution function $F_S(z)$ is defined by:

$$F_S(z)=0 \quad \forall \quad z<z_0 \tag{A.1}$$

For the region $z_i \leq z < z_{i+1}$ $F_S(z)$ is given by

$$F_S(z)=G_i+[(G_{i+1}-G_i)/2]*[1-\cos\{\pi(z-z_i)/(z_{i+1}-z_i)\}] \tag{A.2}$$

$$F_S(z)=1 \quad \forall \; z \geq z_{m+1} \tag{A.3}$$

Sweeder showed that this sample distribution function converges uniformly to the underlying distribution function $F_Z(z)$.

In Equation A.2 G_i is a nonparametric plotting position given by some rule such as:

$$G_i=(i+\alpha)/(m+\beta); \; -1 \leq \alpha \leq \beta \leq 1 \tag{A.4}$$

In Equations A.1 and A.3 z_0 and z_{m+1} are extrapolated endpoints such that:

$$G_0=0 \tag{A.5}$$

$$G_{m+1}=1 \tag{A.6}$$

At the data points $z=z_i$ the sample distribution function yields the values:

$$F_S(z_i)=G_i \tag{A.7}$$

Sweeder's work was examined, since it was anticipated that the problems of nuclear survivability would be dominated by small sample statistics, and nonparametric estimation would completely eliminate the problems of density function identification and parameter estimation.

Although the original Reference [14] should be consulted for detail, Sweeder's basic idea is to take the sample defined by the set described above, and break it into a number of subsamples. Each subsample is treated as representative of the entire population, and Equations A.1 through A.3 are used to form estimates of the CDF. These estimates are then averaged. A key parameter in one of

Sweeder's models is thus the number of subsamples to take. The first digit, 5, from Model 5332 denotes the number of subsamples.

Another parameter of importance is the choice of the plotting rule. Table A.1 shows several selections that follow under the general description of Equation A.4. The third choice, Hazen's Rank, is the second parameter in Model 5332.

The third major parameter of importance in Sweeder's algorithm is the choice of the extrapolation constant. For many of the plotting positions of Table A.1, the distribution is not determined at the endpoints. That is, the G_i's do not span the entire space from 0 to 1. Thus, the sample CDF remains undefined in the tails unless one chooses the points z_0 and z_{m+1} in such a way that

$$F_S(z_0)=0 \tag{A.8}$$

$$F_S(z_{m+1})=1 \tag{A.9}$$

For each subsample, Sweeder proposed a general extrapolation given by:

$$z_0=z_1-\Delta_1(z_2-z_1) \tag{A.10}$$

$$z_{m+1}=z_m+\Delta_u(z_m-z_{m-1}) \tag{A.11}$$

where Δ_1 and Δ_u are the lower and upper extrapolation constants. Table A.2 gives the choices of Δ_1 and Δ_u that Sweeder examined. For Model 5332, choice 3 was used.

TABLE A.1

PLOTTING POSITIONS OF THE FORM $G_i=(i+\alpha)/(m+\beta)$

	FORMULA	DESCRIPTION
1.	i/(m+1)	Mean Rank
2.	(i-.3)/(m+.4)	Median Rank Approximation
3.	(i-.5)/m	Hazen Rank
4.	[i-(m+1)/2m]/[m-(1/m)]	Average of Mean and Mode Rank
5.	(i-1)/(m-1)	Mode Rank
6.	i/m	Empirical Distribution Function
7.	(i-.375)/(m+.25)	Efficient Approximation for the Normal Distribution

TABLE A.2

EXTRAPOLATION VALUES

	LOWER VALUE (Δ_l)	UPPER VALUE (Δ_u)
1.	0	0
2.	0.5	0.5
3.	1.0	1.0
4.	1.5	1.5
5.	$G_1/(G_2-G_1)$	$G_1/(G_2-G_1)$

The CDF, including the endpoints, can now be constructed using Sweeder's technique. However, Sweeder added an additional feature in order to reduce some of the numerical noise in the CDF estimate. Once the CDF has been determined, it may be easily inverted by using a Newton-Raphson or other technique. Rather than inverting the distribution randomly, Sweeder used the median rank points (choice 2 of Table A.1) to invert the distribution. These points were then processed again by the algorithm, resulting in a better estimate of the CDF. For Model 5332, choice 2 of Table A.1 is used.

Model 5332 was chosen as a starting point, since for a range of distributions examined, it behaved well with respect to modified Cramer Von Mises (CVM) distance measures [14]. Sweeder applied it to the double exponential, normal, and uniform distributions, representing distributions with a heavy tail, a moderate tail, and a short tail, respectively. Model 5332 was not optimum for any of the distributions considered. However, compared to the 3 other models that Sweeder considered, it ranked second overall for smallest CVM distance averaged over all three distributions. More significantly, Model 5332 was not the worst choice for any distribution considered. Hence, it was selected as the starting point for possible use in a reliability theory approach to nuclear survivability.

In the first series of numerical experiments, designated as Series 1, Model 5332 (with two inversions) was applied to the uniform, normal, double exponential, and lognormal distributions. The lognormal was added as a bench mark since it is asymmetric and is popular with other survivability analysts [49]. Random samples of size 50 were drawn from each of these distributions, and the CDF and PDF estimated by Sweeder's method. The results are illustrated in Figures A.1 through A.4. In these figures the PDF'S have been scaled to their peak values so as to be able to overlay the PDF and CDF on the same plot. The results for each distribution are discussed briefly below.

The uniform distribution shows a rather heavy tailed result compared to the true one. The true endpoints are at 0 and 1, whereas the numerical technique is putting them at -.20 and 1.15. In addition, the PDF has some oscillations. These oscillations exceed the true peak value of the PDF by more than 50%.

The approximation to the normal is, at least visually, somewhat better. The true endpoints are of course at $\pm\infty$ which cannot be matched by this numerical algorithm. A more meaningful comparison is the 98th and 2nd percentiles, which should be at 1 and 0 respectively. The behavior in the right hand tail is better than that in the left. The PDF estimate does fairly well except for the peak which should be at .5. Here noise seems to be a problem.

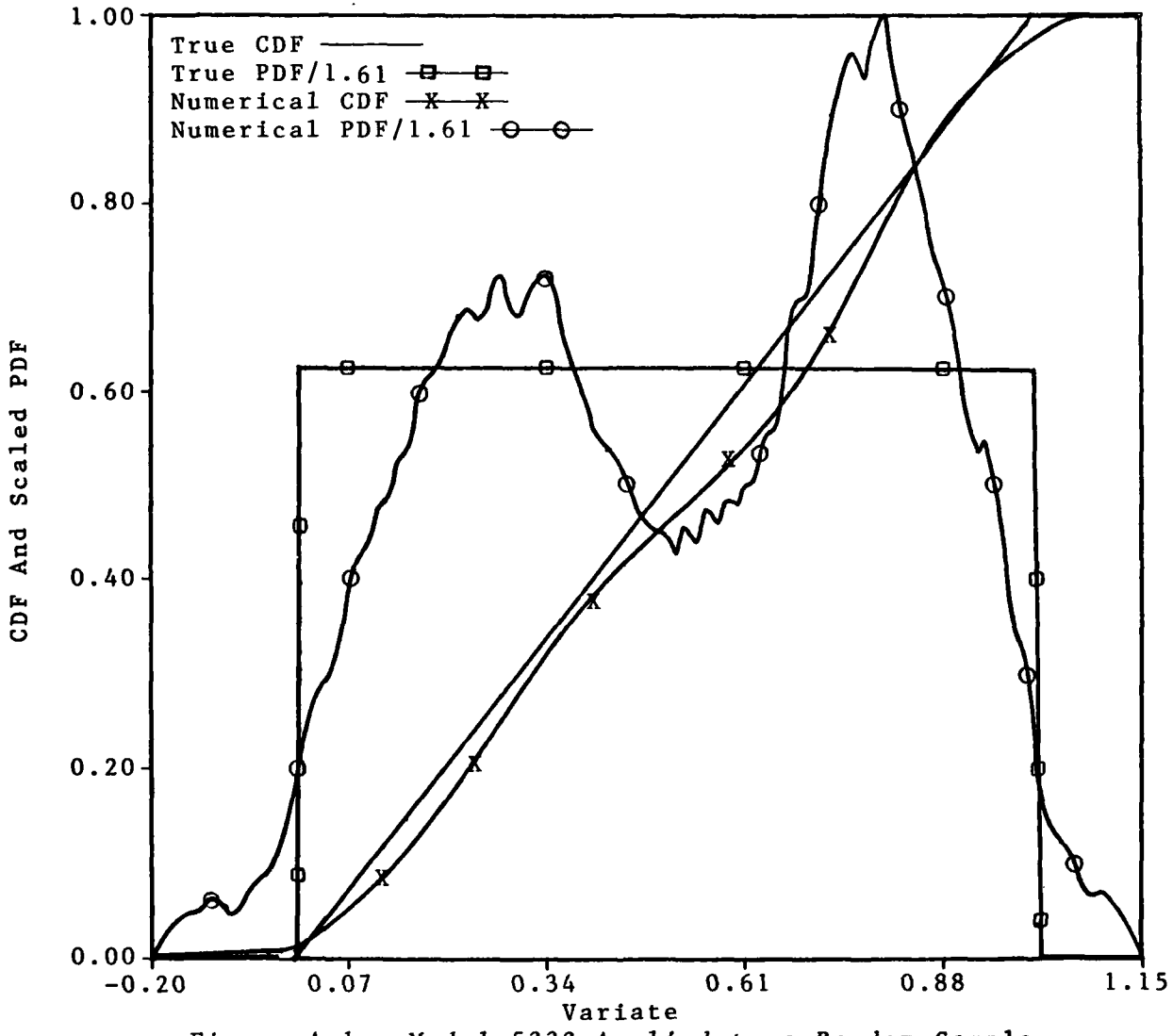

Figure A.1. Model 5332 Applied to a Random Sample From the Uniform Distribution

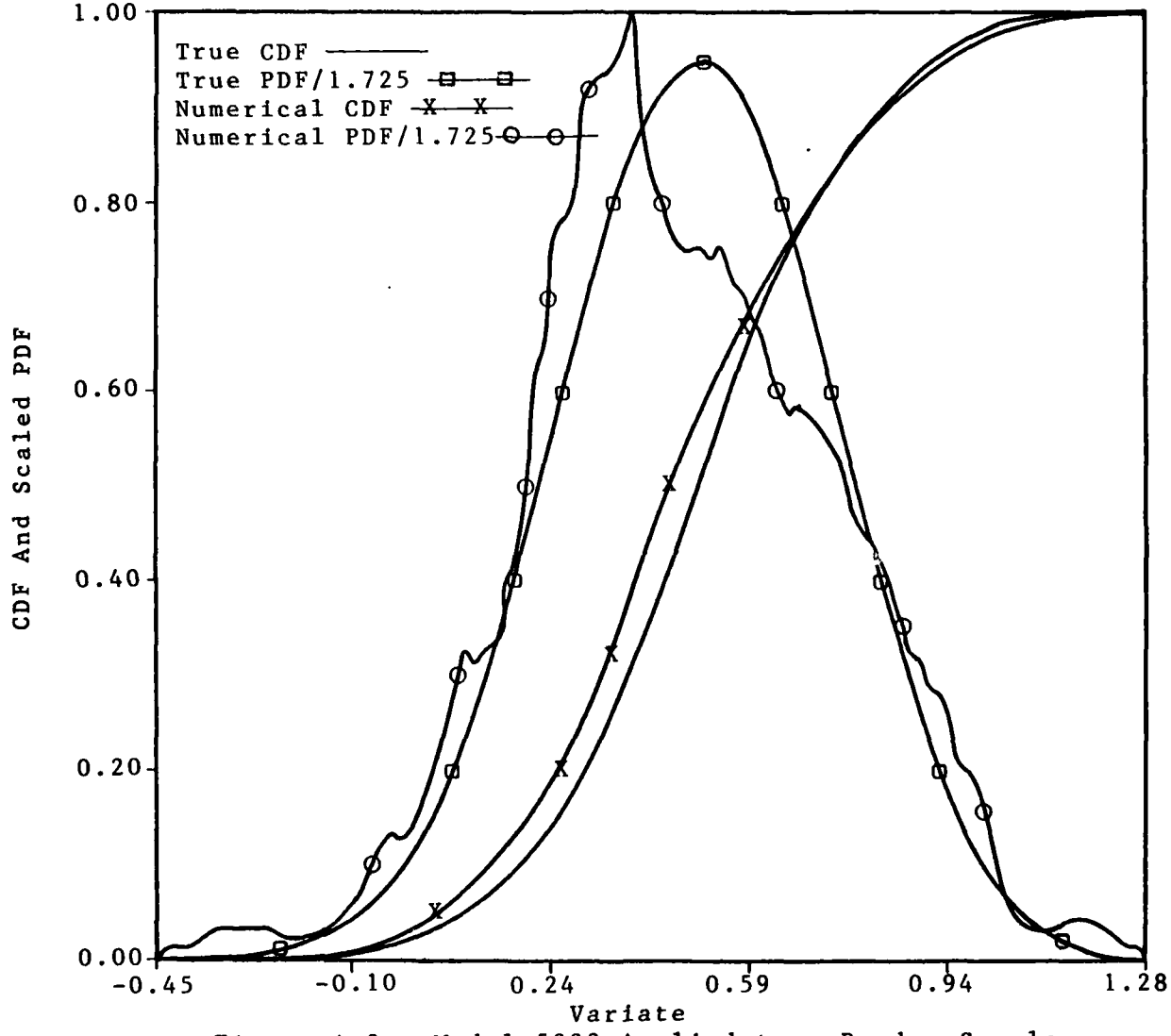

Figure A.2. Model 5332 Applied to a Random Sample From the Normal Distribution

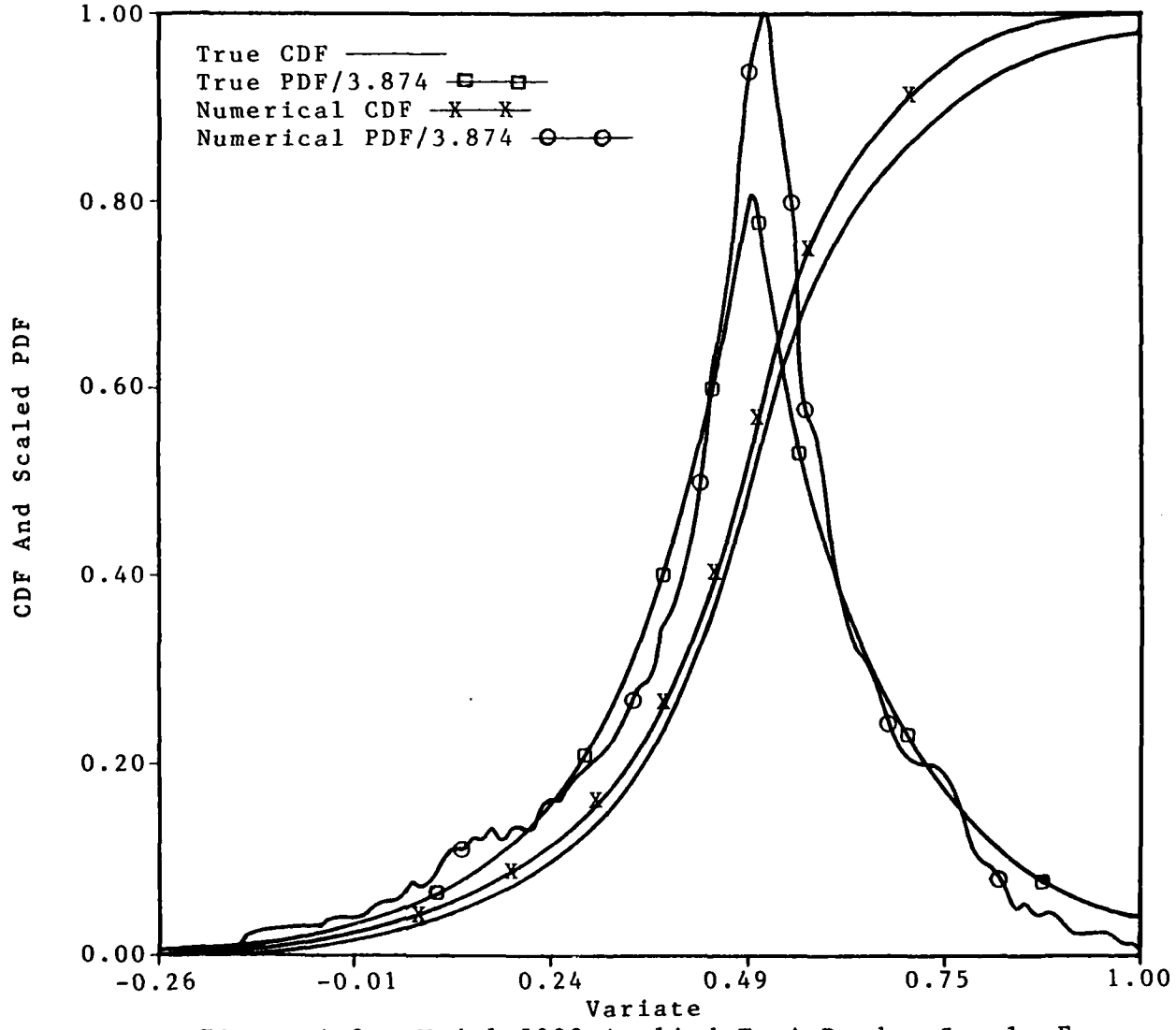

Figure A.3. Model 5332 Applied To A Random Sample From the Double Exponential Distribution

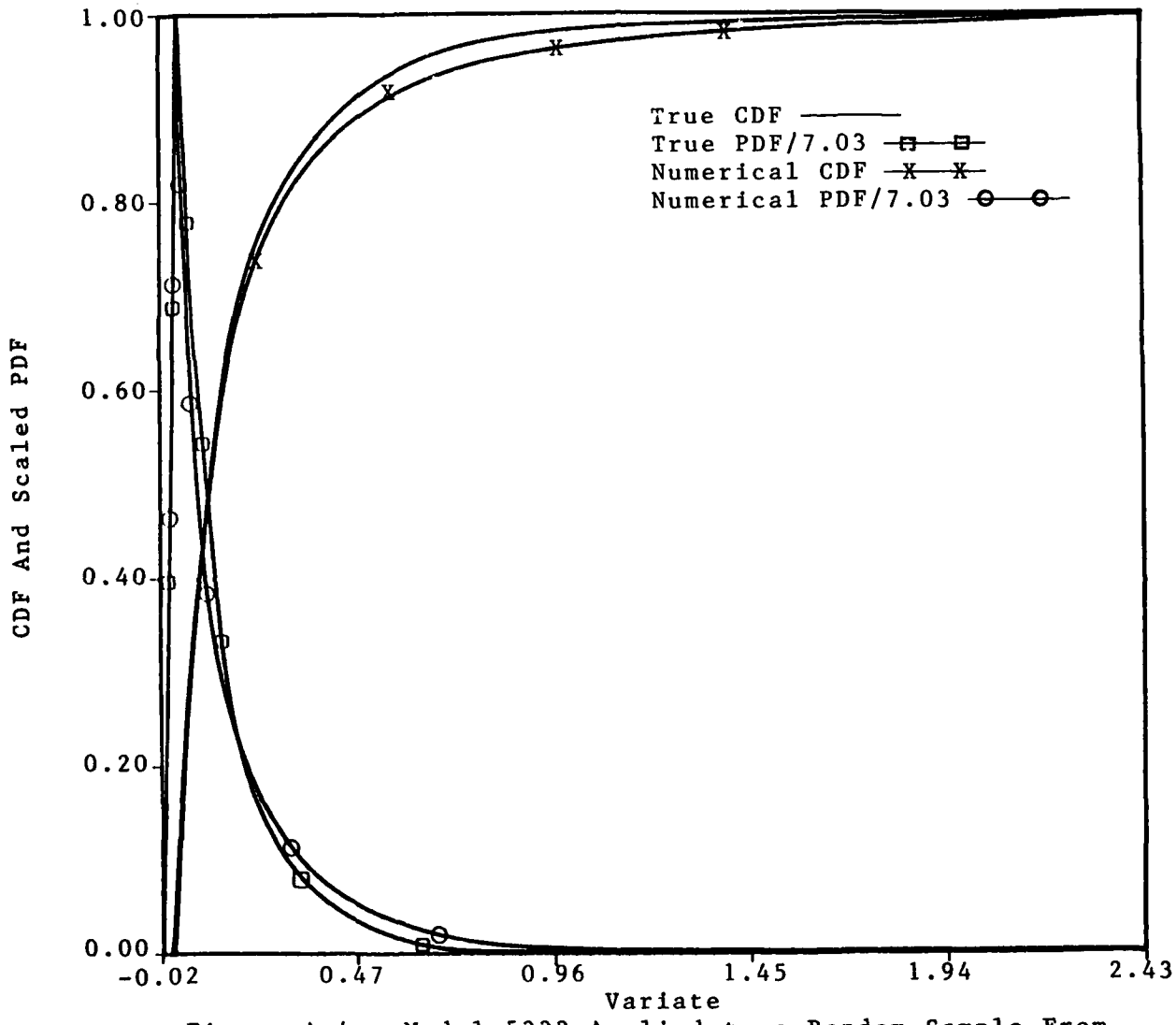

Figure A.4. Model 5332 Applied to a Random Sample From the Lognormal Distribution

The results for the double exponential (DE) shown in Figure A.3 show very clearly the concave shape of the DE PDF. The peak of the PDF is also matched fairly well, but the distribution seems to show considerable asymmetry, being shorter in the right-hand tail than in the left.

The results for the lognormal are displayed in Figure A.4. Sweeder's technique does remarkably well here. Although not developed explicitly for asymmetric density functions, Model 5332 estimates the lognormal CDF and PDF rather well. The asymmetry in the CDF is clearly evident, as is the almost spiking PDF.

Although the overall results are favorable, it is difficult to tell at this point how useful Sweeder's method might be for engineering applications. In particular, it is difficult to tell by observing one random sample from each distribution which features are potential model problems and which are the result of a random draw. This question can be dealt with by considering, and defining in more detail, the idea of a stylized sample, and applying that idea to a second series of numerical experiments.

Model Performance on Stylized Samples

Sweeder does not strictly define the term ''stylized sample'' [14], but basically, a stylized sample is one that best represents a given distribution. This can be defined more precisely by observing the following. Of all the possible random samples that one might choose, there is one

particular sample that yields a best estimate of the underlying distribution. In this set, each z_i of the set satisfies:

$$G_i=F_Z(z_i) \tag{A.12}$$

If each z_i so determined is then plotted using the same plotting rule by which it was drawn, then by Equation A.7, Sweeder's method exactly interpolates the distribution function $F_Z(z)$ at the data points. A stylized sample can thus be defined formally:

Definition: The set of points $\{z_i^*\}$,i=1,m is said to be a stylized sample from the population of the random variable Z, if, for every point in the set,

$$F_S(z_i^*)=F_Z(z_i^*) \tag{A.13}$$

Stylized samples of size 50 were drawn from each of the bench mark distributions. The results are displayed in Figures A.5 through A.8 and are discussed below.

The results for the uniform distribution are displayed in Figure A.5. Clearly, the situation has improved. The PDF shows very clear features of the true PDF, and the peak PDF value is very close. The CDF is also much improved, but one still sees a rather long tail, which is now symmetric about .50.

The behavior of Model 5332 on a stylized sample from the normal distribution is shown in Figure A.6. The PDF estimation is almost outstanding. However, one can still see that the CDF does not match exactly, even though the

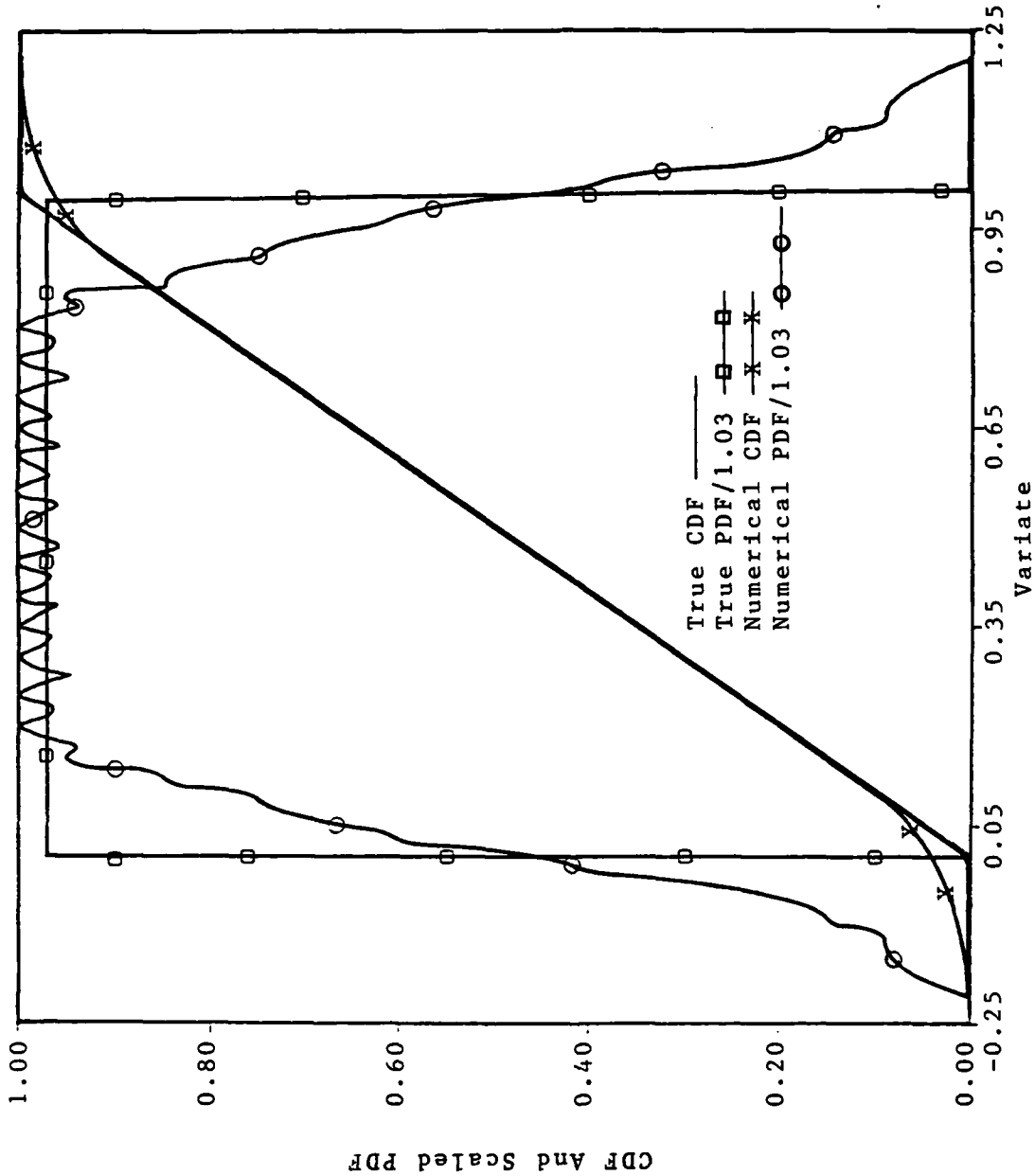

Figure A.5. Model 5332 Applied to a Stylized Sample From the Uniform Distribution

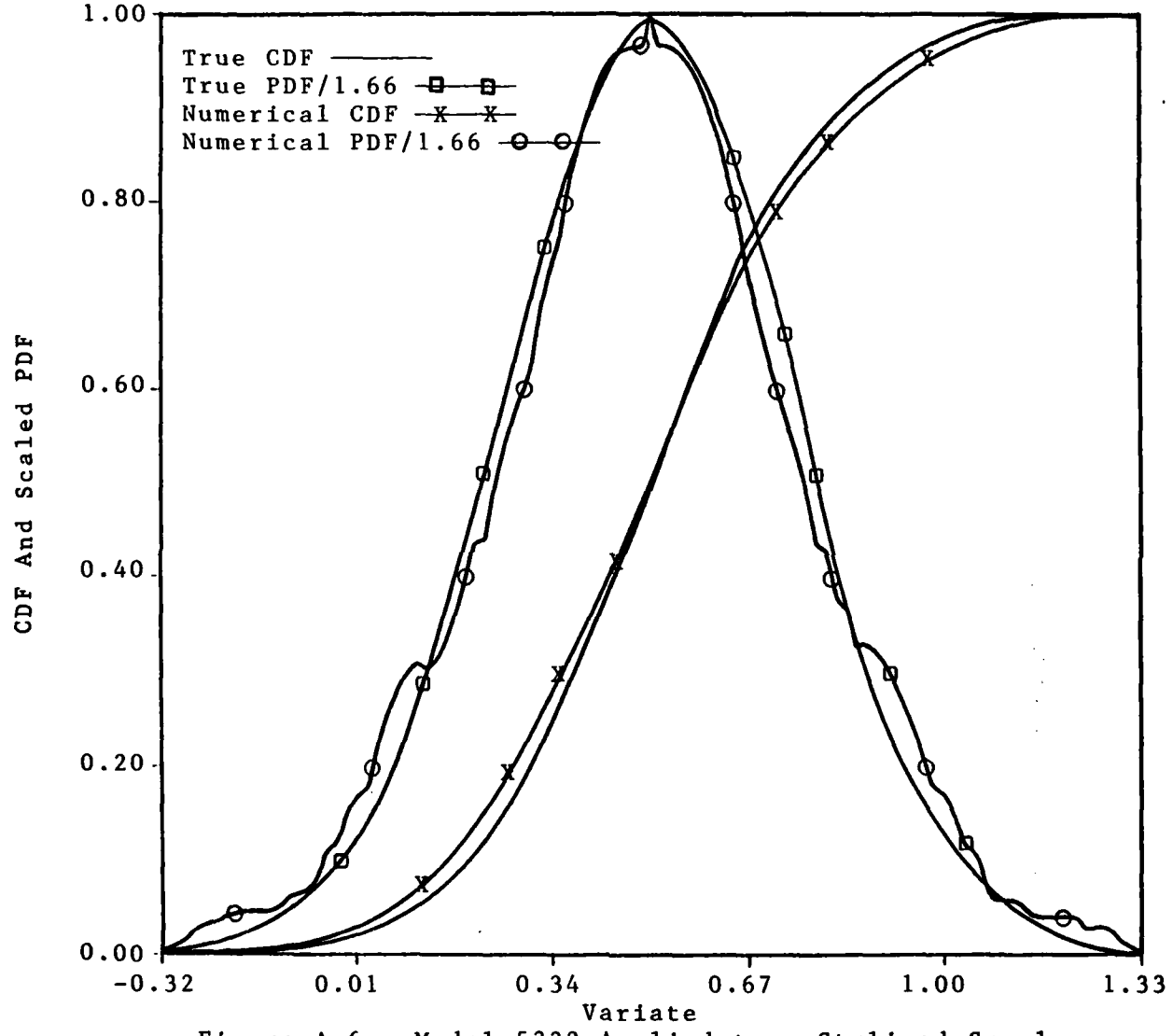

Figure A.6. Model 5332 Applied to a Stylized Sample From the Normal Distribution

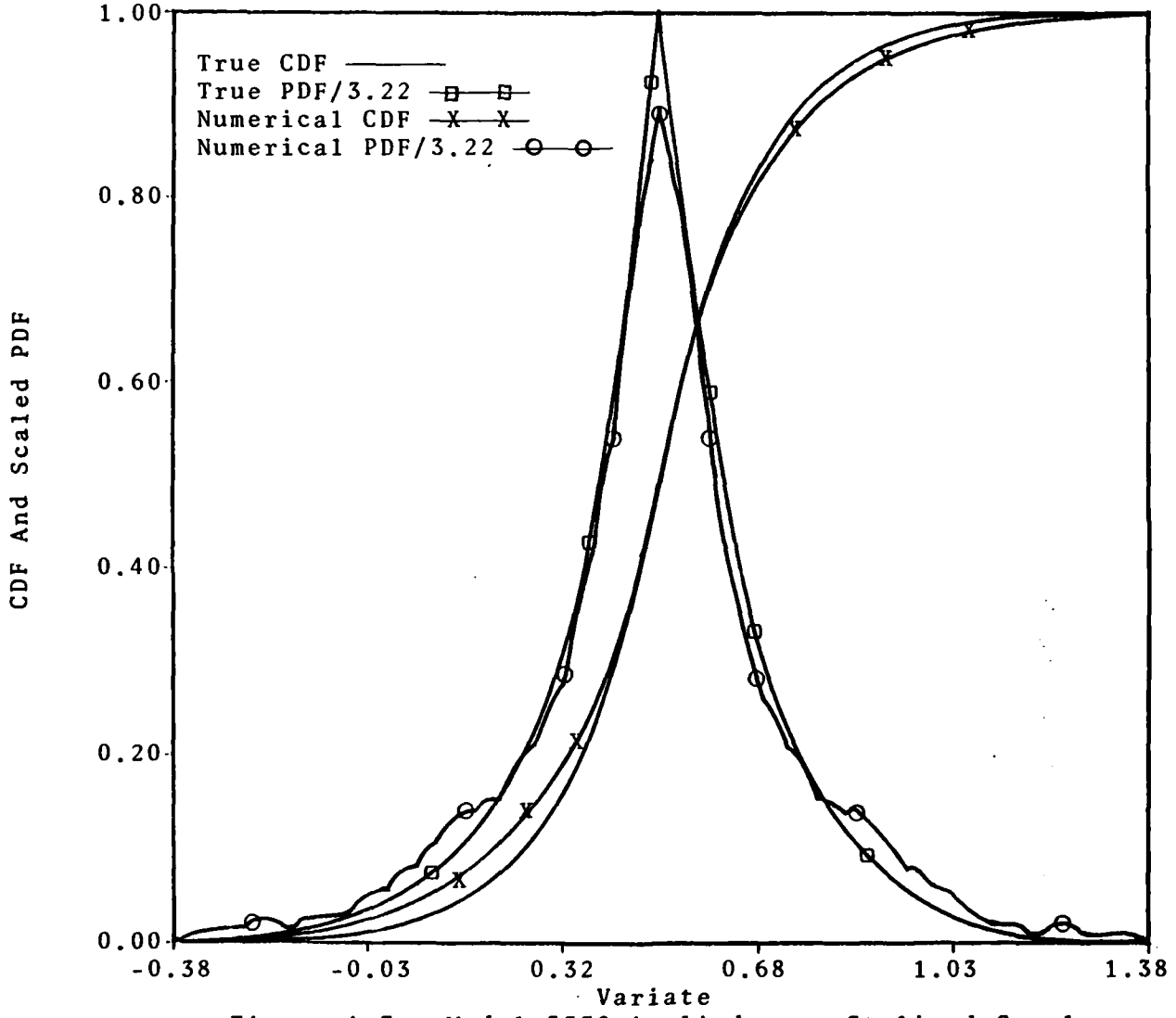

Figure A.7. Model 5332 Applied to a Stylized Sample From the Double Exponential Distribution

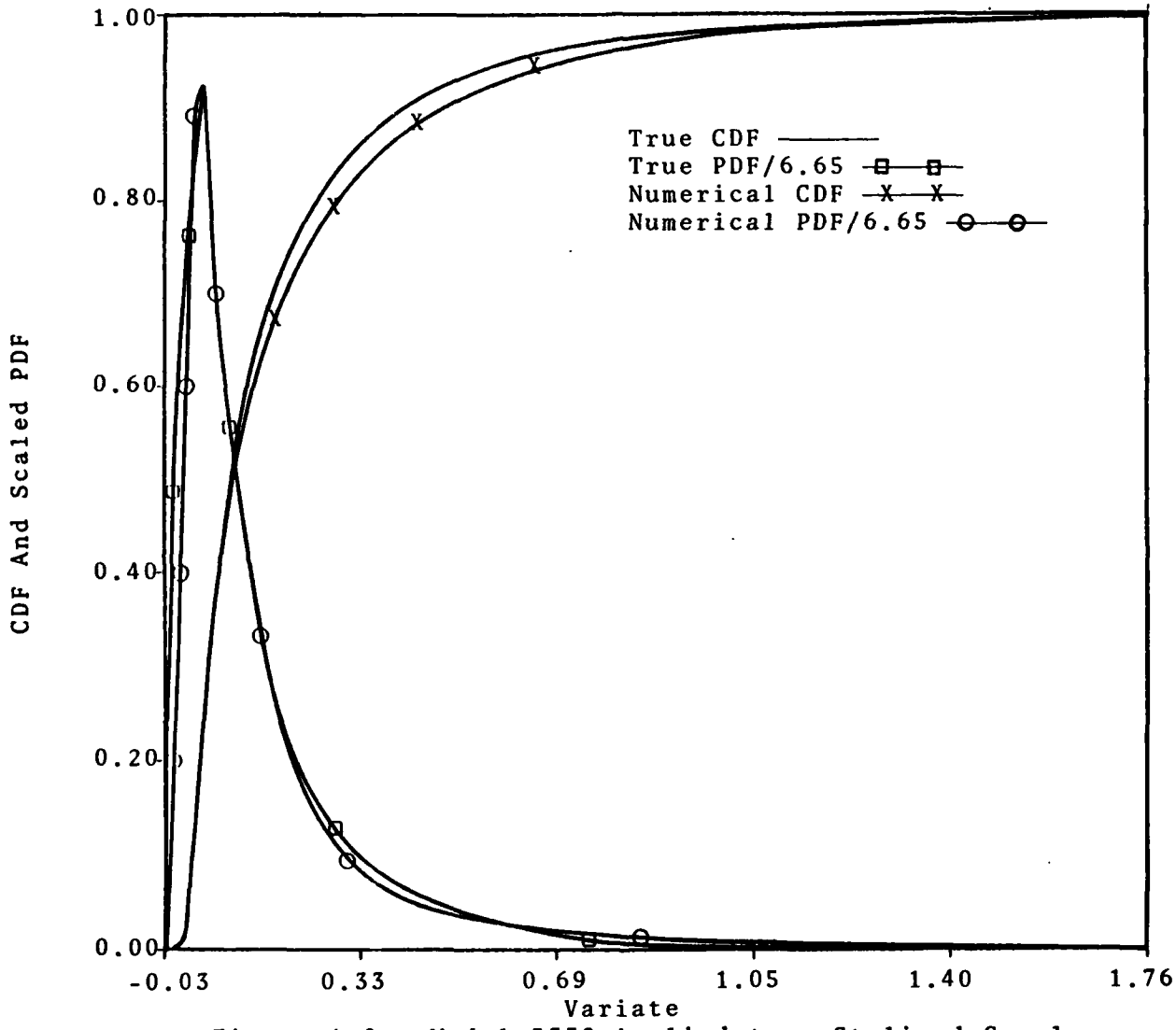

Figure A.8. Model 5332 Applied to a Stylized Sample from the Lognormal Distribution

endpoints are symmetric about the median.

The DE distribution as estimated by using Model 5332 is illustrated in Figure A.7. Again, the PDF estimate looks very good, while the CDF estimate is not quite as good. Again, symmetry about .50 is obvious, with slightly more tail than in the normal case.

Finally, the lognormal distribution as estimated by Sweeder's technique is shown in Figure A.8. The PDF behavior is a little hard to see on such a scale since it rises so fast, but it matches fairly well. However, the CDF seems to have a noticeable problem between the 70th and 98th percentiles.

In summary, the Series 2 experiments allow one to see the power of Sweeder's method on stylized samples. The performance is very good for the normal and double exponential distributions, and is less satisfactory for both the uniform and lognormal. The outstanding problems seem to be undue weight in the tails of the uniform, and somewhat weak estimation of the asymmetric lognormal. These difficulties are overcome by actually modifying the model.

Elimination of Subsampling

At the moment, two problems remain: (a) the improper tail weight given to the uniform distribution, and (b) somewhat poor performance in CDF estimation, especially for the uniform and lognormal distribution functions.

These two problems were found to be related. Based on the previous definition of a stylized sample, if one treated the entire sample as a single subsample and plotted it by Hazen's Rule, then the CDF estimate should be exact (for m=50) at the CDF values .01(.02).99. The Series 2 experiments did not yield exact results at these points owing to the subsampling and averaging process.

A third series of experiments was performed. For this series, the subsampling was eliminated. Said another way, Sweeder's Model 5332 was altered, using his nomenclature, to Model 1332. The results are shown in Figures A.9 through A.12. For these experiments no inversions were necessary, decreasing computer execution time by a factor of 20 or so.

The use of this new model on a stylized sample from the uniform distribution is shown in Figure A.9. This Figure is truly enlightening, as will be discussed shortly. The CDF estimate is nearly perfect, and the tail weight problem has all but vanished. In short, the CDF estimate is precisely as predicted. However, the PDF estimate is much worse. Instead of having a flat line at the value 1.0, sinusoidal variations exist which oscillate between 0 and $\pi/2$.

The new estimate of the normal distribution is displayed in Figure A.10. Again, the CDF estimate is very good, while the PDF estimate has failed.

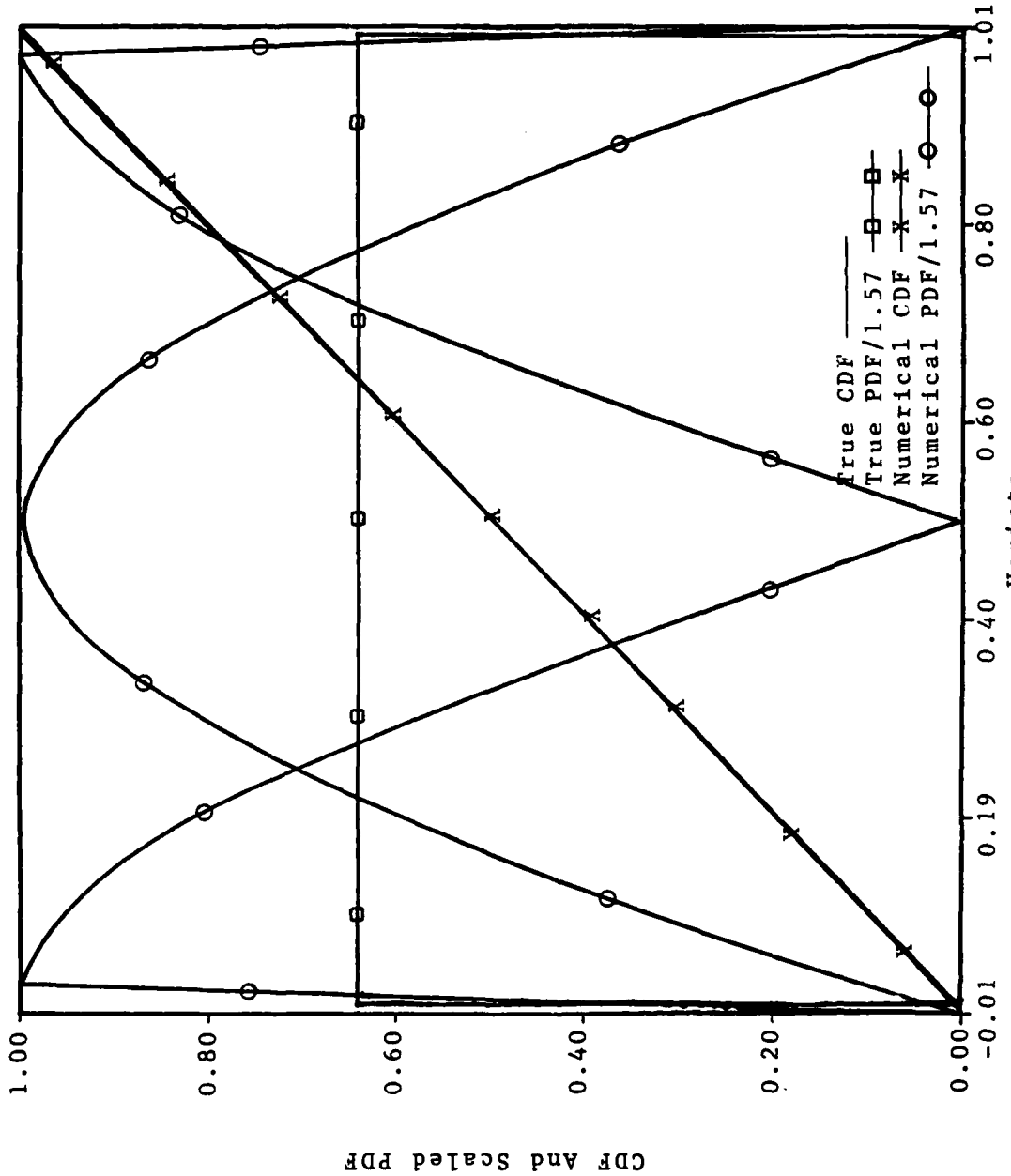

Figure A.9. Model 1332 Applied to a Stylized Sample From the Uniform Distribution

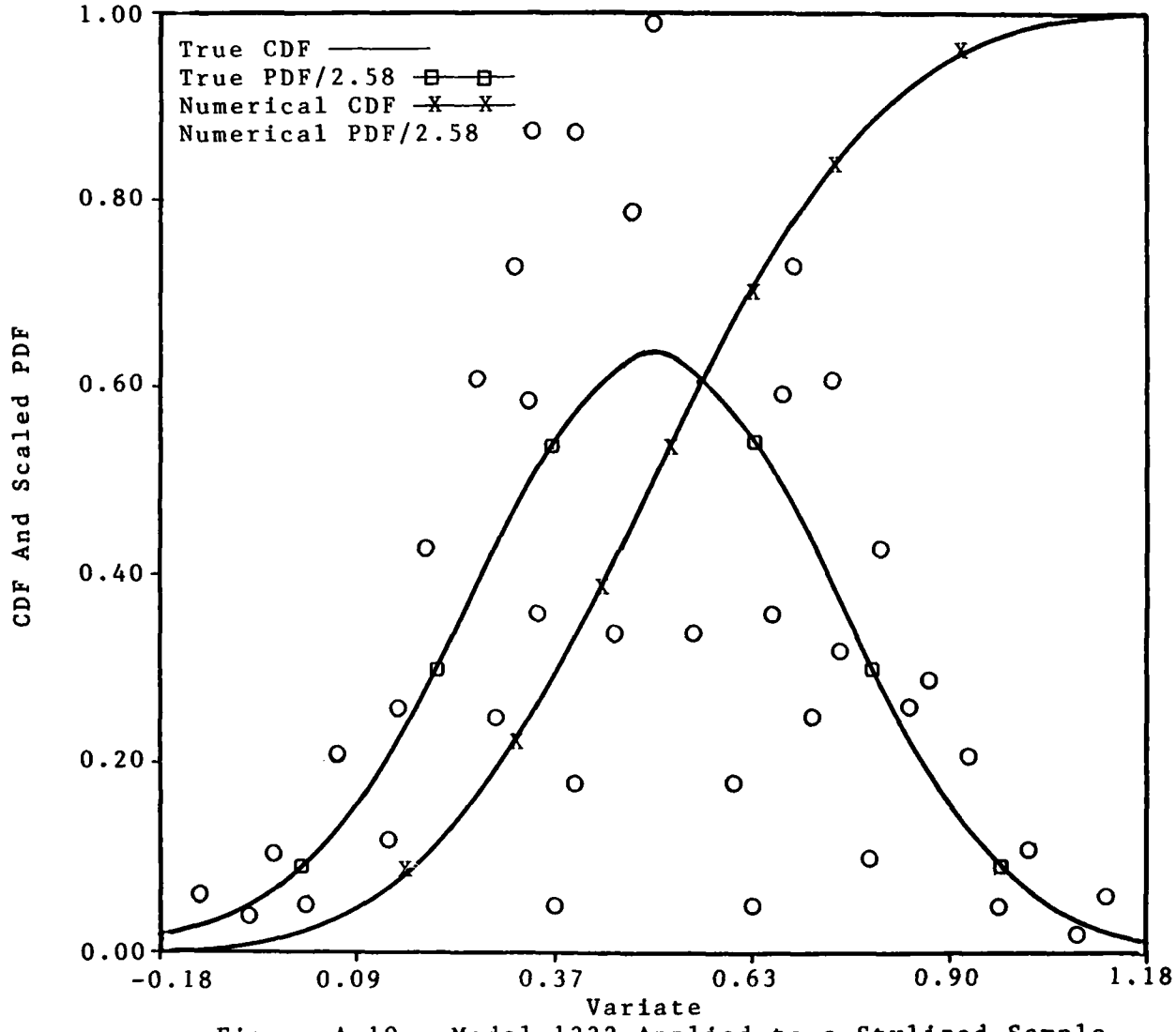

Figure A.10. Model 1332 Applied to a Stylized Sample From the Normal Distribution

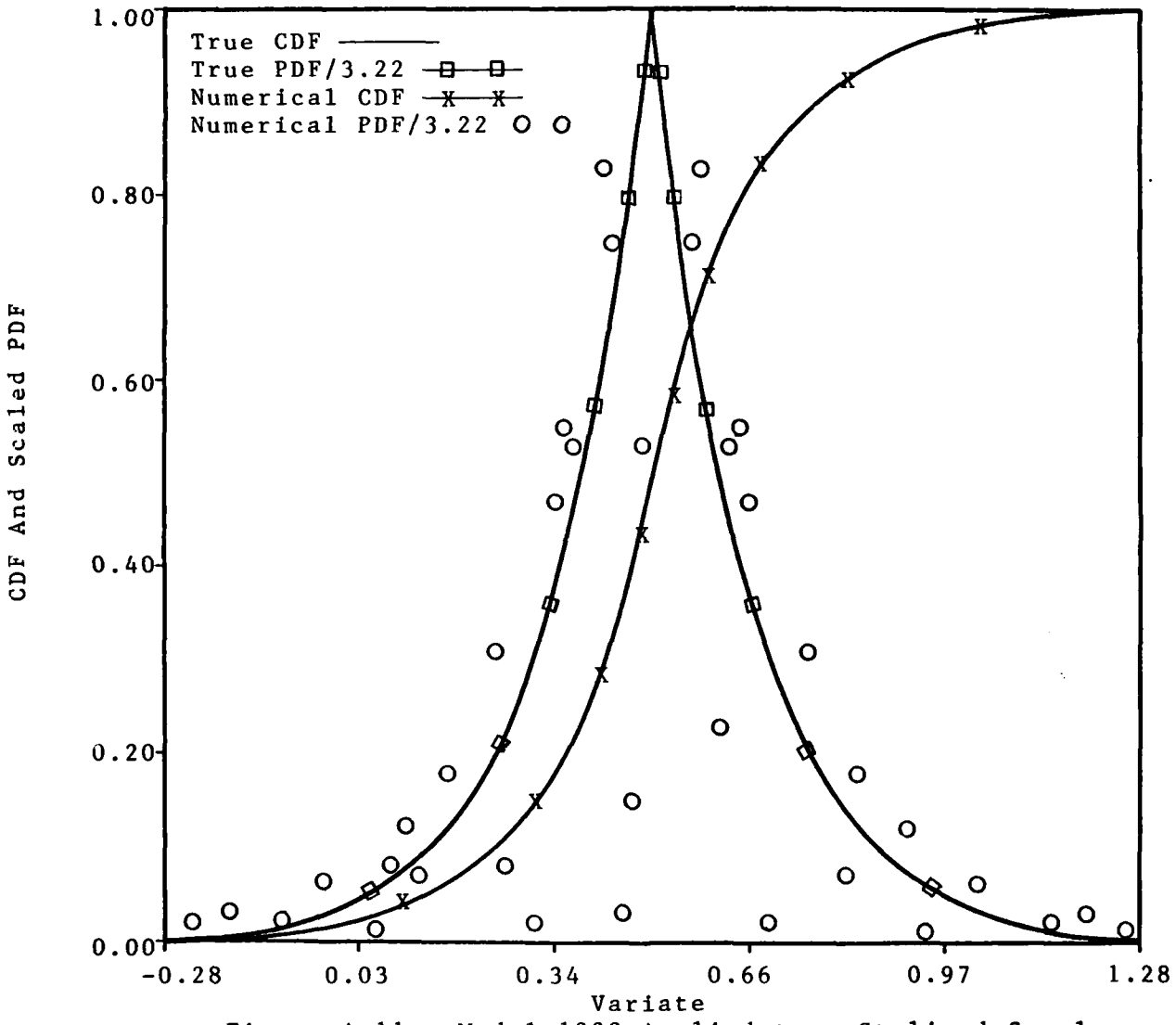

Figure A.11. Model 1332 Applied to a Stylized Sample From the Double Exponential Distribution

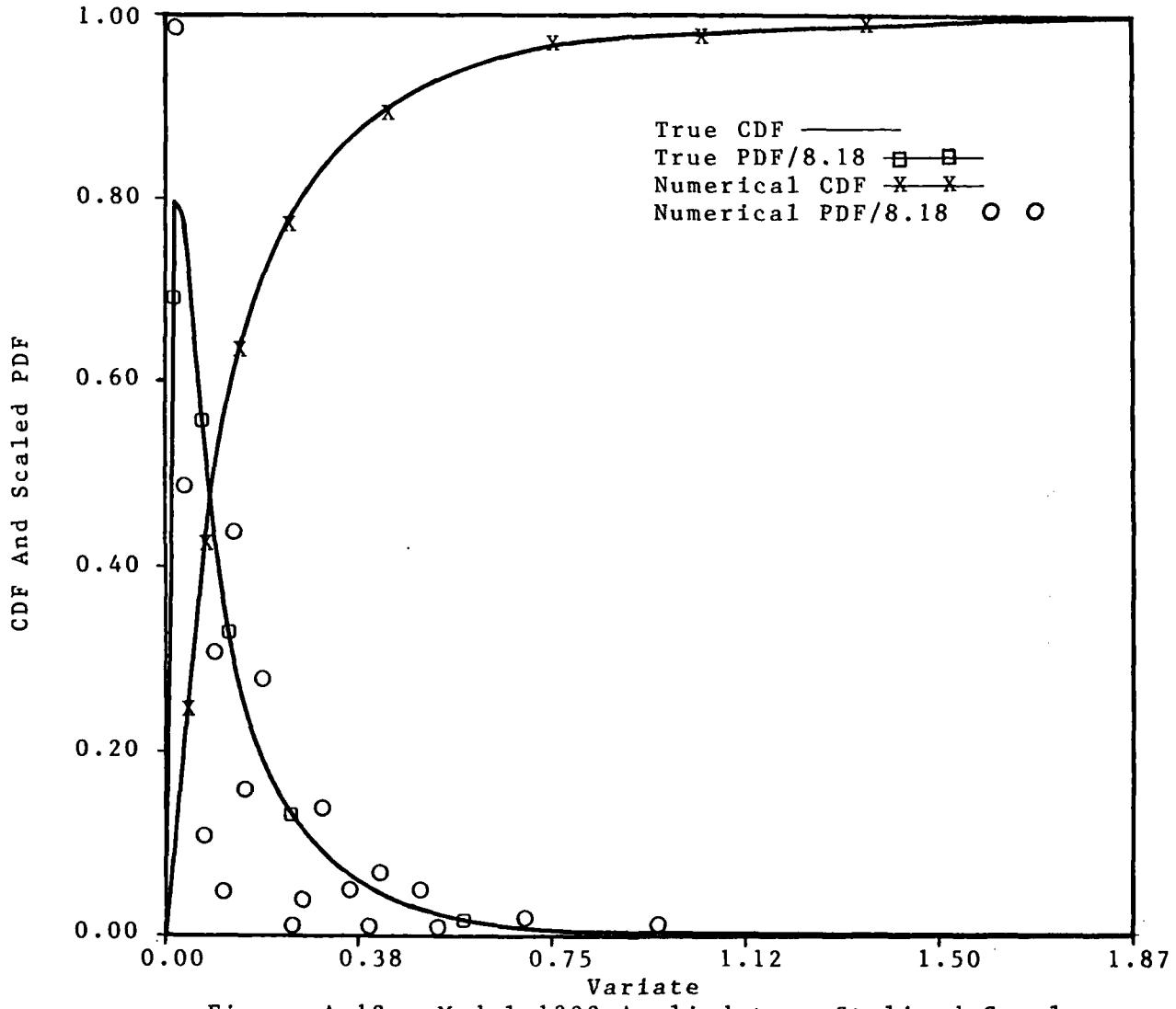

Figure A.12. Model 1332 Applied to a Stylized Sample From the Lognormal Distribution

The behavior of the new model on the DE and lognormal distributions is shown in Figures A.11 and A.12. Again, the general result is a very good estimate of the CDF and a badly oscillating PDF. This problem led to a fourth series of numerical experiments.

Modification of the PDF Estimation Method

At the conclusion of the Series 3 experiments two observations were made. First, the CDF estimate was behaving exactly as anticipated based on the concept of stylized sampling. Second, the PDF estimate had gone badly awry. Sweeder's subsampling technique clearly helps the PDF estimate a good deal. Why is this so?

The PDF mystery is solved by examining in detail Sweeder's method for finding the PDF. He simply differentiated Equations A.1 through A.3 resulting in:

$$f_S(z)=0 \quad \forall \quad z<z_0 \tag{A.14}$$

For the region $z_i \leq z < z_{i+1}$ the PDF is given by:

$$f_S(z)=(\pi f_{i+1/2}/2)\sin\{\pi(z-z_i)/(z_{i+1}-z_i)\} \tag{A.15}$$

$$f_S(z)=0 \quad \forall \quad z \geq z_{m+1} \tag{A.16}$$

The term $f_{i+1/2}$ in Equation A.15 is defined by:

$$f_{i+1/2}=(G_{i+1}-G_i)/(z_{i+1}-z_i) \tag{A.17}$$

The quantity $f_{i+1/2}$ is the classic centered-difference approximation to the derivative. If the true value of the derivative is a constant 1.0, one sees from Equation A.15 that the PDF estimate is a sinusoidal function with a peak amplitude of $\pi/2$, exactly as observed in Figure A.9.

AD-A163 218 AIRCRAFT NUCLEAR SURVIVABILITY METHODS(U) AIR FORCE INST OF TECH WRIGHT-PATTERSON AFB OH SCHOOL OF ENGINEERING H A UNDEM SEP 85 AFIT/DS/PH/84-3 3/3

UNCLASSIFIED F/G 18/3 NL

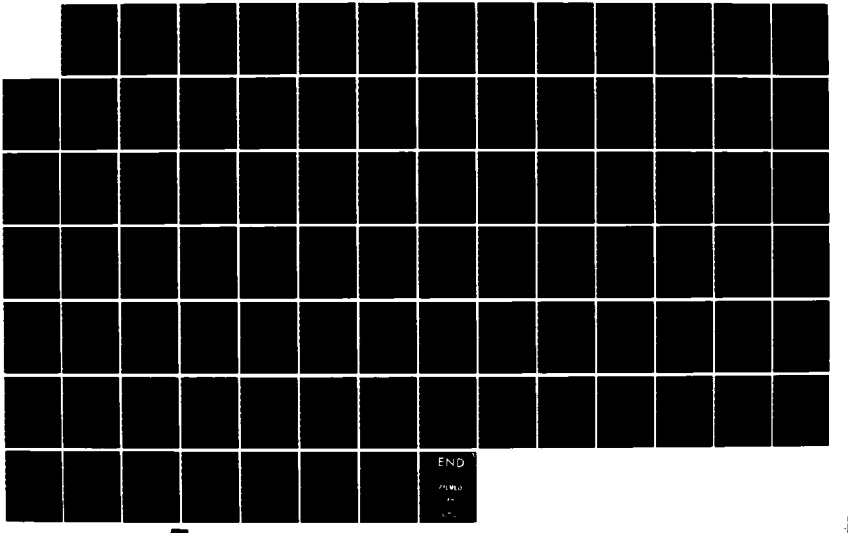

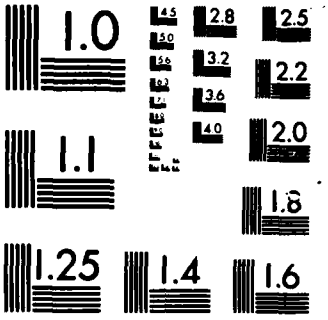

MICROCOPY RESOLUTION TEST CHART
NATIONAL BUREAU OF STANDARDS-1963-A

One also sees from Equation A.15 that increasing the number of points does nothing to improve the PDF estimate. The PDF always goes to zero at the data points, and oscillates between 0 and $\pi/2$. In short, the problem is one of posedness, as discussed by Lee [10].

However, one can calculate the average value of Sweeder's derivative over the interval $[z_i, z_{i+1}]$.

$$\langle f_S(z)\rangle = \int_{z_i}^{z_{i+1}} f_S(z)dz/(z_{i+1}-z_i) \qquad (A.18)$$

The result is just:

$$\langle f_S(z)\rangle = f_{i+1/2} \qquad (A.19)$$

The average value of Sweeder's PDF is just the numerical centered-difference value. It appears that Sweeder's subsampling technique acts primarily as an averaging algorithm.

If these considerations are true, one can now alter Sweeder's method again. A new CDF estimate can be defined by:

$$F_S(z)=0 \ \forall \ z<z_0 \qquad (A.20)$$

On the interval $[z_i, z_{i+1})$:

$$F_S(z)=G_i+(G_{i+1}-G_i)(z-z_i)/(z_{i+1}-z_i) \qquad (A.21)$$

$$F_S(z)=1 \ \forall \ z\geq z_{m+1} \qquad (A.22)$$

The PDF estimate is given by:

$$f_S(z)=0 \ \forall \ z<z_0 \qquad (A.23)$$

$$f_S(z)=f_{3/2}(z-z_0)/(z_{3/2}-z_0) \ \forall \ z_0\leq z<z_{3/2} \qquad (A.24)$$

On the interval $[z_{i-1/2}, z_{i+1/2})$:

$$f_S(z)=f_{i-1/2}+(f_{i+1/2}-f_{i-1/2})(z-z_{i-1/2}) \\ /(z_{i+1/2}-z_{i-1/2}) \quad \text{(A.25)}$$

On the interval $[z_{m-1/2}, z_{m+1})$ $f_S(z)$ is given by:

$$f_S(z)=f_{m-1/2}(z_{m+1}-z)/(z_{m+1}-z_{m-1/2}) \quad \text{(A.26)}$$

while

$$f_S(z)=0 \ \forall \ z \geq z_{m+1} \quad \text{(A.27)}$$

In Equation A.25 i ranges from 2 to m-1 and $z_{i\pm1/2}$ is defined by:

$$z_{i\pm1/2}=(z_i+z_{i\pm1})/2 \quad \text{(A.28)}$$

The results of the above model on the stylized samples from the benchmark distributions are displayed in Figures A.13 through A.16. One final improvement will be considered, and that is the problem of endpoint extrapolation.

Endpoint Extrapolation

Even though the results displayed in Figures A.13 through A.16 are very rewarding, one nagging issue remains--that of endpoint extrapolation. That is, how should one choose the points z_0 and z_{m+1}? It is not clear that Sweeder's choice of a constant Δ_l and Δ_u remain optimum for the newly developed algorithm. For example, examination of Figures A.5 through A.8 indicates that the resultant endpoint values do not agree with those of Figures A.13 through A.16. The uniform tail length is shorter in Figure A.13, and the lognormal is longer on the right and positive on the

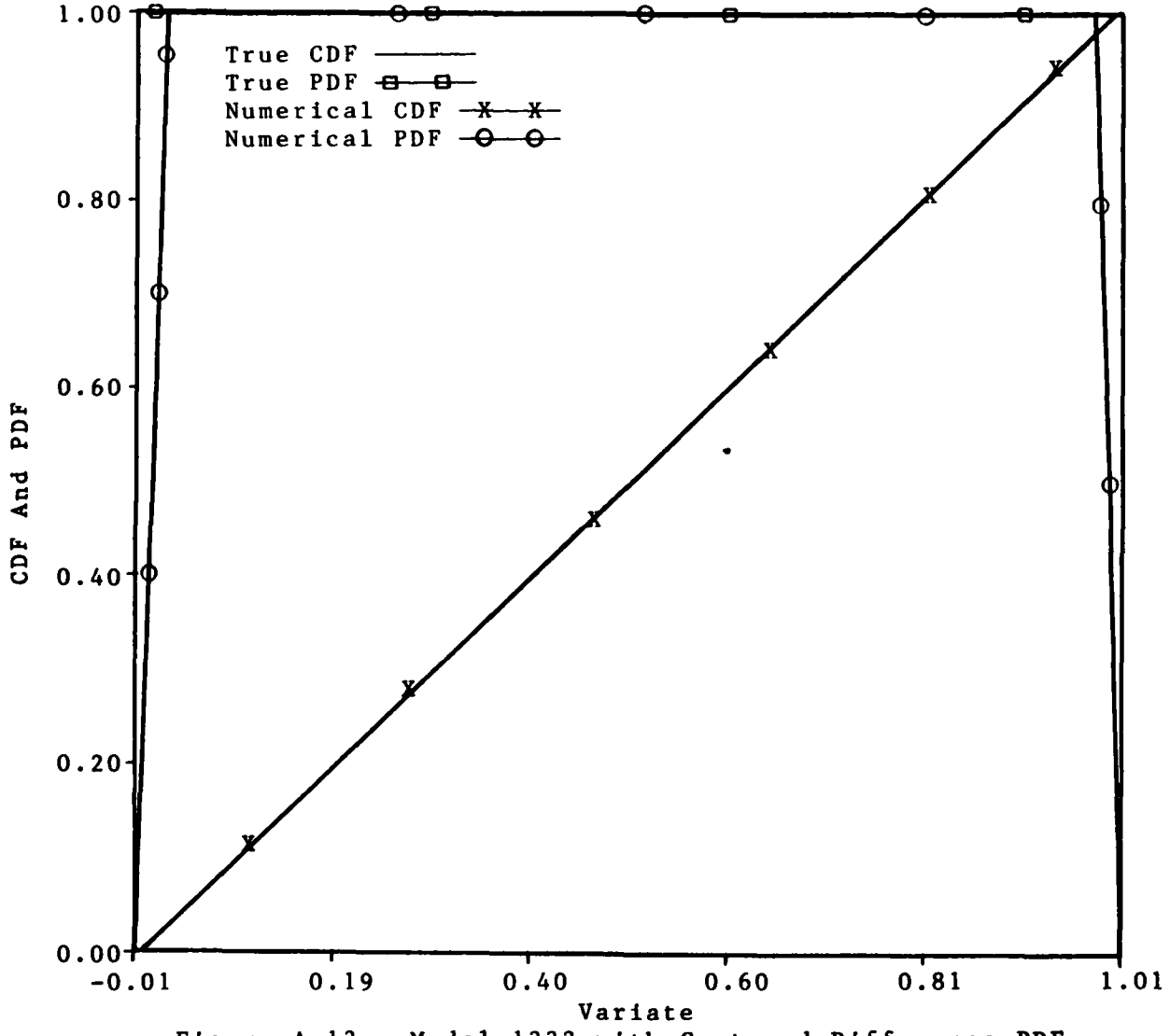

Figure A.13. Model 1332 with Centered Difference PDF Applied to a Uniformly Distributed Variable

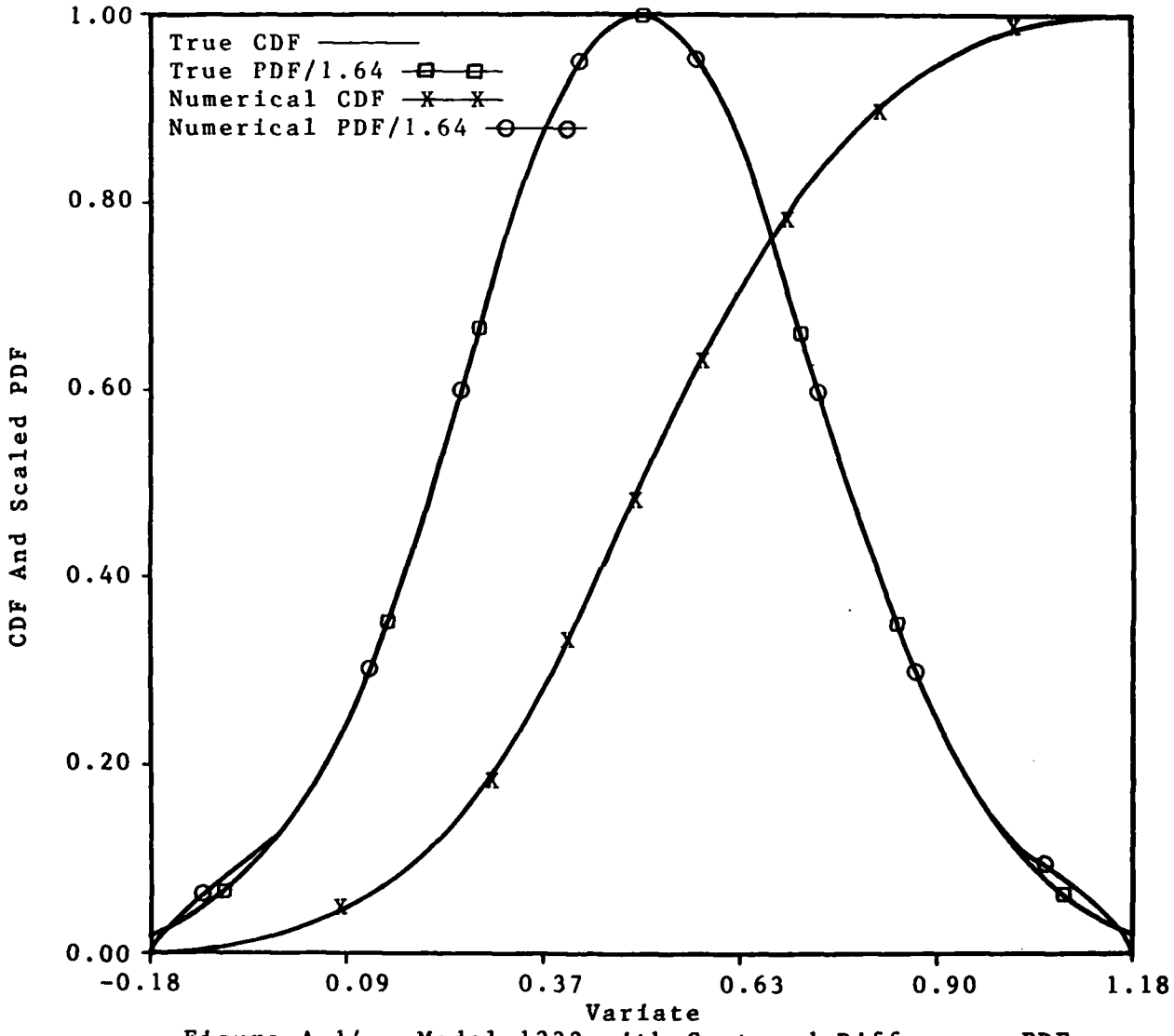

Figure A.14. Model 1332 with Centered Difference PDF Applied to a Normally Distributed Variable

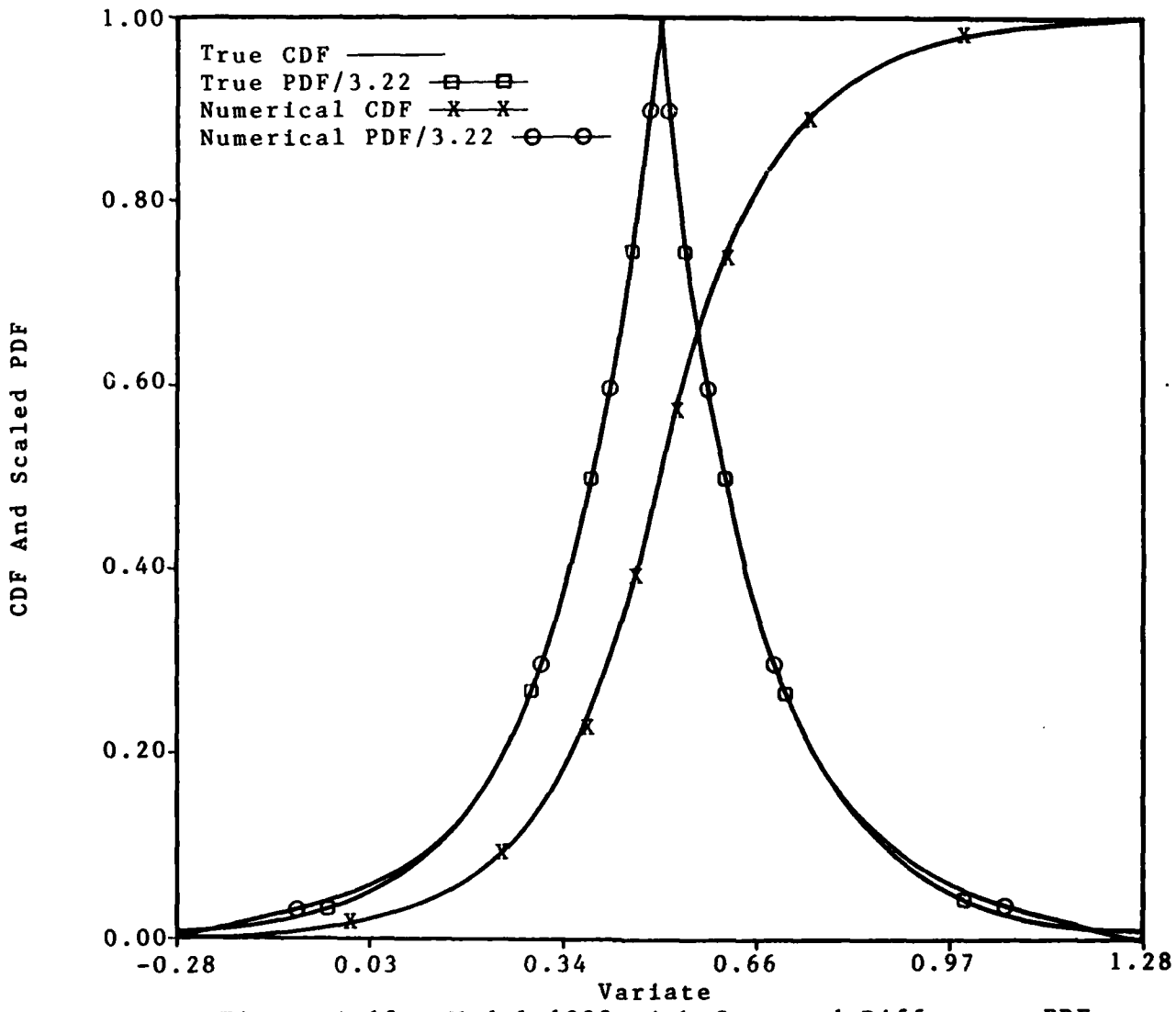

Figure A.15. Model 1332 with Centered Difference PDF Applied to a Double Exponentially Distributed Variable

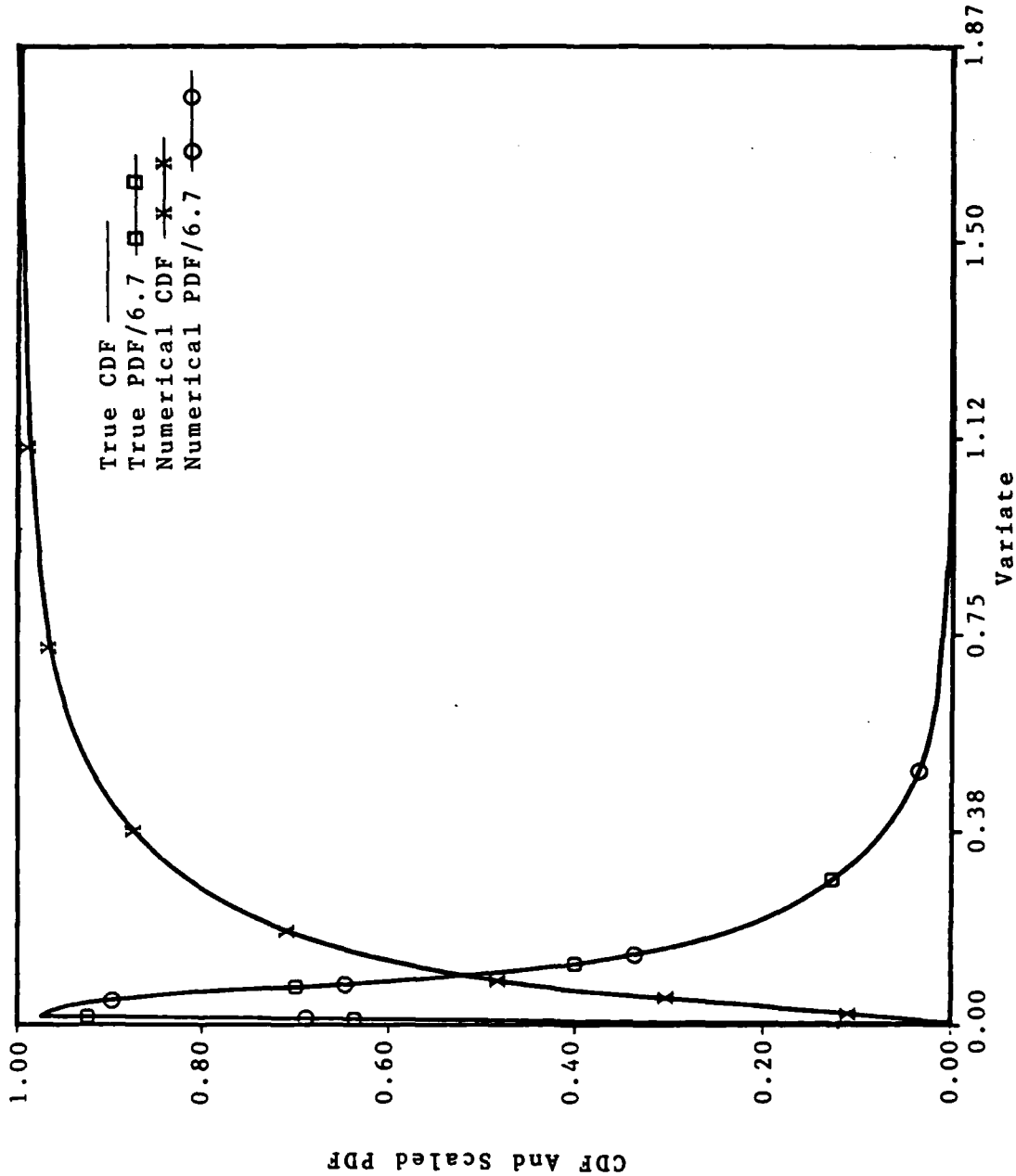

Figure A.16. Model 1332 With Centered Difference PDF Applied to a Lognormally Distributed Variable

left in Figure A.16, as it should be. However, the normal and DE tails in Figures A.14 and A.15, respectively, are shorter, which they should not be.

Sweeder [14] grappled with this problem, developing a number of adaptive models. This approach was not completely successful, since under subsampling and inversion, endpoints were sometimes chosen that eliminated some original data. In addition, one would like to avoid computer intensiveness as much as possible.

An alternate approach is to enforce conservation of probability in the tails of the sample distribution to find the endpoints.

Derivation of the General Form. The numerical situation in the tails is illustrated in Figure A.17. The CDF is known at the circled locations. The PDF is known approximately at the location of the x's. The locations of z_0 and z_{m+1} are desired.

The conservation of probability may be approximately enforced on the intervals $[z_0,z_1]$ and $[z_1,z_2]$ by requiring:

$$F_Z(z_1)=\int_{z_0}^{z_1} f_Z(z)dz \qquad (A.29)$$

$$F_Z(z_2)-F_Z(z_1)=\int_{z_1}^{z_2} f_Z(z)dz \qquad (A.30)$$

Using the relations:

$$F_Z(z_i)=G_i \qquad (A.31)$$

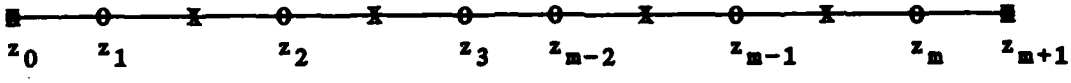

Figure A.17. An Illustration of the Extrapolation Problem

$$\int_{z_i}^{z_{i+1}} f_Z(z)dz \cong (f_{i+1}+f_i)(z_{i+1}-z_i)/2 \qquad (A.32)$$

Equations A.29 and A.30 reduce to:

$$G_1 = f_1(z_1-z_0)/2 \qquad (A.33)$$

$$\Delta G = (f_2+f_1)(z_2-z_1)/2 \qquad (A.34)$$

where

$$\Delta G = G_{i+1}-G_i = G_2-G_1 \qquad (A.35)$$

Since the G_i's are known from the plotting rule of Equation A.4 and f_2 by some method of interpolation on the interval $[z_{3/2}, z_{5/2}]$, the only unknowns above are f_1 and z_0. Solving for z_0 leads to the equation:

$$z_0 = z_1 - 2G_1(z_2-z_1)/\{2\Delta G - f_2(z_2-z_1)\} \qquad (A.36)$$

If Δ_l is defined by:

$$\Delta_l = 2G_1/\{2\Delta G - f_2(z_2-z_1)\} \qquad (A.37)$$

then Equation A.36 has exactly the same form as Sweeder's extrapolation rule Equation A.10. A similar analysis for the right hand tail leads to a similar form and an extrapolation constant Δ_u defined by:

$$\Delta_u = 2(1-G_m)/\{2\Delta G - f_{m-1}(z_m-z_{m-1})\} \qquad (A.38)$$

Exploiting the general form for the G_i's, the extrapolation constants may be written as:

$$\Delta_l = 2(1+\alpha)/\{2-f_2(z_2-z_1)/\Delta G\} \qquad (A.39)$$

$$\Delta_u = 2(\beta-\alpha)/\{2-f_{m-1}(z_m-z_{m-1})/\Delta G\} \qquad (A.40)$$

These extrapolation constants depend on the plotting rule (α,β), the sample size (m), the extreme order statistics (z_1, z_2, z_{m-1}, z_m), and on the choice of interpolation for the derivative (f_2, f_{m-1}).

TABLE A.3

ADAPTIVE EXTRAPOLATION BEHAVIOR

	FORMULA	$2(1+\alpha)$	$2(\beta-\alpha)$
1.	i/(m+1)	2	2
2.	(i-.3)/(m+.4)	1.4	1.4
3.	(i-.5)/m	1.0	1.0
4.	[i-(m+1)/2m]/[m-(1/m)]	(m-1)/m	(m-1)/m
5.	(i-1)/(m-1)	0	0
6.	i/m	2	0
7.	(i-.375)/(m+.25)	1.25	1.25

The dependence of the extrapolation constants on the plotting rule is best seen by examining Table A.3. The adaptive extrapolation constants properly reflect the underlying behavior of the plotting rule. For example, the empirical distribution function (EDF) requires no upper extrapolation ($\Delta_u=0$), while the mode rank requires no upper or lower extrapolation ($\Delta_l=0, \Delta_u=0$).

One also sees that Δ_l and Δ_u remain positive quantities provided:

$$2-f_2(z_2-z_1)/\Delta G>0 \tag{A.41}$$

$$2-f_{m-1}(z_m-z_{m-1})/\Delta G>0 \tag{A.42}$$

Equations A.41 and A.42 are just the requirements that f_1 and f_m be non-negative. Since a numerical approximation is being used for the f_i's, the above equations may not always be satisfied. A number of interpolation schemes are investigated below.

Linear Interpolation. From Figure A.17, and assuming that:

$$f_0=f_{m+1}=0 \tag{A.43}$$

then

$$f_{3/2}\leq f_2\leq f_{5/2} \tag{A.44}$$

$$f_{m-1/2}\leq f_{m-1}\leq f_{m-3/2} \tag{A.45}$$

where, in general,

$$f_{i+1/2}=\Delta G/(z_{i+1}-z_i) \tag{A.46}$$

Linear interpolation consequently leads to:

$$f_2=f_{3/2}+(f_{5/2}-f_{3/2})(z_2-z_{3/2})/(z_{5/2}-z_{3/2}) \tag{A.47}$$

$$f_{m-1}=f_{m-1/2}+(f_{m-3/2}-f_{m-1/2})(z_{m-1}-z_{m-1/2})/(z_{m-3/2}-z_{m-1/2}) \quad (A.48)$$

Average Value Approximation. The above expressions may lead to negative Δ_1 and Δ_u. Another choice for f_2 and f_{m-1} would be to set:

$$f_2 \equiv (f_{3/2}+f_{5/2})/2 \quad (A.49)$$

$$f_{m-1} \equiv (f_{m-1/2}+f_{m-3/2})/2 \quad (A.50)$$

This choice leads to:

$$f_2(z_2-z_1)/\Delta G=(z_3-z_1)/\{2(z_3-z_2)\} \quad (A.51)$$

$$f_{m-1}(z_m-z_{m-1})/\Delta G=(z_m-z_{m-2})/\{2(z_{m-1}-z_{m-2})\} \quad (A.52)$$

In this case, the resulting expressions for Δ_1 and Δ_u remain positive provided that:

$$(z_3-z_1)/(z_3-z_2)<4 \quad (A.53)$$

$$(z_m-z_{m-2})/(z_{m-1}-z_{m-2})<4 \quad (A.54)$$

Extreme Value Approximation. The average value approximation may still yield negative extrapolation constants for heavy-tailed distributions. Using an extreme value approximation, one sets:

$$f_2 \equiv f_{3/2} \quad (A.55)$$

$$f_{m-1} \equiv f_{m-1/2} \quad (A.56)$$

The result here is that:

$$f_2(z_2-z_1)/\Delta G=1 \quad (A.57)$$

$$f_{m-1}(z_m-z_{m-1})/\Delta G=1 \quad (A.58)$$

This choice therefore guarantees that the extrapolation constants remain positive. In fact, for this approximation:

$$\Delta_1=2(1+\alpha) \quad (A.59)$$

$$\Delta_u = 2(\beta - \alpha) \qquad \text{(A.60)}$$

For plotting under Hazen's Rule (α=-.5,β=0), the extrapolation constants reduce to Sweeder's values (Δ_l=1,Δ_u=1).

Final Results. The final results obtained by incorporating these new ideas are illustrated in Figures A.18 through A.22. Some discussion here is in order.

The results for the uniform distribution are illustrated in Figure A.18. It is interesting to note that no changes have occurred in the endpoints. This must mean that Sweeder's rule is correct. That this is true can be seen by examining Equations A.47 and A.48. Using the fact that, for the uniform:

$$\Delta G = z_{i+1} - z_i \quad \forall \; i=1,m \qquad \text{(A.61)}$$

Equations A.47 and A.48 reduce to Equations A.57 and A.58. The linear interpolation scheme reduces naturally to Sweeder's rule under the assumption of a uniform distribution.

The result for the normal distribution is displayed in Figure A.19. An increased tail length is evident compared to the plot of Figure A.14. An expanded left-hand tail is shown in Figure A.20 to illustrate the differences in the approximations. In this figure the smooth curve represents the true PDF, the X's the adaptive extrapolation technique just developed, and the circles Sweeder's rule.

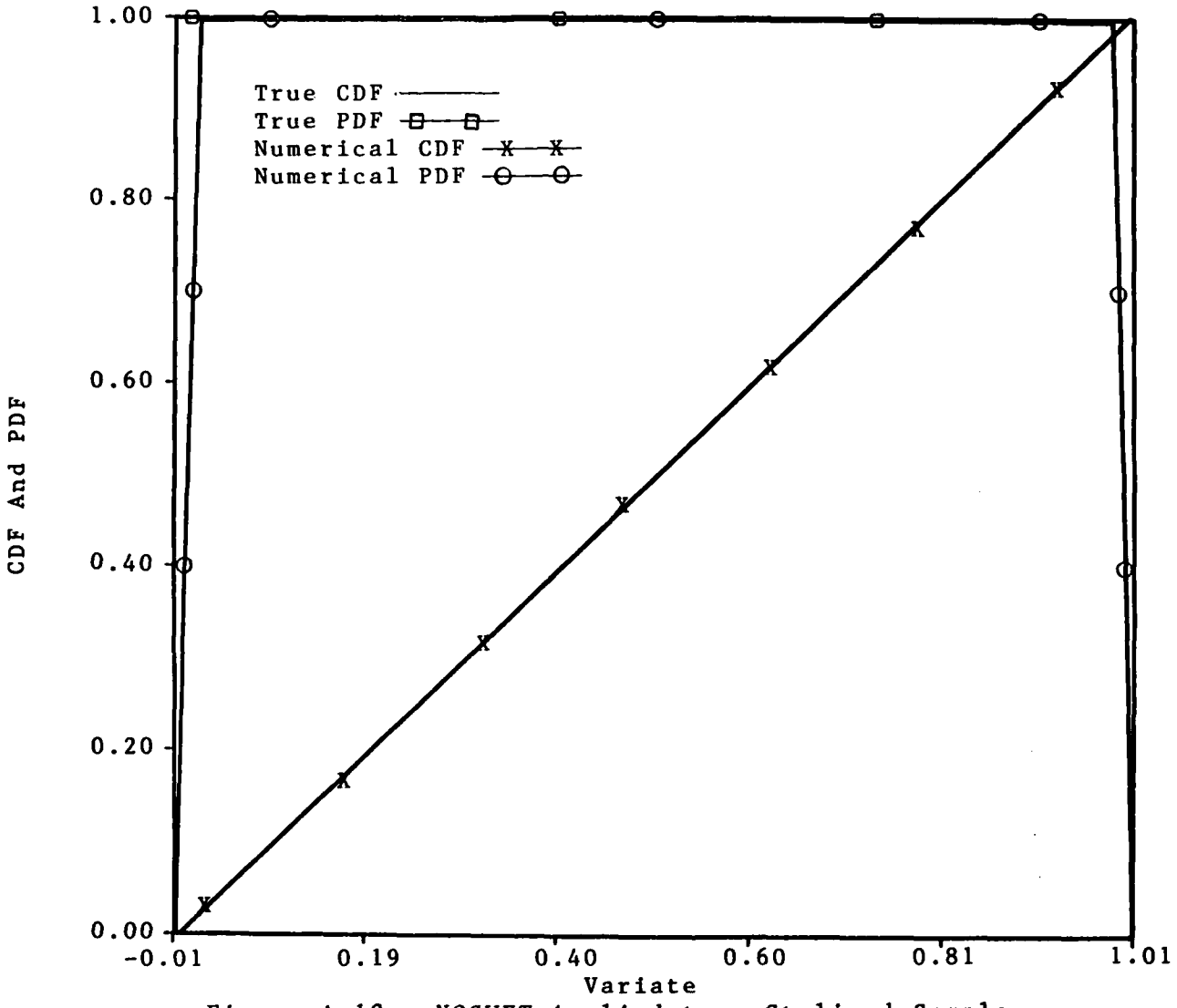

Figure A.18. NOSWET Applied to a Stylized Sample From the Uniform Distribution

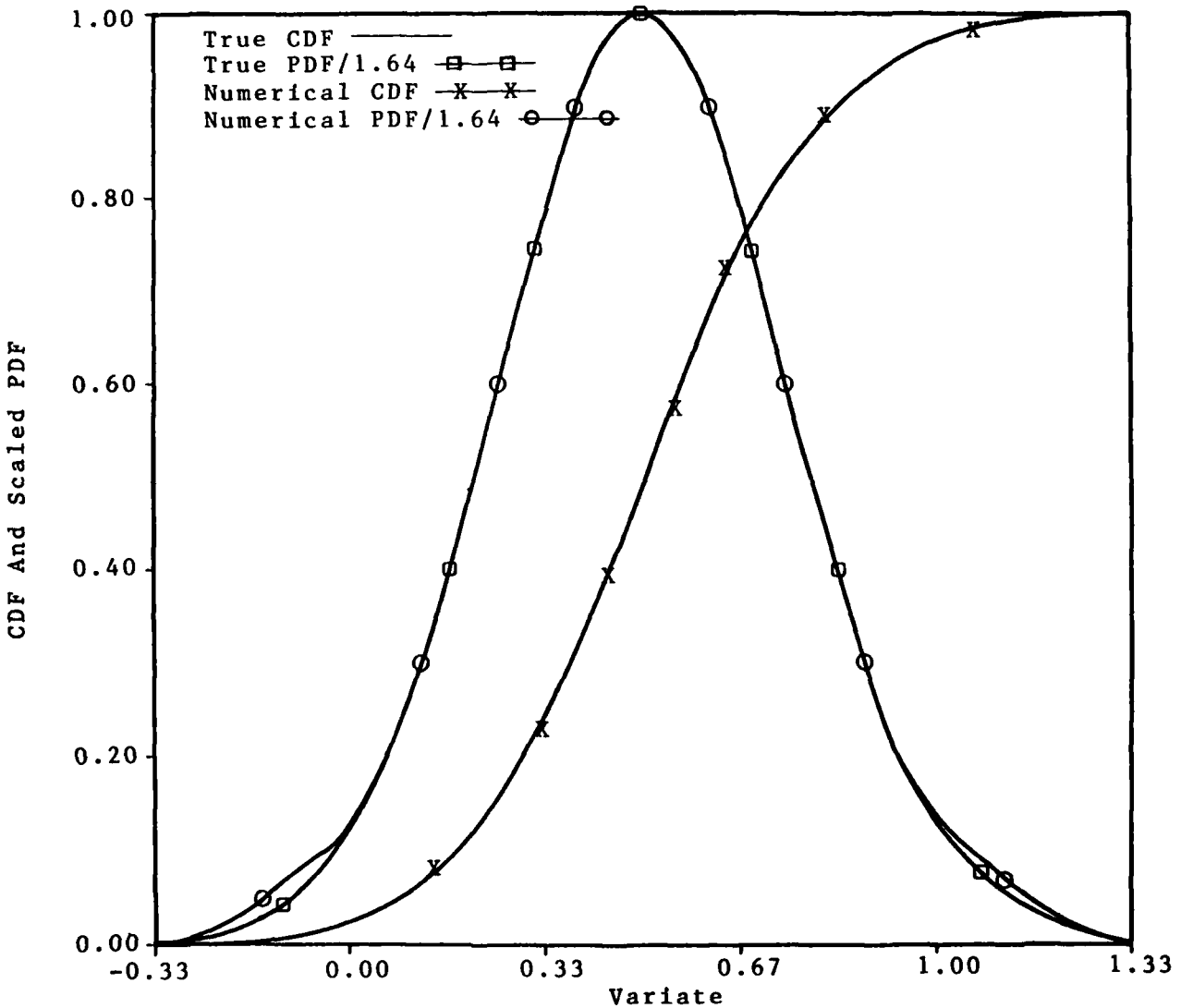

Figure A.19. NOSWET Applied to a Stylized Sample From the Normal Distribution

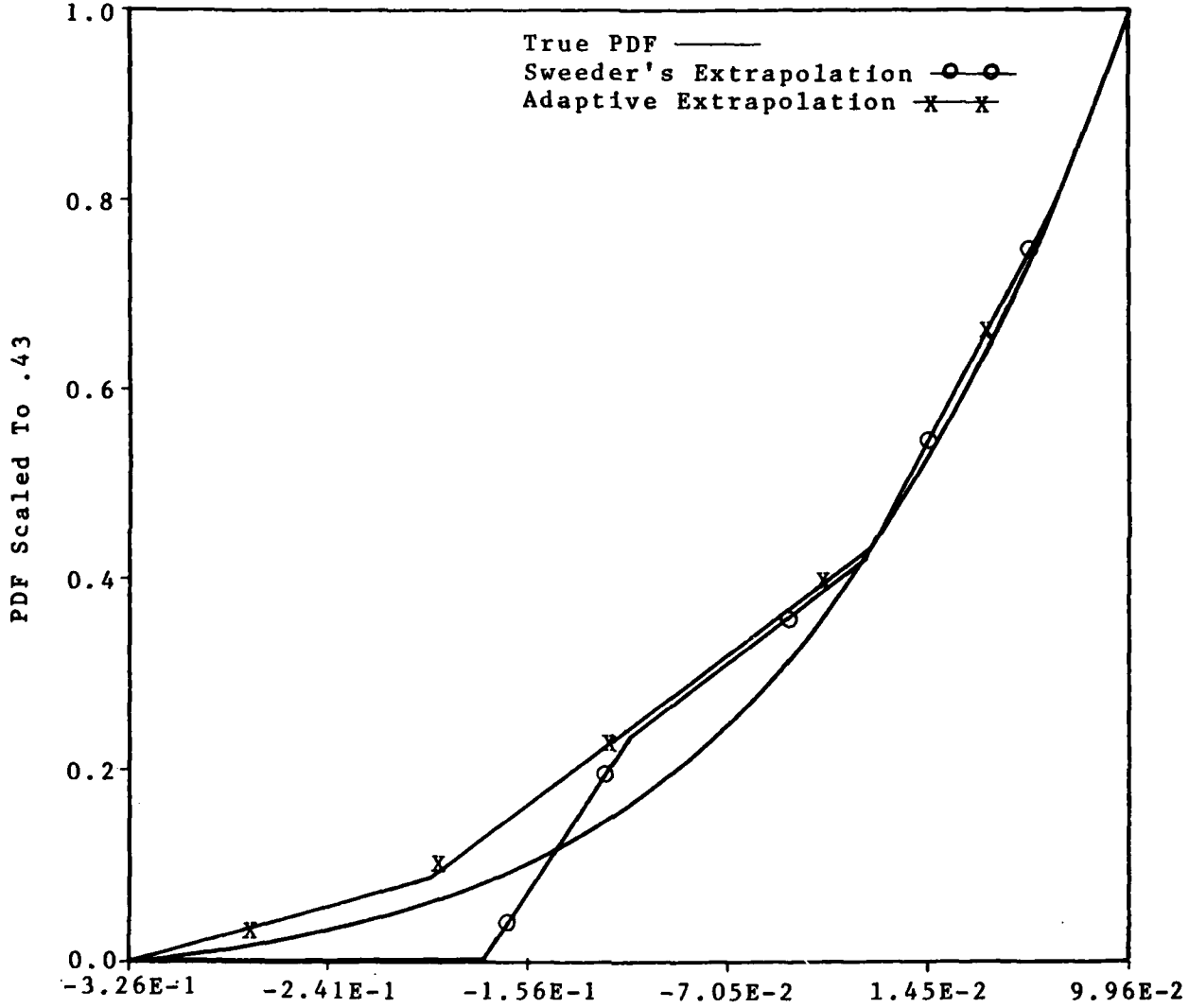

Figure A.20. A Comparison of Extrapolation Methods

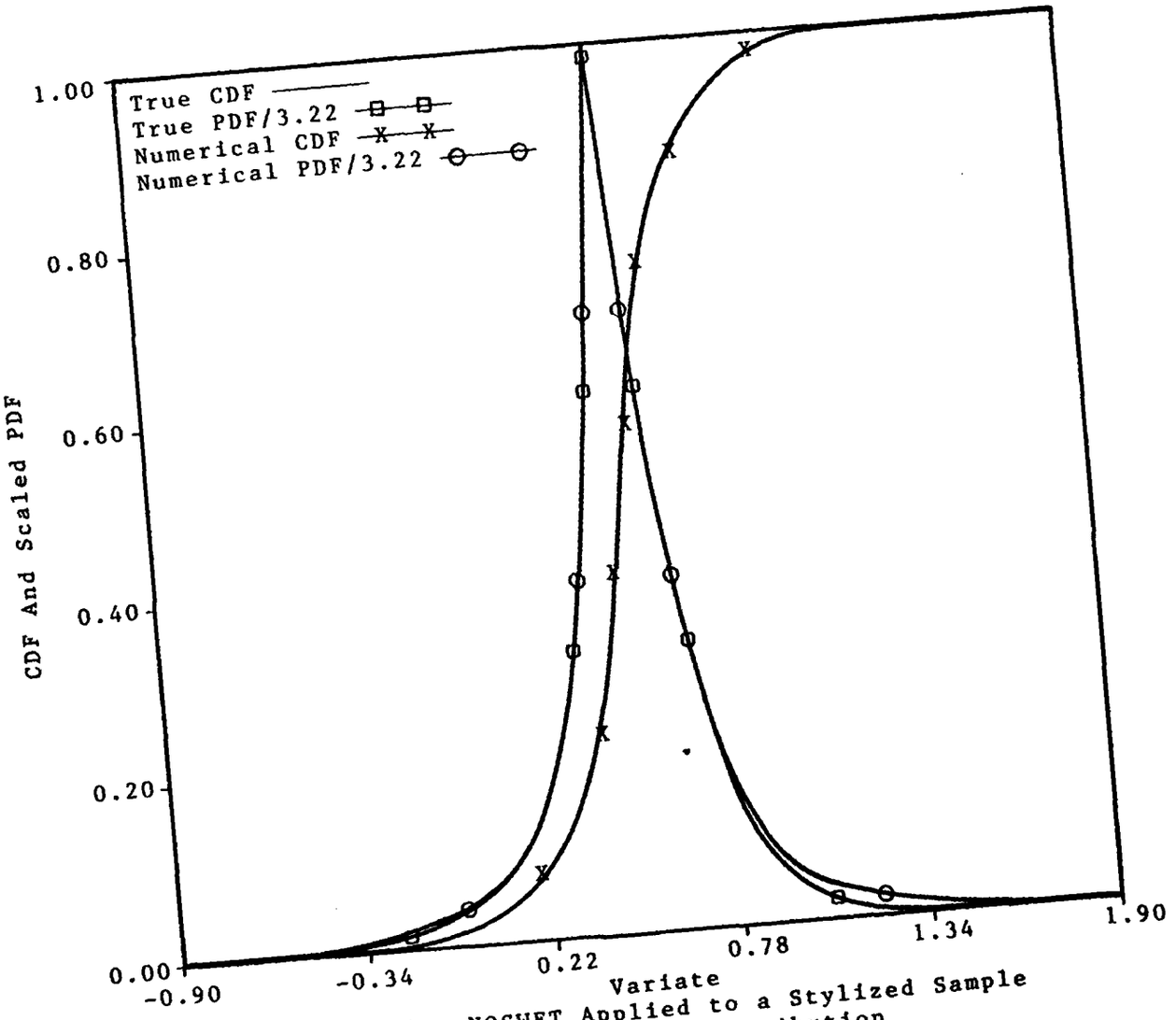

Figure A.21. NOSWET Applied to a Stylized Sample From the Double Exponential Distribution

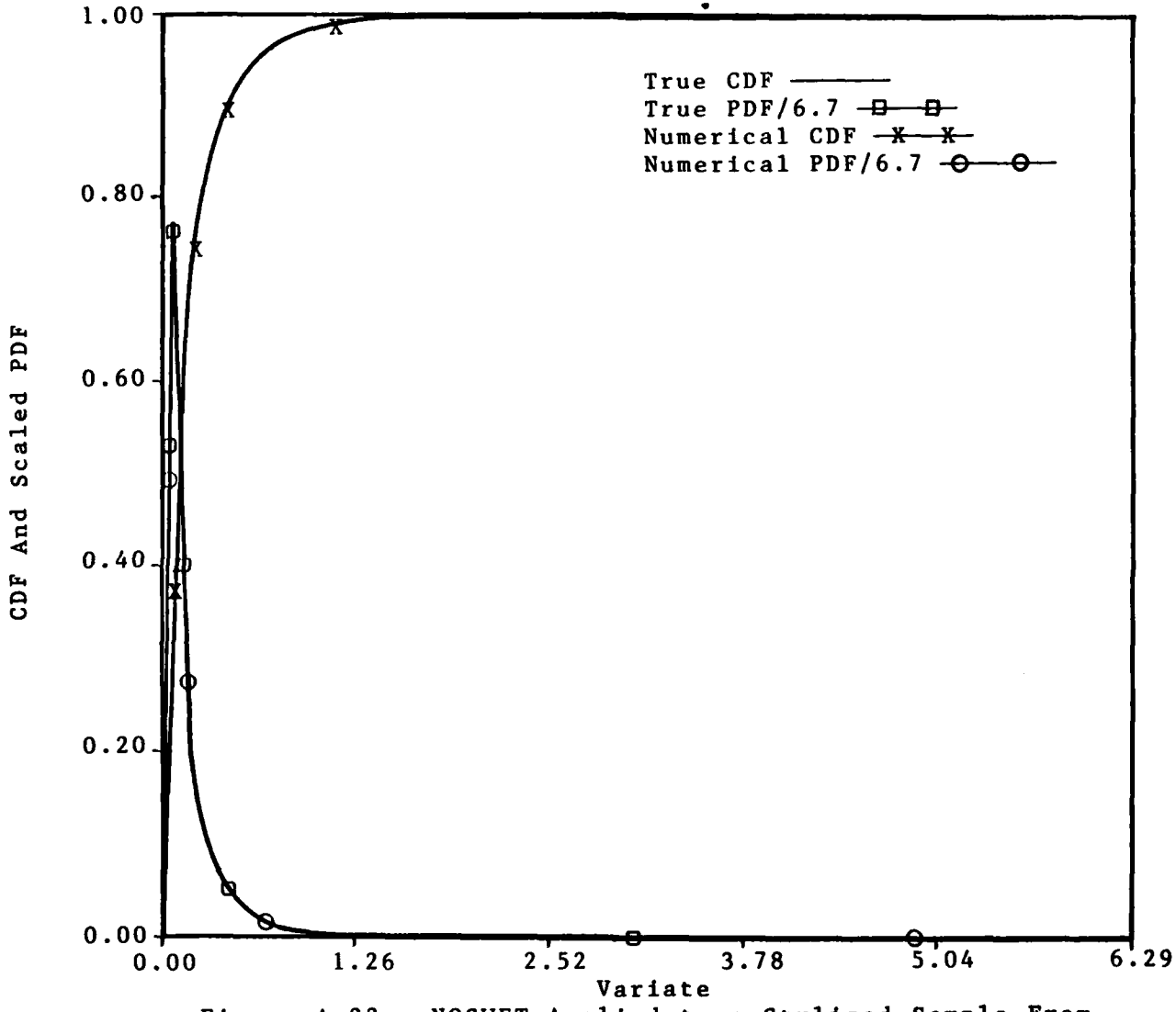

Figure A.22. NOSWET Applied to a Stylized Sample From the Lognormal Distribution

The final result for the DE is illustrated in Figure A.21. The adaptive technique has extended the tails considerably.

The final result for the lognormal is illustrated in Figure A.22. The adaptive endpoint extrapolation here brings the left-hand tail very close to zero, and extends the right-hand tail by more than a factor of 3.

At this point, the developmental task was considered to be finished. The computer code NOSWET was written based on the above considerations. A listing is given in Appendix B, and its primary use is discussed in Appendix C.

Summary

To summarize, Sweeder's method [14] has been modified in four ways. First, the concept of a stylized sample was defined. The performance of one of Sweeder's early research models on stylized samples from the uniform, normal, double exponential, and lognormal distributions led to the elimination of Sweeder's subsampling method. Second, Sweeder's trigonometric method of interpolating the CDF was changed to simple linear interpolation. Third, the PDF estimation method was changed to a centered-difference scheme. Fourth, a general approach to endpoint extrapolation was taken by enforcing the conservation of probability in the tails of the distribution. Sweeder's extrapolation rule [14] was seen to be a special case of this more general approach. The new algorithm, written as computer program NOSWET (NOn-

parametric 'after SWeeder' Estimation Technique), was found to be especially useful in finding the distribution of functions of random variables. The program listing is shown in Appendix B, and its primary use is described in Appendix C.

Appendix B: Listing Of Program NOSWET

```
10 '************PROGRAM NOSWET**********************
20 ' Program NOSWET (NOnparametric 'after SWeeder'
       Estimation Technique)
       Constructs a Nonparametric Distribution and Density
       Function From The Data in the 1D Array XDATA
30 '**************************
40 ' Algorithm is based on NONPARAMETRIC ESTIMATION OF
       DISTRIBUTION AND DENSITY FUNCTIONS WITH APPLICATIONS
       by James Sweeder, Ph.D, Capt, USAF.  AFIT/DS/MA/82-1
50 '**************************
60 ' This Microsoft Basic Code Written By HALVOR A. UNDEM,
       Capt, USAF, DS-83, as an Applications Tool in
       Nuclear Survivability.
70 '**************************
80 '************************************************
90 'In the Fictitious Fortran CALL Statements, Variables
       Preceding the Semicolon Are Input, Those After Are
       Output or Altered.
100 '**************************'
110 COMMON BASICNAME$,SETMIN%,SETMAX%
120 DIM MAX(15),MIN(15),WEIGHT(15)
130 ON ERROR GOTO 5400' DISK I/O ERROR TRAP
140 INPUT "BASICNAME$,SETMIN%,SETMAX%:",BASICNAME$,
     SETMIN%,SETMAX%
150 INPUT "Do You Want a DEBUG$ Run (Y/N) ";DEBUG$
160 INPUT "(S)weeder,(H)istogram, or (C)ontinuous PDF";
     PDFTOGGLE$
170 PRINT "THIS IS PROGRAM NOSWET.015"
180 '    NOSWET.015 FEATURES:     (1)--CHOICE OF KSUBS%
                                  (2)--CHOICE OF EXTRAPOLATION
                                  (3)--CHOICE OF PDF
                                  (4)--WRITES TO DISK IF
                                       MEMORY SHORT
190 '                             (5)--CDF IS LINEAR
                                       INTERPOLATION
200 PREFIX$="A:"
210 FOR SET%=SETMIN% TO SETMAX%
220 PRINT
230 PRINT "NOSWET IS PROCESSING DATA SET ";SET%
240 NUMBER$=STR$(SET%)
250 ADD$=MID$(NUMBER$,2)
260 FILNAM$=BASICNAME$+ADD$
270 'Call LOADER(;XDATA[],SIZE%)
280     GOSUB 1000
290     IF DEBUG$="Y" THEN 300 ELSE 370
300     'THEN Segment--Debug Mode Selected
310             FOR I%=1 TO SIZE%
```

```
320             PRINT XDATA(I%);
330             IF I% MOD 5=0 THEN PRINT
340             NEXT I%
350             PRINT "SIZE% IS ";SIZE%
360             IF SIZE%<2 THEN PRINT "SAMPLE TOO SMALL--
                    LOADER ABORT":STOP
370 'Call SORT(XDATA[],N%;XDATA[])
380     N%=SIZE%
390     GOSUB 1490
400 'Call SUBSAMPL(XDATA[],KSUBS%,SIZE%,;SUBSAMP[],M%,R%,
                    XMAX,XMIN)
410     INPUT "(R)andom or (S)tylized Sample";TOGGLE$
420     IF TOGGLE$="R" THEN KSUBS%=5 ELSE KSUBS%=1
430     IF KSUBS%>N%/3 THEN PRINT "KSUBS% TOO LARGE":GOTO
           410
440     INPUT "(S)weeder or (A)utoranging Extrapolation";
          EXTRAPTOGGLE$
450     GOSUB 1780
460     IF DEBUG$="Y" THEN 470 ELSE 580
470     'THEN Segment--Debug Mode Selected
480             FOR SAMPLE%=1 TO KSUBS%
490             IF SAMPLE%<=R% THEN LASTEL%=M%+2 ELSE
                    LASTEL%=M%+1
500             PRINT "SAMPLE%,LASTEL% ARE ";SAMPLE%;LASTEL%
510             FOR ELEMNT%=0 TO LASTEL%
520             PRINT SUBSAMP(ELEMNT%,SAMPLE%);
530             IF ELEMNT% MOD 5=0 THEN PRINT
540             NEXT ELEMNT%
550             PRINT "PAUSING BEFORE NEXT SAMPLE":STOP
560             NEXT SAMPLE%
570             PRINT "M%,R%,XMAX,XMIN ARE ";M%;R%;XMAX;XMIN
580 'Call JACKNIFE(SUBSAMP[],SIZE%,KSUBS%;SUBSAMP[],
                    XDATA[],ZDATA[])
590     GOSUB 2600
600     IF DEBUG$="Y" THEN 610 ELSE 820
610     'THEN Segment--Debug Mode Selected
620             PRINT "HERE IS THE NEW XDATA ARRAY";
630             FOR I%=1 TO SIZE%
640             PRINT XDATA(I%);
650             IF I% MOD 5=0 THEN PRINT
660             NEXT I%
670             PRINT "HERE IS THE ZDATA ARRAY"
680             FOR I%=1 TO SIZE%
690             PRINT ZDATA(I%);
700             IF I% MOD 5=0 THEN PRINT
710             NEXT I%
720             PRINT "HERE IS THE NEW SUBSAMP ARRAY"
730             FOR SAMPLE%=1 TO KSUBS%
740             IF SAMPLE%<=R% THEN LASTEL%=M%+2 ELSE
                    LASTEL%=M%+1
750             PRINT "SAMPLE%,LASTEL% ARE ";SAMPLE%;LASTEL%
760             FOR ELEMNT%=0 TO LASTEL%
```

```
770             PRINT SUBSAMP(ELEMNT%,SAMPLE%);
780             IF ELEMNT% MOD 5=0 THEN PRINT
790             NEXT ELEMNT%
800             PRINT "PAUSING AFTER SAMPLE% ";SAMPLE%:STOP
810             NEXT SAMPLE%
820 INPUT "Dump XDATA To Disk ";ANS$
830 IF ANS$="Y" THEN 840 ELSE 860
840 'THEN Segment--Dump XDATA To Disk
850     GOSUB 5160
860 INPUT "Want A Look (Y/N)";LOOK$
870 IF LOOK$="Y" THEN 880 ELSE 940
880 INPUT "Input The Value of X ",X
890 'Call CDFPDF(SUBSAMP[],KSUBS%,M%,R%,IPLOT%,X;AVGCDF(X),
                 AVGPDF(X))
900     IPLOT%=3        'Midpoint of EDF
910     GOSUB 3780
920 PRINT "AT X=";X;"CDF,PDF ARE ";AVGCDF;AVGPDF
930 GOTO 860
940 INPUT "Do You Wish To Plot the PDF/CDF ";ANS$
950 IF ANS$="Y" THEN GOSUB 5450'        CALL PLOTPCDF
960 NEXT SET%
970 CHAIN "FAILPROB"
980 END
990 '*****************************
1000 '****'SUBROUTINE LOADER(;XDATA[],SIZE%)'****'
1010 '*****************************
1020 'Subroutine LOADER Loads the XDATA Array From
       The Keyboard or From A Datafile
1030 '************************
1040 'INPUT VARIABLES:  None--Prompts For All
1050 '************************
1060 'OUTPUT VARIABLES: XDATA--The Array Containing SIZE%
                              Elements
1070 '************************
1080 IF DEBUG$="Y" THEN PRINT "LOADER HAS BEEN CALLED"
1090 ANS$="N"
1100 IF ANS$="Y" THEN 1110 ELSE 1190
1110 'THEN Segment--Load XDATA From Random Number Generator
1120    RANDOMIZE
1130    INPUT "What Size is Your Sample ";SIZE%
1140    DIM XDATA(SIZE%)
1150    FOR J%=1 TO SIZE%
1160    XDATA(J%)=RND
1170    NEXT J%
1180    RETURN
1190 'ELSE Segment--Load From Keyboard or Datafile
1200    KEYIN$="T"
1210    IF KEYIN$="K" THEN 1220 ELSE 1290
1220    'THEN Segment--Load Data From Keyboard
1230            INPUT "What Size Is Your Sample";SIZE%
1240            DIM XDATA(SIZE%)
1250            FOR J%=1 TO SIZE%
```

```
1260            PRINT "XDATA(";J%;")=";:INPUT XDATA(J%)
1270            NEXT J%
1280            RETURN
1290    'ELSE Segment--Load Data From Tape
1300            OPEN "I",3,FILNAM$
1310            INPUT #3,SIZE%,NEL%
1320            IF TAPCALL$="T" THEN ERASE XDATA
1330            DIM XDATA(SIZE%)
1340            NREC%=SIZE%\NEL%
1350            IF SIZE% MOD NEL%<>0 THEN NREC%=NREC%+1
1360            XINDEX%=0
1370            FOR RECORD%=1 TO NREC%
1380            FOR ELEMNT%=1 TO NEL%
1390            XINDEX%=XINDEX%+1
1400            IF XINDEX%>SIZE% THEN PRINT "OUT OF
                    DATA":RETURN
1410            INPUT #3,XDATA(XINDEX%)
1420            NEXT ELEMNT%
1430            NEXT RECORD%
1440            CLOSE #3
1450            TAPCALL$="T"
1460            RETURN
1470            END
1480 '''''''''''''''''''''''''''''''''''''
1490 '  SUBROUTINE SORT(XDATA[],N%;XDATA[])"""'
1500 '''''''''''''''''''''''''''''''''''''
1510 'SUBROUTINE SORT Sorts a Data Set From Min to Max
1520 'INPUT VARIABLES:  XDATA--The Array Containing the Data
                        N%-----The Number of Elements
1530 'OUTPUT VARIABLES: XDATA--The Array After Sorting
1540 '*********************************************
1550 IF DEBUG$="Y" THEN PRINT "SORT HAS BEEN CALLED"
1560 FLIPS=1 'FORCE AT LEAST ONE PASS
1570 WHILE FLIPS
1580    FLIPS=0
1590    FOR J%=1 TO N%-1
1600    IF XDATA(J%)>XDATA(J%+1) THEN 1620 ELSE 1660
1610    'THEN Segment--SWAP pair
1620            SWAP XDATA(J%),XDATA(J%+1)
1630            FLIPS=1
1640            GOTO 1660
1650    'ELSE Segment--Look At Next Pair
1660    NEXT J%
1670 WEND
1680 IF DEBUG$="Y" THEN 1690 ELSE 1750
1690 PRINT "HERE IS THE SORTED ARRAY"
1700 FOR I%=1 TO N%
1710 PRINT XDATA(I%);
1720 IF I% MOD 5=0 THEN PRINT
1730 NEXT I%
1740 PRINT
1750 RETURN
```

```
1760 END
1770 '*****************************
1780 '  SUBROUTINE SUBSAMPL(XDATA[],KSUBS%,SIZE%;SUBSAMP[],
       M%,R%,XMAX,XMIN)
1790 '*****************************
1800 'Subroutine SUBSAMPL Loads the 2D Array SUBSAMP from
       the 1D Array XDATA
1810 '*****************************
1820 'INPUT VARIABLES:  XDATA--1D Array Containing
                           Observations
                        SIZE%--Total Dimension of XDATA
                        KSUBS%-Number of Subsamples
                        Desired--Will Be # of Cols of SUBSAMP
1830 '*************************
1840 'OUTPUT VARIABLES: M%--Nominal Number of Elements Per
                           Subsample
                        R%--Number of Subsamples With M%+1
                           Elements
                        SUBSAMP--2D Array--Each Column Is A
                           Subsample
1850 '*************************
1860 'REQUIRED EXTERNALS:       SUBROUTINE ENDPOINT--To Get
                                   XMIN,XMAX
1870 '*************************
1880 IF DEBUG$="Y" THEN PRINT "SUBSAMPL HAS BEEN CALLED"
1890 M%=SIZE%\KSUBS%
1900 R%=SIZE% MOD KSUBS%
1910 IF SAMPCALL%=1 THEN 1920 ELSE 1940
1920 'THEN Segment--SUBSAMPL Previously Called
1930           ERASE SUBSAMP
1940 IF R%=0 THEN 1950 ELSE 1980
1950 'THEN Segment--M% Elements in SUBSAMP--Dimension 1 More
1960    DIM SUBSAMP(M%+1,KSUBS%)
1970    GOTO 2000
1980 'ELSE Segment--M%+1 Elements in SUBSAMP
1990    DIM SUBSAMP(M%+2,KSUBS%)
2000 XINDEX%=0
2010 FOR SAMPLE%=1 TO KSUBS%
2020    IF SAMPLE%<=R% THEN 2030 ELSE 2060
2030    'THEN Segment--M%+1 In This One
2040           SAMPSIZE%=M%+1
2050           GOTO 2080
2060    'ELSE Segment--M% In This One
2070           SAMPSIZE%=M%
2080 WEIGHT(SAMPLE%)=SAMPSIZE%/SIZE%
2090 FOR ELEMNT%=1 TO SAMPSIZE%
2100 XINDEX%=XINDEX%+1
2110 IF TOGGLE$="R" THEN XINDEX%=SAMPLE%+KSUBS%*(ELEMNT%-1)
2120 SUBSAMP(ELEMNT%,SAMPLE%)=XDATA(XINDEX%)
2130 NEXT ELEMNT%
2140 'CALL EXTRAP(SUBSAMP[],TOGGLE$;DELTAL,DELTAU)
2150    GOSUB 5970
```

```
2160 SUBSAMP(0,SAMPLE%)=SUBSAMP(1,SAMPLE%)-DELTAL
     *(SUBSAMP(2,SAMPLE%)-SUBSAMP(1,SAMPLE%))
2170 SUBSAMP(SAMPSIZE%+1,SAMPLE%)=SUBSAMP(SAMPSIZE%,SAMPLE%)
     +DELTAU*(SUBSAMP(SAMPSIZE%,SAMPLE%)
     -SUBSAMP(SAMPSIZE%-1,SAMPLE%))
2180 MIN(SAMPLE%)=SUBSAMP(0,SAMPLE%)
2190 MAX(SAMPLE%)=SUBSAMP(SAMPSIZE%+1,SAMPLE%)
2200 NEXT SAMPLE%
2210 'CALL SUBROUTINE ENDPOINT(MIN[],MAX[],KSUBS%)
2220    GOSUB 2270
2230 SAMPCALL%=1
2240 RETURN
2250 END
2260 '*****************************
2270 '  SUBROUTINE ENDPOINT(MIN[],MAX[],KSUBS%;XMIN,XMAX)
2280 '*****************************
2290 'Subroutine ENDPOINTS Gets The Extrapolated Values
        for A Set of Data Found in Arrays MIN And MAX
2300 '*************************
2310 'INPUT VARIABLES:  MIN--1D Array Containing Mininum
                              Extraps
                        MAX--1D Array Containing Max Extraps
                        KSUBS%--Size of Above Arrays
2320 '*************************
2330 'OUTPUT VARIABLES: XMIN--Minimum Found in MIN
                        XMAX--Maximum Found in MAX
2340 '*************************
2350 'REQUIRED EXTERNALS:       SUBROUTINE SORT
2360 '*************************
2370 IF DEBUG$="Y" THEN PRINT "ENDPOINT HAS BEEN CALLED"
2380 'CALL SORT(XDATA[],N%;XDATA[])
2390    FOR J%=1 TO KSUBS%
2400    SWAP XDATA(J%),MIN(J%)
2410    NEXT J%
2420    N%=KSUBS%
2430    GOSUB 1490
2440 FOR J%=1 TO KSUBS%
2450 SWAP XDATA(J%),MIN(J%)
2460 NEXT J%
2470 XMIN=MIN(1)
2480 'CALL SORT(XDATA[],N%;XDATA[])
2490    FOR J%=1 TO KSUBS%
2500    SWAP XDATA(J%),MAX(J%)
2510    NEXT J%
2520    GOSUB 1490
2530 FOR J%=1 TO KSUBS%
2540 SWAP XDATA(J%),MAX(J%)
2550 NEXT J%
2560 XMAX=MAX(KSUBS%)
2570 RETURN
2580 END
```

```
2590 !****************************
2600 '  SUBROUTINE JACKNIFE(SUBSAMP[],SIZE%,KSUBS%;
          SUBSAMP[],XDATA[],ZDATA[])
2610 !*******!*********************
2620 '""'Subroutine JACKNIFE Samples From the Current
       Distribution, Storing the Sample in ZDATA
2630 !************************
2640 'INPUT VARIABLES:  SUBSAMP--2D Array of Subsamples For
                              Current Distribution
                        SIZE%-----Total Number of Data Points
                                  in Original Sample
                        KSUBS%--Number Of Subsamples Desired
2650 !*************************!
2660 'OUTPUT VARIABLES: ZDATA--Array Containing Last
                                  Pseudodata
                        SUBSAMP--Altered 2D Array For "New"
                                  Distribution
                        XDATA--Now Contains New Dataset
2670 !*************************!
2680 'REQUIRED EXTERNALS:  SUBROUTINE PLOTPNT--To Get Median
                                                  Ranks
                           SUBROUTINE ZOFCDF--To Invert
                                                Distribution
                           SUBROUTINE SUBSAMPL--To Reload Array
                                                SUBSAMP
2690 !*****************************!
2700 IF DEBUG$="Y" THEN PRINT "JACKNIFE HAS BEEN CALLED"
2710 IF JACKCALL$<>"T" THEN DIM ZDATA(SIZE%)
2720 INPUT "Input JACKMAX% (0,1,2):",JACKMAX%
2730 IF JACKMAX%=0 THEN JACKCALL$="T":RETURN
2740 IF JACKCALL$<>"T" AND JACKMAX<>0 AND TOGGLE$="S" THEN
       2750 ELSE 2780
2750    'THEN SEGMENT--Verify Desired Operation
2760    PRINT "YOU ARE JACKNIFING A STYLIZED SAMPLE"
2770    STOP
2780 FOR JACK%=1 TO JACKMAX%
2790 PRINT
2800 PRINT "THIS IS INVERSION NUMBER ";JACK%
2810 ZDATA(0)=XMIN
2820 FOR IJACK%=1 TO SIZE%
2830 'CALL PLOTPNT(IPLOT%,IPNT%,NOBS%;PLOTPNT)
2840    IPNT%=IJACK%
2850    IPLOT%=2'        Median Rank Points
2860    NOBS%=SIZE%
2870    GOSUB 3060
2880 'CALL ZOFCDF(ALFA,ZMIN,ZMAX;ZALFA)
2890    ZMAX=XMAX
2900    ZMIN=ZDATA(IJACK%-1)
2910    ALFA=PLOTPNT
2920    GOSUB 3270
2930 ZDATA(IJACK%)=ZALFA
```

```
2940 PRINT "FOR DATA POINT ";IJACK%;"ALFA,ZDATA ARE ";ALFA;
       ZDATA(IJACK%)
2950 NEXT IJACK%
2960 'CALL SUBSAMPL(XDATA[],KSUBS%,SIZE%;SUBSAMPL[],M%,R%,
                    XMAX,XMIN)
2970    FOR J%=1 TO SIZE%
2980    SWAP XDATA(J%),ZDATA(J%)
2990    NEXT J%
3000    GOSUB 1780
3010 NEXT JACK%
3020 JACKCALL$="T"
3030 RETURN
3040 END
3050 '*****************************
3060 '  SUBROUTINE PLOTPNT(IPLOT%,IPNT%,NOBS%;PLOTPNT)
3070 '*****************************
3080 '  Subroutine PLOTPNT Generates the Plotting Position
       for the I%th Observation out of NOBS%
3090 '*************************
3100 'INPUT VARIABLES:  IPLOT%--Variable Selecting Choice
                              of Plotting Position
                        IPNT%------The I%th Observation
                        NOBS%---The Total Number of
                                  Observations
3110 '*************************
3120 'OUTPUT VARIABLE:  PLOTPNT--The Plotting Position
3130 '*************************
3140 IF DEBUG$="Y" THEN PRINT "PLOTPNT HAS BEEN CALLED"
3150 IF IPNT%=0 THEN PLOTPNT=0:RETURN
3160 IF IPNT%=NOBS%+1 THEN PLOTPNT=1:RETURN
3170 IF IPLOT%=2 THEN 3180 ELSE 3210
3180 'THEN Segment--Approximate Median Ranks
3190    PLOTPNT=(IPNT%-.3)/(NOBS%+.4)
3200    GOTO 3230
3210 'ELSE Segment--Midpoint of EDF
3220    PLOTPNT=(IPNT%-.5)/NOBS%
3230 IF PLOTPNT<0 OR PLOTPNT>1 THEN PRINT "ERROR IN
       PLOTPNT":STOP
3240 RETURN
3250 END
3260 '*****************************
3270 '  SUBROUTINE ZOFCDF(ALFA,ZMIN,ZMAX;ZALFA)
3280 '*****************************
3290 'Subroutine ZOFCDF Finds the Value of z such that
       Pr[Z<=z]=ALFA
3300 '*************************
3310 'INPUT VARIABLES:  ALFA--PERCENTILE DESIRED
                        ZMIN--MINIMUM VALUE OF VARIATE
                        ZMAX--MAXIMUM VALUE OF VARIATE
3320 '*************************
3330 'OUTPUT VARIABLES: ZALFA--Value of Z Satisfying
       Equation
```

```
3340 '**************************
3350 'REQUIRED EXTERNALS:       SUBROUTINE CDFPDF--To Supply
                                                    CDF Values
3360 '**************************
3370 IF DEBUG$="Y" THEN PRINT "ZOFCDF HAS BEEN CALLED"
3380 ICOUNT%=0
3390 CRIT=1
3400 HIVALUE=ZMAX
3410 LOVALUE=ZMIN
3420 WHILE CRIT>.000001
3430    IF HIVALUE=LOVALUE THEN 3440 ELSE 3480
3440    'THEN Segment--Nonconvergence Problem
3450            PRINT "ZOFCDF CANNOT CONVERGE"
3460            PRINT "ALFA,ZALFA,CRIT ARE ";ALFA;ZALFA;CRIT
3470            STOP
3480    'ELSE Segment--Normal Search Continues
3490    ICOUNT%=ICOUNT%+1
3500    IF ICOUNT%>212 THEN 3510 ELSE 3580
3510    'THEN Segment--Tolerance Not Met
3520            PRINT "TOLERANCE NOT MET"
3530            PRINT "ALFA,ZALFA,CRIT ARE ";ALFA;GUESS;CRIT
3540            PRINT "HIVALUE,LOVALUE ARE ";HIVALUE;LOVALUE
3550            INPUT "Execute Recovery Routine ";ANS$
3560            IF ANS$="Y" THEN X=(HIVALUE+LOVALUE)/2:GOTO
                    3740
3570            PRINT "ZOFCDF HAS ABORTED":STOP
3580    IF PDF<>0 AND ICOUNT%>1 THEN 3590 ELSE 3620
3590    'THEN Segment--Newton-Raphson Estimate
3600           GUESS=GUESS+(ALFA-CDF)/PDF
3610            IF GUESS>HIVALUE OR GUESS<LOVALUE THEN 3630
                    ELSE 3640
3620    'ELSE Segment--Halve the Interval Estimate
3630            GUESS=(HIVALUE+LOVALUE)/2
3640    'CALL CDFPDF(SUBSAMP[],KSUBS%,M%,R%,IPLOT%,X;
                        AVGCDF(X),AVGPDF(X))
3650            IPLOT%=3        'Midpoint of EDF
3660            X=GUESS
3670            GOSUB 3780
3680            CDF=AVGCDF
3690            PDF=AVGPDF
3700    IF CDF>ALFA THEN HIVALUE=GUESS
3710    IF CDF<ALFA THEN LOVALUE=GUESS
3720    CRIT=ABS(CDF-ALFA)
3730 WEND
3740 ZALFA=X
3750 RETURN
3760 END
3770 '*****************************
3780 'SUBROUTINE CDFPDF(SUBSAMP[],KSUBS%,M%,R%,IPLOT%,X;
                        AVGCDF(X),AVGPDF(X))
3790 '*****************************
```

```
3800 'Subroutine CDFPDF Gets the Value of The CDF and
       PDF Using Sweeder's Estimation Technique
3810 '*************************
3820 'INPUT VARIABLES:  KSUBS%--THE NUMBER OF SUBSAMPLES
                       X-------VARIATE OF DISTRIBUTION
                       SUBSAMP-2D ARRAY CONTAINING
                               PARTITIONED SAMPLE
                       R%--NUMBER OF COLS OF SUBSAMP WITH
                           M%+1 ELEMENTS
                       M%--NUMBER OF ELEMNTS IN SAMPLES%
                           R%+1 ON
3830 '                 IPLOT%--CHOICE OF PLOTTING POSITION
3840 '*****************************
3850 'OUTPUT VARIABLES: AVGCDF--Average CDF Over KSUBS%
                               Subsamples
                       AVGPDF--Average PDF Over KSUBS%
                        Subsamples (Both Evaluated at X)
3860 '*****************************
3870 'EXTERNALS REQUIRED:       SUBROUTINE LOADXDUM--To Load
                                        Dummy Array
                                SUBROUTINE POINTCDF--To Get
                                        Point CDF,PDF Valus
3880 '*****************************
3890 IF DEBUG$="Y" THEN PRINT "CDFPDF HAS BEEN CALLED"
3900 SUMCDF=0
3910 SUMPDF=0
3920 FOR SAMPLE%=1 TO KSUBS%
3930 'CALL LOADXDUM(SUBSAMP[],XDUM[],SAMPLE%,R%,M%)
3940    GOSUB 4080
3950 'CALL POINTCDF(XDUM[],SAMPSIZE%,X,IPLOT%)
3960    SAMPSIZE%=LASTEL%
3970    GOSUB 4430
3980 IF DEBUG$="Y" THEN 3990 ELSE 4000
3990 PRINT "FOR SAMPLE=";SAMPLE%;"CDF,PDF ARE ";CDF,PDF
4000 SUMCDF=SUMCDF+WEIGHT(SAMPLE%)*CDF
4010 SUMPDF=SUMPDF+WEIGHT(SAMPLE%)*PDF
4020 NEXT SAMPLE%
4030 AVGCDF=SUMCDF
4040 AVGPDF=SUMPDF
4050 RETURN
4060 END
4070 '*****************************
4080 '  SUBROUTINE LOADXDUM(SUBSAMP[],M%,R%,SAMPLE%;XDUM[])
4090 '*****************************
4100 'Subroutine LOADXDUM Loads the XDUM Array For Later
       Use By Subroutine POINTCDF--It Acts As The
     Fictitious Data Array And is Loaded From Array SUBSAMP
4110 '*****************************
```

```
4120 'INPUT VARIABLES:  SAMPLE%--IDENTIFIES COLUMN OF
                                 SUBSAMP
                        R%-------FIRST R% COLUMNS OF SUBSAMP
                                HAVE ONE MORE DATA Point
                        SUBSAMP--2X2 Array Containing Data--
                              Row is ELEMNT%, Col is SAMPLE%
                        M%-------Number of Elements Per
                                 Sample
4130 '""""""""""""""""""""""""""!
4140 'OUTPUT VARIABLES: XDUM-----DUMMY SORTED DATA Array-1D
4150 '""""""""""""""""""""""""""!
4160 IF DEBUG$="Y" THEN PRINT "LOADXDUM HAS BEEN CALLED"
4170 IF DEBUG$="Y" THEN PRINT "SAMPLE%,R%,M% CAME IN AS
          ";SAMPLE%;R%,M%
4180    IF SAMPLE%<=R% THEN 4190 ELSE 4220
4190    'THEN Segment--Set Has M%+1 Elements
4200            LASTEL%=M%+2    'Because of Extrapolated
                                 Points
4210            GOTO 4240
4220    'ELSE Segment--Set Has M% Elements
4230            LASTEL%=M%+1
4240 IF CALLXDUM$="T" THEN ERASE XDUM
4250 DIM XDUM(LASTEL%)
4260 FOR I%=0 TO LASTEL%
4270 XDUM(I%)=SUBSAMP(I%,SAMPLE%)
4280 NEXT I%
4290 IF DEBUG$="Y" THEN 4300 ELSE 4360
4300 'THEN Segment--Debug Mode Selected
4310    PRINT "HERE IS THE XDUM ARRAY FOR SAMPLE ";SAMPLE%
4320    FOR IDEX%=0 TO LASTEL%
4330    PRINT XDUM(IDEX%);
4340    IF IDEX% MOD 5=0 THEN PRINT
4350    NEXT IDEX%
4360 'ELSE Segment--Normal Termination
4370    CALLXDUM$="T"
4380    RETURN
4390 END
4400 '"""""""""""""""""""""""""""""
4410 'SUBROUTINE POINTCDF(XDUM[],SAMPSIZE%,X,IPLOT%;
                                              CDF,PDF)
4420 '"""""""""""""""""""""""""""""
4430 '  Subroutine POINTCDF Estimates the CDF and PDF
     Nonparametrically From a Data Set Found in XDUM--
4440 '""""""""""""""""""""""""""!
4450 'INPUT VARIABLES:  XDUM--DUMMY ARRAY CONTAINING THE
                              DATA INCLUDING THE ENDPOINTS
                        SAMPSIZE%--TOTAL SIZE OF THE ARRAY
                        X----POINT WHERE CDF,PDF WANTED
4460 '                  IPLOT%--Choice of Plotting Position
4470 '""""""""""""""""""""""""""!
4480 'OUTPUT VARIABLES: CDF--Value of CDF At Point X
                        PDF--Value of PDF At Point X
```

```
4490 '***************************
4500 'REQUIRED EXTERNALS:        SUBROUTINE PLOTPNT
4510 '***************************
4520 IF DEBUG$="Y" THEN PRINT "POINTCDF HAS BEEN CALLED"
4530 PI=4*ATN(1)
4540 DUMIN=XDUM(0)
4550 DUMAX=XDUM(SAMPSIZE%)
4560 IF X<=DUMIN THEN CDF=0:PDF=0:RETURN
4570 IF X>=DUMAX THEN CDF=1:PDF=0:RETURN
4580 FOR I%=0 TO SAMPSIZE%-1
4590 IF XDUM(I%)<=X AND X<XDUM(I%+1) THEN 4600 ELSE 4710
4600 'THEN Segment--Interval Found
4610    'CALL PLOTPNT(I%,IPLOT%,SAMPSIZE%)
4620             IPNT%=I%
4630             NOBS%=SAMPSIZE%-1
4640             GOSUB 3060
4650             G=PLOTPNT
4660    'CALL PLOTPNT(I%+1,IPLOT%,SAMPSIZE%)
4670             IPNT%=I%+1
4680             GOSUB 3060
4690             GPLUS=PLOTPNT
4700    GOTO 4740
4710 'ELSE Segment--Look Again
4720    NEXT I%
4730 PRINT "ABORT IN POINTCDF--X NOT FOUND":STOP
4740 ARG=(X-XDUM(I%))/(XDUM(I%+1)-XDUM(I%))
4750 CDF=G+(GPLUS-G)*ARG
4760 IF PDFTOGGLE$="S" THEN CDF=G+(GPLUS-G)/2
                                  *(1-COS(PI*ARG))
4770 IF CDF<-6E-09 OR CDF>1 THEN PRINT "CDF ABORT IN
       POINTCDF":STOP
4780 IF PDFFLAG$="S" THEN PRINT "PDF ABORTED":PDF=0:RETURN
4790 IF PDFTOGGLE$="S" THEN 4800 EL  4830
4800 ' THEN Segment--Use Sweeder's ( iginal PDF
4810    PDF=PI/2*(GPLUS-G)/(XDUM(I%-1)-XDUM(I%))*SIN(PI*ARG)
4820    GOTO 5130
4830 IF PDFTOGGLE$="H" THEN PDF=(GPLUS-G)/(XDUM(I%+1)-
       XDUM(I%)):GOTO 5130
4840 IF X<=.5*(XDUM(I%)+XDUM(I%+1)) THEN 4850 ELSE 5020
4850 'THEN Segment--Interpolate From Previous Derivative
4860    IF XDUM(I%+1)=XDUM(I%) THEN 4870 ELSE 4890
4870             PRINT "DUPLICATE SAMPLE--PDF ABORT"
4880             PDFFLAG$="S":PDF=0:RETURN
4890    PDFMAX=(GPLUS-G)/(XDUM(I%+1)-XDUM(I%))
4900    XHI=.5*(XDUM(I%)+XDUM(I%+1))
4910    IF I%=0 THEN PDFMIN=0:XLO=DUMIN:GOTO 5120
4920    'CALL PLOTPNT(I%-1),IPLOT%,SAMPSIZE%;PLOTPNT)
4930             IPNT%=I%-1
4940             GOSUB 3060
4950    GMINUS=PLOTPNT
4960    IF XDUM(I%)=XDUM(I%-1) THEN 4970 ELSE 4990
4970       PRINT "DUPLICATE SAMPLE--PDF ABORTS"
```

```
4980       PDFFLAG$="S":PDF=0:RETURN
4990     PDFMIN=(G-GMINUS)/(XDUM(I%)-XDUM(I%-1))
5000     XLO=.5*(XDUM(I%-1)+XDUM(I%))
5010     GOTO 5120
5020 'ELSE Segment--Interpolate To Next Derivative
5030     PDFMIN=(GPLUS-G)/(XDUM(I%+1)-XDUM(I%))
5040     XLO=.5*(XDUM(I%)+XDUM(I%+1))
5050     IF I%=SAMPSIZE%-1 THEN PDFMAX=0:XHI=DUMAX:GOTO 5120
5060     'CALL PLOTPNT(I%+2,IPLOT%,SAMPSIZE%;PLOTPNT)
5070             IPNT%=I%+2
5080             GOSUB 3060
5090     GHIGH=PLOTPNT
5100     PDFMAX=(GHIGH-GPLUS)/(XDUM(I%+2)-XDUM(I%+1))
5110     XHI=.5*(XDUM(I%+1)+XDUM(I%+2))
5120 PDF=PDFMIN+(PDFMAX-PDFMIN)/(XHI-XLO)*(X-XLO)
5130 IF PDF<0 THEN PRINT "PDF ABORT IN POINTCDF":STOP
5140 RETURN
5150 END
5160 '  SUBROUTINE DUMPDATA(XDATA[],SIZE%)
5170 ON ERROR GOTO 5410
5180 IF MID$(FILNAM$,2,1)=":" THEN FILNAM$=MID$(FILNAM$,3)
5190 FILE$=PREFIX$+FILNAM$
5200 OLDFIL$=FILE$+".BAK"
5210 KILL OLDFIL$
5220 NAME FILE$ AS OLDFIL$
5230 OPEN "O",1,FILE$
5240 NEL%=5
5250 NREC%=SIZE%\NEL%
5260 IF SIZE% MOD NEL%<>0 THEN NREC%=NREC%+1
5270 XINDEX%=0
5280 PRINT #1,SIZE%;NEL%
5290 FOR RECORD%=1 TO NREC%
5300 FOR ELEMNT%=1 TO NEL%
5310 XINDEX%=XINDEX%+1
5320 IF XINDEX%>SIZE% THEN PRINT #1,:CLOSE 1:RETURN
5330 PRINT #1,XDATA(XINDEX%);
5340 NEXT ELEMNT%
5350 PRINT #1,
5360 NEXT RECORD%
5370 CLOSE 1
5380 RETURN
5390 END
5400 '******SUBROUTINE DISKERR*********
5410 IF ERR=53 AND ERL<>1300 THEN RESUME NEXT
5420 ON ERROR GOTO 0
5430 RETURN
5440 END
5450 '******SUBROUTINE PLOTPCDF***********
5460 MEMORY=FRE(0)
5470 PRINT "MEMORY LEFT IS ";MEMORY;"BYTES"
5480 MEM=1000
5490 IF MEMORY<MEM THEN 5520
```

```
5500 INPUT "Do You Want Plotdata Written To Disk";ANS$
5510 IF ANS$="Y" THEN 5520 ELSE 5630
5520    COMMON MAXPDF,XMIN,XMAX,FILE$
5530    DIM X(1),Y(1),Y2(1)'    Sets Starting Addresses
5540    CLOSE
5550  INPUT "MUST WRITE TO DISK. INPUT FILNAM$:",FILNAM$
5560    IF MID$(FILNAM$,2,1)=":" THEN
          FILNAM$=MID$(FILNAM$,3)
5570    FILE$=PREFIX$+FILNAM$
5580    OLDFIL$=FILE$+".BAK"
5590    KILL OLDFIL$
5600    NAME FILE$ AS OLDFIL$
5610    OPEN "O",1,FILE$
5620    GOTO 5660
5630    COMMON X(),Y(),Y2()
5640    FILE$="A:"'     Sets Address
5650    DIM X(101),Y(101),Y2(101)
5660 PRINT "XMAX AND XMIN ARE ";XMAX;XMIN:INPUT "CHANGE
       VALUES";CHANGE$
5670 IF CHANGE$="Y" THEN  INPUT "INPUT XMIN,XMAX:",XMIN,XMAX
5680 HX=(XMAX-XMIN)/100
5690 FOR POINT%=1 TO 101
5700    INDEX%=POINT%-1
5710    X=XMIN+INDEX%*HX
5720            GOSUB 3770
5730    PRINT "AT X=";X;"CDF,PDF ARE ";AVGCDF;AVGPDF
5740    IF AVGPDF>MAXPDF THEN MAXPDF=AVGPDF
5750    IF MEMORY<MEM OR ANS$="Y" THEN 5760 ELSE 5780
5760            PRINT #1,X;AVGPDF;AVGCDF
5770            GOTO 5790
5780            X(INDEX%)=X:Y(INDEX%)=AVGPDF:
                        Y2(INDEX%)=AVGCDF
5790 NEXT POINT%
5800 IF MEMORY<MEM OR ANS$="Y" THEN 5810 ELSE 5870
5810    PRINT #1,MAXPDF;XMIN;XMAX
5820    CLOSE
5830    PRINT "MAXPDF;XMIN;XMAX;FILE$=";MAXPDF;XMIN;
                XMAX;FILE$
5840    INPUT "Chain In PLOTCDF (Y/N)";ANS$
5850    IF ANS$="N" THEN PRINT "NORMAL TERMINATION":STOP
5860    CHAIN "PLOTCDF"
5870    PRINT "MAXPDF IS ";MAXPDF
5880    INPUT "CHANGE MAXPDF ";PDF$
5890    IF PDF$="Y" THEN INPUT "Input MAXPDF:",MAXPDF
5900    FOR INDEX%=0 TO 100
5910            Y(INDEX%)=Y(INDEX%)/MAXPDF
5920    NEXT INDEX%
5930    PRINT "MAXPDF,XMIN,XMAX ARE
          ";MAXPDF;XMIN;XMAX;"PAUSING":STOP
5940    CHAIN "MXPLOT.002"
5950    RETURN
5960 END
```

```
5970 'SUBROUTINE EXTRAP(SUBSAMP[],TOGGLE$;DELTAL,DELTAU)
5980 ALFAPLOT=-.5:BETAPLOT=0
5990 IF TOGGLE$="R" OR PDFTOGGLE$="S" THEN
          DELTAL=1:DELTAU=1:RETURN
6000 IF EXTRAPTOGGLE$="S" THEN DELTAL=1:DELTAU=1:RETURN
6010 RL1=2*SUBSAMP(2,SAMPLE%)-SUBSAMP(1,SAMPLE%)
          -SUBSAMP(3,SAMPLE%)
6020 RL2=SUBSAMP(2,SAMPLE%)-SUBSAMP(1,SAMPLE%)
6030 RL3=SUBSAMP(3,SAMPLE%)-SUBSAMP(2,SAMPLE%)
6040 RL4=SUBSAMP(3,SAMPLE%)-SUBSAMP(1,SAMPLE%)
6050 RL=RL1*RL2/(RL3*RL4)
6060 IF RL>=1 THEN 6070 ELSE 6150
6070    PRINT "EXACT EXTRAPOLATION FAILS FOR DELTAL":STOP
6080    RL=RL4/RL3
6090    IF RL>=4 THEN 6100 ELSE 6130
6100            PRINT "METHOD 2 FAILS FOR DELTAL":STOP
6110            DELTAL=2*(1+ALFAPLOT)
6120            GOTO 6160
6130            DELTAL=2*(1+ALFAPLOT)/(2-.5*RL)
6140            GOTO 6160
6150    DELTAL=2*(1+ALFAPLOT)/(1-RL)
6160 RH1A=SUBSAMP(SAMPSIZE%,SAMPLE%)
          -SUBSAMP(SAMPSIZE%-1,SAMPLE%)
6170 RH1B=SUBSAMP(SAMPSIZE%-1,SAMPLE%)
          -SUBSAMP(SAMPSIZE%-2,SAMPLE%)
6180 RH1=RH1A/RH1B
6190 RH2A=2*SUBSAMP(SAMPSIZE%-1,SAMPLE%)
          -SUBSAMP(SAMPSIZE%-2,SAMPLE%)
          -SUBSAMP(SAMPSIZE%,SAMPLE%)
6200 RH2B=SUBSAMP(SAMPSIZE%,SAMPLE%)
          -SUBSAMP(SAMPSIZE%-2,SAMPLE%)
6210 RH2=RH2A/RH2B
6220 RH=RH1+RH2
6230 IF RH>=2 THEN 6240 ELSE 6320
6240    PRINT "EXACT EXTRAPOLATION FAILS FOR DELTAU":STOP
6250    RH=RH2B/RH1B
6260    IF RH>=4 THEN 6270 ELSE 6300
6270            PRINT "METHOD 2 FAILS FOR DELTAU":STOP
6280            DELTAU=2*(BETAPLOT-ALFAPLOT)
6290            GOTO 6330
6300            DELTAU=2*(BETAPLOT-ALFAPLOT)/(2-.5*RH)
6310            GOTO 6330
6320    DELTAU=2*(BETAPLOT-ALFAPLOT)/(2-RH)
6330 RETURN
6340 END
```

Appendix C: Distribution Of A Function Monotonic In N Random Variables

Overview

This Appendix provides a demonstration of a powerful alternative to random Monte Carlo sampling when used to find the distribution of a function of one or more random variables. Appendix A provided an introduction to Sweeder's method [14] of non-parametric estimation of distribution and density functions. In that Appendix, the concept of a stylized sample was presented, and improvements were made to one of Sweeder's basic numerical techniques. These ideas are briefly reviewed. The problem of finding the distribution of a function of a single random variable is considered. It is shown that a set of stylized points from the population of the random variable X maps into a set of stylized points from the population of Z, where Z=g(X), and the function g(x) is monotonic. Two examples are presented. Functions of two independent random variables are then considered, and two examples again presented. Functions monotonic in N random variables are discussed.

A Review of Sweeder's Method

Given a set of observations from the population of the random variable Z with distribution function $F_Z(z)$, one can order the set from smallest to largest. Given this set, denoted by:

$\{z_i\}, i=1,m$

where $z_i < z_{i+1}$ then one may construct the sample distribution function $F_S(z)$ as follows:

$$F_S(z)=0 \quad \forall \; z<z_0 \tag{C.1}$$

$$F_S(z)=G_i+(G_{i+1}-G_i)(z-z_i)/(z_{i+1}-z_i) \quad \forall \; z_i \leq z < z_{i+1} \tag{C.2}$$

$$F_S(z)=1 \quad \forall \; z \geq z_{m+1} \tag{C.3}$$

Sweeder [14] showed that such a sample distribution function converges uniformly to the underlying distribution function $F_Z(z)$.

In Equation C.2, G_i is a nonparametric plotting position, given by some rule such as:

$$G_i=(i+\alpha)/(m+\beta); \quad -1 \leq \alpha \leq \beta \leq 1 \tag{C.4}$$

In Equations C.1 and C.3, z_0 and z_{m+1} are extrapolated endpoints such that:

$$F_S(z_0)=G_0=0 \tag{C.5}$$

$$F_S(z_{m+1})=G_{m+1}=1 \tag{C.6}$$

The simplist linear transformation is given by:

$$Z=X \tag{C.7}$$

If X is a random variable with distribution function $F_X(x)$, then the distribution function of Z is given by:

$$F_Z(z(x))=F_X(x) \tag{C.8}$$

Now, provided $F_X(x)$ is known, one can collect the particular set of m values:

$\{x_i^*\}$; $i=1,m$

in such a way that the x_i^* satisfy:

$$G_i = F_X(x_i^*) = \int_{x_0}^{x_i^*} f_X(x)dx \qquad (C.9)$$

where

$$F_X(x_0) = 0 \qquad (C.10)$$

By Equations C.2 and C.9 one sees that:

$$F_S(x_i^*) = F_X(x_i^*) \qquad (C.11)$$

For this particular set of points, the sample distribution function $F_S(x)$ is exact at the drawn data points, x_i^*. Such a set of points (reference Appendix A) will be referred to as a **stylized sample**. The definition is repeated below:

Definition: The set of points $\{x_i^*\}$, i=1,m, is defined as a stylized sample from the population of X if, for every element of the set,

$$F_S(x_i^*) = F_X(x_i^*) \qquad (C.12)$$

and $x_i^* < x_{i+1}^*$.

Referring back to Equation C.7, one sees that the distribution function $F_S(z)$ is also exact at points z_i^* given by

$$z_i^* = x_i^* \qquad (C.13)$$

since

$$F_S(z_i^*) = F_S(x_i^*) = G_i \qquad (C.14)$$

Hence, the motivation is provided to search for a new technique in finding the distribution of a function of a random variable.

Monotonic Functions of a Single Random Variable

One may now consider the case where the random variable Z is an arbitrary monotonic function of the single random variable X. That is,

$$Z=g(X) \tag{C.15}$$

where g'(x) has no zeroes throughout the range of X.

From the previous discussion, if one could somehow obtain a stylized sample from the population of Z, then the sample distribution function $F_S(z)$ is exact at the points $\{z_i^*\}$, i=1,m. With a minor restriction on the plotting rule of Equation C.4, such a set of z's is found by simply evaluating the function g(x) at the points $\{x_i^*\}$.

HYPOTHESIS: Given Z=g(X), with g(x) monotonic, and a stylized sample from the population of X, $\{x_i^*\}$, i=1,m, then the stylized sample from Z, $\{z_i^*\}$, i=1,m; is found by evaluating g(x) at the points $\{x_i^*\}$, i=1,m. This is true provided the x_i^* are drawn by the rule:

$$G_i=(i+\alpha)/(m+\beta)=F_X(x_i^*)=\int_{x_0}^{x_i^*} f_X(x)dx \tag{C.16}$$

and $$\beta-2\alpha=1 \tag{C.17}$$

PROOF: The equation of total probability [1,6] can be used to find the density function $f_Z(z)$ given the conditional density function $f_{Z|X}(z(x))$. That is:

$$f_Z(z)=\int_{x_0}^{x_{m+1}} f_X(x)f_{Z|X}(z(x))dx \tag{C.18}$$

where x_0 and x_{m+1} satisfy:

$$F_X(x_0)=0 \tag{C.19}$$

$$F_X(x_{m+1})=1 \tag{C.20}$$

Since the objective is to draw or construct a stylized sample from the population of Z, one might seek the point z_j^* that satisfies the equation:

$$G_j = F_Z(z_j^*) \tag{C.21}$$

That is, z_j^* is one of the members of a stylized sample from the population of Z.

The distribution function may be found by integrating the density function. Equation C.18 may be integrated to the point z_j^*, and the integral over z taken inside the integral over all x. Recalling the definition of the conditional distribution function leads to the result:

$$F_Z(z_j^*) = \int_{x_0}^{x_{m+1}} f_X(x) F_{Z|X}(z_j^*) dx \tag{C.22}$$

The z_j^* must satisfy Equation C.22 for every j=1,m.

Now, $F_{Z|X}(z_j^*)$ is known explicitly. Since z is a function of x only, the density function of Z|X is the Dirac delta function with parameter ζ given by:

$$\zeta = g(x) \tag{C.23}$$

That is:

$$f_{Z|X}(z) = \delta(z-\zeta) \tag{C.24}$$

and

$$F_{Z|X}(z_j^*) = \int_{-\infty}^{z_j^*} \delta(z-\zeta) dz \tag{C.25}$$

By the properties of the Dirac delta function [2,11], $F_{Z|X}(z_j^*)$ takes only two values:

$$F_{Z|X}(z_j^*) = 0 \quad \forall \quad z_j^* < \zeta \tag{C.26}$$

$$F_{Z|X}(z_j^*) = 1 \quad \forall \quad z_j^* \geq \zeta \tag{C.27}$$

Equations C.26 and C.27 can be put to use in Equation C.22 by transforming the integral in Equation C.22 to an integral over ζ. From Equation C.23,

$$d\zeta = g'(x)dx \tag{C.28}$$

$$x = g^{-1}(\zeta) \tag{C.29}$$

The transformed integral is:

$$G_j = F_Z(z_j^*) = \int_{g(x_0)}^{g(x_{m+1})} f_X(g^{-1}(\zeta)) F_{Z|X}(z_j^*) d\zeta / g'(g^{-1}(\zeta)) \tag{C.30}$$

One may now consider increasing versus decreasing functions of X.

Monotonically Increasing Functions. For monotonically increasing functions of X,

$$g'(x) > 0 \quad \forall \; x \tag{C.31}$$

For this case the integrand in Equation C.30 is always non-negative. By Equation C.26,

$$F_{Z|X}(z_j^*) = 0 \quad \forall \; \zeta > z_j^* \tag{C.32}$$

and is unity elsewhere. Using Equation C.32 in C.30 reduces that expression to:

$$G_j = F_Z(z_j^*) = \int_{g(x_0)}^{z_j^*} f_X(g^{-1}(\zeta)) d\zeta / g'(g^{-1}(\zeta)) \tag{C.33}$$

provided that

$$z_j^* < g(x_{m+1}) \tag{C.34}$$

Transforming back to the variable in x yields:

$$G_j = F_Z(z_j^*) = \int_{x_0}^{g^{-1}(z_j^*)} f_X(x) dx \tag{C.35}$$

However,

$$G_j = F_X(x_j^*) = \int_{x_0}^{x_j^*} f_X(x) dx \tag{C.36}$$

Since Equation C.34 holds and g(x) is increasing it follows that

$$g^{-1}(z_j^*) < x_{m+1} \tag{C.37}$$

$$f_X(g^{-1}(z_j^*)) > 0 \tag{C.38}$$

Comparison of Equations C.35 and C.36 implies that

$$g^{-1}(z_j^*) = x_j^* \tag{C.39}$$

or $$z_j^* = g(x_j^*) \tag{C.40}$$

The hypothesis is verified for increasing functions of X.

Monotonically Decreasing Functions. For monotonically decreasing functions of X,

$$g'(x) < 0 \quad \forall \quad x \tag{C.41}$$

For this case, the integrand in Equation C.30 is always non-positive. Since positive integrands are preferred, one can use the relation:

$$|g'(x)| = -g'(x) \tag{C.42}$$

in Equation C.30. This results in the expression:

$$F_Z(z_j^*) = -\int_{g(x_0)}^{g(x_{m+1})} f_X(g^{-1}(\zeta)) F_{Z|X}(z_j^*) d\zeta / |g'(g^{-1}(\zeta))| \tag{C.43}$$

Reversing the limits of integration leads to:

$$F_Z(z_j^*) = \int_{g(x_{m+1})}^{g(x_0)} f_X(g^{-1}(\zeta)) F_{Z|X}(z_j^*) d\zeta / |g'(g^{-1}(\zeta))| \tag{C.44}$$

Exploiting again Equations C.26 and C.27:

$$G_j = F_Z(z_j^*) = \int_{g(x_{m+1})}^{z_j^*} f_X(g^{-1}(\zeta)) d\zeta / |g'(g^{-1}(\zeta))| \tag{C.45}$$

provided that

$$z_j^* < g(x_0) \tag{C.46}$$

A variable transformation back to x space yields:

$$G_j = F_Z(z_j^*) = -\int_{x_{m+1}}^{g^{-1}(z_j^*)} f_X(x) |g'(x)| dx / |g'(x)| \tag{C.47}$$

Exploiting Equation C.29 and again reversing limits leads to:

$$G_j=F_Z(z_j^*)=\int_{g^{-1}(z_j^*)}^{x_{m+1}} f_X(x)dx \qquad (C.48)$$

Equation C.48 is just the statement that:

$$G_j=F_Z(z_j^*)=Pr\{X>g^{-1}(z_j^*)\}=1-F_X(g^{-1}(z_j^*)) \qquad (C.49)$$

Since Equation C.46 holds and g(x) is decreasing, it follows that

$$g^{-1}(z_j^*)>x_0 \qquad (C.50)$$

$$f_X(g^{-1}(z_j^*))>0 \qquad (C.51)$$

So there must exist an x_j, such that

$$x_j,>x_0 \qquad (C.52)$$

and $$g^{-1}(z_j^*)=x_j, \qquad (C.53)$$

or $$z_j^*=g(x_j,) \qquad (C.54)$$

The question is, is this x_j, one of the members of the set of stylized points drawn from the population of X? It is if it satisfies Equation C.36 for j=j'. However, it must also satisfy the equation just derived, Equation C.49. Evidently, one must require that

$$G_j=1-G_j, \text{ for some } j=1,m; \text{ some } j'=1,m \qquad (C.55)$$

Using Equation C.4 in the above, j and j' must satisfy

$$j=m+\beta-2\alpha-j' \qquad (C.56)$$

But the restriction of Equation C.17 reduces the above to:

$$j=m+1-j' \qquad (C.57)$$

Examination of the above equation (see Table C.1) shows that under the restriction of Equation C.17, the set of G_j's

remain unchanged under the transformation of Equation C.55. It is interesting to note that of all the plotting rules considered (Table C.2), only the EDF fails to satisfy the condition $\beta-2\alpha=1$.

In conclusion then, Equations C.54 and C.57 imply that:

$$z_j^*=g(x_j,)=g(x_{m+1-j}^*) \qquad (C.58)$$

The hypothesis is therefore verified for decreasing functions of X, completing the proof.

Sample Calculations. To illustrate the above considerations, two sample problems will be worked--one involving a known increasing function of X, the other a known decreasing function of X.

Distribution of a Linear Transform. An example of an increasing function of X is:

$$Z=(\ln X-\alpha_X)/\beta_X \qquad (C.59)$$

where X is lognormally distributed with location parameter α_X and scale parameter β_X. The input distribution is from Figure A.22. The stylized sample is formed by finding

$$z_i=(\ln x_i-\alpha_X)/\beta_X \quad \forall \; i=1,m \qquad (C.60)$$

The distribution of Z, which should be normal with mean zero and standard deviation 1, is found using the method previously described. The results are illustrated in Figure C.1.

TABLE C.1

REFLECTION OF THE PLOTTING RULE UNDER J=M+1-J'

J	J'
1	M
2	M-1
3	M-2
.	.
.	.
M-2	3
M-1	2
M	1

TABLE C.2

PLOTTING RULE BEHAVIOR WITH RESPECT TO $\beta-2\alpha$

	FORMULA	α	β	$\beta-2\alpha$
1.	i/(m+1)	0	1	1
2.	(i-.3)/(m+.4)	-.3	.4	1
3.	(i-.5)/m	-.5	0	1
4.	[i-(m+1)/2m]/[m-(1/m)]	-(m+1)/2m	-1/m	1
5.	(i-1)/(m-1)	-1	-1	1
6.	i/m	0	0	0
7.	(i-.375)/(m+.25)	-.375	.25	1

Distribution of the Log of an Inverse. An example of a decreasing monotonic function is:

$$Z=\ln(1/X) \tag{C.61}$$

where X is uniformly distributed on the interval [0,1]. The input distribution is that of Figure A.18. The stylized sample from the population of Z is found by finding

$$z_i=\ln(1/x_i) \quad \forall \; i=1,m \tag{C.62}$$

The random variable Z should have density function

$$f_Z(z)=e^{-z} \quad \forall \; z>0 \tag{C.63}$$

and distribution function

$$F_Z(z)=1-e^{-z} \quad \forall \; z>0 \tag{C.64}$$

The numerical method is compared to the true CDF and PDF in Figure C.2.

Monotonic Functions of Two Independent Random Variables

One may now seek to extend the above theory to functions monotonic in two independent random variables, say X and Y. That is, given

$$Z=g(X,Y) \tag{C.65}$$

where

$$\partial g/\partial x \neq 0 \text{ and } \partial g/\partial y \neq 0 \quad \forall \; x,y \tag{C.66}$$

the distribution function $F_Z(z)$ is desired. The distribution functions $F_X(x)$ and $F_Y(y)$ are presumed known so that stylized samples of any size from the populations of X and Y may be drawn at will. The set drawn from Y may be denoted by

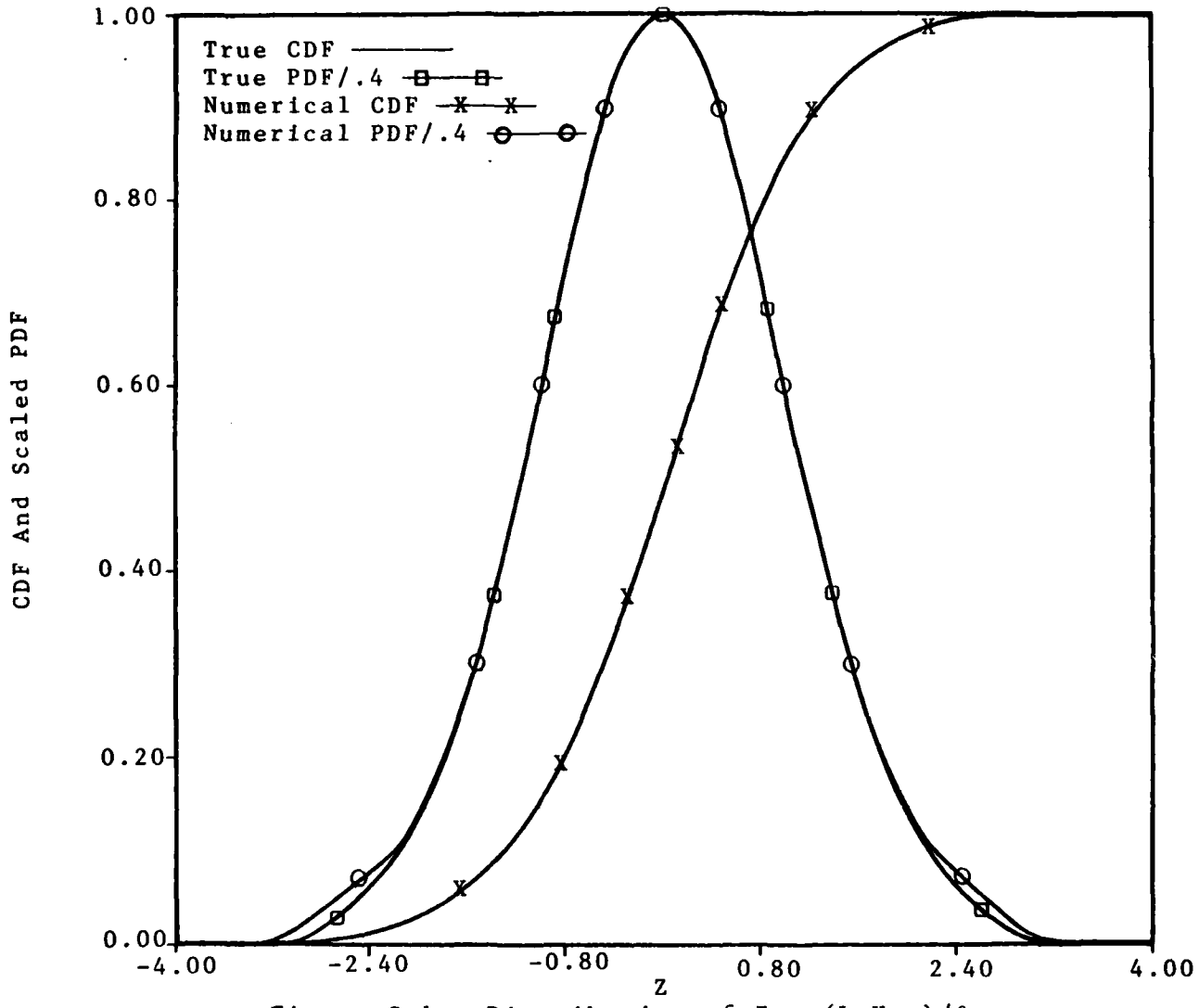

Figure C.1. Distribution of Z = (LnX-α)/β

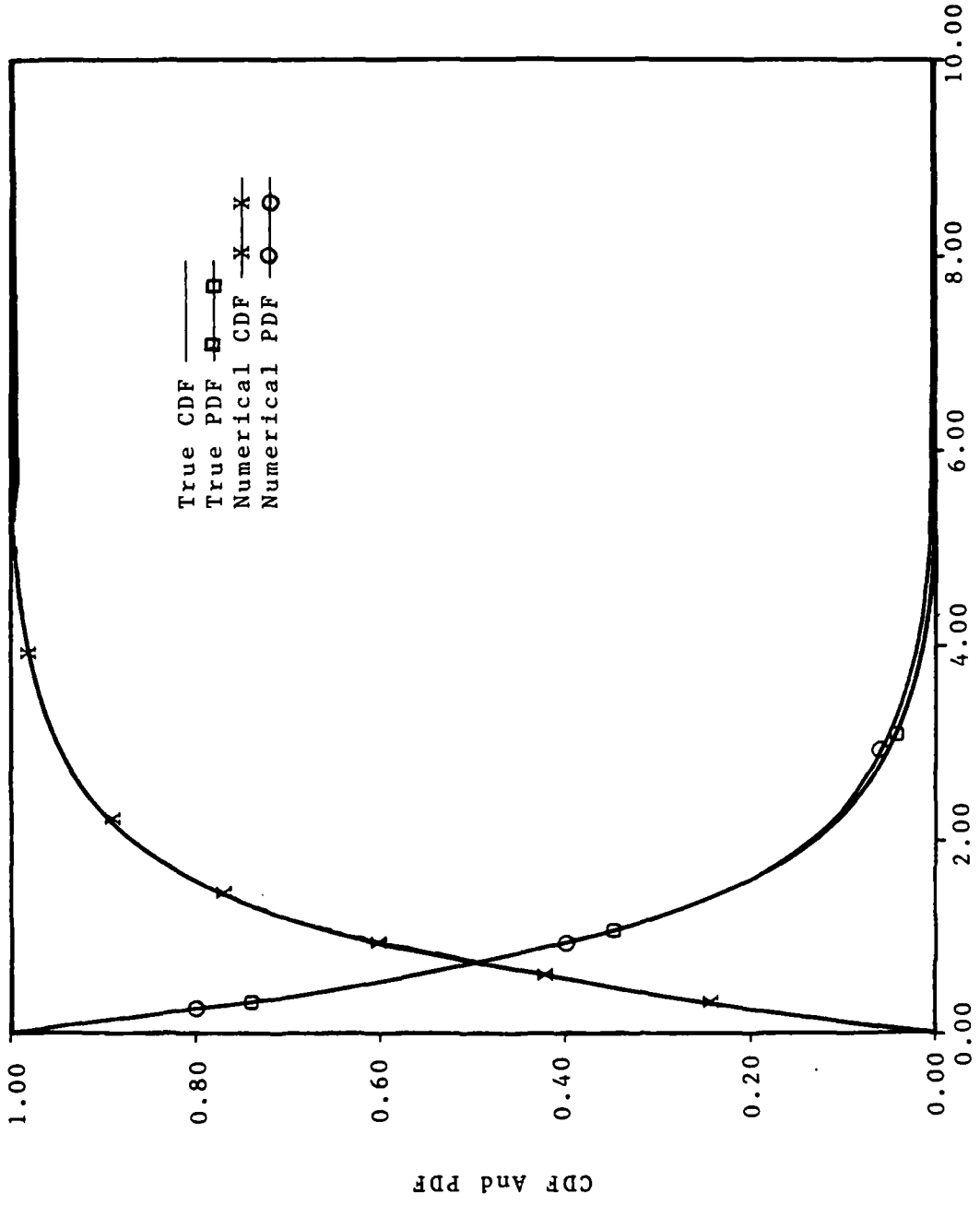

Figure C.2. Distribution of Z = Ln (1/X)

$\{y_i^*\}$, i=1,m

where as usual the y_i^* satisfy

$$G_i=(i+\alpha)/(m+\beta)=F_Y(y_i^*)=\int_{y_0}^{y_i^*} f_Y(y)dy \qquad (C.67)$$

and the restriction of Equation C.17 holds. As usual, y_0 and y_{m+1} are extrapolated endpoints such that:

$$F_Y(y_0)=0 \qquad (C.68)$$

$$F_Y(y_{m+1})=1 \qquad (C.69)$$

Selecting a particular y_i^* one can in principle construct the conditional density function $f_{Z|y_i^*}(z)$ from the equation,

$$f_{Z|y_i^*}(z)=f_X(x(z))\left|\partial x(z)/\partial z\right| \qquad (C.70)$$

If Equation C.70 is analytically tractable, the conditional distribution function may be found by direct integration, i.e.

$$F_{Z|y_i^*}(z)=\int_{-\infty}^{z} f_{Z|y_i^*}(z')dz' \qquad (C.71)$$

If Equation C.70 is not easily integrable, one can define the conditional random variables Z^i as:

$$Z^i=Z|y_i^*;\ i=1,m \qquad (C.72)$$

Since there are m elements in the set of stylized points from the population of Y, m conditional random variables may be defined. From the argument just completed for functions of a single random variable, stylized sets of points for each of the Z^i may be drawn by holding y_i^* fixed and forming the sets from the rule:

$$\{z_j^{i*}\}=\{g(x_j^*,y_i^*)\};\ j=1,m \qquad (C.73)$$

Thus, one may construct m sets of conditional random

variables with m elements each, requiring, at most, m^2 calls to the function g(x,y).

In any case, the conditional distribution function $F_{Z|y_i}(z)$ is readily available.

The density function of Z is given by Equation C.18, and the distribution function by:

$$F_Z(z)=\int_{y_0}^{y_{m+1}} f_Y(y)F_{Z|Y}(z)dy \qquad (C.74)$$

Since the function $F_Y(y)$ is known, as are the functions $F_{Z|Y}(z)$, the integral of Equation C.74 may be solved by Mellin transform [9], also known as the graphical method [8]. The exact details of this using stylized sets are described in Appendix D.

Again, the objective is to construct a stylized set of points from the population of Z. That is, one finds the z_j^* satisfying

$$G_j=(j+\alpha)/(m+\beta)=F_Z(z_j^*) \quad \forall \; j=1,m \qquad (C.75)$$

or, one seeks solutions to the inverse equation,

$$z_j^*=F_Z^{-1}(G_j) \qquad (C.76)$$

The approach now is direct solution of Equation C.76 by numerical iterative methods. Two examples using this formulation are presented at this time.

<u>Distribution of A Sum of Squares</u>. An example of a function monotonic in two independent random variables is

$$Z=X^2+Y^2 \qquad (C.77)$$

where both X and Y are independent and distributed uniformly on the interval [0,1]. Again, the input distribution for

either X or Y is that shown in Figure A.18. The stylized sample from the population of Z is found by solution of Equation C.76.

Some tedious analytic work yields the exact distribution and density functions given respectively by:

$$F_Z(z)=0 \quad \forall \quad z\leq 0 \tag{C.78}$$

$$F_Z(z)=\pi z/4 \quad \forall \quad 0\leq z\leq 1 \tag{C.79}$$

For the region $1\leq z\leq 2$,

$$F_Z(z)=z\{\mathrm{Sin}^{-1}[1/z^{1/2}]-\mathrm{Sin}^{-1}[((z-1)/z)^{1/2}]\}/2 + (z-1)^{1/2} \tag{C.80}$$

$$F_Z(z)=1 \quad \forall \quad z\geq 2 \tag{C.81}$$

$$f_Z(z)=0 \quad \forall \quad z\leq 0 \tag{C.82}$$

$$f_Z(z)=\pi/4 \quad \forall \quad 0\leq z\leq 1 \tag{C.83}$$

For the region $1\leq z\leq 2$,

$$f_Z(z)=\{\mathrm{Sin}^{-1}[1/z^{1/2}]-\mathrm{Sin}^{-1}[((z-1)/z)^{1/2}]\}/2 \tag{C.84}$$

$$f_Z(z)=0 \quad \forall \quad z\geq 2 \tag{C.85}$$

Equation C.76 was solved iteratively for various numbers of stylized points by the method just described. The resulting convergence with increasing number of stylized points is illustrated in Figures C.3 through C.6. These figures illustrate the overall convergence of both the distribution and density functions as the number of stylized points increases. For purposes of illustration, Sweeder's trigonometric interpolation was used for these plots. The most interesting of these is Figure C.3 which was done using only 5 stylized points from each of the input distributions.

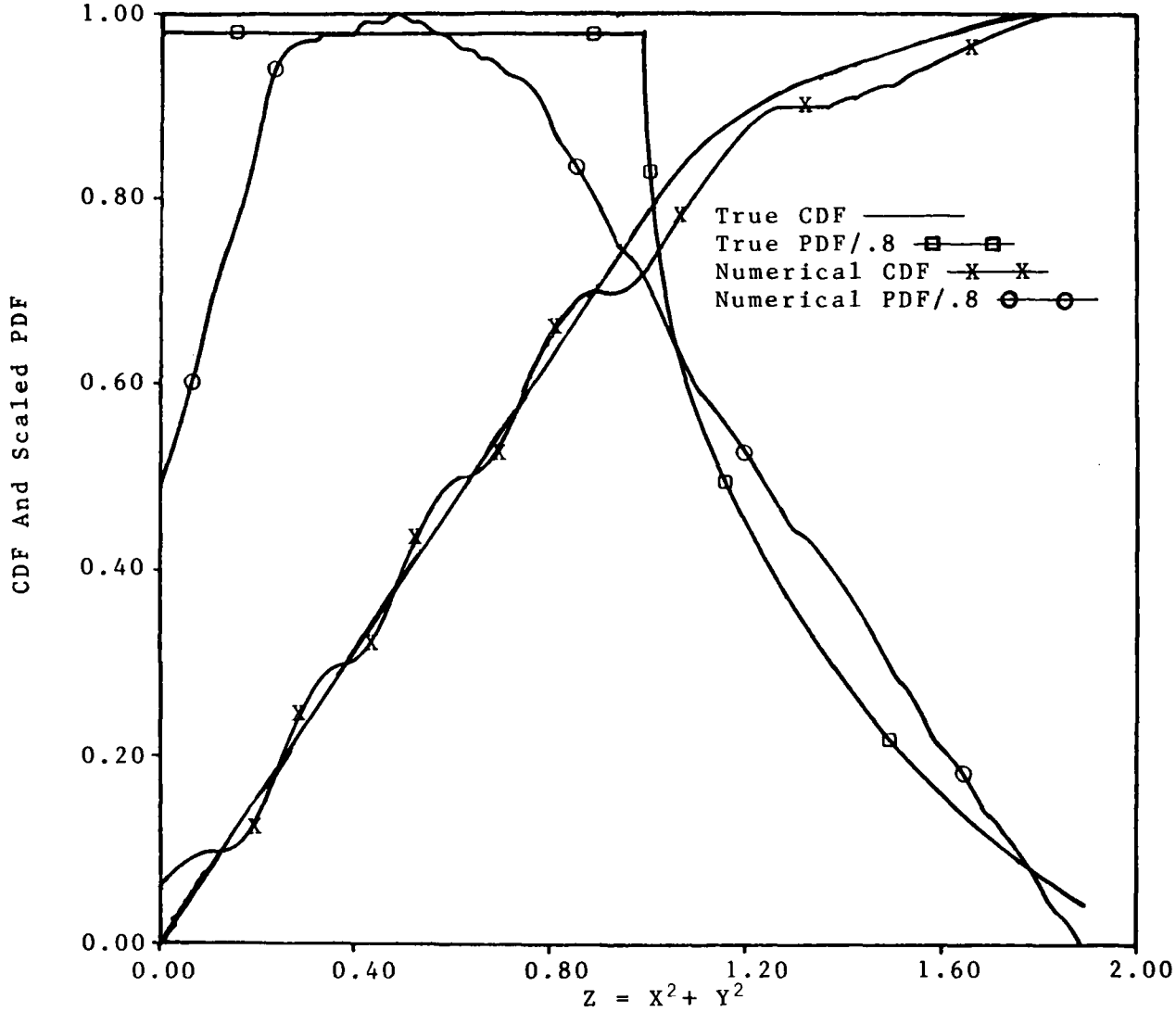

Figure C.3. Distribution of a Sum of Squares Using 5 Stylized Points

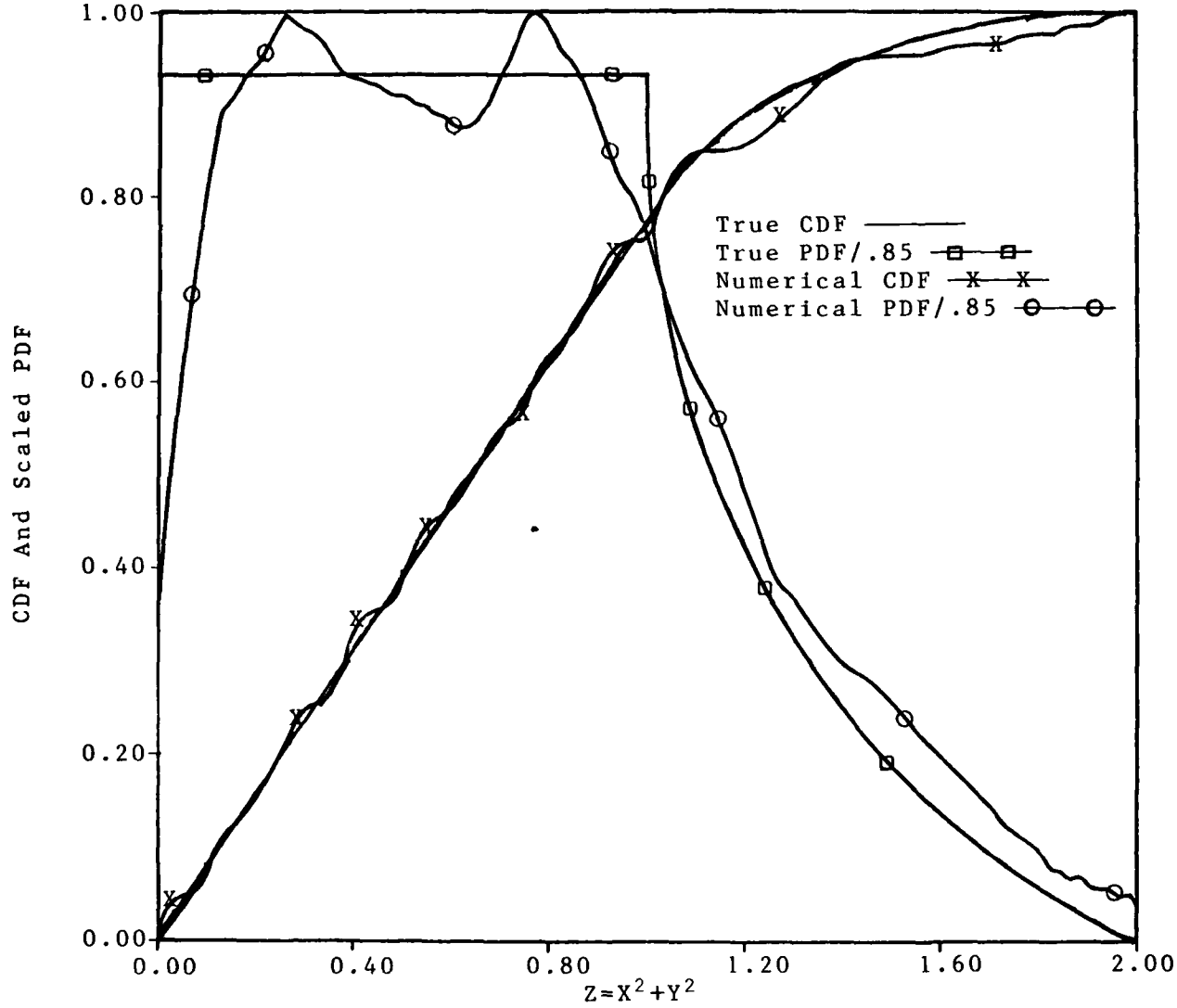

Figure C.4. Distribution of a Sum of Squares Using 10 Stylized Points

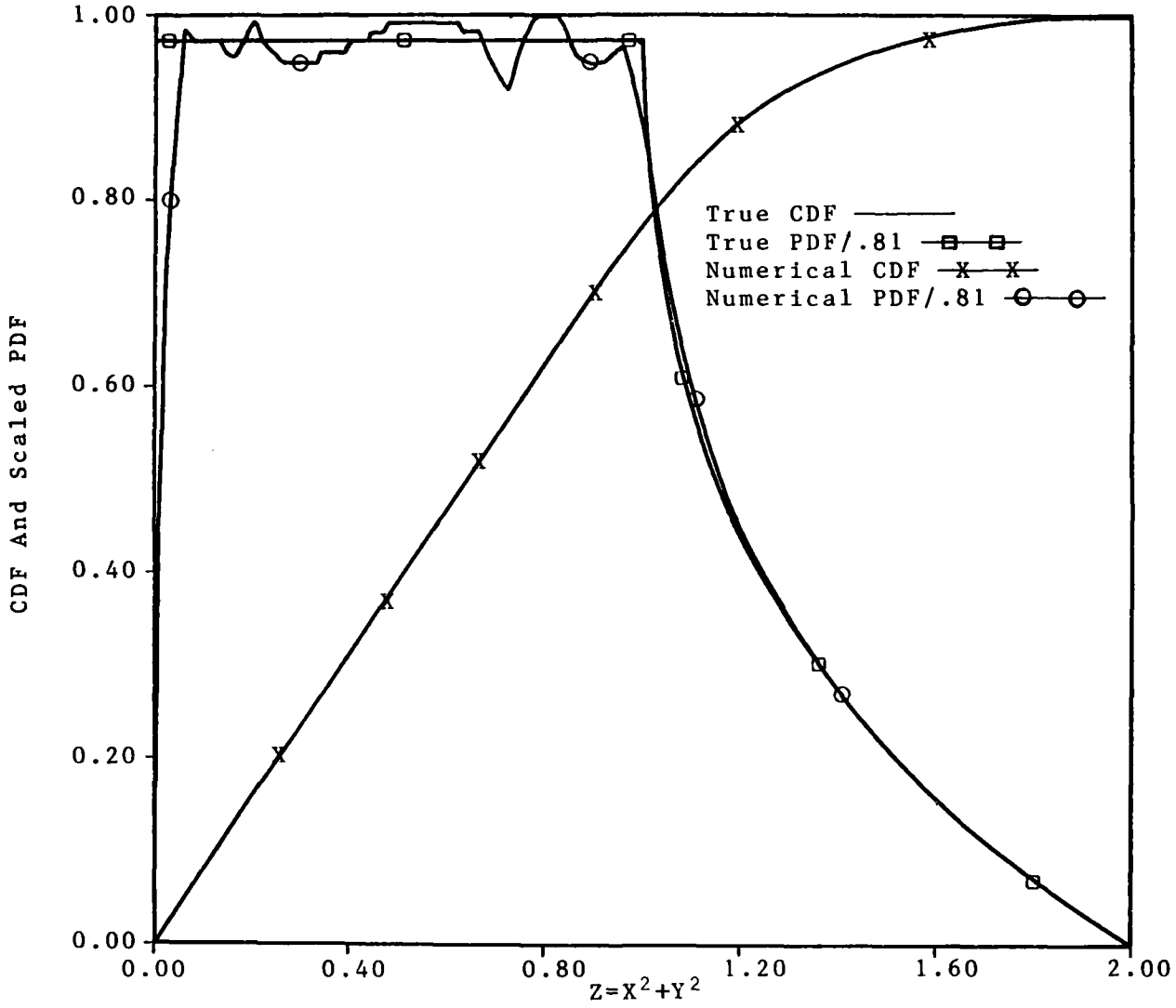

Figure C.5. Distribution of a Sum of Squares Using 25 Stylized Points

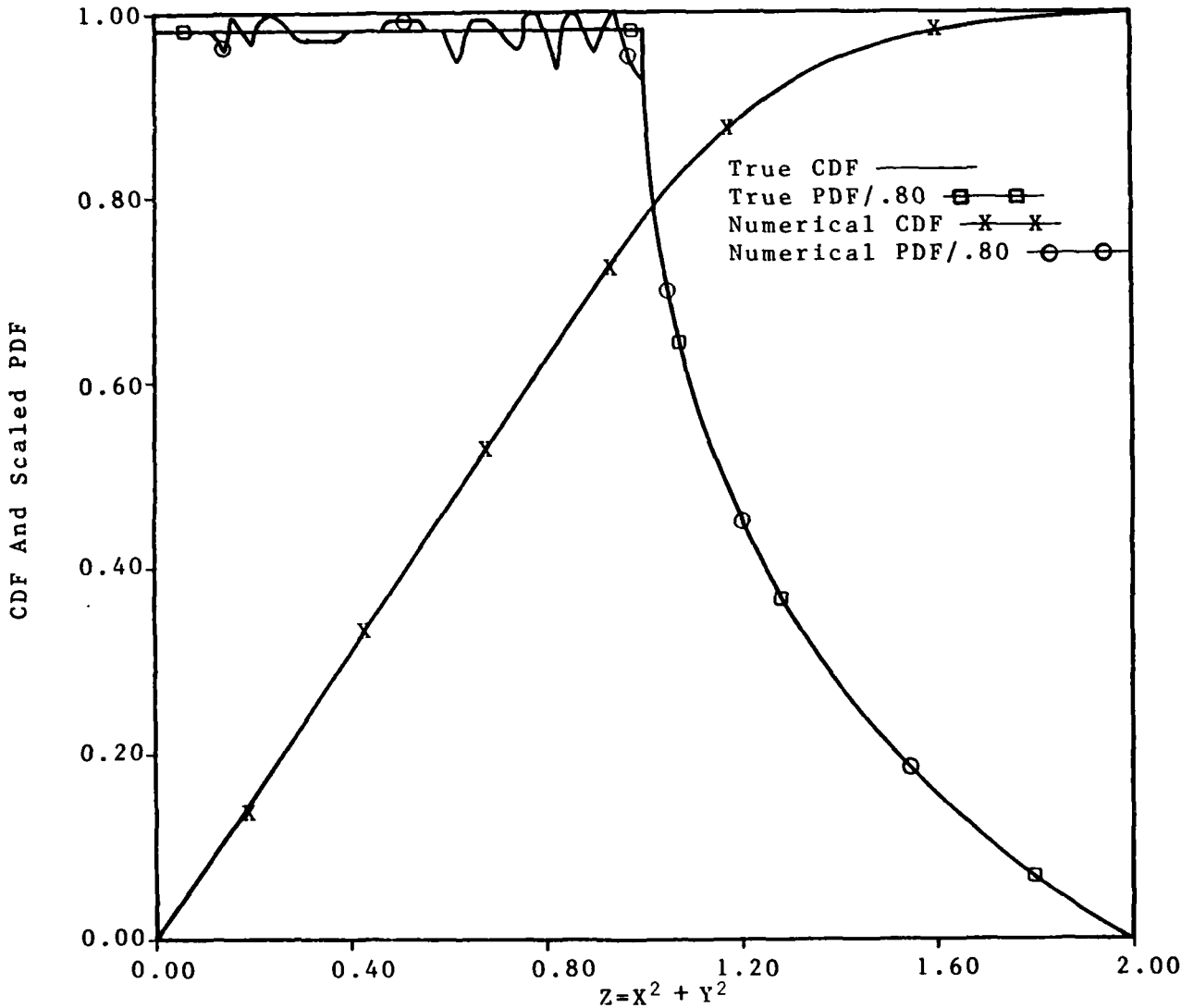

Figure C.6. Distribution of a Sum of Squares Using 50 Stylized Points

The theory just developed predicts that the numerical approximation to the true distribution function should be pinned to the exact distribution function at the percentile points .10(.20).90. The crossover points are very close to these, even though it is expected that integration errors for such a small number of points might lead to erroneous values for the z_j^*. The probability density function is uniform out to z=1, and then has a longer decaying tail. The extrapolated endpoints compare favorably to the exact results of 0 and 2.

Distribution of A Ratio. Finally, consider the distribution of

$$Z=X/Y \tag{C.86}$$

where both X and Y are distributed normally with mean 0 and variance 1. It is known that the distribution of Z is Cauchy with density given by:

$$f_Z(z)=1/\{\pi(1+z^2)\} \tag{C.87}$$

and distribution function given by:

$$F_Z(z)=.5+\mathrm{Tan}^{-1}(z)/\pi \tag{C.88}$$

This was investigated since the Cauchy is particularly troublesome for moment propagation methods, including Shannon maximum entropy [13], and because a hard test of the method was desired for the case when the distribution has infinite support and heavy tails. The results are displayed in Figure C.7.

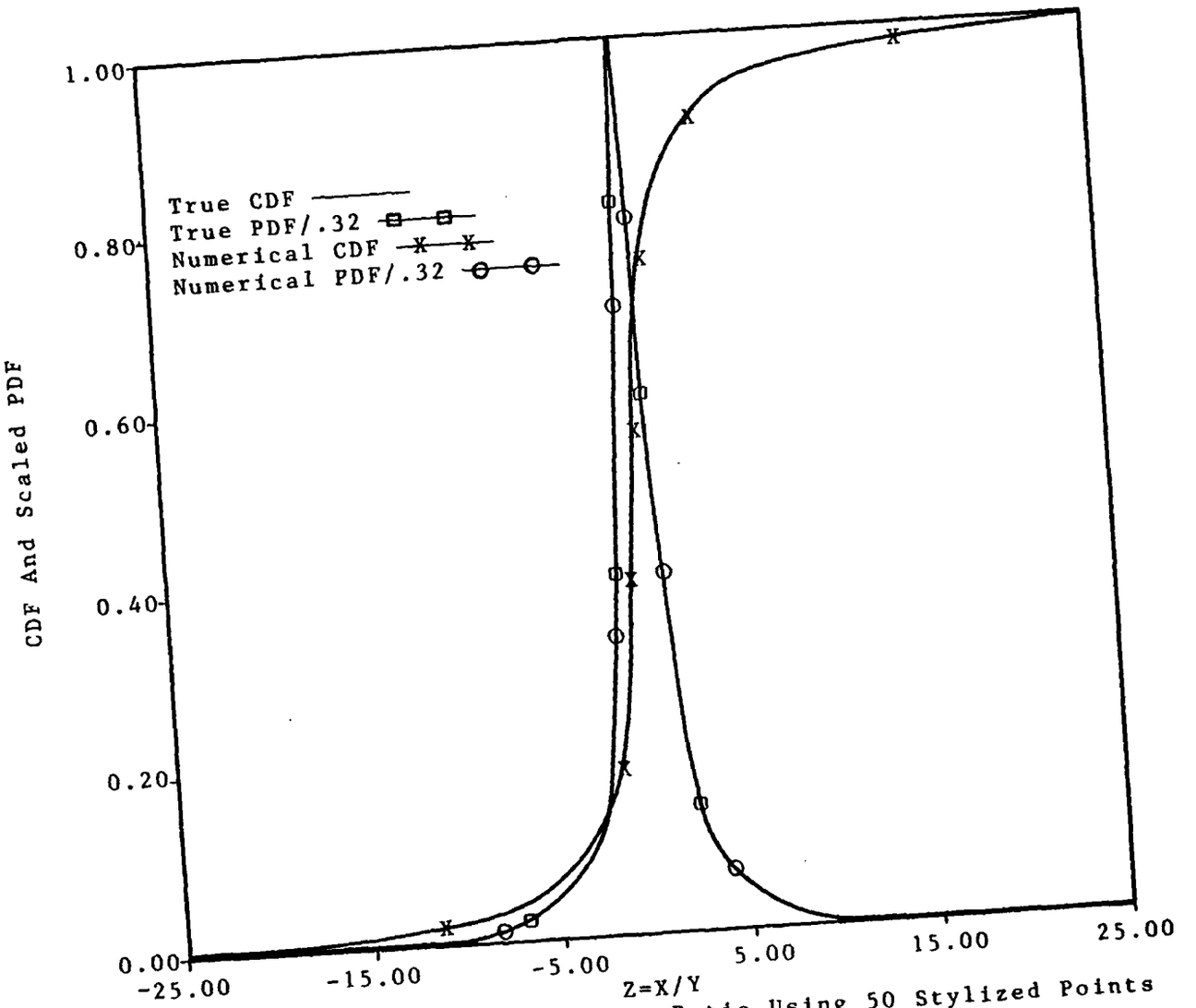

Figure C.7. Distribution of a Ratio Using 50 Stylized Points

Functions Monotonic in N Independent Random Variables

The above considerations lead to the ability to find the distribution of functions monotonic in N random variables, provided that the function can be easily rewritten as combinations of pairs of independent random variables. One then uses the methods of the last section to solve a sequence of binary problems. A relatively simple example is:

$$Z=\{(R-S)W+T\}/U \tag{C.89}$$

where R,S,T,U, and W are all independently distributed random variables with known distributions. The problem can be solved by solving a sequence of problems of two random variables. First, one finds the distribution of

$$V=R-S \tag{C.90}$$

This is done using the methods just described, and once the distribution of V is known, Equation C.89 has been reduced to

$$Z=(VW+T)/U \tag{C.91}$$

Now one can proceed by finding the distribution of X where X is defined as

$$X=VW \tag{C.92}$$

The original problem has been reduced in dimension again to

$$Z=(X+T)/U \tag{C.93}$$

Now Y may be defined by

$$Y=X+T \tag{C.94}$$

and the distribution of Y can be found, since the

distributions of X and T are known. The final problem to solve is thus

$$Z=Y/U \tag{C.95}$$

But this is easily done, since the distributions of Y and U are known, and are independent.

The method is not limited to linear functions. The above simply serves as an illustration of a function of multiple random variables, solved using no additional mathematical complexity than that for two random variables. Actually, the requirement of independence might be relaxed, depending on the problem being considered. If two of the variables are correlated, if the correlation is known, and if those two can be isolated from the other random variables, then the distribution of their combination can be determined. This is done in Chapter IV, where the distribution of the safety factor of a reactor pressure vessel is determined, the safety factor being a function of five random variables, two of them correlated.

Summary

The primary use of algorithm NOSWET has been demonstrated in this Appendix. Sweeder's method of nonparametric estimation, as modified (Reference Appendix A), provides a new tool for finding the distribution of a function of a random variable. After reviewing Sweeder's basic ideas, monotonic functions of a single random variable were considered. It was shown that a stylized sample from the

population of X maps into a stylized sample from the population of Z. The idea of drawing a stylized sample to find the distribution of an output variable leads to a numerical method for finding the distribution of a function of two random variables. Examples were shown, and the problem of a function of multiple random variables was discussed. The technique provides a new tool for the survivability analyst, since the stress and strength distributions are often functions of basic random variables whose input distributions are known. The method provides a powerful alternative to random Monte Carlo methods and propagation of moments techniques.

Appendix D: A Numerical Approximation To The Reliability Interference Integral

The objective of this Appendix is to demonstrate the utility of stylized sets of points (reference Appendix A) in solving conditional probability integrals, like that shown in Equation C.74, reproduced below.

$$F_Z(z)=\int_{y_0}^{y_{m+1}} f_Y(y)F_{Z|Y}(z(y))dy \qquad (D.1)$$

The integral essentially extracts the expected value of a cumulative distribution function (CDF) with respect to a probability density function (PDF). The CDF and PDF need not be independent, as Equation D.1 above explicitly indicates. The relationship of the above to the reliability interference integral may be seen by considering Y as the stress variable s, and Z|Y as the strength variable S. Equation D.1 then becomes the equation for the failure probability p_f, given by

$$p_f=\int_{s_0}^{s_{m+1}} f_s(s)F_S(s)ds \qquad (D.2)$$

A variable transformation technique, known as a Mellin transform [9] may be used to calculate the above integral. (This is also known as the graphical method by some other authors [8].) The variables G and H are defined by

$$G(S)=\int_{S_0}^{S} f_S(S')dS' \qquad (D.3)$$

$$H(s)=\int_{s_0}^{s} f_s(s')ds' \tag{D.4}$$

Then

$$dH=f_s(s)ds \tag{D.5}$$

and Equation D.2 may be written as

$$p_f=\int_0^1 G(H)dH \tag{D.6}$$

The dependence of G on H is seen through the relations

$$H_i=F_s(s_i) \tag{D.7}$$

or $$s_i=F_s^{-1}(H_i) \tag{D.8}$$

At the particular value s_i, G_i is given by

$$G_i=F_S(s_i) \tag{D.9}$$

or, writing G as an explicit function of H,

$$G_i=F_S[F_s^{-1}(H_i)] \tag{D.10}$$

Numerically, one draws a set of stylized points from the stress random variable s, and denotes the set by

$$\{s_i^*\},\ i=1,m$$

where s_0 and s_{m+1} are the extrapolated endpoints found as discussed in Appendix A. Because of the way the stylized points are drawn, the H_i are given exactly by

$$H_i=(i+\alpha)/(m+\beta);\ -1\leq\alpha\leq\beta;\ i=1,m \tag{D.11}$$

where

$$H_0=0 \tag{D.12}$$

and $$H_{m+1}=1 \tag{D.13}$$

The set of stylized points from the strength variable S, denoted by

$$\{S_i^*\},\ i=1,m$$

defines the strength distribution function $F_S(s)$ as defined

in Equation D.9. Consequently, the integral may be calculated over H by writing

$$p_f = \int_{H_0}^{H_{m+1}} G(H)\,dH \tag{D.14}$$

The above integral may be written as the sum of three separate integrals on the intervals $[H_0, H_1]$, $[H_1, H_m]$, and $[H_m, H_{m+1}]$. Application of the trapezoidal rule to each of these integrals in turn yields

$$p_{f1} = (G_1 + G_0) H_1 / 2 \tag{D.15}$$

$$p_{f2} = \Delta H \{ G_1 + 2 \sum_{i=2}^{m-1} G_i + G_m \} / 2 \tag{D.16}$$

$$p_{f3} = (G_{m+1} + G_m)(1 - H_m) / 2 \tag{D.17}$$

where

$$\Delta H = 1 / (m + \beta) \tag{D.18}$$

The sum of the above three terms is approximately the value of the reliability interference integral.

Appendix E: Further Consideration of the Vulnerability of a Box-Beam Wing Structure

Overview

This Appendix provides additional information on the box-beam wing model discussed in Chapter VI. In particular, the following is provided: (a) the basic assumptions about the box-beam and the scenario for the vulnerability calculations, (b) explicit calculations of the stress in each of the four members of the beam, and (c) the relative vulnerability of each of the four components of the beam in the sure-kill, median-failure, and sure-safe regions.

Assumptions

The following assumptions are made regarding the wing model and the scenario for the calculation:

(a) the wing is assumed to be designed for constant bending stress along the length of the wing with a 1g design of 10,000 psi (6.891E7 Pascals);

(b) the wing box is assumed to be free to expand and bend;

(c) the effects of structural discontinuities are neglected;

(d) the aircraft is directly above the burst at burst time, implying that only the lower skin is heated, and it is heated uniformly.

Stress Calculations

There are four components to the box-beam, as shown in Figure 6.9. These include the lower skin, the upper skin, the lower stringers, and the upper stringers. Even though the lower skin is the only heated part, the effects of this heating will be felt by all the members through the integral equations shown in Equations 6.25 and 6.26. These integrals have the explicit values shown below.

$$I_1=\int_{-c-\epsilon}^{-c+\epsilon}\Delta T_p(z,t)dz \qquad (E.1)$$

where c is as shown in Figure 6.9, and ϵ is the half-thickness of the skin. In general terms, I_1 reduces to

$$I_1=2\epsilon\Delta T_p \qquad (E.2)$$

Similarly, the integral in Equation 6.26 is given by:

$$I_2=\int_{-c-\epsilon}^{-c+\epsilon}z\Delta T_p(z,t)dz \qquad (E.3)$$

This integral reduces to:

$$I_2=-2c\epsilon\Delta T_p \qquad (E.4)$$

With these integrals determined, and denoting the stress in the lower skin, upper skin, lower stringer, and upper stringer by σ_1, σ_2, σ_3, and σ_4, respectively, one finds the results:

$$\sigma_1=\sigma_{1g}N_L-.3582\alpha_1E(T_p)\Delta T_p \qquad (E.5)$$

$$\sigma_2=-\sigma_{1g}N_L-.04177\alpha_1E(T_p)\Delta T_p \qquad (E.6)$$

$$\sigma_3=5\sigma_{1g}N_L/6+.5848\alpha_1E(T_p)\Delta T_p \qquad (E.7)$$

$$\sigma_4=-5\sigma_{1g}N_L/6+.01519\alpha_1E(T_p)\Delta T_p \qquad (E.8)$$

where, in the above equations, N_L is the dimensionless load factor on the wings, α_1 is the coefficient of linear expan-

sion, $E(T_p)$ is the modulus of elasticity, and T_p is the peak temperature of the skin at blast arrival time. Since the constants in the above equations are dimensionless, English or metric units may be used. For reference purposes, the calculations were done using an α_1 of 12.7E-6 in/(in-^{o}F) and an $E(T_0)$ of 1E7 psi. (These correspond to metric values of 2.286E-5 m/(m-^{o}K) and 6.891E10 Pascals, respectively.)

Relative Vulnerability

The relative vulnerability to the combined effects of both gust and thermal are shown in Table E.1. The three aircraft are located in the sure-kill (308 meters range), median-failure (366.5 meters range), and sure-safe (438 meters range) regions. Each aircraft is directly above the weapon at burst time, traveling with a velocity of 130 meters/second (250 knots). The blast wave catches each aircraft at a different time, resulting in a gust/thermal synergism that changes character. The measure of vulnerability is taken as the point ratio of the yield stress of 6061-T6 aluminum to the applied stress. This is the safety factor. A discussion of the relative vulnerabilities in each region follows.

The Sure-Kill Region--The upper skin appears to be the most vulnerable assembly in the sure-kill region. In each structure, the thermal contribution to the total stress load is small, but this is particularly true for the upper skin. The upper skin structure exhibits no pronounced gust/thermal

TABLE E.1

RELATIVE VULNERABILITIES OF A BOX-BEAM WING

REGION	ITEM	GUST LOAD (Pa)	THERMAL LOAD (Pa)	TOTAL STRESS (s-Pa)	STRENGTH (S-Pa)	SAFETY FACTOR (S/s)
SK	Lower Skin	4.13E8	-2.50E7	3.88E8	2.71E8	.70
	Lower Stringer	3.44E8	4.08E7	3.84E8	2.76E8	.72
	Upper Stringer	-3.44E8	1.06E6	-3.42E8	2.76E8	.81
	Upper Skin	-4.13E8	-2.91E6	-4.16E9	2.76E8	.66
MF	Lower Skin	2.75E8	-1.87E7	2.56E8	2.74E8	1.07
	Lower Stringer	2.30E8	3.05E7	2.60E8	2.76E8	1.06
	Upper Stringer	-2.30E8	7.93E5	-2.29E8	2.76E8	1.20
	Upper Skin	-2.75E8	-2.18E6	-2.77E8	2.76E8	1.00
SS	Lower Skin	1.99E8	-1.37E7	1.85E8	2.76E8	1.49
	Lower Stringer	1.67E8	2.24E7	1.89E8	2.76E8	1.46
	Upper Stringer	-1.67E8	5.82E5	-1.66E8	2.76E8	1.66
	Upper Skin	-1.99E8	-1.60E6	-2.01E8	2.76E8	1.37

synergism, since the load stress is dominated by the gust, and the strength depends on fixed room temperature material properties. The lower skin does exhibit gust/thermal synergism. The load stress, as in the upper skin, is dominated by the gust term, but the strength properties depend on the thermal behavior. Because of this, this structure was chosen for the sample calculation done in Chapter VI.

The Median-Failure Region.--In this region, the most vulnerable assembly is the upper skin. This is because the thermal stress contribution acts in the same direction (compressive) as the gust load contribution. Even so, the gust/thermal synergism is slight, the thermal contributing only a very small fraction of the total load stress.

In contrast, the lower stringer, though a relatively hard assembly, exhibits the most gust/thermal synergism. The thermal stress term contributes the order of 12% of the total stress load. The stress distribution here would then depend on both the load factor and peak temperature random variables. The strength function depends only on room temperature material properties.

The Sure-Safe Region--Again, the most vulnerable assembly is the upper skin, with both gust and thermal stress terms acting compressively. Again, the synergism is slight, since the thermal contribution remains a small fraction of the total. The comments made above regarding the lower stringer apply here also.

Summary

This Appendix has provided a more detailed analysis of the box wing model discussed in Chapter VI. The assumptions of the model and the calculational scenario have been presented. In addition to this, the thermal stress terms have been explicitly shown, as well as the relative vulnerabilities of the four components in the sure-kill, median-failure, and sure-safe regions.

Appendix F: Glossary

Chapter III Nomenclature

Acronyms And Abbreviations

CDF=Cumulative Distribution Function

DOD=Department of Defense

LLNL=Lawrence Livermore National Laboratory, Livermore, CA

PDF=Probability Density Function

SK=A Sure-Kill Stress Value

Variables

$F_S(s)$=CDF of the Strength Random Variable

$f_S(s)$=PDF of the Strength Random Variable

$F_s(s)$=CDF of the Stress Random Variable

$f_s(s)$=PDF of the Stress Random Variable

p_f=Failure Probability

S=Strength Random Variable

s=Stress Random Variable

s or S=A particular value of Stress or Strength

X_i=Random Variable Inputs

Z=Random Variable Output

$\delta(s-\bar{s})$=Dirac Delta PDF with parameter $\bar{s}$

η=Safety Factor Random Variable (dimensionless)

ξ=Margin Random Variable (stress units)

Chapter IV Nomenclature

Acronyms And Abbreviations

CDF=Cumulative Distribution Function

cm=centimeters

KPa=Kilopascals

PDF=Probability Density Function

psi=pounds per square inch

Variables

A=Modeling coefficient random variable (dimensionless)

a=Weibull scale parameter (KPa)

b=Weibull shape parameter (dimensionless)

c=Weibull location parameter (KPa)

D=Outer wall diameter random variable (cm)

d=Inner wall diameter random variable (cm)

$F_P(p)$=CDF of the applied pressure

F_{cyl}=Strain functional random variable (dimensionless)

G_i=ith percentile ($0 \leq G_i \leq 1$)

i=observation index integer

m=number of observations

P=Applied pressure random variable (KPa)

P_b=Burst pressure random variable (KPa)

P_0=Pressure constant (KPa)

p=Particular value of the applied pressure (KPa)

p_i=ith observation of the applied pressure (KPa)

t=Wall thickness random variable (cm)

W=Ratio of diameters random variable (dimensionless)

X_i=Random Input Variables

X_1=Log of W random variable (dimensionless)

X_2=Product of σ'_u and F_{cyl} (KPa)

X_3=Product of A with X_1 (dimensionless)

X_4=Ratio of X_3 to P (KPa^{-1})

Z=Random Output Variable

α=constant of the plotting rule (dimensionless)

β=constant of the plotting rule (dimensionless)

ϵ_u=Strain random variable (dimensionless)

ϵ'_u=Elongation random variable (dimensionless)

η=Safety factor random variable (dimensionless)

σ'_u=Ultimate tensile strength random variable (KPa)

ξ=Margin random variable (KPa)

Chapter V Nomenclature

Acronyms And Abbreviations

AFIT=Air Force Institute of Technology, WPAFB, OH

AFR=Air Force Regulation

AFWL=Air Force Weapons Laboratory, Kirtland AFB, NM

CDF=Cumulative Distribution Function

DASIAC=Defense Atomic Support Information and Analysis Center

DIALOG=Tradename of An Information Retrieval Service

DNA=Defense Nuclear Agency

DOD=Department of Defense

KT=Kiloton (Energy Equivalent of 10^{12} Joules)

MC=Mission Completion

PDF=Probability density function

psi=pounds per square inch

RK=A sure-kill range value (meters)

RS=A sure-safe range value (meters)

SK=A sure-kill stress value

SS=A sure-safe stress value

S/V=Survivability/Vulnerability

WPAFB=Wright-Patterson Air Force Base, Ohio

Variables

A=Wing area (meters^2)

A_f=Fuselage area (meters^2)

A_t=Tail area (meters^2)

a_x=Scale parameter of power function distribution of X

B=Total bending moment (nt-meters)

B_f=Fuselage bending moment (nt-meters)

B_t=Vertical tail bending moment (nt-meters)

b_x=Shape parameter of power function distribution

C_{df}=Fuselage drag coefficient (dimensionless)

C_{dt}=Vertical tail drag coefficient (dimensionless)

C_L=Coefficient of lift (dimensionless)

C_{L0}=Initial coefficient of lift

d_z=z coordinate of aircraft with respect to burst-plane (m)

$F_X(x)$=Cumulative Distribution Function of X

$f_X(x)$=Probability Density Function of X

L_f=Fuselage lever arm (meters)

L_t=Vertical tail lever arm (meters)

n_L=Load factor (g's--multiples of weight)

P=Random Overpressure (Pascals) From A Nuclear Weapon

p=Particular Overpressure Value (Pascals)

p_a=Ambient atmospheric pressure (pascals)

p_f=probability of failure

r, s_r=Slant range (meters) from a nuclear burst

S=General strength random variable

s=General stress random variable

s=Particular Value of S or s

s_0=Velocity of sound in air (meters/sec)

s_r, r=Slant range (meters) from a nuclear burst

S_{UL}=Ultimate Load Stress (A Design Parameter)

u_1=Peak wind velocity behind the shock front (m/sec)

$u_{1ax,y,z}$=Components of u_1 in aircraft reference frame

u_p=Component of wind perpendicular to vertical tail (m/sec)

$u_{rx,y,z}$=Resultant velocity components in aircraft frame

v=Lift wind velocity (meters/second)

v_0=Initial aircraft velocity (meters/second)

W=Weight (newtons)

X=Random Ratio of Failure Stress to Ultimate Load Stress

x=Particular Value of the Random Variable X

x_b=x coordinate of bomb in burst-plane (meters)

x_t=x coordinate of aircraft in burst-plane (meters)

Y=Log safety factor random variable

y=particular value of Y

y_b=y coordinate of bomb in burst-plane (meters)

z=Standard Normal Variate

α=Angle of attack (radians)

α_0=Initial angle of attack (radians)

α_x=Location Parameter of Lognormal Distribution of X

β_x=Scale parameter of lognormal distribution of X

$\Phi(z)$=CDF of standard normal variate evaluated at z

ρ=Air density behind the shock front (kg/m^3)

ρ_0=Ambient air density (kg/m^3)

μ_y=mean value of Y

σ_y=standard deviation of Y

Chapter VI Nomenclature

Acronyms And Abbreviations

AFWL=Air Force Weapons Laboratory

CDF=Cumulative Distribution Function

KT=Kiloton (10^{12} joules energy equivalent)

PDF=Probability Density Function

SS=Sure-Safe

SK=Sure-Kill

Variables

A_x=Area Cross Section of Wing ($meter^2$)

b=Intercept of the SPUTTER vs FLUX Regression Line

b_w=Chordwise Dimension of Wing Section

C_v=Specific Heat (joules/(kg-^{o} Kelvin))

c=Height of Wing Section (meters)

E(T)=Temperature Dependent Elastic Modulus (pascals)

F=Relative Radiated Power Random Variable

$F_s(s)$=CDF of Random Variable s

f(t)=Time Dependent Fractional Radiated Power

f_i=Sample Value of Relative Radiated Power

g(T)=Ratio of Yield Stress to Room Temperature Yield Stress

h= Heat Transfer Coefficient (joules/°-Kelvin-m^2)

I_x=Area Moment of Inertia of Wing Section ($meter^4$)

m=Slope of the SPUTTER vs FLUX Regression Line

N_L=Load Factor Random Variable

n=Number of Observations of SPUTTER

$P(\tau)$=Time Dependent Radiated Power (watts)

$P_m(W)$=Yield Dependent Peak Radiated Power (watts)

$p_f(r)$=Range Dependent Failure Probability

$\bar{R}$=Mean Residual

r=Slant Range (meters)

s=Generic Stress Random Variable

T=Temperature (° Kelvin)

T_{SK}=A Sure-Kill Temperature (° Kelvin)

T_{SS}=A Sure-Safe Temperature (° Kelvin)

T_p=Peak Temperature Random Variable (°-Kelvin)

T_r=Transmittance Factor

T_0=Ambient Temperature (°-Kelvin)

$\hat{T}$=Ratio of Real Temperature to Ambient Temperature

$\hat{T}_c$=Characteristic Temperature

$\hat{T}_k$=Geometric Part of Characteristic Temperature

t=Time (sec)

t_c=Cooling Time (sec)

t_m=Time to Peak Radiated Power (sec)

W=Weapon Yield (joules)

Y_f=Value of FLUX (watts)

Y_s=Radiated Power Random Variable (watts)

Y_s=Median Value of SPUTTER (watts)

Y_{th}=Thermal Yield (watts)

y_i=Observed SPUTTER value (watts)

Z=Standard Normal Random Variable

z=Coordinate (meters) Measured From Center of Wing Section

z_i=A Variate From the Standard Normal Distribution

α_b=Absorptivity of Skin Surface

α_l=Coefficient of Linear Expansion ($^\circ K^{-1}$)

α_p=Location Parameter of Distribution of Radiated Power

β_p=Scale Parameter of Distribution of Radiated Power

ΔT=Temperature Difference ($^\circ$-Kelvin)

Δx=Skin Thickness (meters)

ϵ=Wing Skin Half Thickness (meters)

γ=Ratio of t_m to t_c

$\theta(t)$=Time Dependent Look Angle (Radians)

ρ=Mass Density (kg/m^3)

$\sigma_{S|F}$=Conditional Standard Deviation of SPUTTER given FLUX

σ_{1g}=Design Stress (pascals)

σ_g=Stress (pascals) Due to Gust Loads

σ_{SK}=Sure-Kill Stress (pascals)

σ_{thi}=Stress (pascals) Due to Thermal Loads

σ_x=Stress (pascals)

τ=Dimensionless Time (Ratio of t to t_m)

Topical Bibliography

Probability, Statistics, And Reliability Theory

1. Ang, A.H., and W.H. Tang, Probability Concepts in Engineering Planning and Design, Volume I, Basic Principles, John Wiley and Sons, Inc., New York, NY, 1975.

2. Arfken, G., Mathematical Methods for Physicists, Academic Press, New York, NY, 1973.

3. Ashley, C., Probabilistic and Statistical Considerations in Assuring Hardness of Complex Systems by Individual Control of Many Independent Piece-Parts, Air Force Weapons Laboratory, Kirtland AFB, NM, April, 1979.

4. Cook, I.D., The H-Function and Probability Functions of Certain Algebraic Combinations of Independent Random Variables with H-Function Probability Distributions, Air Force Institute of Technology, work performed at University of Texas, Austin, TX, AFIT/DS/81/47D Wright-Patterson AFB, OH, May, 1981.

5. Dhillon, B.S. and C. Singh, Engineering Reliability--New Techniques and Applications, John Wiley and Sons, Inc., New York, NY, 1981.*

6. Hoel, P.G., Introduction to Mathematical Statistics, Fourth Edition, John Wiley and Sons, New York, NY, 1971.

7. Johnston, G.O., "A Review of Probabilistic Fracture Mechanics Literature", Relibility Engineering, Vol. 3, No. 61, pps. 423-448, 1982.

8. Kapur, K.L., and L.R. Lamberson, Reliability in Engineering Design, John Wiley and Sons, New York, NY, 1977.

9. Kececioglu, D., "Probabilistic Design Methods for Reliability and Their Data and Research Requirements", Failure Prevention and Reliability, 1977.

10. Lee, D., Lecture 21 in Math 674, Numerical Analysis I , Air Force Institute of Technology, Wright-Patterson AFB, OH, May 1981.

11. Maybeck, P., Stochastic Models, Estimating, and Control. New York, Academic Press, 1979.

12. Shapiro, S.S., and A.J. Gross, Statistical Modeling, Marcel Dekker, Inc., New York, NY, 1981.

13. Siddall, J.N., and Y. Diab, "The Use in Probabilistic Design of Probability Curves Generated by Maximizing the Shannon Entropy Function Constrained by Moments", Journal of Engineering for Industry, August 1975.

14. Sweeder, J., Nonparametric Estimation of Distribution and Density Functions With Applications, Air Force Institute of Technology, AFIT/DS/MA/82-1,Wright-Patterson AFB, OH, May, 1982.

15. Thoft-Christensen, P., and M.J. Blake, Structural Reliability Theory and Its Applications, Springer-Verlag, Berlin, Heidelberg, New York, NY, 1982.

Risk Analysis

16. Anderson, R.G., Reduction of Uncertainty in Structural Design and Decision Making by First Order Bayesian Information Analysis, Thesis presented to the Massachusetts Institute of Technology, Cambridge, MA, 1971.*

17. Ang, A.H-S., Structural Risk Analysis and Reliability-Based Design, ASCE Journal of Structural Division, Vol. 99, No. ST9, September 1973.*

18. Ang, A.H-S., and N.M. Newmark, A Probabilistic Seismic Safety Assessment of the Diablo Canyon Nuclear Power Plant, N.M. Newmark Consulting Engineering Services, Report to U.S. Nuclear Regulatory Commission, November 1977.*

19. Ang, A.H-S., and W.H. Tang, Probability Concepts in Engineering Planning and Design--Volume II, John Wiley and Sons, 1984.*

20. Chenoweth, H.B., "The Error Function of Analytical Structural Design", Proceedings of the 23rd Annual Technical Meeting of the Institute of Environmental Sciences, pps. 231-234, 1977.

21. Chenoweth, H.B., "Aircraft Structural Reliability Prediction Based on Dynamic Loads and Ultimate Strength Test Data", Proceedings of the 24th Annual Meeting of the Institute of Environmental Sciences, pps. 352-355, 1978.

22. Chenoweth, H.B., "An Indicator of the Reliability of Analytical Structural Design", AIAA Journal of Aircraft, Vol. 7, No. 1, pp. 13-17, January-February 1970.

23. Ditlevsen, O., Uncertainty Modeling, McGraw-Hill, New York, NY, 1981.

24. Freudenthal, A.M., and P.Y. Wang, "Ultimate Strength Analysis of Aircraft Structures", AIAA J. of Aircraft, Vol. 7, No. 3, May-June 1970.

25. Henley, E.J., and H. Kumamoto, Reliability Engineering and Risk Assessment, Prentice-Hall, Englewood Cliffs, NJ, 1981.

26. Jablecki, L.S., Analysis of Premature Structural Failures in Static Tested Aircraft, Dissertation, Die Eidgenossichen Technesche Hochschule, Zurich, Switzerland, 1955.

27. Kiuereghian, A.D., "An Integrated Approach To The Reliability of Engineering Systems", Nuclear Engineering and Design, Vol. 71, No. 3, pps. 277-279, 1982.

28. Klingmuller, O., "Some Mechanical Aspects of the Probability of Failure", Nuclear Engineering and Design, Vol. 71, No. 3, pps. 349-354, 1982.

29. McCormick, N.J., Reliability and Risk Analysis: Methods and Nuclear Power Applications, Academic Press, New York, NY, 1981.

30. Rojiani, K.B. "A Probabilistic Analysis of Steel Beam-Columns", Engineering Structures, Vol. 4, p.233, 1982.

31. Russell, S.O., "Flood Probability Estimation", Journal of the Hydraulics Division-ASCE, Vol. 8, No. 1, pps. 63-73, 1982.

32. Stancampiano, P.A., "Monte Carlo Approaches to Stress-Strength Interference Theory", Failure Prevention and Reliability, 1977.

33. Tang, W.H., "A Bayesian Evaluation of Information for Foundation Engineering Design", Proceedings of the First International Conference on Application of Statistics and Probability to Soil and Structural Engineering, Hong Kong University Press, September 1971.*

34. Evaluation of Seismic Design Basis and Analysis Pertaining to Diablo Canyon, Nuclear Regulatory Commission, NRC-78-100-200-37, Washington, DC, 1978.*

Survivability Methods

35. Air Force Weapons Laboratory, A Study of Nuclear Airblast Simulators for Aircraft Testing, AFWL-TR-79-211, Kirtland AFB, NM, August 1980.

36. Anderson, D.J., and L.H. Skinner, FLEE.2 User and Analyst Manual, BDM Corporation, BDM/TAC-77-544-TR-R1, Albuquerque, NM, 29 December 1978.

37. Ang, A.H-S., Approximate Probabilistic Methods for Survivability/Vulnerability Analysis of Strategic Structures, Defense Nuclear Agency, DNA-4907F, Washington, DC, July 1978.

38. Badessa, M.E., QUANTA-Users Manual, Air Force Weapons Laboratory, AFWL-TR-79-193, Kirtland AFB, NM, July 1980.

39. Baker, G., Personal Communication, 1983.

40. Bevensee, R.M., H.S. Cabayan, F.J. Deadrick, L.C. Martin, and R.W. Mensing, Probabilistic Approach to EMP Assessment, United States Department of Energy, Lawrence Livermore National Laboratory, University of California, UCRL-52804-REV-1, Livermore, CA, September 1980.

41. Bevensee, R.M., H.S. Cabayan, F.J. Deadrick, L.C. Martin, and R.W. Mensing, Characterization of Errors Inherent in System Vulnerability Assessment Programs, United States Department of Energy, Lawrence Livermore National Laboratory, University of California, UCRL-52954, Livermore, CA, October 1980.

42. Boeing Computer Services, STRAT-SURVIVOR Analysts Manual, Hq USAF, Assistant Chief of Staff, Studies and Analysis, Washington, DC, 2 May 1977.

43. Breuer, D.W., Personal Communication, Air Force Institute of Technology, WPAFB, OH, August 1983.

44. Bridgman, C.J., The Use of Weapon Radius in Nuclear Survivability Calculations, 6th Annual Mini-Symposium, AIAA, Wright-Patterson AFB, OH, March 1980.

45. Bridgman, C.J., A Graduate Design Course On Aircraft Survivability, AIAA Aircraft Systems And Technology Conference, Paper AIAA-81-1727, Dayton, OH, 11-13 August 1981.

46. Bridgman, Charles J., "Nuclear Survivability--Armor in the Nuclear Age", AOG Quarterly, Vol. 2, No. 4, Air Force Institute of Technology Association of Graduates, Miamisburg, OH, Winter 1981/82.

47. Carpenter, H.J., and A.L. Kuhl, Nuclear Blast Environments for Base Escape Assessments, Defense Nuclear Agency, DNA-5316F, Washington, DC, January 1979.

48. Collins, J., Personal Communication, 1983.

49. Collins, J.D., "Hardened System Vulnerability Analysis," The Shock and Vibration Bulletin, The Shock and Vibration Information Center, Naval Research Laboratory, Bulletin 47, Washington, DC, September 1977.

50. Collins, J.D., and J.M. Hudson, "Applications of Risk Analysis to Nuclear Structures", Proceedings of the ASCE Structures Division, Symposium on Probabilistic Methods in Structural Engineering, ASCE, St. Louis, MO, October 1981.

51. Crawford, M., An Evaluation of Modified Sachs and Ledsham- Pike Scaling of a Nuclear Air Blast, Air Force Institute of Technology, Ph.D. Dissertation, Wright-Patterson AFB, OH, In Publication, December 1982.

52. Crowley, P.P., and W.J. Ladroga, Materials Data Handbook, Space and Missile Systems Organization, RADS III, Final Report, Vol. X, SAMSO-TR-69-158, Bks 1 and 2, January 1969.*

53. Defense Intelligence Agency, Physical Vulnerability Handbook--Nuclear Weapons, AP-550-1-2-69-INT, Washington, DC, June 1969.

54. Defense Nuclear Agency, Handbook for Analysis of Nuclear Weapon Effects on Aircraft, Vol. 1 and Vol. II, DNA-2048H1 and DNA-2048H2, Washington, DC 1976.

55. Defense Nuclear Agency, Application of Probabilistic Methods to MX, Washington, DC.

56. Defense Nuclear Agency, The Vulnerability of In-Flight Soviet Aircraft to Nuclear Weapon Blast Effects, DNA-5014F, Washington, DC, June 1979.

57. Defense Nuclear Agency, User's Manual-Volume I, Failure Analysis By Statistical Techniques, DNA 3336F-1, Washington, DC, September 1974.

58. Donahoe, L.H., J.J. Farrell, and G.M. Teraoka, Hardness Evaluation of Reentry Vehicles with the FAST Methodology, Defense Nuclear Agency, DNA-4500F, Washington, DC, January 1978.

59. Evans, R.D., Importance of Predamaged Material Properties in Lethality Analyses, AVCO Systems Division, Technical Report AVSD-0507-69-RR, Vol. III, July 1970.*

60. Friedberg, R., and P.S. Hughes, Experimental Study of Aircraft Structural Response to Blast: Vol. I-Analysis and Correlation, Naval Weapons Evaluation Facility, NWEF-1145 V.1, Kirtland AFB, NM, December 1977.

61. Gatewood, B.E., Thermal Stresses with Applications to Airplanes, Missiles, Turbines, and Nuclear Reactors, McGraw-Hill Book Company, New York, NY, 1957.

62. Glasstone, S. and P.J. Dolan, The Effects of Nuclear Weapons, United States Department of Defense and United States Department of Energy, 3rd Edition, Washington, DC, 1977.

63. Gragg, D.B., Aircraft Hardness to Nuclear Gusts--Uncertainties and Failure Criteria, Toyon Research Corporation, Santa Barbara, CA, April 1982.

64. Harner, E.L., and D.A. Reitz, Air Blast and Thermal Effects on Aircraft--Data Compendium, Kaman-Tempo, SR-168, Santa Barbara, CA, December 1978.

65. Hobbs, N.P., G. Zartarian, and J.P. Walsh, TRAP--A Digital Computer Program for Calculating the Response of Aircraft to the Thermal Radiation from a Nuclear Explosion, Vol. I, Theory and Program Description, Air Force Weapons Laboratory, AFWL-TR-71-61, Kirtland AFB, NM, October 1972.

66. Horizons Technology, Inc., Aircraft Vulnerability, DNA-2048H1, CROM ACV-1 With Nuclear Weapons Effects Programs Manual, San Diego, CA, 18 December 1978 and 17 March 1980.

67. Jordano, R.J., Treatment of Nuclear Effects Uncertainties, Effects on LF Propagation, Defense Nuclear Agency, DNA-5862T, Washington, DC, January 1982.

68. Kaman AviDyne Staff, Handbook for Analysis of Nuclear Weapon Effects on Aircraft, Vol I and Vol II, Defense Nuclear Agency, DNA-2048H1 and DNA-2048H2, Washington, DC, 18 March 1976.

69. Kaman Tempo, Operation PLUMBOB--Technical Summary of Military Effects, AD-A995-075, Santa Barbara, CA, October 1979.

70. Kaman Tempo, Operation REDWING--Technical Summary of Military Effects, AD-A995-132, Santa Barbara, CA, October 1979.

71. Longinow, A., K.H. Chu, and N.T. Thomopoulos, "Probability of Survival In Blast Environment", Journal of Engineering Mechanics, Vol. 108, No. 2, pps. 309-330, 1982.

72. Mihora, D.J., P.K. Abbey, and R.K. Crawford, Nuclear Gust Hardness Derived From Inherent Aircraft Strength, Defense Nuclear Agency, DNA-TR-81-46, Washington, DC, December 1981.

73. Needham, C.E., and J.E. Crepeau, The DNA Nuclear Blast Standard (1 KT), Defense Nuclear Agency, DNA-5648T, Washington, DC, January 1981.

74. Needham, C.E., et.al., Nuclear Blast Standard (1 KT), Air Force Weapons Laboratory, AFWL-TR-73-55 (Revised), Kirtland AFB, NM, January 1981.

75. Ostermann, L.E., and J.D. Collins, "Optimization of Hardened Facility Designs for Nuclear Attack", Proceedings of the Shock and Vibration Symposium, October 1981.

76. Peery, D.J., Aircraft Structures, McGraw-Hill Book Company, Inc., New York, NY, 1954.

77. Sharp, Alfred L., A Thermal Source Model From SPUTTER Calculations, Air Force Weapons Laboratory, AFWL-TR-72-49, Kirtland AFB, NM, March 1973.

78. Stefansky, T., A. Mazzella, K. Triebes, and J. Shea, Material Properties Measurements Using Pulsed Electron Beams, Physics International Company, PIFR-174, February 1971. *

79. Stefansky, T., K. Triebes, and J. Shea, Temperature-Induced Degradation of Mechanical Properties Following Instantaneous Heating, Air Force Weapons Laboratory, AFWL-TR-71-62, Kirtland AFB, NM, September 1971.

80. Optical Interactions, the SPUTTER Program, RTD-TR-63-3128, May 1964.

* This entry has not been referenced in the text, but is cited for the interested reader.

Vita

Halvor Andrew Undem was born on 29 December 1950 in Minot, North Dakota. He graduated from Garretson High School in Garretson, South Dakota on 27 May 1969. He attended South Dakota State University in Brookings, South Dakota, and received the Bachelor of Science degree in Engineering Physics, and a commission in the United States Air Force on 21 December 1973. Under the auspices of the Air Force Educational Delay program, he attended the University of North Dakota at Grand Forks, earning the Master of Science in Physics on 15 May 1977. He entered active duty on 15 July 1977, serving as an Electromagnetic Pulse Analyst at the Air Force Weapons Laboratory, Kirtland Air Force Base, New Mexico, until entering the School of Engineering at the Air Force Institute of Technology, Wright-Patterson Air Force Base, Ohio in July of 1980.

Permanent Address: Box 464

Viborg, South Dakota 57070

UNCLASSIFIED

SECURITY CLASSIFICATION OF THIS PAGE

REPORT DOCUMENTATION PAGE

1a. REPORT SECURITY CLASSIFICATION: UNCLASSIFIED	1b. RESTRICTIVE MARKINGS
2a. SECURITY CLASSIFICATION AUTHORITY	3. DISTRIBUTION/AVAILABILITY OF REPORT: Approved for public release; distribution unlimited.
2b. DECLASSIFICATION/DOWNGRADING SCHEDULE	
4. PERFORMING ORGANIZATION REPORT NUMBER(S): AFIT/DS/PH/84-3	5. MONITORING ORGANIZATION REPORT NUMBER(S)
6a. NAME OF PERFORMING ORGANIZATION: School of Engineering; 6b. OFFICE SYMBOL (If applicable): AFIT/ENP	7a. NAME OF MONITORING ORGANIZATION
6c. ADDRESS (City, State and ZIP Code): Air Force Institute of Technology, Wright-Patterson AFB, Ohio 45433	7b. ADDRESS (City, State and ZIP Code)
8a. NAME OF FUNDING/SPONSORING ORGANIZATION; 8b. OFFICE SYMBOL (If applicable)	9. PROCUREMENT INSTRUMENT IDENTIFICATION NUMBER
8c. ADDRESS (City, State and ZIP Code)	10. SOURCE OF FUNDING NOS. — PROGRAM ELEMENT NO. / PROJECT NO. / TASK NO. / WORK UNIT NO.
11. TITLE (Include Security Classification): See Box 19	
PERSONAL AUTHOR(S): Halvor A. Undem, B.S., M.S., Capt, USAF	
13a. TYPE OF REPORT: PhD Dissertation; 13b. TIME COVERED: FROM _____ TO _____	14. DATE OF REPORT (Yr., Mo., Day): 1985 September 2; 15. PAGE COUNT: 278
16. SUPPLEMENTARY NOTATION	

17. COSATI CODES			18. SUBJECT TERMS (Continue on reverse if necessary and identify by block number)
FIELD	GROUP	SUB. GR.	Nuclear Survivability, Interference Theory, Reliability, Nonparametric Statistics, Nuclear Blast, Nuclear Thermal
18	03		
15	06		

19. ABSTRACT (Continue on reverse if necessary and identify by block number)

Title: AIRCRAFT NUCLEAR SURVIVABILITY METHODS

Dissertation Chairman: Charles J. Bridgman

Approved for public release: IAW AFR 190-1.
LYNN E. WOLAVER 16 oct 85
Dean for Research and Professional Development
Air Force Institute of Technology (AFIT)
Wright-Patterson AFB OH 45433

20. DISTRIBUTION/AVAILABILITY OF ABSTRACT	21. ABSTRACT SECURITY CLASSIFICATION
UNCLASSIFIED/UNLIMITED ☒ SAME AS RPT. ☐ DTIC USERS ☐	UNCLASSIFIED

22a. NAME OF RESPONSIBLE INDIVIDUAL	22b. TELEPHONE NUMBER (Include Area Code)	22c. OFFICE SYMBOL
Charles J. Bridgman	513-255-2012	AFIT/ENP

DD FORM 1473, 83 APR — EDITION OF 1 JAN 73 IS OBSOLETE.

UNCLASSIFIED

SECURITY CLASSIFICATION OF THIS PAGE

A new approach for assessing the survivability of aircraft components in nuclear blast and thermal environments is presented in this dissertation. A nonparametric technique is developed for use in calculating the reliability interference integral. This approach eliminates the need for density function identification and parameter estimation. Furthermore, the method can be used without resorting to large-sample random Monte Carlo simulation or propagation of moments. In addition to this, the derived cumulative distribution function using such a technique exactly interpolates the true distribution function at selected points. The method is applied to the problem of aircraft survivability in nuclear blast environments using failure (strength) distributions found in the literature. It is also applied to the case of aircraft survivability in nuclear thermal environments where direct failure data is not available. Inputs to the engineering models involved are treated statistically and the method is used to rigorously determine the statistical nature of the output variables.

END

FILMED

2-86

DTIC